



Design, synthesis and evaluation of novel c-FLIP inhibitors in order to sensitise breast cancer cells and breast cancer stem cells to TRAIL

A thesis submitted in accordance with the conditions governing
candidates for the degree of

Philosophiae Doctor in Cardiff University

Gilda Giancotti

Under the supervision of **Prof. Andrea Brancale**

Co-supervised by **Prof. Andrew Westwell** and **Dr. Richard Clarkson**

April 2018

Cardiff School of Pharmacy and Pharmaceutical Science

Cardiff University

Declaration

This work has not been submitted in substance for any other degree or award at this or any other university or place of learning, nor is being submitted concurrently in candidature for any degree or other award.

Signed (candidate)

Date

STATEMENT 1

This thesis is being submitted in partial fulfillment of the requirements for the degree of PhD.

Signed (candidate)

Date

STATEMENT 2

This thesis is the result of my own independent work/investigation, except where otherwise stated, and the thesis has not been edited by a third party beyond what is permitted by Cardiff University's Policy on the Use of Third Party Editors by Research Degree Students. Other sources are acknowledged by explicit references. The views expressed are my own.

Signed (candidate)

Date

STATEMENT 3: PREVIOUSLY APPROVED BAR ON ACCESS

I hereby give consent for my thesis, if accepted, to be available online in the University's Open Access repository and for inter-library loans **after expiry of a bar on access previously approved by the Academic Standards & Quality Committee.**

Signed (candidate)

Date

Acknowledgements

Firstly I would like to thank my supervisor Andrea, for giving me the opportunity of this PhD. I am extremely thankful for the constant guidance and the great support he provided during these three years and for all the precious things I have learnt from him. I would also like to thank my co-supervisor Andrew, for his kindness, his advises and for his invaluable help during these three years. I must also thank my co-supervisor Richard, and my colleagues at the European Cancer Stem Cells Research Institute, Liv and Rhiannon, for patiently helping me with any biology-related issues. My gratitude goes also to Tiziana Life Sciences for funding my PhD project.

My greatest thanks goes to all the people I have met during the last three years, all of them contributed to make this experience invaluable. A million thanks to my guardian angel Marcella, for her brilliance, for all the things she taught me, for being such a lovely friend and for her immense help during these years. A great thank you to Salvo, for the loughs and for the funny days in the lab with his uncountable jokes. I would also like to thank all the past and present members of the Brancale's group, for the long chats in the chemistry lab, all the funny moments and the lovely time spent together. I am deeply thankful to all the big group of people who shared with me Friday's beers and crazy nights out, and a particular thanks to Salvia, Vito and Divesh for our short but unforgettable trips. An immense thanks to Carlotta, for her brightness, for being such a lovely person and for bringing positivity in my life. A special thanks to my little Cardiff family, Elisa, Massimo e la mia coinqui Ale, for making me feel home and for always be there for me. The biggest thanks goes to my mum, dad and Kekka, my beloved family, for everything they have done for me, for being patient, for waiting awake for our late-night skype calls, for all their advises and for their constant love and support. I will never thank them enough.

Abstract

Tumour Necrosis Factor-Related Apoptosis Inducing Ligand (TRAIL) is a protein belonging to the TNF family of ligands. TRAIL is able to induce apoptosis in tumour cells, whilst leaving normal cells unaltered, representing therefore an attractive anti-cancer agent. In breast cancer, however, different cell lines are resistant to TRAIL. Moreover, many studies have demonstrated that breast cancer stem cells (bcSCs), the cells that are the most responsible for relapses and metastasis development, are resistant to TRAIL. Cellular FLICE-Like Inhibitory Protein (c-FLIP) plays a crucial role in TRAIL-resistance due to its ability to interfere with the TRAIL pathway, preventing therefore the apoptosis. In the course of a previous study, the homology model of c-FLIP has been constructed and using a structure-based virtual screening of commercially available compounds, one hit compound (**3**) able to inhibit c-FLIP at micromolar concentrations has been identified. Starting from the structure of the hit compound, several new derivatives belonging to four different structural families were designed and synthesised: sulfonamide derivatives, amine derivatives, amide derivatives and methylene derivatives. All the newly synthesised compounds were tested in an *in vitro* assay for their ability to sensitise TRAIL-resistant MCF-7 breast cancer cell line to TRAIL. Different derivatives retained the ability to increase TRAIL sensitisation showing a similar or slightly improved activity compared to the original hit. Some of the most promising compounds were further evaluated in *in vitro* pharmacokinetic assays, dose-response and cytotoxicity studies. The results obtained from these studies suggested the identification of a novel hit compound (**88**) which showed the ability to increase TRAIL sensitisation with an IC₅₀ value in the range of 15-19 µM and improved metabolic stability compared to **3**. Additionally, molecular docking analyses suggested a potential ability of the newly synthesised derivatives to occupy the pocket of c-FLIP. Taking into consideration all these results, a series of novel potential small molecule c-FLIP inhibitors showing ability to increase TRAIL sensitisation in resistant breast cancer cells and breast cancer stem cells was developed. Although further studies are needed to confirm the role of the newly synthesised compounds as c-FLIP inhibitors, these early results obtained are promising for the development of new therapeutic strategies in breast cancer treatment.

Abbreviations and Acronyms

ADME: Absorption, distribution, metabolism, excretion

AI: Aromatase inhibitor

AIBN: Azobisisobutyronitrile

Arg: Arginine

Akt: Threonine protein kinase

Apaf-1: Apoptotic protease activating factor-1

Asp: Aspartate

ATP: Adenosine triphosphate

ATRA: All trans retinoic acid

BCSCs: Breast cancer stem cells

BCL-2: B-cell lymphoma 2

BCL-xl: B-cell lymphoma extra large

BRCA-1: BReast CAncer gene 1

BRCA-2: BReast CAncer gene 2

BSE: Breast self-examination

c-FLIP: Cellular-Flice like inhibitor protein

CFA: Colony forming assay

CFU: Colony forming units

CMH: 4-(4-chloro-2-methylphenoxy)-N-hydroxybutanamide

Co-IP: Co-immunoprecipitation

COX-2: Cyclooxygenase-2

Cyt-C: Cytochrome C

CDI: N-N' carbonyldiimidazole

CSC: Cancer stem cell

DCIS: Ductal carcinoma *in situ*

DCM: Dichloromethane

DcR: Decoy receptor

DD: Death domain

DED: Death effector domain

DIPEA: *N,N*-Diisopropylethylamine
DISC: Death inducing signalling complex
DMF: Dimethylformamide
DR: Death receptor
EDTA: Ethylenediaminetetraacetic acid
EGFR: Epidermal growth factor receptor
EGR1: Early growth response 1
ER⁺: Oestrogen receptor positive
ER⁻: Oestrogen receptor negative
FADD: Fas-associated death receptor
FBS: Fetal bovine serum
Foxo3: Forkhead box O3
FRET: Fluorescence resonance energy transfer
Glu: Glutamate
HDACi: Histone deacetylase inhibitors
HEPES: (4-(2-hydroxyethyl)-1-piperazineethanesulfonic acid)
HER-2⁺: Human epidermal growth factor 2 positive
HER-2⁻: Human epidermal growth factor 2 negative
hERG: Human ether-a-go-go-related gene
His: Histidine
HPLC: High-performance liquid chromatography
HSP: Heat shock protein
IDC: Infiltrating ductal carcinoma
IC₅₀: Half maximal inhibitory concentration
JNK: c-Jun-N-terminal kinases
LBDD: Ligand-based drug design
LCIS: Lobular carcinoma *in situ*
Leu: Leucine
Lys: Lysine
MAPK: Mitogen activated protein kinase

MCV: Molluscum contagiosum virus
MD: Molecular dynamics
MDR: Multidrug resistance
MEK: MAPK/Erk kinase
MFU: Mammosphere forming units
MOE: Molecular operating environment
MRI: Magnetic resonance imaging
MRP1: Multidrug resistance associated protein 1
MS: Mass spectrometry
mTOR: Mammalian target of rapamycin
NBS: N-bromosuccinimide
NF- κ B: Nuclear factor kappa-light-chain-enhancer of activated B cells
NMR: Nuclear magnetic resonance
OPG: Osteoprotegerin
PARP: Poly (ADP-ribose) polymerase
PBS: Phosphate-buffered saline
Phe: Phenylalanine
PI3K: Phosphatidylinositol-4,5-bisphosphate 3-kinase
PR⁺: Progesterone receptor Positive
PR⁻: Progesterone receptor Negative
RF: Retention factor
rh(TRAIL): Recombinant human TRAIL
RIP: Receptor-interacting protein
RMSD: Root-mean -square deviation
Rt: Retention time
SAHA: Suberoyl anilide hydroxamic acid
SERM: Selective estrogen receptor modulators
SBDD: Structure-based drug design
SiRNA: Small interfering RNA
SP1/3: Specificity protein 1/3

TBTU: 2-(1H-Benzotriazol-1-yl)-N,N,N',N'tetramethylamminium tetrafluoroborate

Th cells: T-helper cells

THF: Tetrahydrofuran

TMS: Tetramethylsilane

TNBC: Triple negative breast cancer

TNF: Tumour necrosis factor

TLC: Thin layer chromatography

TRAF: TNFR-associated factor

TRAIL: Tumour necrosis factor-related apoptosis inducing ligand

Tyr: Tyrosine

UPLC: Ultra-performance liquid chromatography

v-FLIP: Viral-fllice-like inhibitory

XIAP: X-linked inhibitor of apoptosis protein

Contents

Chapter 1: Introduction	2
1.1 Breast Cancer	2
1.1.1 Risk factors.....	2
1.1.2 Signs, Symptoms and Diagnosis.....	3
1.1.3 Breast Cancer subtypes	4
1.1.3.1 Histopathology.....	4
1.1.3.2 Hormone Receptor Status	4
1.1.3.3 Molecular Subtypes	5
1.1.4 Breast Cancer Treatment.....	6
1.1.4.1 Surgery	6
1.1.4.2 Radiotherapy.....	6
1.1.4.3 Hormone therapy.....	6
1.1.4.4 Targeted therapy	7
1.1.4.5 Chemotherapy	7
1.1.4.6 Limitations of current treatments	9
1.1.5 Challenges in Breast Cancer treatment.....	10
1.1.5.1 Drug resistance in breast cancer.....	10
1.1.5.2 Breast Cancer Heterogeneity.....	11
1.1.5.3 Breast Cancer Stem Cells (BCSCs)	11
1.1.5.3.1 Cancer Stem Cell (CSC) Hypothesis.....	11
1.1.5.3.2 BCSCs Hypothesis.....	12
1.1.5.3.3 BCSCs-resistance to treatment and relapse	12
1.1.5.3.4 BCSCs experimental models	13
1.1.5.3.5 Targeting BCSCs	14
1.2 Apoptosis.....	15
1.2.1 Tumour necrosis factor-Related Apoptosis Inducing Ligand (TRAIL).....	16
1.2.1.1 TRAIL-induced apoptosis.....	17
1.2.1.2 Regulation of TRAIL and TRAIL signalling.....	17
1.2.1.3 TRAIL and non-transformed cells.....	18
1.2.1.4 TRAIL as anti-cancer agent.....	19
1.2.1.5 TRAIL resistance in breast cancer	20
1.2.1.6 Combinational therapies.....	20
1.3 Cellular-FLICE-Like Inhibitory Protein (c-FLIP).....	21

1.3.1 c-FLIP structure	21
1.3.2 c-FLIP-expression regulation	22
1.3.3 c-FLIP function.....	22
1.3.3.1 c-FLIP and proliferation pathways	22
1.3.3.2 c-FLIP in necroptosis and autophagy	22
1.3.3.3 c-FLIP in apoptosis.....	23
1.3.4 c-FLIP in cancer.....	26
1.3.5 c-FLIP as a therapeutic target: current inhibitors	26
1.4 Previous Molecular Modelling Studies	27
1.4.1 c-FLIP and Caspase-8 homology models.....	28
1.4.2 c-FLIP:FADD interaction	29
1.4.3 Pharmacophore generation and Virtual Screening	30
1.5 <i>In vitro</i> assays and lead compound identification	31
1.6 Evaluation of purchased analogues of 3	32
1.7 Mechanism of action of 3	33
1.7 Project aims.....	35
1.8 References.....	36
Chapter 2: Computational Studies.....	50
2.1 Introduction	50
2.2 c-FLIP:FADD interaction and c-FLIP pocket analysis	50
2.3 Hit 3:c-FLIP interaction.....	52
2.4 Design of new derivatives	53
2.5 Molecular Docking Studies.....	54
2.6 New potential interaction sites.....	55
2.6.1 Protein:Protein Docking.....	55
2.6.2 Molecular Dynamics Simulation	57
2.7 Conclusions	59
2.8 References.....	60
Chapter 3: Sulfonamide Derivatives	62
3.1 Design of sulfonamide derivatives.....	62
3.2 Synthesis of hit 3	65
3.3 Synthesis of sulfonamide derivatives.....	65
3.3.1 Synthesis of methyl(arylsulfonamidobenzoates) (21-37, 42-43).....	65
3.3.2 Synthesis of methyl(arylsulfonamido)benzoate (42-43)	66

3.3.3 Synthesis of alkyl(arylsulfonamido)benzoates (50-57).....	70
3.3.4 Synthesis of (arylsulfonamido)benzoic acids (63-67, 69-70, 72-76).....	71
3.3.4.1 Synthesis of compounds 63-67	71
3.3.4.2 Synthesis of compounds 69-70, 71	72
3.3.4.3 Synthesis of compounds 72-76	73
3.3.5 Synthesis of alkyl(arylsulfonamido)benzoates (78, 80-82).....	73
3.3.6 Synthesis of (arylsulfonamido)N-(1H-tetrazol-5-yl)phenyls (86-93).....	76
3.3.7 Synthesis of (arylsulfonamido)N-(5-oxo-2,5-dihydro-1,2,4-oxadiazol-3-yl)phenyls (97-98)	78
3.3.8 Synthesis of alkyl(arylsulfonamido)benzamides (101-106).....	81
3.4 Conclusions	84
3.5 References.....	85
Chapter 4: Amine Derivatives	87
4.1 Design of amine derivatives	87
4.2 Synthesis of amine derivatives.....	89
4.2.1: Synthesis of (aryl)amino)benzoic acids (113-120).....	89
4.2.2 Synthesis of methyl((aryl)amino)benzoates (121-124, 129-134, 137-138).....	90
4.2.2.1 Synthesis of methyl((aryl)amino)benzoates (121-124)	90
4.2.2.2: Synthesis of methyl((aryl)amino)benzoates (129-134)	91
4.2.2.3 Synthesis of methyl((aryl)amino)benzoates (137-138)	92
4.2.3 Synthesis of (aryl)amino)benzoic acids (139-143)	92
4.2.4 Synthesis of derivatives 144-149, 150	93
4.2.4.1 Synthesis of ((aryl)amino)N-(1H-tetrazol-5-yl)phenyl (144-149).....	93
4.2.4.2 Synthesis of (arylamino)N-(5-oxo-2,5-dihydro-1,2,4-oxadiazol-3-yl)phenyl (150).....	94
4.2.5: Synthesis of 2-(((aryl)amino)methyl)benzoic acids (155-157).....	94
4.3 Conclusions	99
4.4 References.....	100
Chapter 5: Methylene and Amide Derivatives.....	102
5.1 Design of methylene and amide derivatives	102
5.2 Synthesis of methylene derivatives	103
5.2.1 Synthesis of methyl(benzyl)benzoates (169-171).....	103
5.2.2 Synthesis of benzyl benzoic acids (172-173).....	105
5.3: Synthesis of the amide derivatives	106
5.3.1: Synthesis of alkyl 2-arylamido benzoates (178-183)	106
5.3.2 Synthesis of the 3-chloro-2-methy benzoyl chloride (177)	107

5.3.3: Synthesis of 2-(3-chloro-4-methylbenzamido)benzoic acid (186).....	107
5.4 Conclusions	109
5.5 References.....	110
Chapter 6: Biological Evaluation	112
6.1 Introduction	112
6.2 Colony Forming Assay (CFA)	112
6.2.1 Compounds evaluation	113
6.3 Breast cancer cell line	113
6.4 Biological Results.....	114
6.4.1 Sulfonamide Derivatives	114
6.4.1.1 Alkyl(arylsulfonamido)benzoates (21-37, 42-43, 50-57, 71, 78-81).....	114
6.4.1.2 (Arylsulfonamido)benzoic acids (63-70, 72-76).....	119
6.4.1.3 (Arylsulfonamido)N-(1H-tetrazol-5-yl)phenyls (86-93)	122
6.4.1.4 Alkyl(arylsulfonamido)benzamides (101-106).....	124
6.4.1.5 Structure-activity relationships.....	125
6.4.2 Amine Derivatives	127
6.4.2.1 (Aryl)amino)benzoic acids (113-120, 139-143, 156).....	127
6.4.2.2 Methyl((aryl)amino)benzoates (121-124, 129-134, 137-138).....	130
6.4.2.3 ((Aryl)amino)N-(1H-tetrazol-5-yl)phenyls and (arylamino)N-(5-oxo-2,5-dihydro-1,2,4-oxadiazol-3-yl)phenyls (144-150).....	133
6.4.2.4 2-(alkyl)isoindolin-1-ones (158-159).....	135
6.4.2.5 Structure-activity relationships.....	136
6.4.3 Methylene and Amide Derivatives	137
6.4.3.1 Methylene Derivatives (169-170, 172-173).....	137
6.4.3.2: Amide Derivatives (178-183, 186)	138
6.4.3.3 Structure-activity relationships.....	140
6.4.4 Conclusions	141
6.5 <i>In vitro</i> pharmacokinetic studies	145
6.6 Dose-response studies	146
6.7 Cytotoxicity Studies.....	150
6.7.1 Cell Viability Assay.....	150
6.8 Conclusions	151
6.9 Pancreatic Studies.....	153
6.9.1 Cell Viability Assay.....	153

6.10 References.....	155
Chapter 7: Molecular Docking Studies.....	158
7.1 Molecular Docking Studies.....	158
7.1.2 Sulfonamide derivatives.....	158
7.1.3 Amine Derivatives	161
7.1.3 Methylene and amide derivatives	164
7.2 Conclusions	165
7.3 References.....	166
Chapter 8: Conclusion and Future Perspectives	168
8.1 Conclusion	168
8.2 Future Perspectives.....	170
8.2.1 Biological Evaluation	170
8.2.1.1 Mammosphere Assay.....	170
8.2.1.2 <i>In Vivo</i> Studies.....	170
8.2.2 Mechanism Of Action Studies.....	170
8.2.2.1 Caspase-8 Activity Assay	170
8.2.2.2 Co-immunoprecipitation.....	170
8.2.2.3 Fluorescence Resonance Energy Transfer (FRET).....	171
8.3 References.....	172
Chapter 9: Experimental	174
9.1 General Information.....	174
9.1.1 Chemistry	174
9.1.2 Biology.....	174
9.1.2.1 Cell Lines	174
9.1.2.2 Cell Culture Maintenance	175
9.1.2.3 Cell Storage	175
9.1.2.4 Cell-Based Assays	175
9.1.2.4.1 Cell Counting.....	175
9.1.2.4.2 Colony Forming Assay ⁽⁴⁾	175
9.1.2.4.3 CellTiter Blue Viability Assay ⁽⁵⁾	176
9.1.3 Molecular Modelling.....	176
9.1.3.1 Molecular Docking	176
9.1.3.2 Molecular Dynamics (MD)	176
9.2 Synthesis of sulfonamide derivatives.....	177

9.2.1: Arylsulfonamido benzoic acids (3, 63-67).....	185
9.2.2: Methyl(arylsulfonamidobenzoates) (21-37, 42-43, 78, 86-93)	191
9.2.3 Arylsulfonyl chlorides (40-41)	219
9.2.4 Alkyl(arylsulfonamido)benzoates (50-57).....	221
9.2.5 Arylsulfonamido benzoic acids (69-70).....	229
9.2.6 Arylsulfonamido benzoic acid (72-76)	231
9.2.7 Aryl(alkyl)esters (71, 77, 79)	236
9.2.8: <i>Tert</i> -Butyl(arylsulfonamido) benzoate (80-81)	239
9.2.9 (1 <i>H</i> -Tetrazol-5yl) anilines (84-85)	241
2-(1 <i>H</i> -Tetrazol-5-yl)aniline (84).....	241
9.2.10 Alkyl(arylsulfonamido) carboxamide (101-105)	243
9.3 Synthesis of amine derivatives.....	248
9.3.1 Arylamino derivatives (113-120, 129-134, 144-150).....	253
9.3.2 Methyl((aryl)amino)benzoates (121-124)	274
9.3.3 (Aryl)amino)benzoic acids (139-143, 156).....	278
9.3.4 Methyl 2-(aryl)amino)methyl)benzoates (162-164)	284
Lactam Derivatives (158-160)	287
9.4 Synthesis of methylene derivatives	290
9.4.1 Methyl(benzyl)benzoates (169-170).....	292
9.4.2 Benzyl benzoic acids (172-173).....	294
9.5 Synthesis of amide derivatives.....	296
9.5.1 Alkyl 2-arylamido benzoates (178-183)	299
9.6 References.....	305

Chapter 1

Introduction

Chapter 1: Introduction

1.1 Breast Cancer

Breast cancer is a disease caused by a proliferation of breast cells which are exposed to mutations in genes that control cell growth and survival.

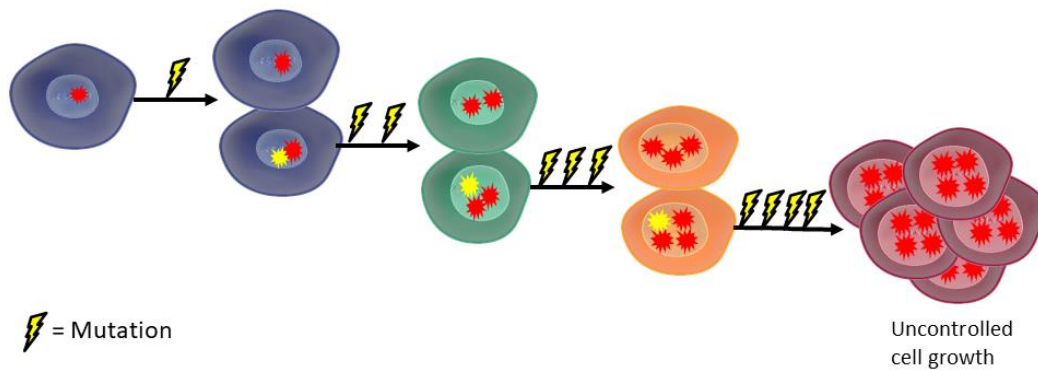


Fig 1.1: Tumour development.

In the UK, in 2014, 55,222 new cases of breast cancer were diagnosed (54,833 in women and 389 in men).⁽¹⁾ In 2012, breast cancer affected around 1,676,000 people worldwide.⁽²⁾ According to these data, breast cancer is categorised as the most prevalent form of cancer in the UK, and the second most common cancer worldwide. Although the breast cancer survival rate has increased in the last forty years, in 2012, around 522,000 women worldwide died from breast cancer.⁽²⁾ In the UK, it is estimated that breast cancer killed around 11,400 women in 2014, 31 women every day on average.⁽¹⁾ Therefore, considering the mortality rates, breast cancer represents one of the most common causes of cancer death overall.

1.1.1 Risk factors

Although the causes of breast cancer are not exactly understood, different risk factors have been identified over the years. The primary risk factor is the female sex. The latest breast cancer incidence statistics for the UK show a female:male ratio of 141:1.⁽³⁾ This is due to the activity of the female oestrogen hormones that stimulate breast cell proliferation, thus promoting errors in DNA replication.⁽⁴⁾ This explains also why even early menarche and late menopause, which expose women to a higher level of hormones, increase the risk of developing breast cancer.⁽⁵⁾ Age is an additional important risk factor with those over 65 years old representing the highest percentage (40%) of affected people.⁽⁶⁾ The probability to develop breast cancer is highly influenced by genetic predisposition as well.⁽⁸⁾ The most common hereditary genetic mutation in breast cancer is on genes BRCA1 (BReast CANcer gene 1) and BRCA 2 (BReast CANcer gene 2). Physiologically, these genes are

involved in repairing DNA damage, contributing to the normal breast cell growth. Therefore, mutations on BRCA1 or BRCA2 are associated with genomic instability. ⁽⁸⁾ Women who have mutations on BRCA1 and BRCA2 have a 72% and a 69% risk of developing breast cancer, respectively. ⁽⁹⁾ Although less common, changes in genes such as p53, PTEN and others can also represent important risk factors, due to their important role in suppressing tumours. ^(10,11) The chance of breast cancer is also associated with lifestyle. Obesity, for example, increases the risk of postmenopausal breast cancer. ⁽¹²⁾ Consumption of alcohol has been assessed as a breast cancer risk factor, whilst cigarettes smoking does not influence the probability to develop breast cancer. ⁽¹³⁾ On the other hand, additional dietary components such as vitamins A, C, E and soy, and also regular physical activity are suggested to reduce breast cancer risk. ⁽¹³⁾

1.1.2 Signs, Symptoms and Diagnosis

Several signs and symptoms can occur during a breast cancer onset. In most cases the first sign is a lump which may appear in the breast or in the armpits. ⁽¹³⁾ Additional symptoms are: a change in the size or in the shape of a breast or of a nipple, fluid leaking from the nipple, irritation of the skin around the breast. ⁽¹³⁾

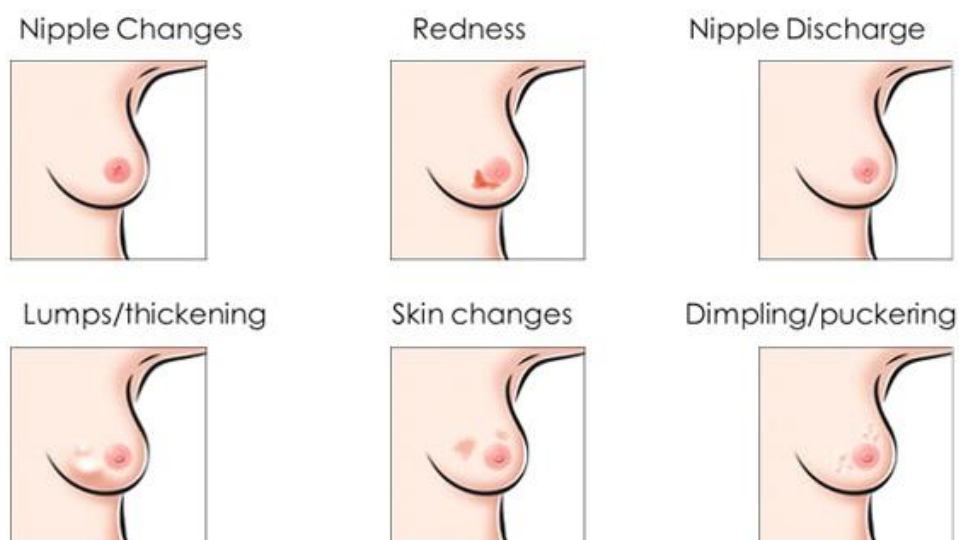


Fig 1.1.2: Breast Cancer signs. ⁽¹⁴⁾

Whenever one or more of these symptoms occur, further analyses are highly recommended. There are different examinations used to diagnose breast cancer. ⁽¹⁵⁾ The first one is the Mammogram, an X-ray of the breast, which allows an accurate analysis for any suspicious areas. ⁽¹⁶⁾ Ultrasound is another exam that uses sound waves to penetrate and scan the breast. ⁽¹⁷⁾ MRI (Magnetic Resonance Imaging), using magnetic energy and radio waves, is an additional analysis useful to understand better the difference between normal and abnormal tissue. ⁽¹⁸⁾ Most frequently, the last

test is the biopsy which, by aspiration of the tissue and microscopic examination is the only procedure that can accurately determine if the suspicious area is cancerous. ⁽¹⁹⁾

1.1.3 Breast Cancer subtypes

Breast cancer categorisation into different subtypes is often useful in order to identify the best therapeutic strategy. Due to the high heterogeneity, breast cancer can be classified on the basis of multiple factors.

1.1.3.1 Histopathology

Breast cancers are generally divided into invasive carcinoma and non-invasive (*in situ*) carcinoma. ⁽²⁰⁾ The non-invasive carcinoma can be additionally classified as ductal carcinoma *in situ* (DCIS) or lobular carcinoma *in situ* (LCIS). Among the two subtypes, the ductal carcinoma is the most common one and it has been divided into 5 different classes: Comedo, Cribiform, Micropapillary, Papillary and Solid. ⁽²⁰⁾ On the other hand, invasive carcinoma have been sub-classified into tubular, ductal lobular, invasive lobular, infiltrating ductal, mucinous and medullary. Among these, infiltrating ductal carcinoma (IDC) represents the most common form (70-80%) and it can be subdivided into three distinct grades on the basis of the difference between cancer cells and normal breast cells. ^(20, 21) When the tumours are well differentiated, with high tubule formation, low nuclear pleomorphism and low mitotic process, they are classified as grade 1. Grade 2 tumours are moderately differentiated, whereas when cancer cells are poorly differentiated, with a tubule formation less than 10%, a high mitotic rate and nuclear pleomorphism, they are defined as grade 3. ⁽²¹⁾ The three different grades are shown in figure 1.1.3.1.

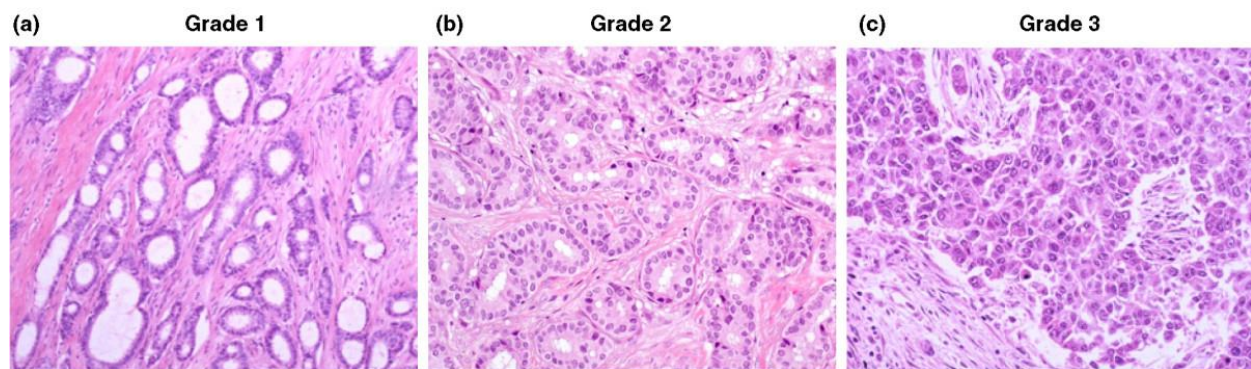


Fig 1.1.3.1: The three different grades. ⁽²¹⁾

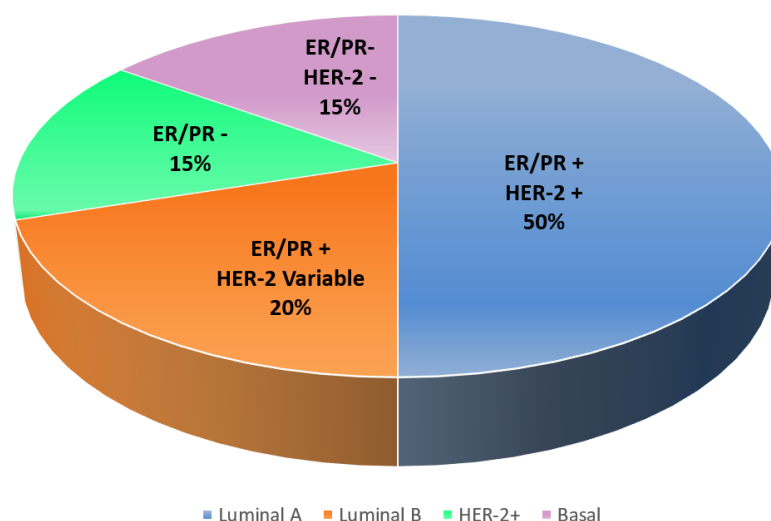
1.1.3.2 Hormone Receptor Status

The hormone receptor status is a common criterion used to classify breast cancer. In this case tumours are separated as receptor 'positive' and 'negative'. When cancer cells overexpress the

oestrogen or progesterone receptor, they are defined as receptor positive (ER⁺, PR⁺).⁽²²⁾ This class of tumours shows a strong response when treated with specific anti-hormonal therapy and they represent the most common breast cancer subtype.⁽²³⁾ In contrast, this therapy is not applicable to negative receptor tumours because they do not display the receptor for the appropriate hormone (ER⁻, PR⁻). The expression of the human epidermal growth factor receptor 2 (HER-2) allows a further classification into HER-2 positive (HER-2⁺) and HER-2 negative (HER-2⁻) tumours.⁽²⁴⁾

1.1.3.3 Molecular Subtypes

The molecular classification is based on the different gene expression pattern and allows the definition of at least three distinct subtypes: luminal, basal and HER-2⁺.⁽²⁵⁾ The first subtype includes tumours that express oestrogen and progesterone receptors and they are divided into luminal A and luminal B, according to the HER-2 expression.⁽²⁶⁾ Luminal A tumours are HER-2 negative and they represent the 50% of invasive breast cancers, whilst luminal B tumours are characterised by a variable expression of HER-2 and they account for 20% of cases.⁽²⁶⁾ The HER-2⁺ tumours are ER/PR negative, however they overexpress the HER-2 gene and additional oncogenes, such as ERBB2, and they represent the 15% of invasive breast cancers.^(26, 27) Finally, the remaining 15% is represented by basal tumours which are characterised by the lack of HER-2 and hormone receptor expression, thus they are also called triple negative breast cancer (TNBC).⁽²⁶⁾ Graph 1.1.3.3 summarises the four different breast cancer subtypes.



Graph 1.1.3.3: Molecular Breast Cancer Subtypes.

This categorisation is helpful in order to improve the accuracy of the diagnosis and to plan individualised treatments.

1.1.4 Breast Cancer Treatment

The early detection of the cancer is fundamental in order to reach a successful result in breast cancer treatment. Currently, the UK breast cancer screening programme offers a breast cancer screening every three years to women aged 50-70 years. ⁽²⁸⁾ The aim of this programme is the diagnosis and the following treatment of breast cancer in its early stage, in order to increase the probability of treatment success. In the UK, it has been estimated that the screening programme reduced the relative risk of dying from breast cancer by 20%. ⁽²⁹⁾ Mammography is the most useful method in breast cancer screening, it is a technique that, using X-ray, takes images of the breast allowing an accurate analysis. Breast Self-Examination (BSE), a self-made inspection, and the clinical examination, a full inspection of the breast, also represent important techniques in early cancer investigation. ⁽³⁰⁾ After the diagnosis, the appropriate therapeutic strategy will be selected according to the grade, the stage and the subtype of the tumour. Currently, five main categories of treatment are available: surgery, radiotherapy, chemotherapy, hormone therapy and targeted therapy. ⁽³¹⁾

1.1.4.1 Surgery

Surgery is, usually the first approach in breast cancer treatment and aims to remove completely the tumour mass and to discover whether any spread has occurred. Two different types of surgical procedure can be considered, mastectomy and breast conservations surgery, the choice depending on factors such as the size or the degree of the tumour. ⁽³²⁾

1.1.4.2 Radiotherapy

Radiotherapy is the use of high-energy beam in order to destroy cancer cells in the part of the body treated with radiation. ⁽³³⁾ In general, it is combined with surgery with the aim to reduce the possibility of breast cancer relapse. A study conducted on 11,000 women has reported that patients treated with postoperative radiation have a 16% lower risk of breast cancer recurrence. ⁽³⁴⁾

1.1.4.3 Hormone therapy

Hormonal treatment is a therapeutic strategy suitable for receptor positive tumours and is based on the use of agents able to inhibit the proliferative action of female hormones. Currently, endocrine therapy is mostly based on drugs belonging to two main classes: the selective estrogen receptor modulators (SERM) and the aromatase inhibitors (AI). ⁽³⁵⁾ Tamoxifen is the most common drug of the SERM family and it represents the first-line therapy, especially in premenopausal women. ⁽³¹⁾ Tamoxifen acts as oestrogen receptor antagonist in the breast, preventing the oestrogen-induced proliferative response in breast cells. ⁽³⁶⁾ Different studies have shown that the risk of breast cancer

recurrence and the risk of mortality is significantly decreased after 5/10 years of Tamoxifen treatment. ^(37,38) The second class of drugs, represented by the aromatase inhibitors, is often the treatment of choice in postmenopausal women. ⁽³⁹⁾ Anastrozole, letrozole and exemestane are the most common aromatase inhibitors and they act via inhibition of the aromatase, that is the enzyme responsible for the oestrogen synthesis. ⁽⁴⁰⁾ A combination of these two classes of drugs is often used in order to increase the efficacy of the treatment. Since lower risk of breast cancer recurrence and higher chance of survival have been demonstrated by the combination of the two therapies, current guidelines recommend the use of tamoxifen for the first 2-5 years followed by the administration of an AI. ⁽⁴¹⁾

1.1.4.4 Targeted therapy

Targeted therapy is based on the possibility to hit cancer cells selectively by targeting specific molecular pathways which are involved in cancer cell proliferation and survival. Tumours which are classified as HER-2⁺ are characterised by the overexpression of the human epidermal growth factor receptor-2, which is a transmembrane tyrosine kinase receptor and controls cell growth, survival and migration ⁽⁴²⁾. Those patients with HER-2⁺ tumours are currently treated with targeted therapies such as monoclonal antibodies directed against HER-2 or other members of the epidermal growth factor receptor family (EGFR), or small molecule tyrosine kinase inhibitors. Trastuzumab is a monoclonal antibody that binds the HER-2 extracellular domain interfering with the signalling pathway. ⁽⁴²⁾ More recently other monoclonal antibodies binding different sites of the HER-2 extracellular domain or other EGFRs have been developed, such as pertuzumab and cetuximab. ^(43,44) Additional targeted treatments are represented by small molecule inhibitors of the tyrosine kinases. The most common one is lapatinib, which is an ErbB1 and ErbB2 inhibitor and interferes with different pathways involved in cell growth and migration. ⁽⁴⁵⁾ Although trastuzumab represents the first-line therapy for HER-2⁺ tumours, a combination with lapatinib or other chemotherapeutic drugs is often used. In particular, a combination with doxorubicin and cyclophosphamide induces a mortality risk reduction of 37%. ⁽⁴⁶⁾

1.1.4.5 Chemotherapy

Chemotherapy implicates the use of anti-cancer drugs and is defined "adjuvant chemotherapy" when it is given after surgery, whereas when the drug administration precedes the surgery it is defined "neoadjuvant chemotherapy". In both cases, the purpose of this treatment is to kill cancer cells and to prevent the tumour recurrence, however, the neoadjuvant therapy has an additional

benefit, indeed drugs can reduce the tumour size permitting a less invasive surgery. ⁽⁴⁷⁾ Several anti-cancer agents have been developed over the years: alkylating agents (e.g. cyclophosphamide and cisplatin), antimetabolites (e.g. methotrexate and 5-fluorouracil), taxanes (e.g. paclitaxel and docetaxel), anthracyclines (e.g. doxorubicin). All these drugs act via inhibition of cell division. ⁽⁴⁸⁾ Despite the highly unselective mechanism of action, chemotherapeutic agents represent the treatment of choice for triple negative breast cancers (TNBCs). Usually anthracyclines (doxorubicin) and taxanes (paclitaxel) as single agents are the first line therapy. ⁽⁴⁹⁾ However, a sequential combination of these agents gives a 20-25% lower breast cancer mortality. ⁽³¹⁾ More recently, several agents which aim to hit specific pathways, such as PI3K inhibitors, PARP inhibitors, MEK inhibitors, HDAC inhibitors and HSP 90 inhibitors have been developed and are under investigations. ⁽⁵⁰⁾ Unfortunately, the overall survival among patients diagnosed with TNBC is currently very low, with only less than 30% of women surviving 5 years after the diagnosis. ⁽⁵⁰⁾

A summary of the most common therapeutic strategies is shown in table 1.1.

Cancer Targets	Type	Mechanism of action	Examples
Luminal	SERM	Oestrogen receptor antagonist	Tamoxifen, Raloxifene, Toremifene
	AI	Inhibition of oestrogen synthesis	Anastrozole, letrozole, exemestane
HER-2 ⁺	Monoclonal Antibodies	Interfere with EGFRs signalling pathways	Trastuzumab, pertuzumab, cetuximab
	TK inhibitors	Interfere with tyrosine kinases signalling pathways	Lapatinib
Basal	Alkylating agents	DNA damage	Cyclophosphamide, Cisplatin
	Antimetabolites	Interfere with the S phase of cell growth	5-fluorouracile, Fludarabine, Methotrexate
	Anthracyclines	Generation of free radicals that break DNA	Doxorubicin, Epirubicin
	Taxanes	Interfere with the M phase of cell cycle stopping cell division	Paclitaxel, Docetaxel

Table 1.1.4: Summary of breast cancer therapeutic strategies.

1.1.4.6 Limitations of current treatments

One of the most important limitation of the therapeutic strategies developed so far is the high cytotoxicity associated with the lack of tumour selectivity. ⁽⁵¹⁾ Commonly, patients undergoing chemotherapy experience an incredible variety of side effects which significantly reduce the quality of life during the treatment: nausea, vomiting, loss of hair, highest risk to acquire infections, anaemia, weight gain, fatigue. ^(52,53) Hormonal treatment for luminal breast cancers is also associated with several side effects such as insomnia, weight gain, hot flashes, joint aches. ⁽⁵⁴⁾ Different side effects have been associated with trastuzumab and tyrosine kinases inhibitors used for the treatment of HER-2⁺ tumours. Cardiac toxicity is the biggest problem for patients treated with trastuzumab, whilst symptoms such as nausea, vomiting, diarrhoea and rash are common in patients treated with lapatinib. ⁽⁵⁵⁾ Therefore, despite the decreased mortality rate in breast cancer

patients reached over the years, the development of more selective targets and novel therapeutic strategies represents a relevant issue.

1.1.5 Challenges in Breast Cancer treatment

Most certainly breast cancer screening and the different therapeutic strategies developed over the years, achieved important results in reducing breast cancer mortality,⁽⁵⁶⁾ however, resistance to treatment and relapses are common events.⁽⁵⁷⁾ Therefore, an accurate analysis of the reasons behind these phenomena is required in order to delineate the challenges in breast cancer treatment.

1.1.5.1 Drug resistance in breast cancer

Although several therapeutic agents have been developed, resistance to these drugs still represents a relevant problem in breast cancer treatment. Drug resistance can either occur at the very beginning of the treatment, in this case defined as *de novo*, or it can be *acquired* when patients, initially responding to the treatment, become refractory.⁽⁵⁸⁾ Drug resistance concerns all different types of breast cancer. Adjuvant endocrine therapy for patients diagnosed with luminal cancer significantly contributed to reduce breast cancer mortality, however resistance to the treatment occurs in one third of the cases.⁽⁵⁹⁾ Although several factors such as different catalytic activity of the enzymes responsible for tamoxifen or other drugs metabolism, or modifications in the phosphorylation events that regulate ERs activity, have been identified, generally the mechanisms of endocrine resistance are still poorly understood.⁽⁶⁰⁾ Drug-resistance represents an important limitation also for the treatment of HER-2⁺ tumours. A very high percentage of patients develop *de novo* or *acquired* resistance to trastuzumab: 65% and 70% respectively.⁽⁶⁰⁾ Activation of other tyrosine kinase signalling pathways that overcome the trastuzumab-induced inhibition of HER-2 pathway, is commonly the main mechanism behind trastuzumab resistance.⁽⁶⁰⁾ The problem of drug resistance in the treatment of TNBCs is also very well-known. Unfortunately, the only therapeutic option for TNBCs is the administration of chemotherapeutic agents. However, resistance to these drugs occurs in most of the cases.⁽⁶¹⁾ Although a range of 30-70% of patients initially respond to the two most common classes of drugs used for the treatment, anthracyclines or taxanes, this response is not long-lasting. Commonly, patients acquire resistance to these agents and a progression of the tumours usually occurs after 6-10 months.⁽⁶¹⁾ Combination therapies, that involve the combined use of chemotherapeutic agents belonging to different classes, have been developed in order to overcome the problem of resistance. However, cross-resistance, also known as multidrug resistance

(MDR), where patients which have been exposed to a single drug develop resistance to several other agents, is very common. ⁽⁶¹⁾ Different mechanisms involved in chemotherapy resistance have been identified. The expression of membrane pumps (P-gp or MRP1) that promote the efflux of drugs from the cell is one of the most common, but other events such as changes in the expression of the drug targets, altered functionality of the enzymes responsible for DNA repair or modifications in the apoptotic signalling pathway, also contribute to drug resistance. ⁽⁶¹⁾ As discussed above, a lot of progress in understanding the mechanisms involved in drug resistance have been made, nevertheless it still represents one of the main challenges in breast cancer treatment.

1.1.5.2 Breast Cancer Heterogeneity

Breast cancer heterogeneity represents an important explanation for the inefficiency of some treatments and is based on the idea that several subpopulations with a different sensitivity to drugs contribute to tumour formation. ⁽⁶²⁾ The heterogeneity is due to multiple factors. The several subtypes of breast cancer, defined according to different characteristics that tumours show, have already been mentioned. However, additional aspects are also involved in breast cancer heterogeneity. The type of genetic alteration that converts a normal cell to cancerous cell (mutation, fusion, amplification), and the different susceptibility of genes to breast cancer, are additional examples of the causes of heterogeneity. ⁽⁶³⁾

1.1.5.3 Breast Cancer Stem Cells (BCSCs)

The nature of the cell, which is originally transformed in a cancer cell, is an additional important factor that contributes to heterogeneity and relapse occurrence.

1.1.5.3.1 Cancer Stem Cell (CSC) Hypothesis

During the last 10-15 years a novel theory on cancer initiation has been developed: the cancer stem cell hypothesis. ⁽⁶⁴⁾ This theory states that only a small subpopulation of cells, known as cancer stem cells is responsible for cancer development and progression. ⁽⁶⁵⁾ This concept is mainly based on the fact that cancer cells show important stem-cell like properties: self-renewal ability, capacity to differentiate into different cell types, resistance to programmed cell death and high metastatic potential. ⁽⁶⁶⁾ Additionally, the probability to accumulate multiple mutations that are responsible for the initiation of the tumour is higher in stem cells due to their enduring nature. ⁽⁶⁶⁾ According to the CSC model, cancer stem cells, as well as normal stem cells, during the self-renewal process, can either generate daughter cancer stem cells (symmetric self-renewal), which are responsible for the

progression of the tumour, or differentiate into the heterogeneous bulk of cancer cells (asymmetric self-renewal), which do not show stem-cell like properties. ^(66,67)

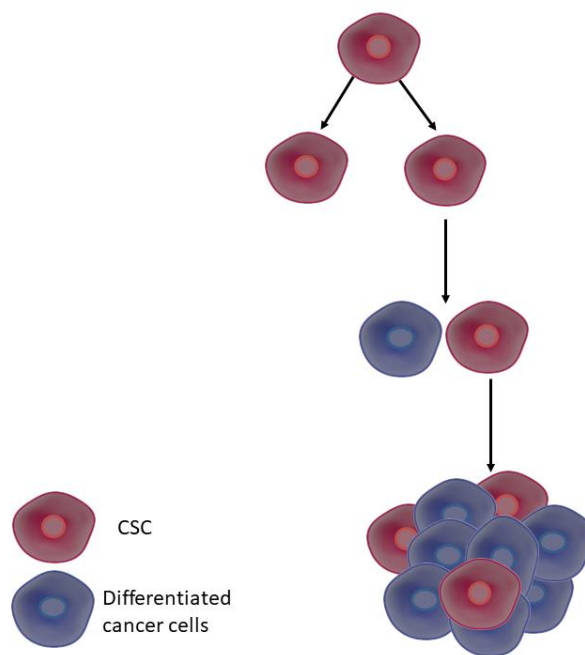


Fig 1.1.5.3.1: Cancer Stem Cells Hypothesis.

Over the years different evidences have supported this theory for a variety of cancers. These studies have demonstrated that only cancer stem cells, identified by the expression of specific markers associated with self-renewal and differentiation properties, were responsible for tumour initiation. ⁽⁶⁵⁾

1.1.5.3.2 BCSCs Hypothesis

The hypothesis that breast tumours originate from cancer stem cells has been demonstrated for the first time in 2003. ⁽⁶⁸⁾ This study showed that only cancer stem cells, defined by specific surface markers such as $CD44^+CD24^{-/low}$ were responsible for tumour initiation. On the contrary, the majority of cancer cells expressing $CD44^-CD24^+$ markers did not show ability to initiate tumours when transplanted in mice. Furthermore, this study demonstrated that tumour initiating cells have stem-cells like properties such as self-renewal and differentiation, indeed those cells expressing $CD44^+CD24^{-/low}$ showed the ability to re-induce tumour formation when passaged and transplanted in new mice, and to generate nontumorigenic cancer cells with different phenotypes. ⁽⁶⁸⁾

1.1.5.3.3 BCSCs-resistance to treatment and relapse

The idea that breast cancer stem cells are responsible for tumour initiation and progression also plays an important role in explaining phenomena such as resistance to treatment and relapse

occurrence. As discussed in paragraph 1.1.4.5, current chemotherapeutic drugs target cells that rapidly undergo cell division. On the contrary, cancer stem cells are quiescent and long-lived cells.⁽⁶⁹⁾ Additionally, BCSCs are characterised by the high expression of anti-apoptotic proteins and ABC-transporters, also recognised as multi-drug resistance transporters.⁽⁶⁵⁾ As a result of these properties, BCSCs do not respond to conventional treatments.⁽⁶⁵⁾ BCSCs resistance to treatment has also relevant implications in the occurrence of relapses, which represents an important problem in breast cancer treatment. Indeed, although current therapeutic strategies have been successful in inducing tumours regression, the self-renewing breast cancer stem cells that survive after the treatment will likely support tumour reoccurrences.⁽⁷⁰⁾ For all these reasons, breast cancer stem cells, represent, nowadays, an important and attractive therapeutic target in order to develop novel therapeutic strategies able to eradicate all the cancer cells within the tumour.

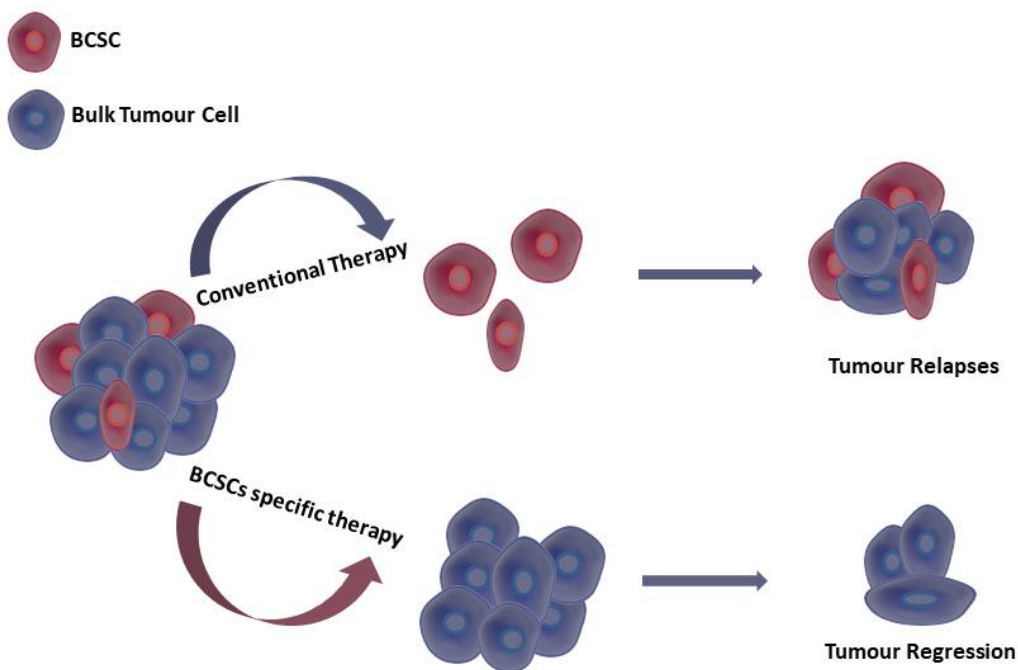


Fig 1.1.5.3.3: Therapeutic strategies of treating cancer.

1.1.5.3.4 BCSCs experimental models

In order to identify novel therapeutic agents able to target breast cancer stem cells, specific *in vivo* and *in vitro* experimental models have been developed. The most reliable *in vitro* assay for the identification of breast cancer stem cells is the mammosphere assay.⁽⁷¹⁾ The assay is based on the selective ability of breast cancer stem cells to form clusters of undifferentiated cells, termed mammospheres, when cultured in non-adherent conditions. Indeed, in these particular conditions most of the cells will die due to anoikis, whilst stem cells will survive and proliferate. In a second passage, mammospheres previously formed will be broken-up and treated in the same conditions

in order to evaluate the self-renewal ability of the breast cancer stem cells, which will result in the formation of new mammospheres. ⁽⁷²⁾ The Colony Forming Assay (CFA) or clonogenic assay is an additional assay used to identify breast cancer stem cells. As well as the mammosphere assay, CFA is based on the ability of a single cell to replicate indefinitely and form colonies composed of at least 50 cells. ⁽⁷³⁾ However, although these *in vitro* assays are convenient in terms of time and resources needed, further *in vivo* studies are often required. The gold standard for *in vivo* study is the serial transplantation assay. ⁽⁶⁷⁾ This assay involves the transplantation of human cancer cells in immunocompromised mice which are assessed at different times for tumour formation. Subsequently cells are isolated from the tumour and transplanted into a second animal, in order to evaluate the ability of these cells to self-renew and re-induce tumour formation. ⁽⁶⁷⁾ Ideally, the development of novel agents targeting breast cancer stem cells should be supported by initial *in vitro* assays, which are suitable for high-throughput screens for compounds, followed by *in vivo* studies.

1.1.5.3.5 Targeting BCSCs

Different strategies are currently under exploration for developing specific breast cancer stem cell therapies. ⁽⁷⁴⁾ One of the most common approaches is to target the different signalling pathways which are involved in survival and self-renewal of breast cancer stem cells, such as Wnt, Notch, Hedgehog, PI3K/Akt/mTOR. ⁽⁷⁵⁾ Several agents, which are currently in clinical trials, showed the ability to affect mammospheres formation *in vitro* and to reduce tumour growth in *in vivo* studies: MK-0752 (gamma-secretase inhibitor), vismodegib (hedgehog inhibitor), PKF118-310 (Wnt inhibitor), everolimus (PI3K/Akt/mTOR inhibitor). ⁽⁷⁵⁾ Other agents, such as salinomycin, or ATRA (All Trans Retinoic Acid) have been evaluated due to their ability to induce cancer stem cells differentiation, but they showed poor clinical results. ⁽⁷⁵⁾ Additionally, existing agents are currently being studied for their ability to affect breast cancer stem cells when combined with conventional chemotherapeutic drugs, lapatinib, trastuzumab and bevacizumab represent a few examples. ⁽⁷⁵⁾ Interestingly, recent studies are also exploring the effect on breast cancer stem cell populations of drugs which have not been used in cancer treatments, such as metformin, or disulfiram. ⁽⁷⁵⁾ Although clinical results for these agents are currently unknown, all these studies prove the importance of the advances made in identifying the molecular pathways involved in breast cancer stem cells survival and in developing *in vitro* and *in vivo* experimental models. This progress is fundamental for the development of more selective targets in order to overcome problems such as relapses and drug resistance and achieve better results in breast cancer treatment.

1.2 Apoptosis

Apoptosis, or programmed cell death, is a physiological process necessary for normal organism development and for the conservation of tissue homeostasis. Alterations in this process are involved in several pathologies: immunological diseases, neurodegenerative diseases, cardiovascular diseases and cancer. ⁽⁷⁶⁾ Immune reactions, pathologies, chemical agents, drugs, and hormones are the most common stimuli that cause the apoptosis initiation. ⁽⁷⁷⁾ Afterwards two different molecular pathways may carry on this process: the intrinsic pathway and the extrinsic pathway.

The intrinsic pathway involves mitochondria and a protein family known as the BCL-2 family. The proteins belonging to this family are characterised by the presence of a BCL-2 homology domain (BH domain). Anti-apoptotic (Bcl-2, Bcl-xl) and pro-apoptotic (Bax, Bak, Boc) proteins are both part of this family. When stressing conditions occur, the pro-apoptotic factors initiate the formation of pores on the mitochondrial membrane, increasing its permeability. This event leads to the conclusion of ATP production due to the variation in mitochondrial membrane potential and finally to the release of multiple proteins, such as Cytochrome C (Cyt C) or the apoptotic protease activating factor-1 (Apaf-1), which recruit the pro-caspase 9, forming the apoptosome that is able to activate the caspase-cascade. ⁽⁷⁷⁾

On the other hand, the extrinsic pathway involves the Tumour Necrosis Factor (TNF) family of proteins. Receptors belonging to this family are generally known as death receptors (DRs). Multiple ligands that show a specific domain, the death domain, bind these receptors, leading to the formation of the Death Inducing Signalling Complex (DISC). ⁽⁷⁸⁾ The DISC generation involves recruitment of adapter proteins which show a particular domain defined as Death Effector Domain (DED). This domain interacts with the DED of the pro-caspase-8 thus leading to the activation of the caspase-cascade. ⁽⁷⁷⁾

Figure 1.2 summarises the two apoptotic signalling pathways.

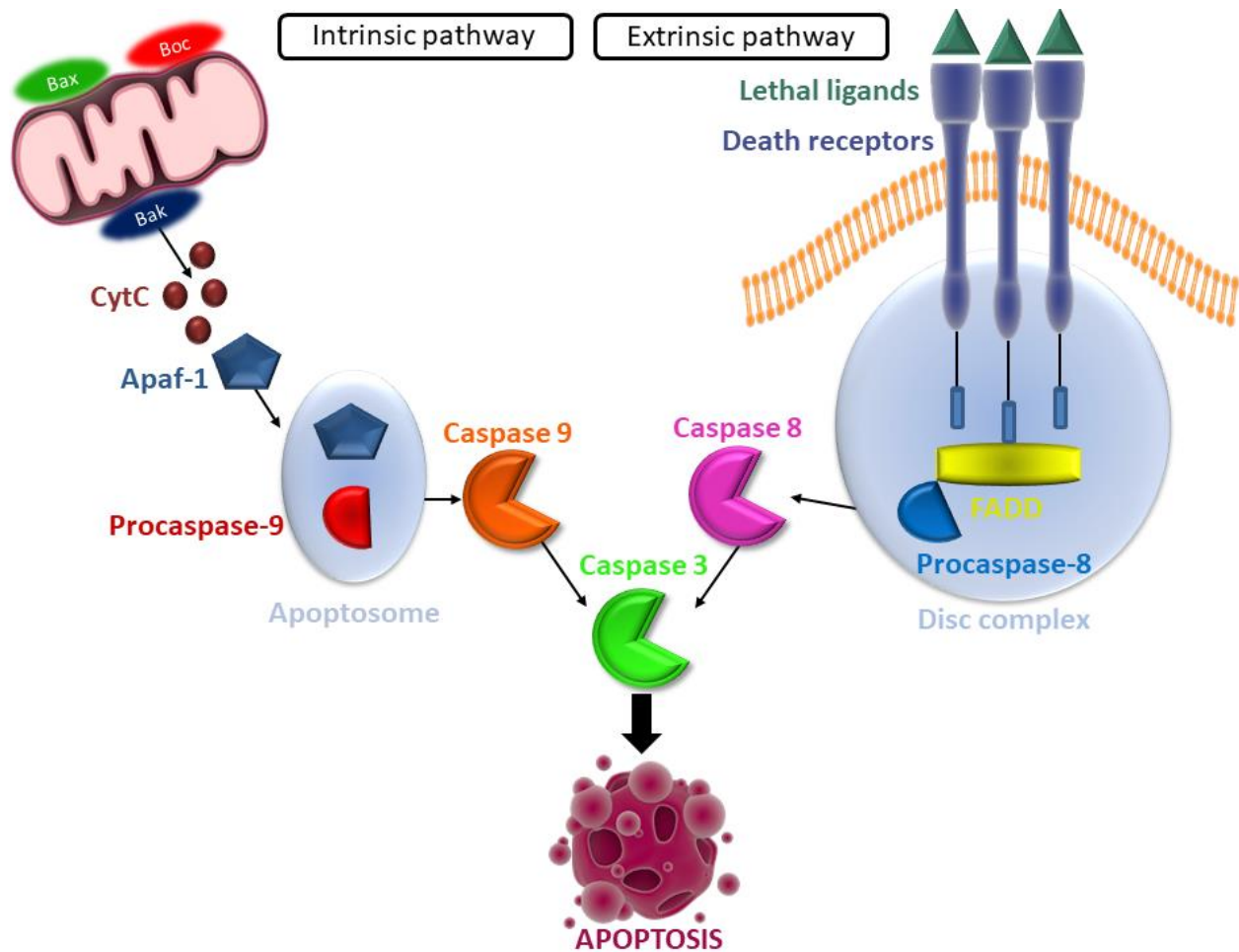


Fig 1.2: Apoptotic Signalling Pathways.

1.2.1 Tumour necrosis factor-Related Apoptosis Inducing Ligand (TRAIL)

TRAIL or the Apo-2 ligand is a type II transmembrane protein composed of 281 amino acids belonging to the TNF family of proteins. ⁽⁷⁹⁾ TRAIL is naturally expressed on cells of the immune system such as dendritic cells, macrophages, T cells and natural killer cells. TRAIL is produced in a pro-form which, after cleavage, results in a soluble homotrimeric molecule. ⁽⁸⁰⁾ As homotrimer, TRAIL is able to bind five different receptors: Death Receptor 4 (DR4), Death Receptor 5 (DR5), Decoy Receptor 1 (DcR1), Decoy Receptor 2 (DcR2), and the last one called Osteoprotegerin (OPG). The two DRs exhibit the Death Domain (DD) which is crucial for initiation of apoptosis, whereas DcRs lack this domain, therefore when overexpressed, they inhibit the activation of the death pathway. ⁽⁸⁰⁾ Although the main function of TRAIL is represented by its role in inducing apoptosis, rarely TRAIL is also able to interfere with other pathways involved in cell survival, such as NF- κ B, MAPKs, PI3K and Akt. ⁽⁸¹⁾ The role of TRAIL in these pathways is still not completely understood, however, a combination of different proteins such as FADD, Caspase-8, c-FLIP, TNFR-type1, TNFF-type2 and others are thought to be involved in this process. ⁽⁸¹⁾

1.2.1.1 TRAIL-induced apoptosis

As discussed in paragraph 1.2.1, as homotrimer TRAIL is able to activate the extrinsic apoptotic pathway via interaction with the Death Receptors (DRs). When activated by TRAIL, DRs change their conformations, acquiring a trimeric form, initiating the formation of the DISC (death inducing signalling complex). The intracellular death domain (DD) of the DRs recruits FADD (Fas-Associated Death Domain), an adapter protein which shows a Death Effector Domain (DED). DED of FADD recognises and binds the DED on procaspase-8. The following procaspase-8 dimerization converts this protein into the active form caspase-8 thus leading to caspase cascade and apoptosis. ⁽⁸²⁾

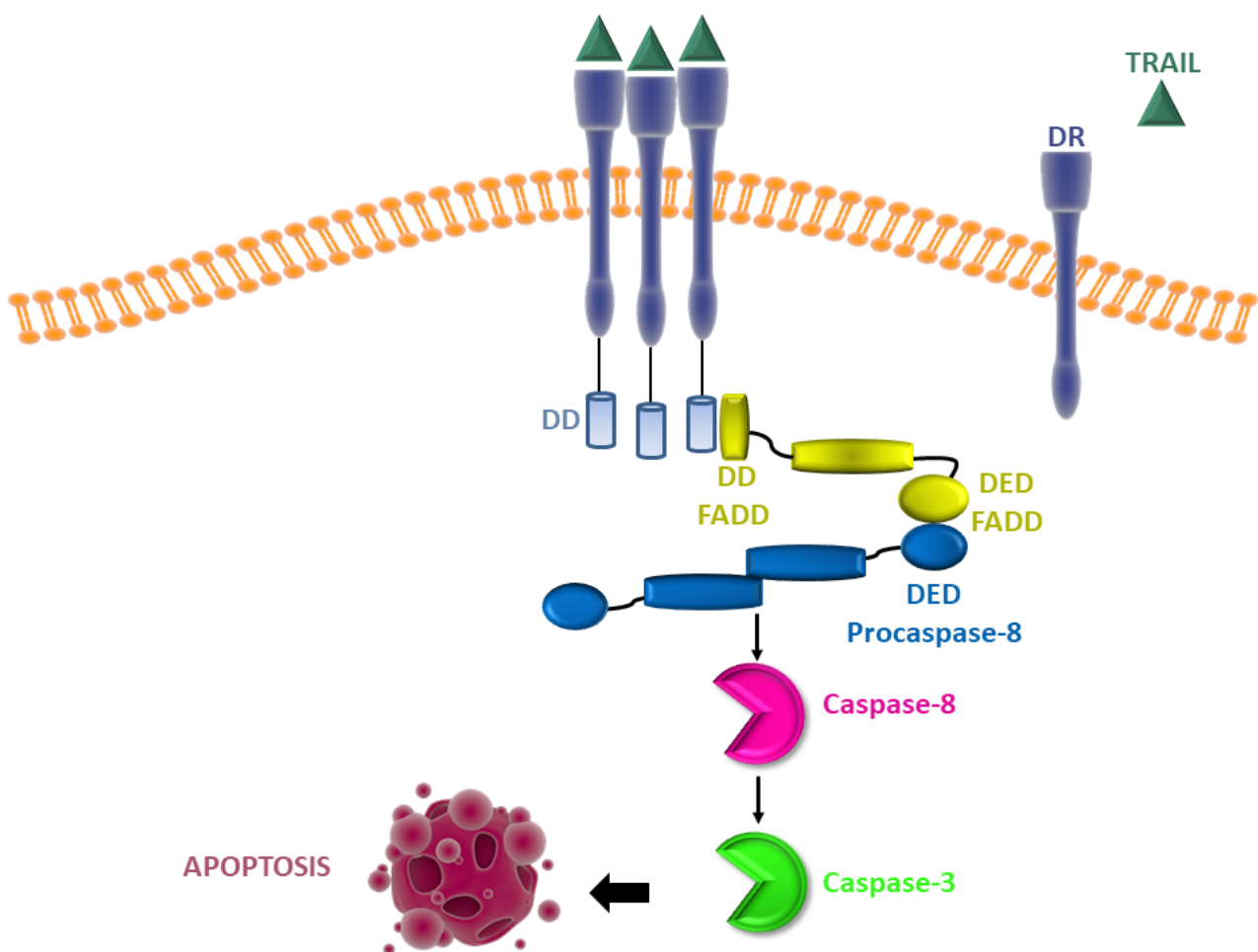


Fig 1.2.1.1: TRAIL-induced apoptosis.

1.2.1.2 Regulation of TRAIL and TRAIL signalling

As endogenous ligand involved in the apoptotic process, the expression of TRAIL is highly regulated by different transcription factors. Interferons, and other transcription factors such as NFAT and NF κ B, or p53 and Foxo3a, which are involved in tumour suppression, promote TRAIL expression, whilst factors such as SP-1 negatively modulate TRAIL gene transcription. ⁽⁸³⁾ The response to TRAIL may be controlled by all the different components belonging to the TRAIL signalling pathway. One

of the main factors that modulates the sensitivity to TRAIL is the expression level of the TRAIL receptors. Lack of DR4 and DR5 is associated with TRAIL resistance. In particular, in breast cancer, endocytosis of the DRs and consequent lack of expression on the cell surface, significantly decrease the response to TRAIL. ^(79, 84) Overexpression of decoy receptors (DcRs) also contribute to TRAIL resistance. These receptors do not show the DD required for the formation of the DISC, therefore, when overexpressed, they prevent the binding between TRAIL and DRs and consequently the activation of the apoptotic signalling pathway. ⁽⁸⁵⁾ Additionally to TRAIL receptors, several other proteins may influence the response to TRAIL. The cellular FLICE-like inhibitory protein (c-FLIP) is a protein involved in the apoptotic process. As well as procaspase-8, c-FLIP shows two death effector domains (DEDs), although lacking caspase activity. When overexpressed, c-FLIP can compete with procaspase-8 for binding to FADD, therefore preventing the activation of the caspase cascade. ⁽⁸⁶⁾ Caspases may also be directly inactivated by the presence of caspase-inhibiting proteins such as XIAP, thus preventing the TRAIL-induced cell death. ⁽⁸⁷⁾ Up-regulation of the transcription factor NFκB, that regulates the expression of genes codifying for the antiapoptotic proteins mentioned above, also promotes TRAIL resistance. ⁽⁸⁸⁾ On the other side, overexpression of the oncogenic factor c-Myc is associated with increased TRAIL sensitivity. The ability of c-Myc to inhibit the NFκB-induced expression of anti-apoptotic proteins and to upregulate the expression of the DR5, represent the main mechanisms involved in the enhancement of the TRAIL response. ^(86, 89)

1.2.1.3 TRAIL and non-transformed cells

Nowadays TRAIL is considered one of the most promising anticancer agents due to the ability to induce apoptosis in cancer cells whilst leaving normal cells unaltered. ⁽⁹⁰⁾ Although different hypotheses have been proposed, the complete mechanism behind TRAIL resistance in non-transformed cells is currently unknown. ⁽⁹⁰⁾ Multiple proteins such as the anti-apoptotic Bcl-2 proteins, c-FLIP, and the caspase-inhibitor XIAP, might be involved. ⁽⁹⁰⁾ However, the suppression of one of these proteins only, do not sensitise normal cells to TRAIL, indicating that these proteins regulate the TRAIL-resistance according to a redundant mechanism. Interestingly, redundancy seems to be lost in different TRAIL-resistant cancer cells, where inhibition of a single anti-apoptotic

protein is sufficient to increase the response to TRAIL.⁽⁹⁰⁾ Surprisingly, no correlation has been found between the expression of decoy receptors in normal cells and TRAIL resistance.⁽⁹⁰⁾

1.2.1.4 TRAIL as anti-cancer agent

Since one of the most relevant limitations of the current treatments is the lack of tumour selectivity, the ability of TRAIL to hit cancer cells only is the most significant reason for the increasing interest in TRAIL as an anti-cancer agent.⁽⁹¹⁾ In order to evaluate TRAIL as potential anticancer treatment, recombinant human TRAIL (rhTRAIL) and agonistic monoclonal antibodies specific for TRAIL death receptors have been developed.⁽⁹²⁾ Among the different forms of rhTRAIL which have been explored over the years, only one form, known as dulanermin, has been developed for clinical application.⁽⁹³⁾ In different phase-I clinical trials, dulanermin demonstrated little antitumor activity as monotherapy in advanced cancers, whilst it showed better efficacy when combined with chemotherapeutic agents, bevacizumab or rituximab in colorectal cancer, lung cancer and lymphoma. Moreover, in all these trials, dulanermin was well-tolerated and generally safe. However, dulanermin failed in randomised controlled trials during phase-II studies, where the rhTRAIL did not show any significant anticancer activity.⁽⁹³⁾ Agonistic antibodies specific for the death receptors have also been clinically evaluated. Currently four of them, mapatumumab (DR4 agonist), conatumumab, tigatuzumab, DS-8273a (DR5 agonists), are in clinical trials.⁽⁹⁴⁾ In preclinical models, mapatumumab was effective in advanced cancers when combined with chemotherapy, and in lymphoma as single agent, whilst the DR5 agonists showed efficacy in lung, colorectal, pancreatic and advanced cancers, but only when combined with chemotherapy.⁽⁹³⁾ Furthermore, in these studies they demonstrated general safety and higher pharmacokinetic stability compared to rhTRAIL.⁽⁹⁴⁾ However, although these promising results, in phase-II studies, little anticancer activity was observed for this class of agents.⁽⁹³⁾ In order to increase the efficacy of this therapy, an alternative approach may be represented by the combined administration of rhTRAIL and agonistic antibodies specific for the DRs. In particular the combination of dulanermin and conatumumab was evaluated in primary ovarian cancer cells.⁽⁹⁵⁾ This study showed that both agents are able to bind DR5, via different epitopes, leading to increased formation of the DISC and improved ability in killing cancer cells.⁽⁹⁵⁾

Therefore, although TRAIL is emerging as very desirable anti-cancer agent, the latest data obtained from phase-II clinical trials indicate the need to develop further strategies in order to improve the efficacy of TRAIL and, additionally, to overcome the problem of TRAIL resistance in cancer cells which represents one of the most relevant limitation associated with TRAIL therapy.

1.2.1.5 TRAIL resistance in breast cancer

One of the most important limitations for the use of TRAIL as an anticancer agent is represented by the fact that approximately the 60-70% of cancer cells are resistant to TRAIL-induced apoptosis.⁽⁹⁰⁾ In breast cancer, *in vitro* studies revealed that most of cell lines derived from TNBCs are TRAIL sensitive, whereas the majority of cell lines isolated from ER⁺ and HER-2⁺ tumours do not respond to TRAIL.⁽⁹⁶⁾ Unfortunately, the molecular mechanisms that determine this different behaviour between breast cancer cell lines have not been identified.⁽⁹⁶⁾ In general, the whole mechanism behind TRAIL resistance is not completely understood, however, all the proteins and receptors belonging to the TRAIL pathway may be involved.⁽⁹⁷⁾ For instance, mutations or lower expression of the death receptors, higher expression of the decoy receptors, dysfunction of FADD, downregulation of caspase-8 may be implicated.⁽⁹⁷⁾ Moreover, other signalling pathways, such as NF- κ B or PI3K-AKT may also contribute to TRAIL resistance. Upregulation of NF- κ B is common in different TRAIL-resistant cancers and, as discussed in paragraph 1.2.1.2, NF- κ B regulates the expression of anti-apoptotic proteins such as XIAP, Bcl-xl or Bcl-2.⁽⁹⁷⁾ TRAIL-resistant cancers also express high levels of constitutively activated AKT (caAKT). Activation of AKT might result in upregulation of c-FLIP, which is one of the most significant proteins involved in regulation of the apoptotic pathway and it will be discussed in section 1.3.⁽⁹⁷⁾

1.2.1.6 Combinational therapies

In order to overcome the problem of TRAIL resistance in cancer cells, novel therapeutic strategies involving the combination of TRAIL with inhibitors of the different anti-apoptotic factors implied in TRAIL resistance, are currently being evaluated. So far, the data obtained from clinical trials exploring the combination of TRAIL with different chemotherapeutic agents such as paclitaxel, doxorubicin, gemcitabine or cisplatin, revealed that these drugs are able to enhance TRAIL-induced apoptosis in different cancers.⁽⁹³⁾ Upregulation of the DRs and activation of p53 which positively modulates expression of DR5, are deemed to be the reasons behind this synergising effect.⁽⁸¹⁾ However, in order to avoid the cytotoxicity associated with chemotherapeutic drugs, more selective agents that inhibit specific factors involved in the apoptotic pathway, such as NF- κ B and PI3K-AKT inhibitors, inhibiting-apoptotic protein (IAP) antagonists and Bcl-2 antagonists are under evaluation.^(81, 93) Currently, YM155, LY2181308 and AEG35156 which downregulate the expression of inhibiting-apoptotic proteins XIAP and survivin, are in clinical trials.⁽⁹⁸⁾ Bcl-2 antagonist, ABT-199 and ABT-263 which targets Bcl-2 and BCL-xL have also entered clinical studies, ABT-263 in particular showed promising TRAIL-sensitising effect in pancreatic and hepatic cancer cells in *in vitro* studies.⁽⁹³⁾

Therefore, these encouraging data indicate that overcoming TRAIL-resistance using selective agents interfering with specific proteins involved in the apoptotic pathway, represents a valid therapeutic strategy which may lead to the development of cancer cell-selective anticancer treatments.

1.3 Cellular-FLICE-Like Inhibitory Protein (c-FLIP)

Cellular FLICE-Like Inhibitory Protein (c-FLIP) is a member of the extrinsic apoptotic signalling pathway which interferes with the formation of the DISC. The first form of FLIP, a viral form known as v-FLIP, was identified in 1997 and it was discovered in molluscum contagiosum virus (MCV).⁽⁹⁹⁾ In the same year, the mammalian cellular homolog, called c-FLIP, was characterised.⁽¹⁰⁰⁾

1.3.1 c-FLIP structure

To date, thirteen different spliced variants of c-FLIP have been reported, even though only three isoforms are expressed as proteins: c-FLIP_S, 26 kDa short form, c-FLIP_R, 24 kDa form and c-FLIP_L, 55 kDa long form.⁽¹⁰¹⁾ All three isoforms exhibit two death effector domains (DEDs) at the N-terminus. The C-terminus of c-FLIP_R is slightly shorter than c-FLIP_S, however these two isoforms are very similar. On the contrary c-FLIP_L shows a longer C-terminus, which contains two caspase-like domains (p20 and p12), and is highly similar to caspase-8⁽¹⁰¹⁾ However, c-FLIP_L is not catalytically active, due to the lack of the amino acids required for the caspase activity, and in particular to the substitution of the crucial cysteine residue by a tyrosine residue.^(101,102) Moreover, c-FLIP_L shows two cleavage sites at positions Asp-376 and Asp-196 which can be processed by caspase-8 to generate the two cleaved fragments p43 and p22 respectively.⁽¹⁰³⁾ The three isoform structures and the cleaved fragments are shown in figure 1.3.1.

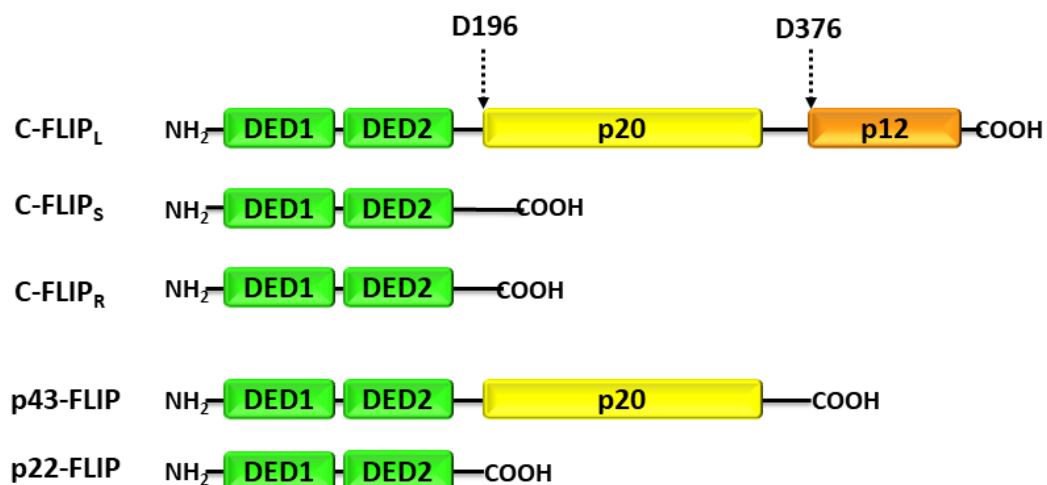


Fig 1.3.1: Structures of the three c-FLIP isoforms and cleaved fragments.

1.3.2 c-FLIP-expression regulation

The expression of c-FLIP can be modulated at different levels. Transcriptionally, c-FLIP expression is induced by several factors such as NF- κ B, p63, EGR1, AR, SP1 whereas factors such as c-myc, c-Fos, SP3, FOXO3a prevent c-FLIP transcription.⁽¹⁰¹⁾ Translationally, c-FLIP expression is mainly regulated by the Akt-mTOR kinase pathway that stimulates c-FLIP-expression.⁽¹⁰¹⁾ Degradation of c-FLIP primarily occurs via ubiquitin-proteasome degradation pathway, however JNK activation and phosphorylation events are also involved in the control of c-FLIP levels.⁽¹⁰¹⁾

1.3.3 c-FLIP function

c-FLIP is an important protein involved in different cellular processes such as regulation of apoptosis, necroptosis and autophagy and activation of proliferation pathways.⁽¹⁰⁴⁾ Additionally, c-FLIP is involved in human Th cell differentiation and in embryonic development.^(105, 106, 107)

1.3.3.1 c-FLIP and proliferation pathways

Different studies have demonstrated that, when overexpressed, c-FLIP acts as activator of signalling pathways associated with properties such as survival and proliferation.⁽¹⁰⁴⁾ c-FLIP_L, when overexpressed, activates the NF- κ B signalling pathway and the MAP kinase Erk by interacting with factors such as TNFR-associated factors 1 and 2 (TRAF1/2), RIP and Raf-1.⁽¹⁰⁸⁾ Co-immunoprecipitation studies in cancer cells have shown that c-FLIP interacts with Akt, increasing its anti-apoptotic function.⁽¹⁰⁹⁾ Additionally, c-FLIP is able to inactivate signalling pathways involved in the activation of apoptosis, such as JNK pathway.⁽¹¹⁰⁾ Furthermore, an ability of c-FLIP to induce cancer cell proliferation has been demonstrated in prostate cancer, where overexpression of c-FLIP is associated with reduced degradation of β -catenin and following higher levels of the proliferative factor cyclin D1.⁽¹¹¹⁾

1.3.3.2 c-FLIP in necroptosis and autophagy

Necroptosis and autophagy are programmed cellular mechanisms which are activated by inflammatory conditions or damage to cytoplasmic components. Several studies have demonstrated that c-FLIP is involved in the activation or suppression of these processes.⁽¹⁰⁴⁾ In necroptosis, the different c-FLIP isoforms play two distinct roles during the formation of the ripoptosome, which is a complex of several cell death-inducing proteins: c-FLIP_L blocks the ripoptosome assembly, whilst c-FLIP_S promotes its formation.⁽¹¹²⁾ On the contrary, in autophagy, c-FLIP only acts as an inhibitory protein, binding and blocking Atg3 which is an essential factor for the

formation of the autophagosome and the following degradation of damaged cytoplasmic components. ⁽¹¹³⁾

1.3.3.3 c-FLIP in apoptosis

The role that c-FLIP plays as apoptosis regulator represents one of the most important c-FLIP functions. Although c-FLIP is recognised as an anti-apoptotic protein, many studies have demonstrated that the two major protein isoforms, c-FLIP_s and c-FLIP_L, have different regulative functions. ^(104, 114, 115) The short isoform, c-FLIP_s, only blocks caspase-8 activation, while c-FLIP_L shows a dual functionality, promoting the caspase-8 activation at lower concentration and acting as caspase-8 antagonist at higher concentration. ⁽¹¹⁵⁾ The reasons behind this bifunctional role of c-FLIP_L are not completely understood, however the mechanism of caspase-8 activation seems to involve the cleaved fragments of c-FLIP (p43/p22FLIP) and their ability to heterodimerise with caspase-8 forming a complex which enhances caspase-8 activation. ⁽¹¹⁶⁾ Contrarily, c-FLIP_s that lacks the pseudo-caspase domain and the cleavage sites, only shows anti-apoptotic functions. ⁽¹¹⁶⁾ Although the important role of c-FLIP in preventing apoptosis is widely recognised, the mechanism by which c-FLIP interferes in this process is not clear. Initially a competitive binding between the DED of c-FLIP and the DED of procaspase-8 to FADD was proposed. ⁽¹¹⁷⁾ According to this model, c-FLIP and procaspase-8 compete for binding to the DED of FADD, as shown in figure 1.3.3.3a ⁽¹¹⁷⁾

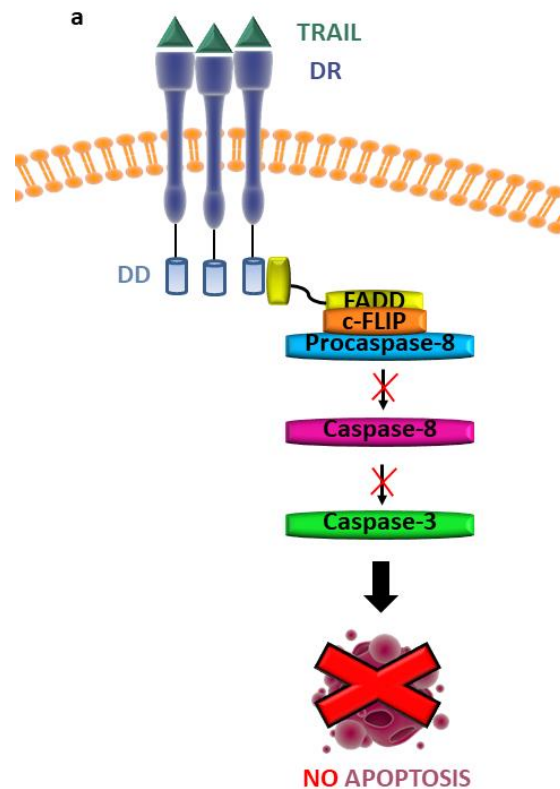


Fig 1.3.3.3a: Competitive Model.

However, more recently, two independent immunoprecipitation and mutational studies, have demonstrated that c-FLIP might interfere with the formation of the DISC in a non-competitive way. ^(118, 115) Although in both cases the results obtained challenge the initial vision of c-FLIP competing with procaspase-8, these studies propose two different potential mechanisms of action: the two-step model and the co-operative and hierarchical model. ^(118, 115) The two step-model suggests that both proteins, c-FLIP and procaspase-8, bind the two faces of the DED of FADD to form a tripartite complex. In this complex, c-FLIP_{L/S} and procaspase-8 can interact via DEDs. When c-FLIP_L is recruited to the complex, the caspase-like domain of c-FLIP_L interacts with the caspase domain of procaspase-8, generating a catalytically active complex, which promotes procaspase-8 dimerization and following caspase-8 activation. On the other side, c-FLIP_S, lacking the caspase-like domain, interacts with procaspase-8 via DEDs without inducing the conformational changes required for the activation of the enzyme. ⁽¹¹⁸⁾

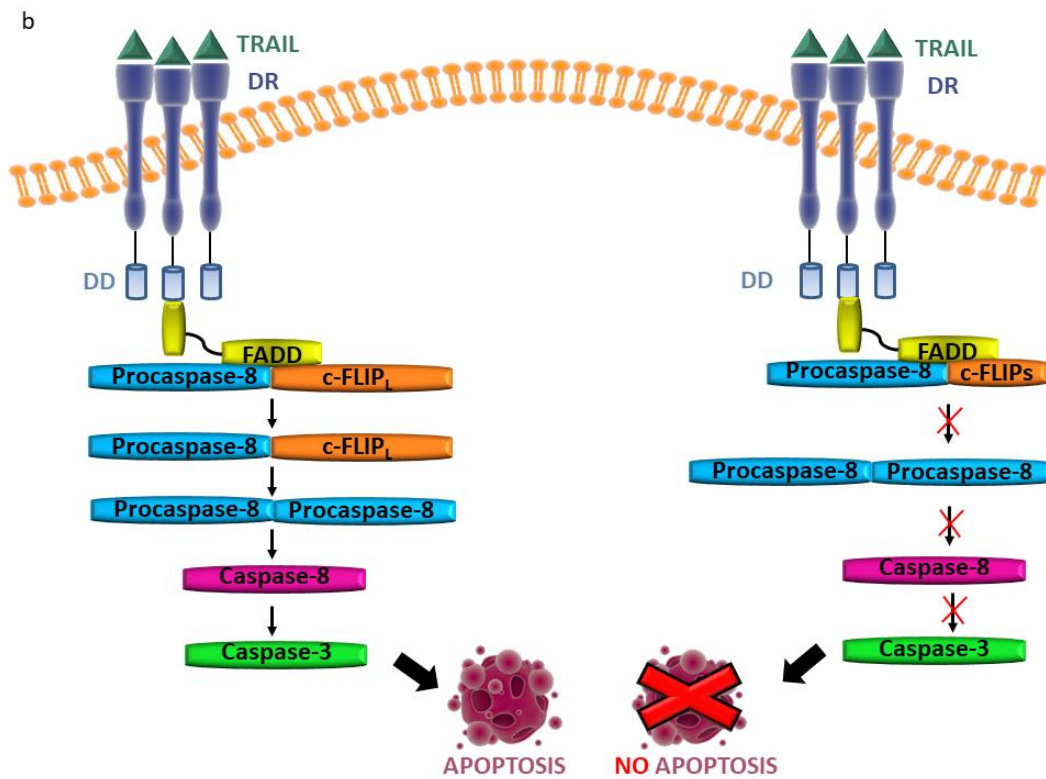


Fig 1.3.3.3b: Two-step Model.

A different mechanism of action is proposed in the co-operative and hierarchical model. According to this model, the amount of c-FLIP that directly binds FADD is limited, whereas the main form of c-FLIP recruitment to the DISC occurs via interaction with procaspase-8. At physiological levels, c-FLIP_L interacts with procaspase-8, forming FLIP_L/procaspase-8 heterodimers, which induce activation of caspase-8. Procaspase-8 preferentially binds c-FLIP molecules, however, when the levels of c-FLIP_L decrease, additional procaspases-8 are recruited to form homodimers that, after proteolytic cleavage, activate caspase-8. Contrarily, c-FLIP_S does not induce DED-mediated procaspase-8 oligomerization, therefore, when recruited, c-FLIP_S forms heterodimers with procaspase-8 which are catalytically inactive. ⁽¹¹⁵⁾

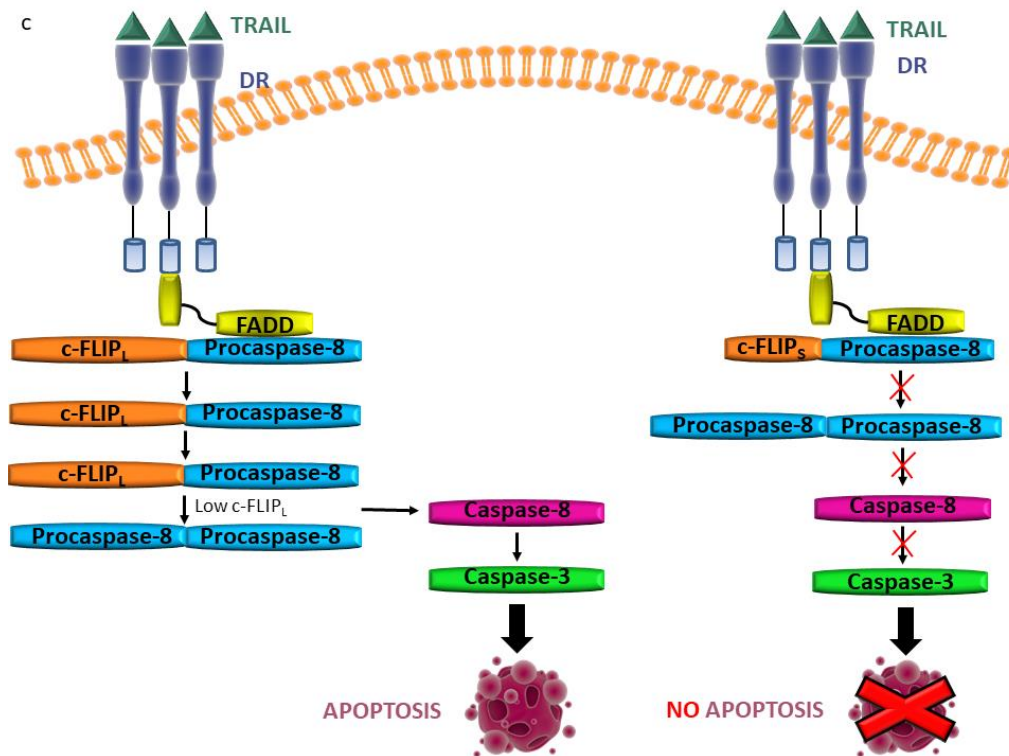


Fig 1.3.3.3c: Co-operative and hierarchical Model.

1.3.4 c-FLIP in cancer

The ability of c-FLIP to inhibit the extrinsic apoptotic pathway might play an important role in cancer cells TRAIL resistance. Multiple cancer cell lines, resistant to TRAIL-induced apoptosis, show elevated levels of c-FLIP. Gastric carcinoma, melanoma, cervical carcinoma, ovarian carcinoma, colorectal carcinoma, Hodgkin's lymphoma, prostate carcinoma, pancreatic carcinoma are all examples of tumours where c-FLIP is overexpressed.⁽¹⁰⁴⁾ In breast cancer, the association between c-FLIP and TRAIL resistance has been demonstrated by a siRNA study, where inhibition of c-FLIP expression using siRNA in different breast cancer cells, sensitise these cells to TRAIL treatment.⁽¹¹⁹⁾

1.3.5 c-FLIP as a therapeutic target: current inhibitors

Considering its ability to prevent apoptosis leading to the survival of breast cancer cells, c-FLIP-inhibition is now recognised as a valid and promising therapeutic target.⁽¹²⁰⁾ Initially, the first attempts to modulate the expression of c-FLIP involved the use of siRNA or agents stimulating c-FLIP degradation.^(121, 122) Although these approaches have been efficient in sensitising breast cancer cells to TRAIL, the several off-target effects which may occur, and the lack of carriers for the delivery into the cells, preclude any possible *in vivo* action.⁽¹²²⁾ A broad class of compounds able to reduce the expression of c-FLIP is represented by histone deacetylase inhibitors (HDACi). SAHA (Suberoyl anilide hydroxamic acid) and CMH (4-(4-chloro-2-methylphenoxy)-N-hydroxybutanamide) are

examples of this class. ^(123, 122) These agents induce an increased response of cancer cells to TRAIL because of their ability to downregulate c-FLIP at the transcriptional level. ⁽¹²²⁾ However, CMH for instance, is active at 100 μM , and at the same concentration it causes the degradation of poly(ADP-ribose) polymerase (PARP), which is an off-target effect. ⁽¹²²⁾ Additional agents which interfere with c-FLIP levels are the Akt inhibitors. Among them, API-1 (pyrido[2,3-*d*]pyrimidine) for example, stimulates c-FLIP degradation. ⁽¹²⁴⁾ Celecoxib is a known COX-2 inhibitor which is also able to inhibit Akt, promoting c-FLIP degradation. ⁽¹²⁵⁾ However additional Akt inhibitors, such as API-2, are not associated with the ability to modulate c-FLIP levels, therefore it is likely that the way these agents work is non-specific for c-FLIP. ⁽¹²³⁾

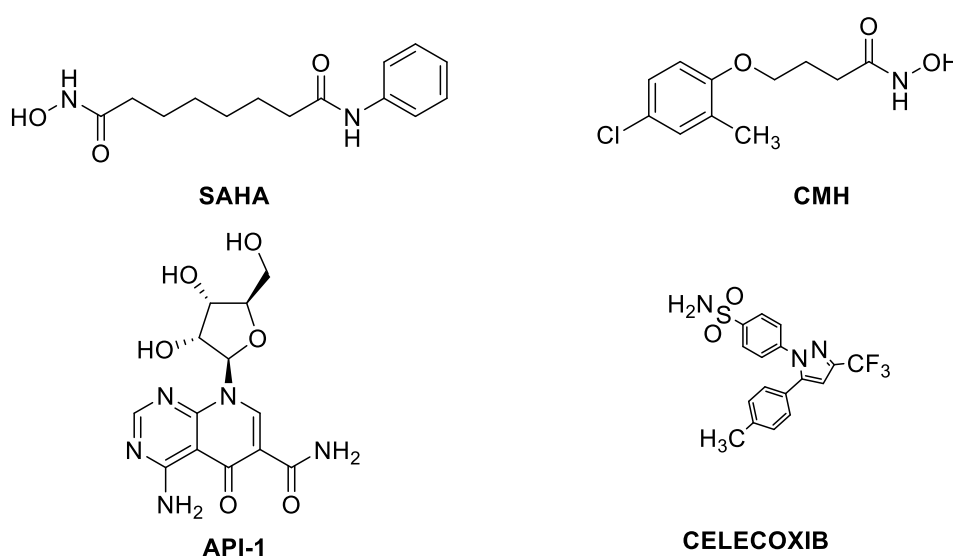


Fig 1.3.5 Chemical Structure of current c-FLIP inhibitors.

Therefore, several agents are recognised as effective at increasing TRAIL sensitivity through the modulation of c-FLIP expression, nevertheless none of these agents can be defined as a specific c-FLIP inhibitor. For this reason, novel small molecules able to inhibit specifically c-FLIP are needed. ⁽¹⁰¹⁾

1.4 Previous Molecular Modelling Studies

Computational techniques represent an important tool in the drug discovery process. ⁽¹²⁶⁾ In general, computer-aided drug design methodologies are based on two different approaches: the ligand-based drug design and the structure-based drug design. ⁽¹²⁷⁾ Structure-based drug design techniques (SBDD) can be used when the three-dimensional structure of the biological target has been experimentally determined, or a model based on the crystal structure of homologous proteins can be built using homology modelling techniques. ⁽¹²⁷⁾ In order to identify compounds that can bind

into the binding site of the protein, virtual screenings of libraries of compounds, followed by molecular docking analyses, are usually performed. ⁽¹²⁸⁾ The ligand-based drug design (LBDD) approach can be adopted when the structure of the biological target is not available, and the structure of known active compounds can be used to perform ligand-based virtual screening studies. ⁽¹²⁹⁾

In the course of a previous study performed in our research group by Dr Olivia Hayward, following a structure-based drug design approach, molecular modelling techniques were used in order to analyse the interactions occurring between the DED domains of FADD, c-FLIP and caspase-8. The final purpose was to identify the features responsible for the interaction FADD:c-FLIP and FADD:caspase-8 in order to develop novel small molecule inhibitors able to target c-FLIP selectively. ⁽¹³⁰⁾

1.4.1 c-FLIP and Caspase-8 homology models

At the beginning of the study, the crystal structures for c-FLIP and caspase-8 were not available. A homologous protein had been identified in MC159 (PDB ID: 2BBR), a viral form of c-FLIP, which has been used in different studies in order to model DED interactions. ^(115, 118) This protein showed a sequence identity of 33% and 29% with c-FLIP and caspase-8, respectively. Considering also the highly conserved nature of the DEDs regions, the MC159 crystal structure was chosen as template to build the homology models of the DED structures of c-FLIP and caspase-8. ^(118, 130) The two models are shown in figure 1.4.1.1 A and B.

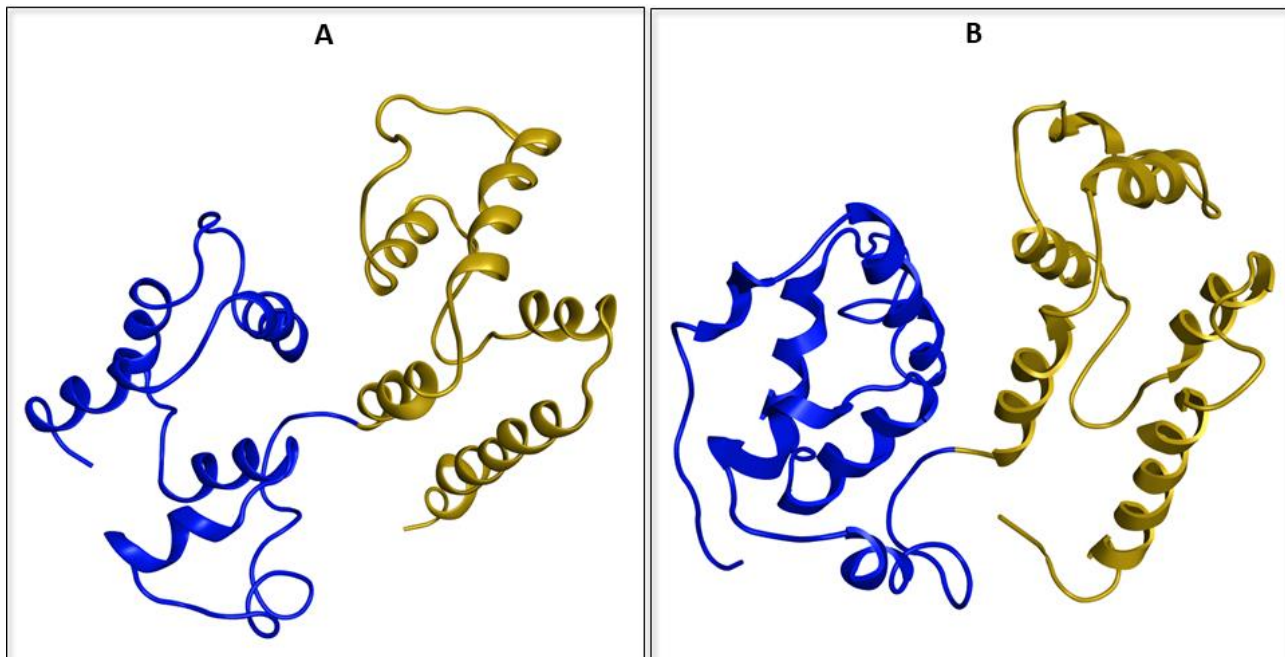


Fig 1.4.1.: Homology Models of c-FLIP (A) and caspase-8 (B). In both proteins DED1 is in blue and DED2 is in yellow.

The interactions between the DEDs of FADD and c-FLIP/caspase-8 were then modelled. A previous study had demonstrated the importance of a particular motif, the FL motif (Phe25/Leu26), in FADD/Caspase-8 binding.⁽¹³⁰⁾ Mutations in this motif generate a relevant reduction of caspase-8 activation due to the decreased caspase-8 recruitment to the DISC. Furthermore, it has been shown that the FL motif causes an intramolecular interaction between DED1 and DED2 in all the proteins that exhibit the two domains. Specifically, the FL motif situated on DED1 interacts with the hydrophobic surface of DED2. This interaction does not occur in FADD because of the presence of only one DED, therefore the FL motif of FADD is available to interact with DEDs of c-FLIP and caspase-8.⁽¹³¹⁾ On the basis of this known intramolecular interaction between DED1 and DED2, the intermolecular interactions between the DED of FADD and the hydrophobic pockets located on the DED1 of c-FLIP and caspase-8 were modelled.⁽¹³⁰⁾

1.4.2 c-FLIP:FADD interaction

According to the c-FLIP-FADD model generated in the previous study, the Phe25 of FADD, which is deemed to have a crucial role for the recruitment of c-FLIP and procaspase-8, fits a small hydrophobic pocket on the DED1 of c-FLIP, as shown in figure 1.4.2.⁽¹³⁰⁾

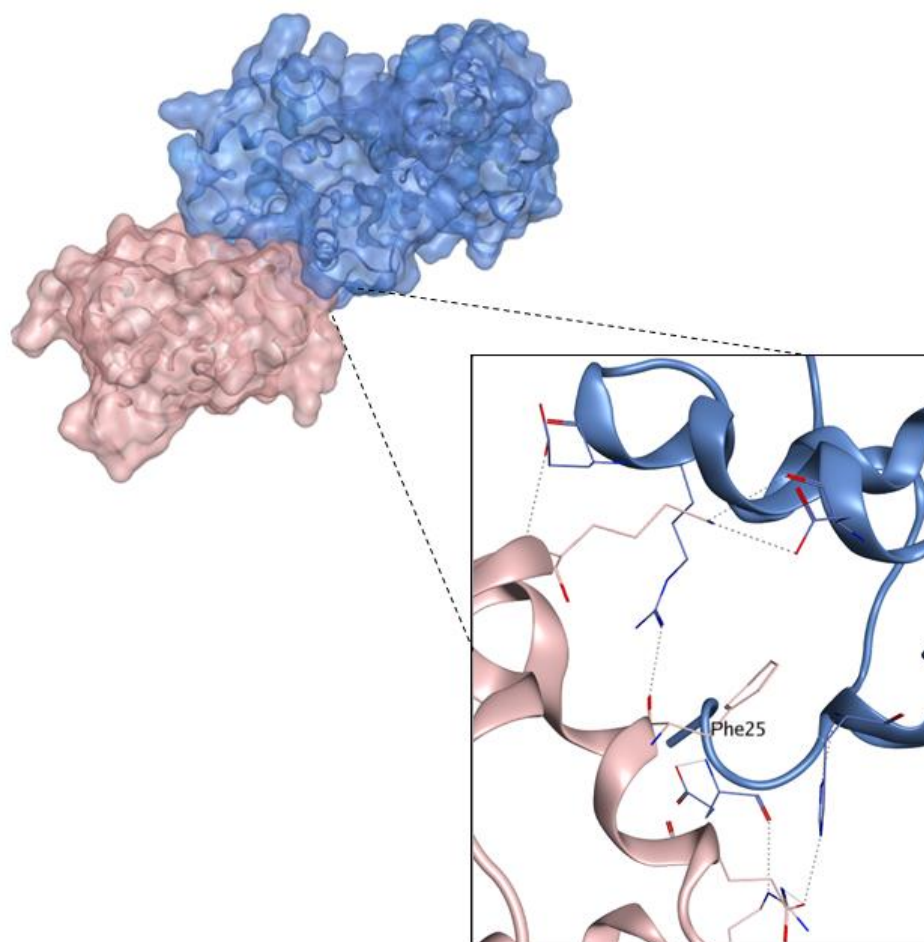


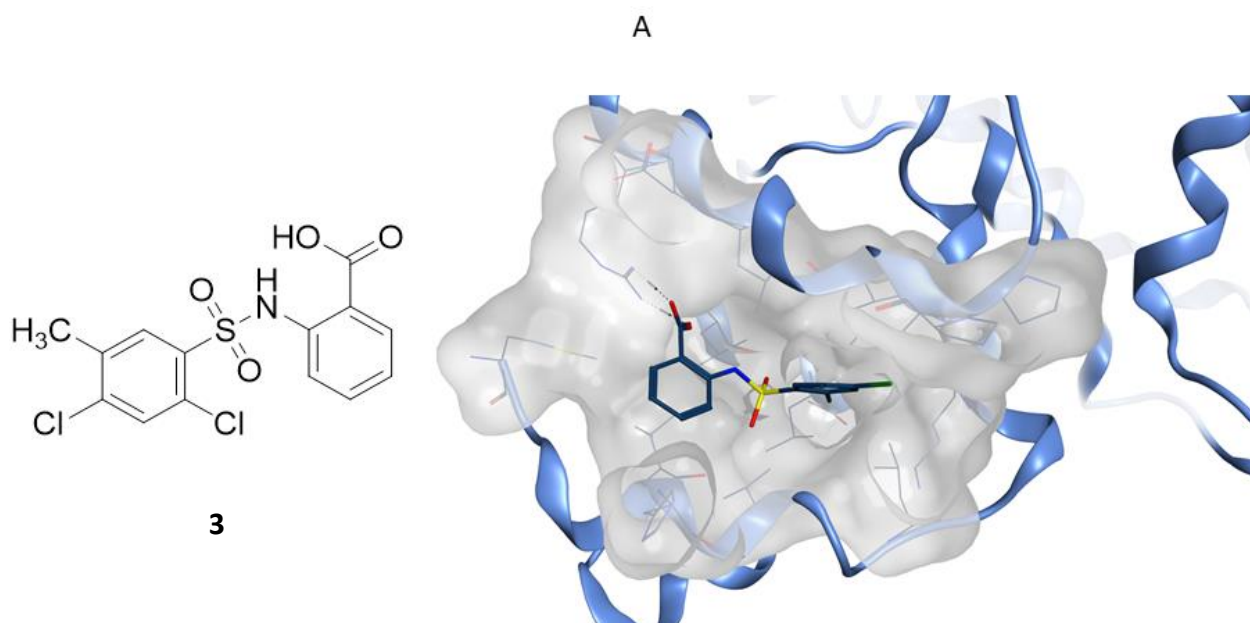
Fig 1.4.2: Model of the interactions occurring between FADD (pink) and c-FLIP (blue).

1.4.3 Pharmacophore generation and Virtual Screening

The interacting c-FLIP pocket was used to generate a pharmacophore model in order to identify features which may be used as targets for possible inhibitors. Once the pharmacophore was developed, it was used to run a structure-based virtual screening, starting from a database of 350,000 known compounds (Specs Database, Delft).⁽¹³²⁾ Among them, 14,000 compounds satisfied the pharmacophore query, and they were docked in the pocket of c-FLIP. Following scoring and rescoring steps, 2,000 compounds were selected. An additional selection step was performed by docking the 2,000 compounds in the pocket of caspase-8. The final aim was to select those compounds potentially able to bind c-FLIP selectively, with a poor predicted ability to fit the pocket of caspase-8. Therefore, according to the docking scores obtained, 100 common compounds with the highest and lowest score for c-FLIP and caspase-8 respectively, were selected and visually inspected. After visual inspection, 19 compounds were selected for testing.⁽¹³⁰⁾

1.5 *In vitro* assays and lead compound identification

All the 19 selected compounds were tested in different *in vitro* assays. ⁽¹³⁰⁾ Two TRAIL-resistant breast cancer cell lines were used to assess the compounds: MCF-7 (ER+) and BT474 (ER+). ⁽¹¹⁹⁾ The Cell Viability Assay was used as first screening. This assay allowed the selection of those compounds that did not affect cell viability when administered alone, demonstrating lack of toxicity, whilst inducing a significant reduction in cell viability when associated with TRAIL, showing ability in sensitising the TRAIL-resistant cancer cells to TRAIL-induced cell death. From this assay, the three best compounds were selected and evaluated in two additional *in vitro* assays: the Mammosphere Assay ⁽⁷²⁾ and Colony Forming Assay. ⁽⁷³⁾ Both these tests are specific for cancer stem cells, therefore they were used to investigate the ability of the selected compounds to induce TRAIL-sensitisation in breast cancer stem cells. In both cell lines and in both assays, one compound in particular, compound **3**, gave the best results. This compound reduced the ability of cancer cells to form mammospheres or colonies when administered in association with TRAIL at low micromolar concentrations, indicating that the increased TRAIL-sensitisation observed in the cell viability assay concerns also breast cancer stem cells. The chemical structure of **3**, its predicted binding mode in the pocket of c-FLIP as well as some of the results obtained in this part of the study are shown in Fig 1.5 A and B. ⁽¹³⁰⁾



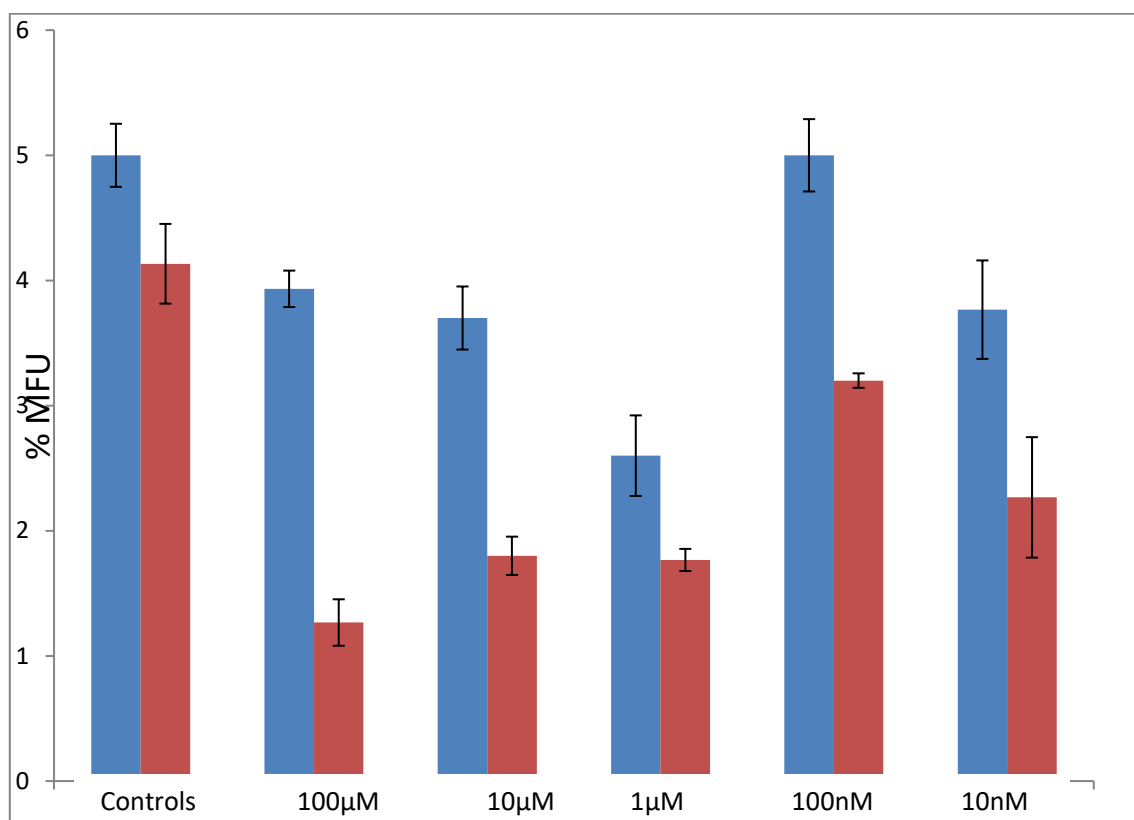


Fig 1.5 A: Chemical structure of **3** and its predicted binding mode in the pocket of c-FLIP. B: Mammosphere Assay in BT474 cells. Blue bars represent compound **3** tested alone, red bars represent compound **3** in association with TRAIL. Different molarities were used. At 100 μM concentration, compound **3** showed the best activity in reducing the number of mammospheres formed, measured as mammosphere forming units (MFU).⁽¹³⁰⁾

1.6 Evaluation of purchased analogues of **3**

The identification of the hit compound **3** was followed by biological evaluation of additional eight analogues of **3**, which were purchased from SPECS. Table 1.6.1 illustrates the chemical structures of these compounds.

3.1	
3.2	
3.3	

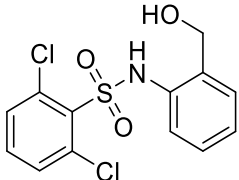
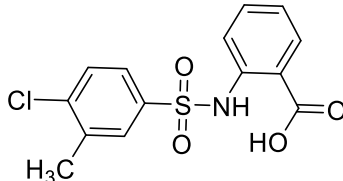
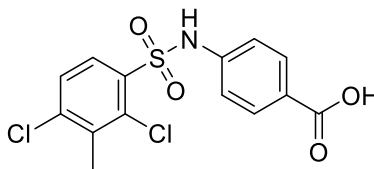
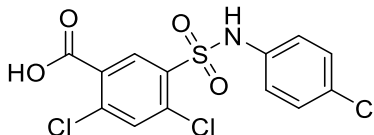
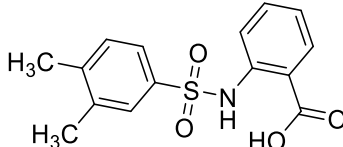
3.4	
3.5	
3.6	
3.7	
3.8	

Table 1.6.1: Analogues of **3** tested.

Analogues **3.1** and **3.7** show a different position of the carboxylic acid which is placed on the ring substituted with hydrophobic groups, while in **3.4** the carboxylic function is replaced by the alcohol group. In all other analogues the hydrophobic ring is modified with different hydrophobic groups at different positions. The Colony Forming Assay and Mammosphere Assay on MCF-7 and BT474 cells were performed in order to assess whether these compounds showed an improved efficacy compared to the original hit. The molecules were tested at 100 μ M concentration. In both assays and cell lines, the analogues showed a decreased ability to reduce the number of colonies and mammospheres formed compared to **3**.⁽¹³⁰⁾

1.7 Mechanism of action of **3**

Several experiments have been performed in the previous work in order to investigate the mechanism of action of **3**, with the final aim to confirm its role as selective c-FLIP inhibitor.⁽¹³⁰⁾ In order to assess the ability of **3** to induce TRAIL sensitisation via the caspase-8 mediated extrinsic apoptotic pathway, the caspase-glo 8 luminescence assay, which measures caspase-8 activity, was performed.⁽¹³³⁾ The results obtained showed a significant increased caspase-8 activity when MCF-7 cells were treated with the combination **3**-TRAIL, whilst **3** alone did not induce any relevant changes in caspase-8 activity. Furthermore, the FRET (Fluorescence Resonance Energy Transfer) assay, a

specific method used to evaluate protein-protein interactions, was performed. This assay is based on the possibility to detect the energy transfer occurring between two interacting proteins, via fluorophore-labelling these proteins and measuring the changes in fluorescence emission which are observable when the two proteins interact. ⁽¹³⁴⁾ Preliminary data obtained from this experiment gave promising results: while c-FLIP:FADD interaction was detected in cells treated with TRAIL only, in cells treated with the combination TRAIL-**3** no interaction between the two proteins was observed, suggesting the ability of **3** to disrupt c-FLIP:FADD interaction. ⁽¹³⁰⁾ Similar early results were obtained in the co-immunoprecipitation assay (Co-IP), which is currently being performed by Dr Richard Clarkson's research group (European Cancer Stem Cells Research Institute, Hadyr Ellis Building, Cardiff University). The Co-IP technique is based on the precipitation of complexes formed by two interacting proteins via using specific antibody and antibody-binding proteins attached to a beaded support. ⁽¹³⁵⁾ In accordance with the FRET results, the early data obtained from the Co-IP assay suggested the ability of **3** to promote the interaction between FADD and caspase-8. Therefore, all these data together confirmed that **3** is able to induce TRAIL sensitisation via the specific TRAIL-caspase-8-mediated apoptotic pathway. Moreover, the preliminary observation that in presence of **3**, the c-FLIP:FADD interaction is disrupted, while the interaction between FADD and caspase-8 is promoted, is very promising in order to confirm the potential role of **3** as selective c-FLIP inhibitor. Additionally, a concomitant study performed in Dr Richard Clarkson's research group, exploring the effect of a combined **3**-paclitaxel therapy, had demonstrated that **3** is able to induce paclitaxel sensitisation in resistant cancer stem cells. These preliminary *in vitro* results were confirmed by *in vivo* studies that showed the ability of **3** to reduce tumour size, when associated with paclitaxel, and, more importantly, to prevent tumour recurrence. ⁽¹³⁶⁾

1.7 Project aims

Although c-FLIP is recognised as an interesting target in breast cancer therapy, currently all therapeutic strategies available aim to reduce the protein expression, acting as c-FLIP transcription inhibitors or increasing c-FLIP degradation. The primary inhibition of c-FLIP using small molecules has not been explored before because of the high similarity with caspase-8. Effectively, a non-selective inhibitor may likely also inhibit caspase-8 preventing apoptosis. However, previous studies performed in our research group have demonstrated that, with the support of computational modelling techniques, the identification of novel small molecules that selectively inhibit c-FLIP may be an achievable result. Therefore, the purpose of this project will be the design and development of analogues of **3**. The synthesis of new compounds will aim to improve the chemical and physical properties of the original hit in order to enhance its ability to cross the cellular membrane. Furthermore, all variations made on the original scaffold will be used to investigate the structure-activity relationships. Molecular docking techniques will be used to visualise the predicted binding mode of the compounds in the pocket of c-FLIP in order to estimate the activity potential and the selectivity of the future analogues. New synthetic pathways will be designed and optimised. The synthesised molecules will then be tested in specific *in vitro* assays to evaluate their ability to sensitise breast cancer cells and breast cancer stem cells to TRAIL-induced apoptosis and in addition the lack of toxicity in non-cancerous cells.

1.8 References

- 1: Cancer Research UK. <http://www.cancerresearchuk.org> (accessed October 05, 2017).
- 2: Ferlay, J.; Soerjomataram, I.; Ervik, M.; Dikshit, R.; Eser, S.; Mathers, C.; Rebelo, M.; Parkin, D. M.; Forman, D.; Bray, F. Cancer incidence and mortality worldwide: sources, methods and major patterns in GLOBOCAN 2012. *Int. J. Cancer*. **2015**, *136*, 359-386.
- 3: Office for National Statistic, June 2016. <http://www.ons.gov.uk> (accessed October 05, 2017).
- 4: Yue, W.; Yager, J. D.; Wang, J. P.; Jupe, E. R.; Santen, R. J. Estrogen receptor-dependent and independent mechanisms of breast cancer carcinogenesis. *Steroids*. **2013**, *78*, 161-170.
- 5: Dall, G. V.; Britt, K. L. Estrogen effects on the mammary gland in early and late life and breast cancer risk. *Front. Oncol*. **2017**, *17*, 110-115.
- 6: McGuire, A.; Brown, J. A. L.; Malone, C.; McLaughlin, R.; Kerin, M. J. Effects of age on the detection and management of breast cancer. *Cancers*. **2015**, *7*, 908-929.
- 7: Shiovitz, S.; Korde, L. A. Genetics of breast cancer: a topic in evolution. *Ann. Oncol*. **2015**, *26*, 1291-1299.
- 8: Hedenfalk, I.; Duggan, D.; Chen, Y.; Radmacher, M.; Bittner, M.; Simon, R.; Meltzer, P.; Gusterson, B.; Esteller, M.; Raffeld, M.; Yakhini, Z.; Ben-Dor, A.; Dougherty, E.; Kononen, J.; Bubendorf, L.; Fehrl, W.; Pittaluga, S.; Gruvberger, S.; Loman, N.; Johannsson, O.; Olsson, H.; Wilfond, B.; Sauter, G.; Kallioniemi, O.P.; Borg, A.; Trent, J. Gene-expression profiles in hereditary breast cancer. *N. Engl. J. Med*. **2001**, *344*, 539-548.
- 8: King, M.C.; Marks, J.H.; Mandell, J.B. Breast and ovarian cancer risks due to inherited mutations in BRCA1 and BRCA2. *Science*. **2003**, *302*, 643-646.
- 9: Kuchenbaecker, K. B.; Hopper, J. L.; Barnes, D. R.; Phillips, K. A.; Mooij, T. M.; Roos-Blom, M. J.; Jervis, S.; Van Leeuwen, F. E.; Milne, R. L.; Andrieu, N.; Goldgar, D. E.; Terry, M. E.; Rookus, M. A.; Easton, D. F.; Antoniou, A. C. Risks of breast, ovarian, and contralateral breast cancer for BRCA1 and BRCA2 mutation carriers. *J.A.M.A*. **2017**, *317*, 2402-2416.
- 10: Walerych, D.; Napoli, M.; Collavin, L.; Del Sal, G. The rebel angel: mutant p53 as the driving oncogene in breast cancer. *Carcinogenesis*. **2012**, *33*, 2007-2017.

- 11:** Saal, L. C.; Gruvberger-Saal, S. K.; Persson, C.; Lövgren, K.; Jumppanen, M.; Staaf, J.; Jönsson, G.; Pires, M. M.; Maurer, M.; Holm, K.; Koujak, S.; Subramaniam, S.; Vallon-Christersson, J.; Olsson, H.; Su, T.; Memeo, L.; Ludwig, T.; Ethier, S. P.; Krogh, M.; Szabolcs, M.; Murty, V. V. V. S.; Isola, J.; Hibshoosh, H.; Parsons, R.; Borg, A. Recurrent gross mutations of the *PTEN* tumor suppressor gene in breast cancers with deficient DSB repair. *Nat. Genet.* **2008**, *40*, 102-107.
- 12:** Lahmann, P. H.; Hoffmann, K.; Allen, N.; Van Gils, C. H.; Khaw, K. T.; Tehard, B.; Berrino, F.; Tjønneland, A.; Bigaard, J.; Olsen, A.; Overvad, K.; Clavel-Chapelon, F.; Nagel, G.; Boeing, H.; Trichopoulos, D.; Economou, G.; Bellos, G.; Palli, D.; Tumino, R.; Panico, S.; Sacerdote, C.; Krogh, V.; Peeters, P. H.; Bueno-de-Mesquita, H. B.; Lund, E.; Ardanaz, E.; Amiano, P.; Pera, G.; Quirós, J. R.; Martínez, C.; Tormo, M. J.; Wirfält, E.; Berglund, G.; Hallmans, G.; Key, T. J.; Reeves, G.; Bingham, S.; Norat, T.; Biessy, C.; Kaaks, R.; Riboli, E. Body size and breast cancer risk: findings from the European Prospective Investigation Into Cancer and Nutrition (EPIC). *Int. J. Cancer.* **2004**, *111*, 762-771.
- 13:** Hulka, B. S.; Moorman, P. G. Breast cancer: hormones and other risk factors. *Maturitas.* **2001**, *38*, 103-113.
- 13:** Cancer Research UK. <http://www.cancerresearchuk.org> (accessed October 15, 2017).
- 14:** Canadian Breast Cancer Foundation. <http://www.cbcbf.org> (accessed October 15, 2017).
- 15:** Weier, R. C.; Reisinger, S. A.; Paskett, E. D. Breast Cancer Screening. In *Psycho-Oncology*, 3rd ed.; Holland, J. C., BreitBart, S. W., Butow, P. N., Jacobsen, P. B., Loscalzo, M. G., Mccorkle, R, Eds.; Oxford University Press: New York, 2015; pp 58-60.
- 16:** Smith, R. A.; Duffy, S. W.; Tabar, L. Breast cancer screening. *Oncology.* **2012**, *26*, 471-475, 479-481, 485-486.
- 17:** Warner, E.; Plewes, D. B.; Hill, K. A.; Causer, P. A.; Zubovits, J. T.; Jong, R. A.; Cutrara, M. R.; DeBoer, G.; Yaffe, M. J.; Messner, S. J.; Meschino, W. J.; Piron, C. A.; Narod, S. A. Surveillance of BRCA1 and BRCA2 mutation carriers with magnetic resonance imaging, ultrasound, mammography, and clinical breast examination. *J.A.M.A.* **2004**, *292*, 1317-1325.
- 18:** Kriege, M.; Brekelmans, C. T.; Boetes, C.; Besnard, P. E.; Zonderland, H. M.; Obdeijn, I. M.; Manoliu, R. A.; Kok, T.; Peterse, H.; Tilanus-Linthorst, M. M.; Muller, S. H.; Meijer, S.; Oosterwijk, J. C.; Beex, L. V.; Tollenaar, R. A.; de Koning, H. J. Efficacy of MRI and mammography for breast-cancer screening in women with a familial or genetic predisposition. *N. Engl. J. Med.* **2004**, *351*, 427-437.

- 19:** Nelson, H. D.; Tyne, K.; Naik, A.; Bougatsos, C.; Chan, B. K.; Humphrey, L. Screening for breast cancer. *Ann. Intern. Med.* **2009**, *151*, 727-737.
- 20:** Malhotra, G. K.; Zhao, X.; Band, H.; Band, V. Histological, molecular and functional subtypes of breast cancers. *Cancer Biol. Ther.* **2010**, *10*, 955-960.
- 21:** Rakha, E. A.; Reis-Filho, J. S.; Baehner, F.; Dabbs, D. J.; Decker, T.; Eusebi, V.; Fox, S. B.; Ichihara, S. U.; Jacquemier, J.; Lakhani, S. R.; Palacios, J.; Richardson, A. L.; Schnitt, F. J.; Schmitt, F. C.; Tan, P. H.; Tse, G. M.; Badve, S.; O Ellis, I. Breast cancer prognostic classification in the molecular era: the role of histological grade. *Breast Cancer Res.* **2010**, *12*, 207-227.
- 22:** Althuis, M. D.; Fergenbaum, J. H.; Garcia-Closas, M.; Brinton, L. A.; Madigan, M. P.; Sherman, M. E. Etiology of hormone receptor-defined breast cancer: a systematic review of the literature. *Cancer Epidemiol. Biomarkers.* **2004**, *13*, 1558-1568.
- 23:** Buzdar, A.U. Role of biologic therapy and chemotherapy in hormone receptor and HER₂-positive breast cancer. *Ann. Oncol.* **2009**, *20*, 993-999.
- 24:** Piccart-Gebhart, M. J.; Procter, M.; Leyland-Jones, B.; Goldhirsch, A.; Untch, M.; Smith, I.; Gianni, L.; Baselga, J.; Bell, R.; Jackisch, C.; Cameron, D.; Dowsett, M.; Barrios, C. H.; Steger, G.; Huang, C.; Andersson, M.; Inbar, M.; Lichinitser, M.; Láng, I.; Nitz, U.; Iwata, H.; Thomssen, C.; Lohrisch, C.; Suter, T. M.; Rüschoff, J.; Sütő, T.; Greatorex, V.; Ward, C.; Straehle, C.; McFadden, E.; Dolci, M. S.; Gelber, R. D. Trastuzumab after adjuvant chemotherapy in HER2-positive breast cancer. *N. Engl. J. Med.* **2005**, *353*, 1659-1672.
- 25:** Perou, C. M.; Sørlie, T.; Eisen, M. B.; Van de Rijn, M.; Jeffrey, S. S.; Rees, C. A.; Pollack, J. R.; Ross, D. T.; Johnsen, H.; Akslen, L. A.; Fluge, O.; Pergamenschikov, A.; Williams, C.; Zhu, S. X.; Lønning, P. E.; Børresen-Dale, A. L.; Brown, P. O.; Botstein, D. Molecular portraits of human breast tumours. *Nature.* **2000**, *406*, 747- 752.
- 26:** Eliyatkin, N.; Yalçın, E.; Zengel, B.; Aktaş, S.; Vardar, E. Molecular classification of breast carcinoma: from traditional, old-fashioned way to a new age, and a new way. *J. Breast. Health.* **2015**, *11*, 59-66.
- 27:** Schnitt, S. J.; Classification and prognosis of invasive breast cancer: from morphology to molecular taxonomy. *Modern Pathol.* **2010**, *23*, 60-64.
- 28:** NHS Choice. <https://www.nhs.uk>. (accessed October 19, 2017).

- 29:** Marmot, M. G.; Altman, D. G.; Cameron, D. A.; Dewar, J. A.; Thompson, S. G.; Wilcox, M. The benefits and harms of breast cancer screening: an independent review. *Lancet*. **2012**, *380*, 1778-1786.
- 30:** Elmore, J. G.; Armstrong, K.; Lehman, C. D.; Fletcher, S.W. Screening for breast cancer. *J.A.M.A.* **2005**, *293*, 1245-1256.
- 31:** Senkus, E.; Kyriakides, S.; Ohno, S.; Penault-Llorca, F.; Poortmans, P.; Rutgers, E.; Zackrisson, S.; Cardoso, F. Primary breast cancer: ESMO Clinical Practice Guidelines for diagnosis, treatment and follow-up. *Annal. Oncol.* **2015**, *26*, 8-30.
- 32:** Association of Breast Surgery at BASO 2009. *E.J.S.O.* **2009**, *35*, 1-22.
- 33:** Cuzick, J. Radiotherapy for Breast Cancer. *J. Natl. Cancer Inst.* **2005**, *97*, 406-407.
- 34:** Buchholz, T. A. Radiotherapy and survival in breast cancer. *Lancet*. **2011**, *378*, 1680-1682.
- 35:** Deroo, B. J.; Korach, K. S. Estrogen receptors and human disease. *J. Clin. Invest.* **2006**, *116*, 561-570.
- 36:** Lewis, J. S.; Jordan, V. C. Selective estrogen receptor modulators (SERMs): Mechanisms of anticarcinogenesis and drug resistance. *Mutat. Res.* **2005**, *591*, 247-263.
- 37:** Early Breast Cancer Trialists' Collaborative Group (EBCTCG). Relevance of breast cancer hormone receptors and other factors to the efficacy of adjuvant tamoxifen: patient-level meta-analysis of randomised trials. *Lancet*. **2011**, *378*, 771-784.
- 38:** Davies, C.; Pan, H.; Godwin, J.; Arriagada, R.; Raina, V.; Abraham, M.; Alencar, V. H. M.; Badran, A.; Bonfill, X.; Bradbury, J.; Clarke, M.; Collins, R.; Davis, S. R.; Delmestri, A.; Forbes, J.; Haddad, P.; Hou, M. F.; Peto, R. Long-term effects of continuing adjuvant tamoxifen to 10 years versus stopping at 5 years after diagnosis of oestrogen receptor-positive breast cancer: ATLAS, a randomised trial. *Lancet*. **2013**, *381*, 805-816.
- 39:** Winer, E. P.; Hudis, C.; Burstein, H. J.; Wolff, A. C.; Pritchard, K. I.; Ingle, J. N.; Chlebowski, R. T.; Gelber, R.; Edge, S. B.; Gralow, J.; Cobleigh, M. A.; Mamounas, E. P.; Goldstein, L. J.; Whelan, T. J.; Powles, T. J.; Bryant, J.; Perkins, C.; Perotti, J.; Braun, S.; Langer, A. S.; Browman, G. P.; Somerfield, M. R. American society of clinical oncology technology assessment on the use of aromatase inhibitors as adjuvant therapy for postmenopausal women with hormone receptor-positive breast cancer: status report 2004. *J. Clin. Oncol.* **2005**, *3*, 619-629.

- 40:** Brueggemeier, R. W.; Hackett, J. C.; Diaz-Cruz, E. S. Aromatase inhibitors in the treatment of breast cancer. *Endocrine Society*. **2013**, *26*, 307.
- 41:** Burstein, H. J.; Prestrud, A. A.; Seidenfeld, J.; Anderson, H.; Buchholz, T. A.; Davidson, N. E.; Gelmon, K. E.; Giordano, S. H.; Hudis, C. A.; Malin, J.; Mamounas, E. P.; Rowden, D.; Solky, A. J.; Sowers, M. R.; Stearns, V.; Winer, E. P.; Somerfield, M. R.; Griggs, J. J. American society of clinical oncology clinical practice guideline: update on adjuvant endocrine therapy for women with hormone receptor–positive breast cancer. *J. Clin. Oncol.* **2010**, *23*, 3784-3796.
- 42:** Spector, N. L.; Blackwell, K. L. Understanding the mechanisms behind trastuzumab therapy for human epidermal growth factor receptor 2–positive breast cancer. *J. Clin. Oncol.* **2009**, *34*, 5838-5847.
- 43:** Malenfant, S. J.; Eckmann, K. R. Pertuzumab: A new targeted therapy for HER2-positive metastatic breast cancer. *Pharmacotherapy*. **2013**, *34*, 60-71.
- 44:** Bedard, P. L.; de Azambuja, E.; Cardoso, F. Beyond trastuzumab: overcoming resistance to targeted HER-2 therapy in breast cancer. *Curr. Cancer Drug Tar.* **2009**, *9*, 148-162.
- 45:** Piccart, M. Circumventing de novo and acquired resistance to trastuzumab: new hope for the care of ErbB2-positive breast cancer. *Clin. Breast Cancer*. **2008**, *8*, 110-113.
- 46:** Perez, E. A.; Romond, E. H.; Suman, V. J.; Jeong, J.; Sledge, G.; Geyer, C. E.; Martino, S.; Rastogi, P.; Gralow, J.; Swain, S. M.; Winer, E. P.; Colon-Otero, G.; Davidson, N. E.; Mamounas, E.; Zujewski, J.; Wolmark, N. Trastuzumab plus adjuvant chemotherapy for human epidermal growth factor receptor 2–positive breast cancer: planned joint analysis of overall survival from NSABP B-31 and NCCTG N9831. *J. Clin. Oncol.* **2014**, *33*, 3744-3752.
- 47:** Mauri, D.; Pavlidis, N.; Ioannidis, J. P. A. Neoadjuvant versus adjuvant systemic treatment in breast cancer: a meta-analysis. *J. Natl. Cancer Inst.* **2005**, *97*, 188-194.
- 48:** Hassan, M. S. U.; Ansari, J.; Spooner, D.; Hussain, S. A. Chemotherapy for breast cancer (review). *Oncol. Rep.* **2010**, *24*, 1121-1131.
- 49:** Cardoso, F.; Costa, A.; Senkus, E.; Aapro, M.; André, F.; Barrios, C. H.; Bergh, J.; Bhattacharyya, G.; Biganzoli, L.; Cardoso, M. J.; Carey, L.; Corneliussen-James, D.; Curigliano, G.; Dieras, V.; El Saghir, N.; Eniu, A.; Fallowfield, L.; Fenech, D.; Francis, P.; Gelmon, K.; Gennari, A.; Harbeck, N.; Hudis, C.; Kaufman, B.; Krop, I.; Mayer, M.; Meijer, H.; Mertz, S.; Ohno, S.; Pagani, O.; Papadopoulos, E.;

Peccatori, F.; Penault-Llorca, F.; Piccart, M. J.; Pierga, J. Y.; Rugo, H.; Shockney, L.; Sledge, G.; Swain, S.; Thomssen, C.; Tutt, A.; Vorobiof, D.; Xu B.; Norton, L.; Winer, E. 3rd ESO–ESMO international consensus guidelines for Advanced Breast Cancer (ABC 3). *Annal. Oncol.* **2017**, *28*, 16-33.

50: Bianchini, G.; Balko, J. M.; Mayer, I. A.; Sanders, M. E.; Gianni, L. Triple-negative breast cancer: challenges and opportunities of a heterogeneous disease. *Nat. Rev. Clin. Oncol.* **2016**, *13*, 674-690.

51: Chari R. V. J. Targeted cancer therapy: conferring specificity to cytotoxic drugs. *Acc. Chem. Res.* **2008**, *41*, 98-107.

52: Carlotto, A.; Hogsett, V. L.; Maiorini, E. M.; Razulis, J. G.; Sonis, S. T. The economic burden of toxicities associated with cancer treatment: review of the literature and analysis of nausea and vomiting, diarrhoea, oral mucositis and fatigue. *Pharmacoeconomics.* **2013**, *31*, 753-766.

53: Shapiro, C. L.; Recht, A. Drug therapy: side effects of adjuvant treatment of breast cancer. *N. Eng. J. Med.* **2001**, *344*, 1997-2008.

54: Garreau, J. R.; DeLaMelena, T.; Walts, D. R. N.; Karamlou, K.; Johnson, N. Side effects of aromatase inhibitors versus tamoxifen: the patients' perspective. *Am. J. Surg.* **2006**, *192*, 496-498.

55: Ross, J. S.; Slodkowska, E. A.; Symmans, W. F.; Pusztai, L.; Ravdin, M. P.; Hortobagyi, G. N. Targeted Anti-Her-2 therapy and personalized medicine. *Oncologist.* **2009**, *14*, 320-368.

56: Schmitz, K. H.; Speck, R. M.; Rye, S. A.; DiSipio, T.; Hayes, S. C. Prevalence of breast cancer treatment sequelae over 6 years of follow-up. *Cancer.* **2012**, *118*, 2217-2225.

57: Galmarini, C. M.; Tredan, O.; Galmarini, C. F. Concomitant resistance and early-breast cancer: should we change treatment strategies?. *Cancer Metastasis Rev.* **2014**, *33*, 271-283.

58: Ahmad, A. Pathways to breast cancer recurrence. *ISRN Oncol.* **2013**, *2013*, 290568.

59: Musgrove, E. A.; Sutherland, R. L. Biological determinants of endocrine resistance in breast cancer. *Nat. Rev. Cancer.* **2009**, *9*, 631-643.

60: Martin, H. L.; Smith, L.; Tomlinson, D. C. Multidrug-resistant breast cancer: current perspectives. *Breast Cancer (Dove Med. Press.).* **2014**, *6*, 1-13.

61: Rivera, E.; Gomez, H. Chemotherapy resistance in metastatic breast cancer: the evolving role of ixabepilone. *Breast Cancer Res.* **2010**, *12*, S2.

- 62:** Marusyk, A.; PolyaK, K. Tumor heterogeneity: causes and consequences. *Biochim. Biophys. Acta.* **2010**, *1805*, 105-117.
- 63:** Lawrence, M. S.; Stojanov, P.; Polak, P.; Kryukov, G. V.; Cibulskis, K.; Sivachenko, A.; Carter, S. L.; Stewart, C.; Mermel, C. H.; Roberts, S. A.; Kiezun, A.; Hammerman, P. S.; McKenna, A.; Drier, Y.; Zou, L.; Ramos, A. H.; Pugh, T. J.; Stransky, N.; Helman, E.; Kim, J.; Sougnez, C.; Ambrogio, L.; Nickerson, E.; Shefler, E.; Cortès, M. L.; Auclair, D.; Staksena, G.; Voet, D.; Noble, M.; DiCara, D.; Lin, P.; Lichtenstein, L.; Heiman, D. I.; Fennel, T.; Imielinski, M.; Hernandez, B.; Hodis, E.; Baca, S.; Dulak, S.; Lohr, J.; Landau, D. A.; Wu, C. J.; Zajgla, J. M.; Hidalgo-Miranda, A.; Koren, A.; McCarroll, S. A.; Mora, J.; Lee, R. S.; Crompton, B.; Onofrio, R.; Parkin, M.; Winckler, W.; Ardlie, K.; Gabriel, S. B.; Roberts, C. W. M.; Biegel, J. A.; Stegmaier, K.; Bass, A. J.; Garraway, L. A.; Meyerson, M.; Golub, T. R.; Gordenin, D. A.; Sunyaev, S.; Lander, E.; Gets, G. Mutational heterogeneity in cancer and the search for new cancer-associated genes. *Nature.* **2013**, *499*, 214-218.
- 64:** Reya, T; Morrison, S. J.; Clarke, F. M.; Weissman, I. L. Stem cells, cancer, and cancer stem cells. *Nature.* **2001**, *414*, 105-111.
- 65:** Lawson, J.; Blatch, G.; Edkins, A. Cancer stem cells in breast cancer and metastasis. *Breast Cancer Res. Treat.* **2009**, *118*, 241-254.
- 66:** Wicha, M. S.; Liu, S.; Dontu, G. Cancer stem cells: an old idea-a paradigm shift. *Cancer Res.* **2006**, *66*, 1883-1890.
- 67:** Clarke, M. F.; Dick, J. E.; Dirks, P. B.; Eaves, C. J.; Jamieson, C. H. M.; Jones, D. L.; Visvader, J.; Weissman, I. L.; Wahl, G. M. Cancer stem cells-perspectives on current status and future directions: AACR workshop on cancer stem cells. *Cancer Res.* **2006**, *66*, 9339-9344.
- 68:** Al-Hajj, M.; Wicha, M. S.; Benito-Hernandez, A.; Morrison, S. J.; Clarke, M. F. Prospective identification of tumorigenic breast cancer cells. *Proc. Natl. Acad. Sci. USA.* **2003**, *100*, 3983-3988.
- 69:** Al-Ejeh, F.; Smart, C. E.; Morrison, B. J.; Chenevix-Trench, G.; Lopez, J. A.; Lakhani, R. S.; Brown, M. P.; Khanna, K. K. Breast cancer stem cells: treatment resistance and therapeutic opportunities. *Carcinogenesis.* **2011**, *32*, 650-658.
- 70:** Dean, M.; Fojo, T.; Bates, S. Tumour stem cells and drug resistance. *Nat. Rev. Cancer.* **2005**, *5*, 275-284.
- 71:** Han, L.; Shi, S.; Gonz, T.; Zhang, Z.; Sun, Z. Cancer stem cells: therapeutic implications and perspectives in cancer therapy. *Acta. Pharm. Sin. B.* **2013**, *3*, 65-75.

- 72:** Dontu, G.; Al-Hajj, M.; Abdallah, W. M.; Clarke, M. F.; Wicha, M. S. Stem cells in normal breast development and breast cancer. *Cell Prolif.* **2003**, *36*, 59-72.
- 73:** Franken, N. A.; Rodermond, H. M.; Stap, J.; Haveman, J.; Van Bree, C. Clonogenic assay of cells in vitro. *Nat. Protoc.* **2006**, *1*, 2315-2319.
- 74:** Dragu, D. L.; Necula, L. G.; Bleotu, C.; Diaconu, C. C.; Chivu-Economescu, M. Therapies targeting cancer stem cells: current trends and future challenges. *World J. Stem Cells.* **2015**, *7*, 1185-1201.
- 75:** Chiotaki, R.; Polioudaki, H.; Theodoropoulos, P. A. Cancer stem cells in solid and liquid tissue of breast cancer patients: characterization and therapeutic perspectives. *Curr. Cancer Drug Tar.* **2015**, *15*, 256-269.
- 76:** Zimmermann, K. C.; Green, R. D. How cells die: Apoptosis pathways. *J. Allergy Clin. Immun.* **2001**, *108*, 99-103.
- 77:** Elmore, S. Apoptosis: A review of programmed cell death. *Toxicol. Pathol.* **2007**, *35*, 495-516.
- 78:** Favalaro, B.; Allocati, N.; Graziano, V.; Di Ilio, C.; Di Ilio, V.; De Laurenzi, V. Role of Apoptosis in disease. *AGING.* **2012**, *4*, 330-349.
- 79:** Wang, S.; El-Deiry, S. W. TRAIL and apoptosis induction by TNF-family death receptors. *Nature.* **2003**, *22*, 8628-8633.
- 80:** Thorburn, A. Tumor Necrosis Factor-Related Apoptosis-Inducing Ligand (TRAIL) pathway signalling. *J. Thorac. Oncol.* **2007**, *2*, 461-465.
- 81:** Johnstone, R. W.; Frew, A. J.; Smyth, M. J. The TRAIL apoptotic pathway in cancer onset, progression and therapy. *Nat. Rev. Cancer.* **2008**, *8*, 782-798.
- 82:** Ashkenazi, A.; Salvesen, G. Regulated cell death: signalling and mechanism. *Annu. Rev. Cell. Dev. Biol.* **2014**, *30*, 337-356.
- 83:** Allen, J. E.; El-Deiry, W. S. Regulation of the human TRAIL gene. *Cancer Biol. Ther.* **2012**, *13*, 1143-1151.
- 84:** Zhang, Y.; Zhang, B. TRAIL resistance of breast cancer cells is associated with constitutive endocytosis of death receptors 4 and 5. *Mol. Cancer. Res.* **2008**, *6*, 1861-1871.
- 85:** LeBlanc, H. N.; Ashkenazi, A. Apo2L/TRAIL and its death and decoy receptors. *Cell Death Differ.* **2003**, *10*, 66-75.

- 86:** Mahalingam, D.; Szegezdi, E.; Keane, M.; De Jong, S.; Samali, A. TRAIL receptor signalling and modulation: are we on the right TRAIL?. *Cancer Treat. Rev.* **2009**, *35*, 280-288.
- 87:** Falschlehner, C.; Emmerich, C. H.; Gerlach, B.; Walczak, H. TRAIL signalling: decisions between life and death. *Int. J. Biochem.* **2007**, *39*, 1462-1475.
- 88:** MacFarlane, M. TRAIL-induced signalling and apoptosis. *Toxicol. Lett.* **2003**, *139*, 89-97.
- 89:** Ricci, M. S.; Kim, S. H.; Ogi, K.; Plastaras, G. P.; Ling, J.; Wang, W.; Jin, Z.; Dicker, D.; Chiao, P. J.; Flaherty, K. T.; Smit, D. C.; El-Deiry, W. S. Reduction of TRAIL-induced Mcl-1 and cIAP2 by c-Myc or sorafenib sensitizes resistant human cancer cells to TRAIL-induced death. *Cancer Cell.* **2007**, *12*, 66-80.
- 90:** Van Dijk, M.; Halpin-McCormick, A.; Sessler, T.; Samali, A.; Szegezdi, E. Resistance to TRAIL in non-transformed cells is due to multiple redundant pathways. *Cell Death Dis.* **2013**, *4*, e702.
- 91:** Koschny, R.; Walczak, H.; Ganten, T.M. The promise of TRAIL-potential and risk of a novel anticancer therapy. *J. Mol. Med.* **2007**, *85*, 923-935.
- 92:** Duiker, E. W.; Mom, C. H.; De Jong, S.; Willemse, P. H. B.; Gietema, J. A.; Van deer Zee, A. G. J.; De Vries, E. G. E. The clinical trail of TRAIL. *Eur. J. Cancer.* **2006**, *42*, 2233-2240.
- 93:** Lemke, J.; Von Karstedt, S.; Zinngrebe, J.; Walczak, H. Getting TRAIL back on track for cancer therapy. *Cell Death Differ.* **2014**, *21*, 1350-1364.
- 94:** Von Karstedt, S.; Montinaro, A.; Walczak, H. Exploring the TRAILs less travelled: TRAIL in cancer biology and therapy. *Nat. Rev. Cancer.* **2017**, *17*, 352-366.
- 95:** Tuthill, M. H.; Montinaro, A.; Zinngrebe, J.; Prieske, K.; Draber, P.; Prieske, S.; Newsom-Davis, T.; Von Karstedt, S.; Walczak, H. TRAIL-R2-specific antibodies and recombinant TRAIL can synergise to kill cancer cells. *Oncogene.* **2014**, *34*, 2138-2144.
- 96:** Rahman, M.; Pumphrey, J. G.; Lipkowitz, S. The TRAIL to targeted therapy of breast cancer. *Adv. Cancer Res.* **2009**, *103*, 43-73.
- 97:** Wang, F.; Lin, J.; Xu, R. The molecular mechanisms of TRAIL resistance in cancer cells: help in designing new drugs. *Curr. Pharm. Des.* **2014**, *20*, 6714-6722.
- 98:** Mahalingam, D.; Oldenhuis, C. N. A. M.; Szegezdi, E.; Giles, F. J.; De Vries, E. G. E.; De Jong, S.; Nawrocki, S. T. Targeting Trail Towards the Clinic. *Curr. Drug Targets.* **2011**, *12*, 2079-2090.

- 99:** Thome, M.; Schneider, P.; Hofmann, K.; Fickenscher, H.; Meinel, E.; Neipel, F.; Mattmann, C.; Burns, K.; Bodmer, J. L.; Schröter, M.; Scaffidi, C.; Krammer, P. H.; Peter, M. E.; Tschopp, J. Viral FLICE-inhibitory proteins (FLIPs) prevent apoptosis induced by death receptors. *Nature*. **1997**, *386*, 517-521.
- 100:** Irmeler, M.; Thome, M.; Hahne, M.; Schneider, P.; Hofmann, K.; Steiner, V.; Bodmer, J. L.; Schröter, M.; Burns, K.; Mattmann, C.; Rimoldi, D.; French, L. E.; Tschopp, J. Inhibition of death receptor signals by cellular FLIP. *Nature*. **1997**, *388*, 190-195.
- 101:** Safa, A.R. c-FLIP, a master anti-apoptotic regulator. *Exp. Oncol.* **2012**, *34*, 176-184.
- 102:** Hazlehurst, L. A.; Landowski, T. H.; Dalton, W. S. Role of the tumor microenvironment in mediating de novo resistance to drugs and physiological mediators of cell death. *Oncogene*. **2003**, *22*, 7396-7402.
- 103:** Matsuda, I.; Matsuo, K.; Matsushita, Y.; Haruna, Y.; Niwa, M.; Kataoka, T. The C-terminal domain of the long form of cellular FLICE-Inhibitory Protein (c-FLIPL) inhibits the interaction of the caspase 8 prodomain with the receptor-interacting protein 1 (RIP1) death domain and regulates caspase 8-dependent nuclear factor κ B (NF- κ B) activation. *J. Biol. Chem.* **2014**, *289*, 3876-3887.
- 104:** Safa, A. R. Roles of c-FLIP in apoptosis, necroptosis and autophagy. *J. Carcinog. Mutagen.* **2013**, *6*, doi:10.4172/2157-2518.S6-003.
- 105:** Kyläniemi, M. K.; Kaukonen, R.; Myllyviita, J.; Rasool, O.; Lahesmaa, R. The regulation and role of c-FLIP in human Th cell differentiation. *PLoS One*. **2014**, *9*, e102022.
- 106:** Yeh, W. C.; Itie, A.; Elia, A. J.; Ng, M.; Shu, H. B.; Wakeham, A.; Mirtsos, C.; Suzuki, N.; Bonnard, M.; Goeddel, D. V.; Mak, T. W. Requirement for Casper (c-FLIP) in regulation of death receptor-induced apoptosis and embryonic development. *Immunity*. **2000**, *12*, 633-642.
- 107:** Sakamaki, K.; Iwabe, N.; Iwata, H.; Imai, K.; Takagi, C.; Chiba, K.; Shukunami, C.; Tomii, K.; Ueno, N. Conservation of structure and function in vertebrate c-FLIP proteins despite rapid evolutionary change. *Biochem. Biophys. Rep.* **2015**, *3*, 175-189.
- 108:** Kataoka, T.; Buddab, R. C.; Hollera, N.; Thomea, M.; Martinona, F.; Irmelera, M.; Burnsa, K.; Hahnea, M.; Kennedyb, N.; Kovacovic, M.; Tschoppa, J. The caspase-8 inhibitor FLIP promotes activation of NF- κ B and Erk signaling pathways. *Curr. Biol.* **2000**, *10*, 640-648.

- 109:** Quintavalle, C.; Incoronato, M.; Puca, L.; Acunzo, M.; Zanca, C.; Romano, G.; Garofalo, M.; Iaboni, M.; Croce, C. M.; Conodorelli, G. c-FLIP_L enhances anti-apoptotic Akt functions by modulation of Gsk3 β activity. *Cell. Death. Differ.* **2010**, *17*, 1908–1916.
- 110:** Nakajima, A.; Komazawa-Sakon, S.; Takekawa, M.; Sasazuki, T.; Yeh, W. C.; Yagita, H.; Okumura, K.; Nakano, H. An antiapoptotic protein, c-FLIP_L, directly binds to MKK7 and inhibits the JNK pathway. *EMBO J.* **2006**, *25*, 5549–5559.
- 111:** Mizushima, N.; Levine, B.; Cuervo, A. M.; Klionsky, D. J. Autophagy fights disease through cellular self-digestion. *Nature.* **2008**, *451*, 1069–1075.
- 112:** Feoktistova, M.; Geserick, P.; Kellert, B.; Dimitrova, D. P.; Langlais, C.; Hupe, M.; Cain, K.; MacFarlane, M.; Häcker, G.; Leverkus, M. cIAPs block Ripoptosome formation, a RIP1/caspase-8 containing intracellular cell death complex differentially regulated by cFLIP isoforms. *Mol. Cell.* **2011**, *43*, 449–463.
- 113:** Leidal, A. M.; Cyr, D. P.; Hill, R. J.; Lee, P. W.; McCormick, C. Subversion of autophagy by Kaposi's sarcoma-associated herpesvirus impairs oncogene-induced senescence. *Cell. Host. Microbe.* **2012**, *11*, 167–180.
- 114:** Bagnoli, M.; Canevari, S.; Mezzanzanica, D. Cellular FLICE-inhibitory protein (c-FLIP) signalling: A key regulator of receptor-mediated apoptosis in physiologic context and in cancer. *Int. J. Biochem. Cell Biol.* **2010**, *42*, 210-213.
- 115:** Hughes, M. A.; Powley, I. R.; Jukes-Jones, R.; Horn, S.; Feoktistova, M.; Fairall, L.; Schwabe, J. W. R.; Leverkus, M.; Cain, K.; MacFarlane, M. Co-operative and hierarchical binding of c-FLIP and Caspase-8: a unified model defines how c-FLIP isoforms differentially control cell fate. *Mol. Cell.* **2016**, *61*, 834-849.
- 116:** Yu, J. W.; Jeffrey, P. D.; Shi, Y. Mechanism of procaspase-8 activation by c-FLIPL. *PNAS.* **2009**, *106*, 8169-8174.
- 117:** Yang, J. K.; Wang, L.; Zheng, L.; Wan, F.; Ahmed, M.; Lenardo, M. J.; Wu, H. Crystal structure of MC159 reveals molecular mechanism of DISC assembly and FLIP inhibition. *Mol. Cell.* **2005**, *20*, 939-949.
- 118:** Majkut, J.; Sgobba, M.; Holohan, C.; Crawford, N.; Logan, A. E.; Kerr, E.; Higgins, C. A.; Redmond, K. L.; Riley, J. S.; Stasik, I.; Fennel, D. A.; Van Schaeuybroeck, S.; Haider, S.; Johnston, P. G.; Haigh, D.;

Longley, D. B. Differential affinity of FLIP and procaspase 8 for FADD's DED binding surfaces regulates DISC assembly. *Nat. Commun.* **2014**, *5*, doi:10.1038/ncomms4350.

119: Piggott, L.; Omidivar, N.; Pérez, S.M.; Eberl, M.; Clarkson, R. W. E. Suppression of apoptosis inhibitor c-FLIP selectively eliminates breast cancer stem cell activity in response to the anti-cancer agent, TRAIL. *Breast Cancer Res.* **2011**, *13*, S88.

120: Yang, J. K. Flip as anti-cancer therapeutic target. *Yonsei Med. J.* **2008**, *49*, 19-27.

121: Day, T. W.; Safa, A. R. RNA interference in cancer: targeting the anti-apoptotic protein c-FLIP for drug discovery. *Mini Rev. Med. Chem.* **2009**, *9*, 741-748.

122: Bijangi-Vishehsaraei, K.; Saadatzadeh, M. R.; Huang, S.; Murphy, M.P.; Safa, A.R. 4-(4-Chloro-2-methylphenoxy)-N-hydroxybutanamide (CMH) targets mRNA of the c-FLIP variants and induces apoptosis in MCF-7 human breast cancer cells. *Mol. Cell Biochem.* **2010**, *342*, 133-142.

123: Butler, L. M.; Liapis, V.; Bouralexis, S.; Welldon, K.; Hay, S.; Thai, L. M.; Labrinidis, A.; Tilley, W. D.; Findlay, D. M.; Evdokiou, A. The histone deacetylase inhibitor, suberoylanilide hydroxamic acid, overcomes resistance of human breast cancer cells to Apo2L/TRAIL. *Int. J. Cancer.* **2006**, *119*, 944-954.

124: Li, B.; Ren, H.; Yue, P.; Chen, M.; Khuri, F. R.; Sun, S. Y. The novel Akt inhibitor API-1 induces c-FLIP degradation and synergizes with TRAIL to augment apoptosis independent of Akt inhibition. *Cancer Pre. Res.* **2012**, *5*, 612-620.

125: Chen, S.; Cao, W.; Yue, P.; Hao, C.; Khuri, F.R.; Sun, S.Y. Celecoxib promotes c-FLIP degradation through Akt-independent inhibition of GSK3. *Cancer Res.* **2011**, *71*, 6270-81.

126: Kapetanovic, I. Computer-Aided Drug Discovery and Development (CADD): in silico-chemico-biological approach. *Chem. Biol. Interact.* **2008**, *171*, 165-176.

127: Harak, S. S.; Mali, D. R.; Amrutkar, S. V. Computer aided drug design. *I. J. S. R. S. T.* **2017**, *10*, 118-120.

128: Anderson, A. C. The process of structure-based drug design. *Chem. Biol.* **2003**, *10*, 787-797.

129: Acharya, C.; Coop, A.; Polli, J. E.; MacKerell, A. D. Recent advances in ligand-based drug design: relevance and utility of the conformationally sampled pharmacophore approach. *Curr. Comp. Aided Drug Des.* **2011**, *7*, 10-22.

- 130:** Hayward, O. Design and Synthesis of Molecular Inhibitors of c-FLIP Activity as a Therapeutic Strategy to Target Breast Cancer Stem Cells. PhD Thesis. **2015**, Cardiff University.
- 131:** Dickens, L. S.; Boyd, R. S.; Jukes-Jones, R.; Hughes, M. A.; Rbinson, G. L.; Fairall, L.; Schwabe, J. W. R.; Cain, K.; MacFarlane, M. A death effector domain chain DISC model reveals a crucial role for Caspase-8 chain assembly in mediating apoptotic cell death. *Mol. Cell.* **2012**, *392*, 941-945.
- 132:** Specs. <http://www.specs.net> (accessed December 17, 2017).
- 133:** Caspase-Glo® 8 Assay Systems. <https://www.promega.co.uk> (accessed December 2017).
- 134:** Kenworthy, K. A.; Imaging protein-protein interactions using fluorescence resonance energy transfer microscopy. *Methods.* **2001**, *24*, 289-296.
- 135:** Co-immunoprecipitation (co-IP). <https://www.thermofisher.com> (accessed December 2017).
- 136:** Robinson, T. Targeting c-FLIP to inhibit residual cancer stem cells after chemotherapy. PhD Thesis. **2017**, Cardiff University.

Chapter 2

Computational Studies

Chapter 2: Computational Studies

2.1 Introduction

At the beginning of this study the analysis of the features involved in c-FLIP:FADD binding and in c-FLIP:hit **3** was performed according to the homology modelling studies previously performed in our research group. ⁽¹⁾ The aim was to investigate the chemical and structural properties of the c-FLIP pocket in order to design new molecules hypothetically able to block the interaction between c-FLIP and FADD while promoting the FADD:Caspase-8 binding. Following these computational studies, several new compounds were designed and synthesised. For all the new derivatives molecular docking studies were performed, and a brief description of the general methods used is reported in this chapter. Moreover, additional computational studies were performed in order to investigate whether further amino acid residues of c-FLIP may be involved in the interaction with FADD.

2.2 c-FLIP:FADD interaction and c-FLIP pocket analysis

As mentioned in section 1.4.2, in previous studies carried out in our research group, the homology model of FADD interacting with the DED1 of c-FLIP was built. ⁽¹⁾ Previous mutational studies have demonstrated the important role of the Phe25/Leu26 motif of FADD, which is responsible for the interaction occurring with caspase-8, and it is deemed to have a crucial role in c-FLIP and caspase-8 recruitment to the DISC. ⁽²⁾ An analysis of the interactions occurring between this particular motif and the amino acid residues in the pocket of c-FLIP was therefore performed using MOE as visualiser software. According to our model, the Phe25 located on the DED of FADD occupies a small pocket on the DED1 of c-FLIP, forming Van der Waals interactions with the His7 and an H-bond with the Arg45. The interactions occurring between the amino acid residues and the corresponding distances are shown in figure 2.2.1.

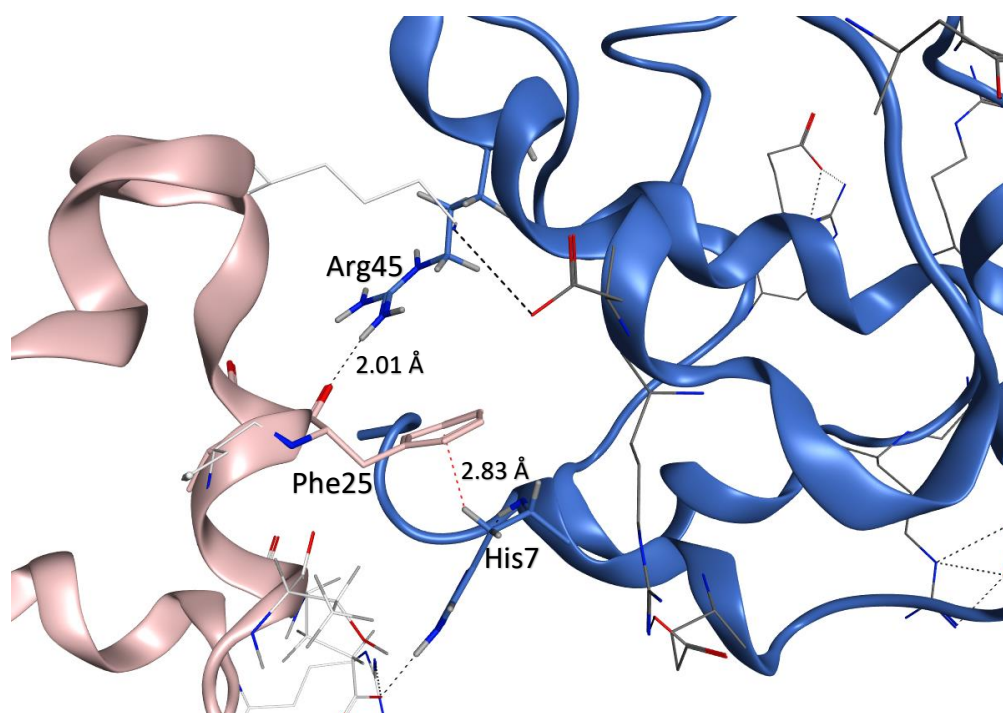


Fig 2.2.1: Phe25 of FADD (pink) forms an H-bond (2.01 Å), indicated by a black dot line, with Arg45 and Van der Waals interaction (2.83 Å), indicated with a red dot line, with His7 in the DED1 of c-FLIP (blue).

The pocket accommodating Phe25 of FADD is a small hydrophobic cavity. As shown in figure 2.2.2, the central portion of the pocket is occupied by two amino acid residues, Glu10 and Arg38. Behind these residues, the pocket bends inward creating a curved-shaped hydrophobic cavity. Arg45, which is responsible for the binding with Phe25 of FADD, is exposed to the surface of the pocket, in proximity to the entrance of the cavity.

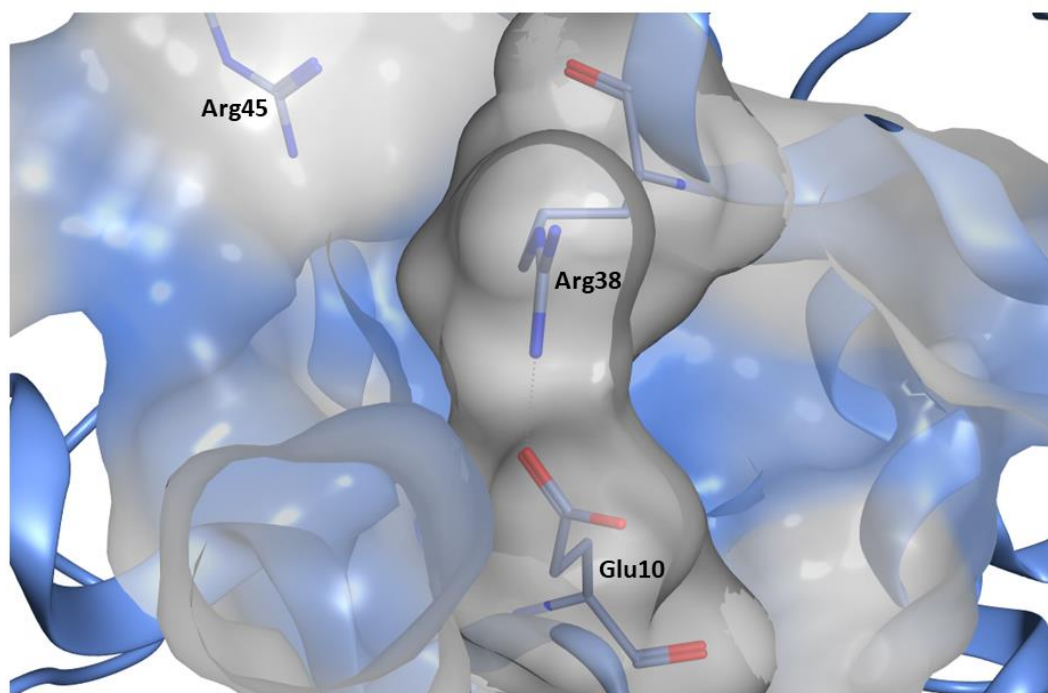


Fig 2.2.2: The c-FLIP pocket.

Considering the features described above, novel small molecules able to fit the curved-shaped hydrophobic cavity in the pocket of c-FLIP might be able to prevent the binding to FADD.

2.3 Hit 3:c-FLIP interaction

In order to investigate the features required for the occupation of c-FLIP pocket, the predicted binding mode of hit **3** was analysed. Looking at figure 2.3.1, which shows the interaction between **3** and c-FLIP, it is possible to outline important relationships between the structural properties of the compound and its binding mode.

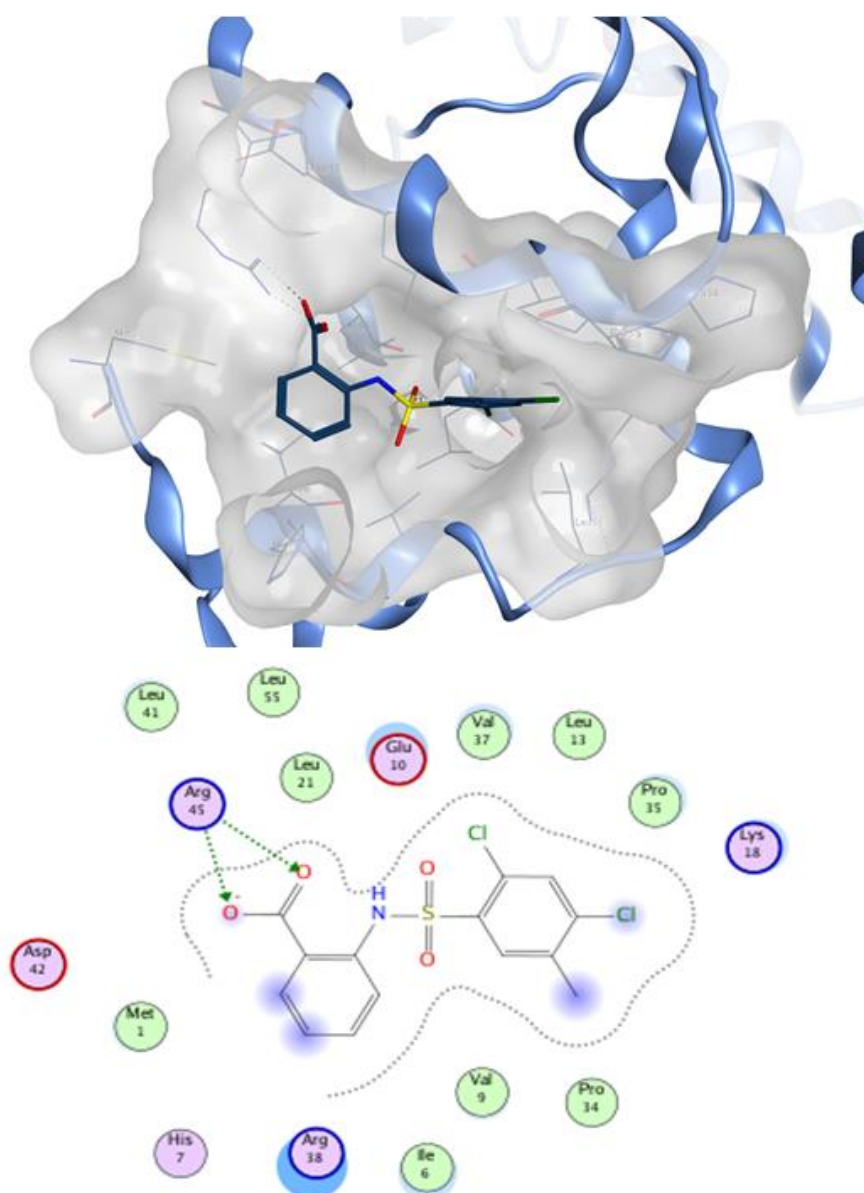


Fig 2.3.1: Predicted binding mode for **3** (dark blue) and its interaction with the amino acid residues. The two amino acid residues Glu10 and Arg38 are not shown in order to provide a better visualisation of the predicted binding mode.

The structure of **3** can be divided into three portions, each of which plays an important role in the binding within the c-FLIP pocket. Figure 2.3.2, which includes the two amino acid residues Arg38

and Glu10, shows the predicted ability of the compound to fit the small pocket. The presence of the sulfonamide linker, located behind the residues Glu10 and Arg38, allows the molecule to acquire a tetrahedral geometry, thus promoting its arrangement in the curved-shaped cavity. The 2,4-dichloro-3-methyl phenyl ring occupies the hydrophobic region of the pocket, whilst the carboxylic acid moiety, on the other aromatic ring, forms an H-bond with Arg45 of c-FLIP.

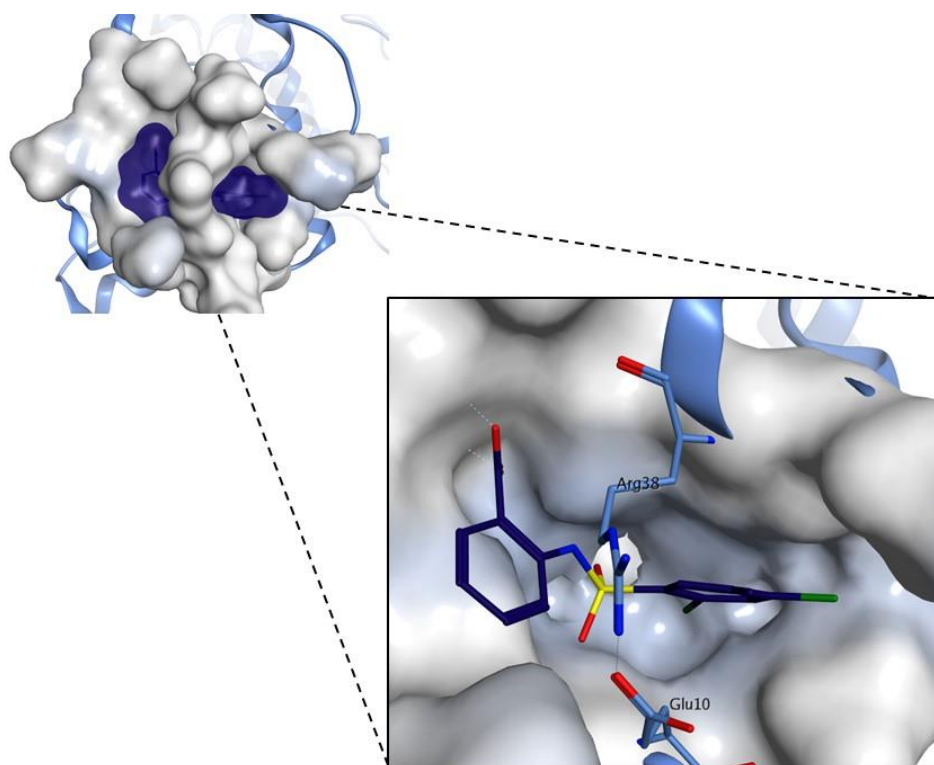


Fig 2.3.2: The small figure represents the predicted ability of the hit compound **3** (surface dark blue) to adapt to the curved-shaped cavity (surface grey). The big figure is an enlargement of the binding pocket which shows how the sulfonamide group (yellow) of **3** (dark blue), occupying the area behind the residues Arg38 and Glu10, allows the molecule to fit the curved-shaped c-FLIP pocket.

The analysis of the structural properties of the c-FLIP pocket and the investigation of the features required for the binding of the original hit **3** within the c-FLIP pocket, in combination with the biological results obtained in the previous work, were used to design new potential c-FLIP inhibitors.

2.4 Design of new derivatives

In order to investigate structure-activity relationships and to improve the activity and the pharmacokinetic properties of **3**, new derivatives were designed. As mentioned in section 2.3, the linker between the two aromatic rings plays a crucial role in the binding within the c-FLIP pocket. Therefore, on the basis of the linker group, four new series of compounds were designed:

sulphonamide derivatives, amine derivatives, methylene derivatives and amide derivatives. The general scaffold of the new series of analogues is represented in table 2.4.

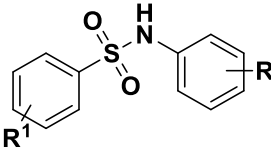
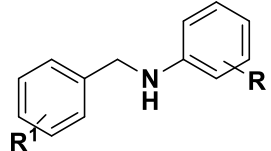
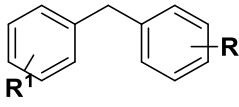
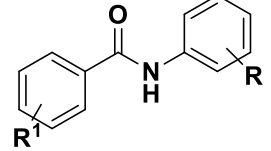
DERIVATIVES	SCAFFOLD
Sulphonamide	
Amine	
Methylene	
Amide	

Table 2.4: General Scaffold of the new derivatives.

For each series different modifications on the two aromatic rings were also explored.

2.5 Molecular Docking Studies

Molecular docking techniques represent an important tool in medicinal chemistry due to their ability to predict the binding mode of a ligand to its molecular target. ⁽³⁾ In general, molecular docking algorithms generate different conformations (poses) for each ligand in the binding site of the biological target. The binding affinity of each pose for the binding site is then estimated using different scoring functions. ⁽⁴⁾ In this work, molecular docking studies were performed in order to investigate the predicted behaviour of all the newly designed derivatives in the pocket of c-FLIP. All molecular docking analyses were performed using Glide SP. ⁽⁵⁾ As a first step, a database containing the structure of the newly designed compounds was created using MOE 2015. ⁽⁶⁾ Using the LigPrep tool in Maestro, ⁽⁵⁾ the ligands included in the database were prepared for docking. The c-FLIP pocket was selected as receptor, and a maximum length of 12Å from the centre of the site, defined by the position predicted to be occupied by hit **3**, was set up to dock the compounds. 15 poses for each compound were included in the post-docking minimisation. The results obtained were exported in MOE, which was used for the visual inspection of all poses and the analysis of the predicted interactions between the ligands and the amino acid residues belonging to the binding pocket.

2.6 New potential interaction sites

In a recent study published in 2016, a new model of c-FLIP recruitment to the DISC was proposed.

⁽⁷⁾ According to the results obtained in this study, based on the reconstitution of the TRAIL DISC, only a small amount of c-FLIP is recruited to the DISC in the absence of procaspase-8, while, interestingly, the amount of c-FLIP recruited is significantly increased when the reconstituted DISC is pre-assembled with procaspase-8. Therefore, this model supports a potential co-operative recruitment of procaspase-8 and c-FLIP to the DISC, thus indicating that c-FLIP and procaspase-8 do not compete for binding to FADD. Furthermore, mutational studies were performed, in order to identify the amino acids involved in the formation of the complexes FADD:procaspase-8 and FADD:c-FLIP. According to the results obtained, Tyr8 in the DED1 of procaspase-8 is the key residue involved in the interaction with FADD, suggesting that FADD recruits procaspase-8 via DEDPhe25:DED1Tyr8 binding, while additional procaspase-8 molecules interact via the DED1 domain with the exposed DED2 of the FADD-bound procaspase-8. On the other side, the mutational studies performed on the complex c-FLIP:FADD revealed the residues Phe114/Leu115 in the DED2 of c-FLIP and His9 of FADD as the crucial amino acids for the interaction between the two proteins. However, the formation of the complex c-FLIP:FADD which occurs via the DED2 of c-FLIP is limited in the absence of procaspase-8, suggesting that c-FLIP may be indirectly recruited to FADD via DED-mediated c-FLIP:procaspase-8 heterodimerization. Therefore, the model suggested in this study involves the initial recruitment of procaspase-8 to Phe25 of FADD via DED1. When c-FLIP is overexpressed, procaspase-8 heterodimerizes with c-FLIP via DED2:DED1 interaction. Thus, c-FLIP is indirectly recruited to the DISC and the exposed DED2 interacts with His9 of FADD. According to the proposed model, c-FLIP blocks the activation of procaspase-8 preventing the dimerization required for the conversion into the active form caspase-8, and additionally inhibiting the recruitment of other pro-caspase-8 molecules to FADD. ⁽⁷⁾

Taking into consideration this information, further molecular modelling analyses were performed in order to explore the potential sites of interaction described above.

2.6.1 Protein:Protein Docking

The suggested interaction between the DED of FADD and the DED2 of c-FLIP was computationally investigated performing a protein:protein docking analysis. The protein-protein docking method is a technique used in computational chemistry to predict the possible interactions which occur between two proteins. ⁽⁸⁾ In this work, the protein-protein docking analysis was performed using

MOE 2015. ⁽⁶⁾ The crystal structure of FADD (PDB ID: 1A1W) was defined as desired receptor, while His9 of FADD, which was the crucial amino acid identified in the study previously mentioned, ⁽⁷⁾ was selected as the binding site. The c-FLIP model was marked as the ligand to dock and all the amino acids of the protein were defined as ligand site in order to explore all the potential interactions deriving from the computational analysis. The docking results were then visually inspected. Interestingly, several results suggested the potential interaction of His9 of FADD with Leu115 of DED2 of c-FLIP, which is one of the key residues involved in the formation of the complex c-FLIP:FADD according to the work previously described. ⁽⁷⁾ Furthermore, among all the poses analysed, one in particular, shown in fig 2.6.1, predicted the interaction between His9 of FADD and both the amino acid residues Phe114 and Leu115 of c-FLIP, revealing a potential correlation with the mutational studies recently published. ⁽⁷⁾ Therefore, this pose was chosen as the best result from protein:protein docking studies.

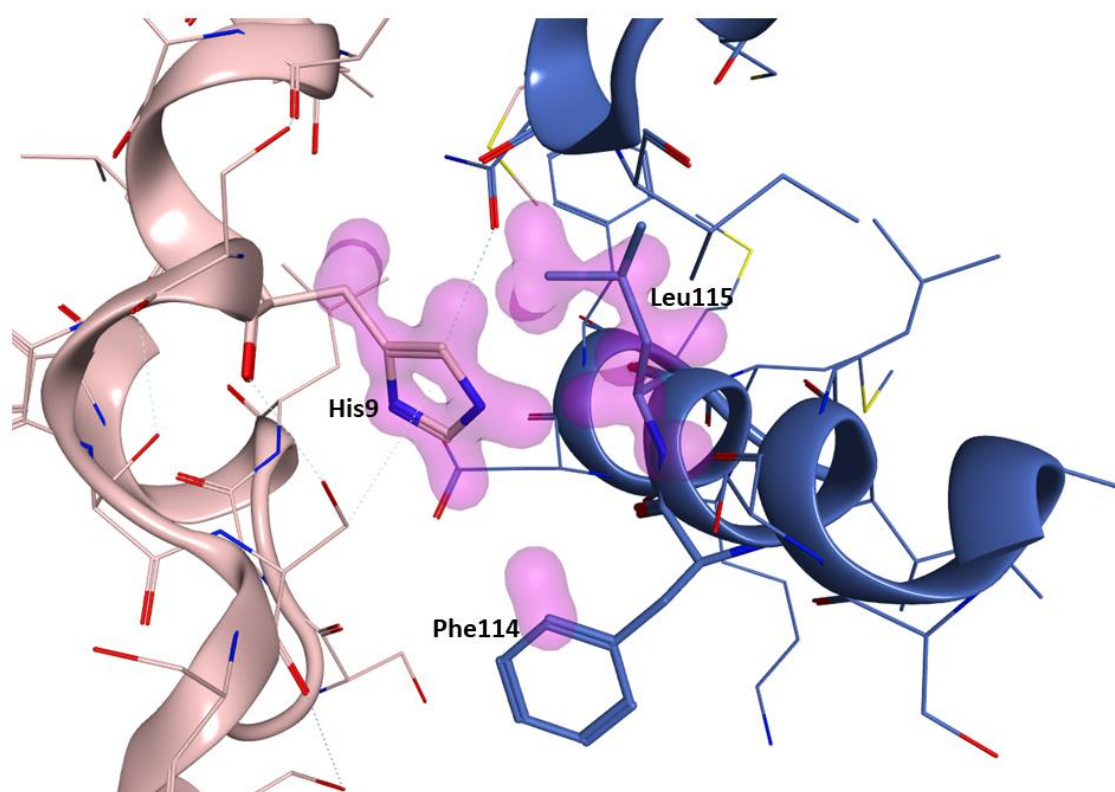


Fig 2.6.1: Protein:protein docking result: The predicted interaction (indicated by the pink cloud) between the His9 of FADD (pink) and the Phe114/Leu115 of c-FLIP (blue).

Following the protein:protein docking, a molecular dynamics simulation was performed in order to analyse the stability of the system over time.

2.6.2 Molecular Dynamics Simulation

A Molecular Dynamics (MD) simulation analyses the spatial coordinates of each atom of the molecular system, through the simultaneous solution, in short time steps, of Newton's second law of motion (equation 2.6.2).⁽⁹⁾

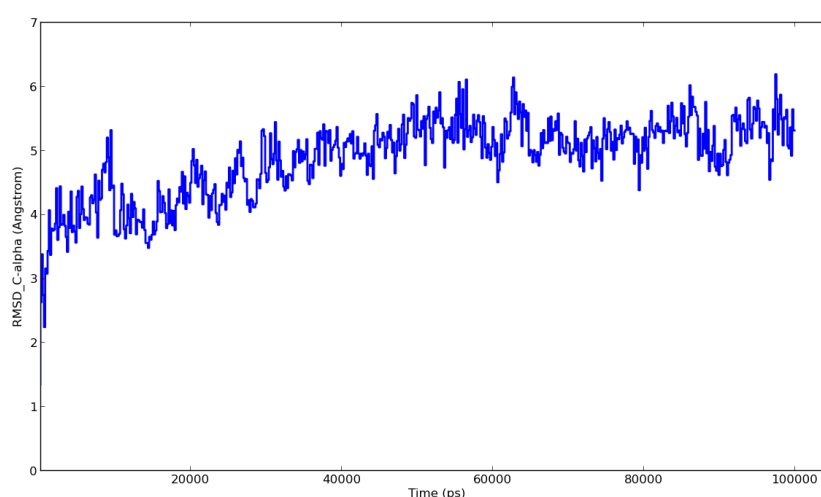
$$F_i = m_i * a_i = m_i * \frac{\delta^2 r_i}{\delta t^2}$$

Equation 2.6.2: Newton's equation of motion.

F=force, m=mass, a=acceleration, r=distance, t=time, $i= 1$ to N ⁽⁹⁾

MD simulations also calculate potential energy and forces between particles using force field functions.⁽⁹⁾ Therefore, MD simulations represent an important technique in computational chemistry in order to analyse the dynamic behaviour of a molecular system as a function of time, thus acquiring information about the motion of the different atoms and about the stability of the molecular system.⁽¹⁰⁾

In this study, a MD simulation was performed using DESMOND⁽¹¹⁾. The simulation time was set to 100 ns and constant values of number of atoms, temperature (300K) and pressure (1 atm) were selected. The specific protocol applied is reported in the Experimental Section. The results obtained were analysed using Maestro. The MD simulation was monitored with C-alpha RMSD evaluation in order to analyse the stability of the system. Graph 2.6.2 shows an increase of the RMSD values from 0 to 50 ns, and the system appears to be stabilised between 50 and 100 ns, indicating also that the MD duration was appropriate.



Graph 2.6.2: RMSD time variations of the protein C-alpha.

The visual inspection of the molecular dynamics results was performed using MOE. The MD result is shown in figure 2.6.2. The predicted interaction between Phe114/Leu115 of c-FLIP and His9 of FADD was retained during the MD simulation, thus supporting the docking results previously obtained and suggesting stability for the predicted interaction over time.

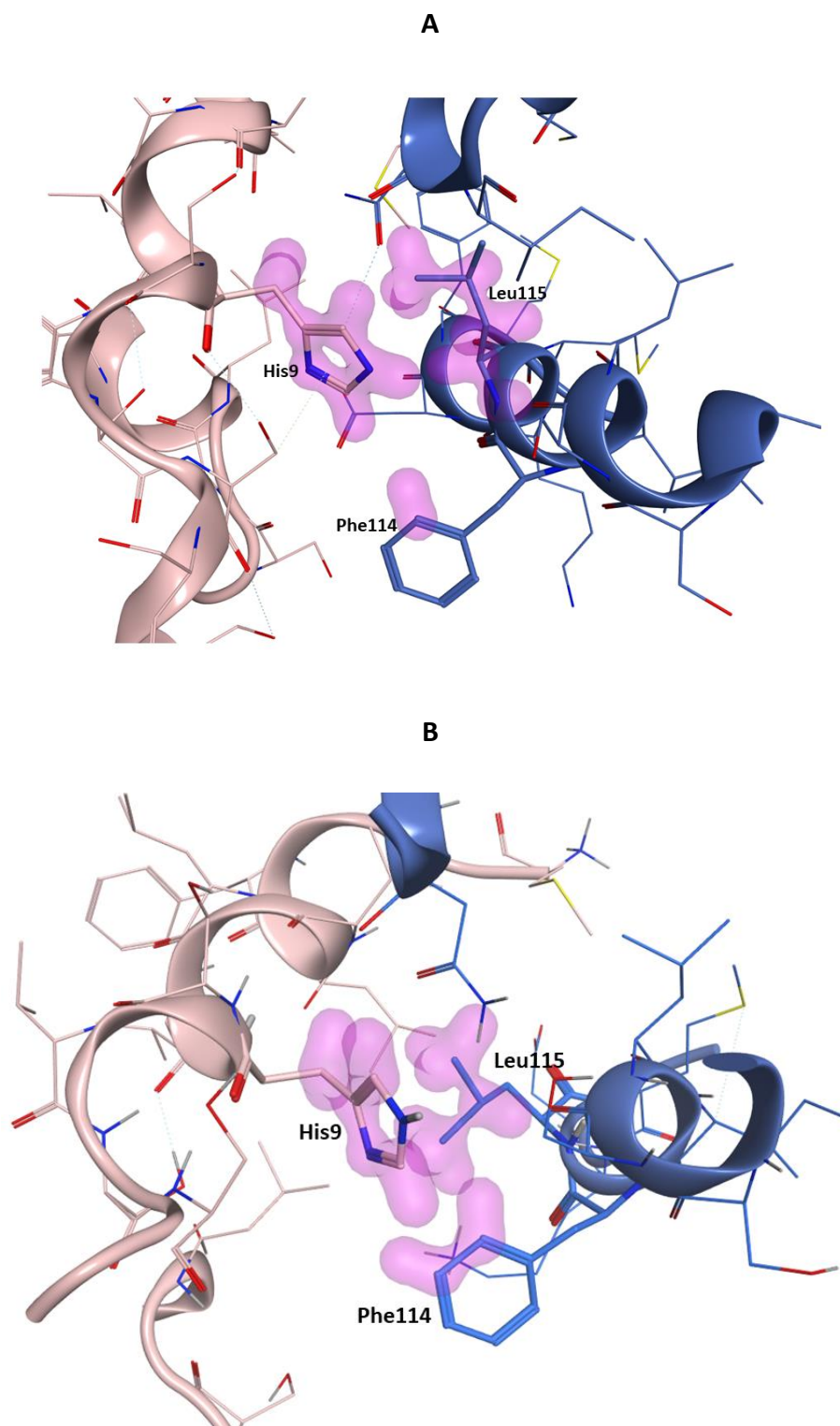


Fig 2.6.2: MD simulation result. A: Before MD simulation B: after MD simulation.

These computational studies suggest the potential involvement of Phe114/Leu115 located on the DED2 of c-FLIP in the binding to FADD, indicating that additional sites as well as the hydrophobic c-FLIP pocket located on the DED1 may be explored as new potential target sites.

2.7 Conclusions

At the beginning of this work, computational studies were performed in order to explore the features required for the binding between c-FLIP and FADD, to investigate the chemical and structural properties of the c-FLIP pocket and eventually to analyse the interactions occurring between c-FLIP and the hit **3**. These studies were used to design four series of analogues of **3** with the final aim to develop novel c-FLIP inhibitors showing improved activity and a better pharmacokinetic profile compared to the original hit. Furthermore, following the publication of a new model of c-FLIP recruitment to the DISC, ⁽⁷⁾ protein:protein docking and molecular dynamics studies were performed, in order to investigate whether additional target sites may be identified. According to the results obtained, two residues located on the DED2 of c-FLIP might be involved in the binding to FADD, Phe114 and Leu115, indicating that, additionally to the DED1, the DED2 of c-FLIP might be also explored as potential target site. This work however will focus on the hydrophobic pocket located on the DED1 of c-FLIP.

2.8 References

- 1: Hayward, O. Design and Synthesis of Molecular Inhibitors of c-FLIP Activity as a Therapeutic Strategy to Target Breast Cancer Stem Cells. PhD Thesis. **2015**, Cardiff University.
- 2: Dickens, L. S.; Boyd, R. S.; Jukes-Jones, R.; Hughes, M. A.; Rbinson, G. L.; Fairall, L.; Schwabe, J. W. R.; Cain, K.; MacFarlane, M. A death effector domain chain DISC model reveals a crucial role for Caspase-8 chain assembly in mediating apoptotic cell death. *Mol. Cell.* **2012**, *392*, 941-945.
- 3: Ferreira, L. G.; Dos Santos, R. N.; Oliva, G.; Andricopulo, A. D. Molecular docking and structure-based drug design strategies. *Molecules.* **2015**, *20*, 13384-13421.
- 4: Xuan-Yu, M.; Hong-Xing, Z.; Mihaly, M.; Meng, C. Molecular Docking: A powerful approach for structure-based drug discovery. *Curr. Comput. Aided Drug Des.* **2011**, *7*, 146-157.
- 5: Schrödinger, Cambridge, MA. www.schrödinger.com (accessed March 27, 2015).
- 6: Chemical Computing Group, Montreal, Canada. www.chemcomp.com (accessed February 20, 2015).
- 7: Hughes, M. A.; Powley, I. R.; Jukes-Jones, R.; Horn, S.; Feoktistova, M.; Fairall, L.; Schwabe, J. W. R.; Leverkus, M.; Cain, K.; MacFarlane, M. Co-operative and hierarchical binding of c-FLIP and Caspase-8: a unified model defines how c-FLIP isoforms differentially control cell fate. *Mol. Cell.* **2016**, *61*, 834-849.
- 8: Ehrlich, L. P.; Wade, R. C. Protein-Protein Docking. In *Reviews in computational chemistry*, 1st ed.; Lipkowitz, K. B., Boyd, D. B., Eds.; Wiley- VCH: New York, 2001, pp 61-98.
- 9: Watanabe, M.; Karplus, M. Dynamics of molecules with internal degrees of freedom by multiple time-step method. *Physical Rev.* **1993**, *99*, 8063-8074.
- 10: Alonso, H.; Bliznyuk, A. A.; Gready, J. E. Combining docking and molecular dynamic simulations in drug design. *Med. Res. Rev.* **2006**, *26*, 531-568.
- 11: Bowers, K. J.; Chow, E.; Xu, H.; Dror, R. O.; Eastwood, M. P.; Gregersen, B. A.; Klepeis, J. L.; Kolossváry, I.; Moraes, M. A.; Sacerdoti, F. D.; Salmon, J. K.; Shan, Y.; Shaw, D. E. Scalable algorithms for molecular dynamics simulations on commodity clusters. *Proceedings of the ACM/IEEE Conference on Supercomputing (SC06)*, Tampa, Florida, November 11–17, **2006**.

Chapter 3

Sulfonamide Derivatives

Chapter 3: Sulfonamide Derivatives

3.1 Design of sulfonamide derivatives

In order to develop novel analogues able to improve the efficacy of **3**, changes on the original structure were considered on the basis of the molecular modelling studies performed and the results previously obtained. At the beginning, given the importance of the sulfonamide linker for the arrangement in the c-FLIP pocket, this functional group was retained. However, in some of the designed derivatives the original linker was elongated by adding one carbon atom. On the other hand, changes on both aromatic rings were contemplated. The original 2,4-dichloro-3-methyl substituent was replaced with numerous hydrophobic groups at different positions of the ring with the aim to investigate whether other hydrophobic substituents may improve penetration and stability of the molecule in the pocket. Moreover, the replacement of the phenyl ring with different heterocycles and bigger rings such as naphthalene and quinoline was explored. Since previous biological data had shown a reduction of activity for compounds lacking the carboxylic acid group or compounds having the carboxylic acid moiety on the hydrophobic ring, this functional group was retained on the original anthranilic ring. The carboxylic acid group is deemed to be crucial for the activity of **3** because of its proposed ability to interact with Arg45 of c-FLIP, thus preventing the binding between this amino acid and Phe25 of FADD. However, the presence of a carboxylic acid moiety is often associated with limitations such as reduced ability to cross the lipophilic layers of the cellular membrane or potential toxicity derived from metabolism. ⁽¹⁾ Replacement of the carboxylic acid group with bioisoster groups such as tetrazole and oxadiazole, or different alkyl esters was therefore considered. Carboxamide and N-alkyl-carboxamides were also explored as substituents of the carboxylic acid in order to investigate how these functional groups may affect activity of the original hit. Several new analogues of **3** were designed as listed in table 3.1. All molecules conserve a central scaffold characterised by the sulfonamide group which connects the two aromatic rings (Fig 3.1). In order to explore whether changes in the hydrophobic ring only or changes in the carboxylic acid moiety only may affect activity of the compounds, for some of the analogues the carboxylic acid moiety was retained and only the hydrophobic ring was modified, whilst for other analogues the hydrophobic ring was kept unchanged while the carboxylic acid was replaced with alkyl esters and tetrazole group in *ortho*, *meta* and *para* position, and oxadiazole and different alkyl carboxamide groups in the *ortho* position. For all the other analogues changes on both sides of the molecule were considered.

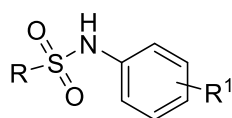


Fig 3.1: Central scaffold of the new analogues.

Molecule	R ¹	R
21	2-methyl ester	(2,4-dichloro-5-methyl)phenyl
22	3-methyl ester	(2,4-dichloro-5-methyl)phenyl
23	4-methyl ester	(2,4-dichloro-5-methyl)phenyl
24	2-methyl ester	(4-trifluoromethyl)phenyl
25	2-methyl ester	(3,4-dimethyl)phenyl
26	2-methyl ester	(3,4-dichloro)phenyl
27	2-methyl ester	(2,4-dichloro)phenyl
28	2-methyl ester	(2,4-dimethyl)phenyl
29	2-methyl ester	(2,5-dimethyl)phenyl
30	2-methyl ester	(2,5-dichloro)phenyl
31	2-methyl ester	(4-tert-butyl)phenyl
32	2-methyl ester	(3,5-bis(trifluoromethyl))phenyl
33	2-methyl ester	1-phenylmethane
34	2-methyl ester	3-pyridine
35	2-methyl ester	2-naphtalene
36	2-methyl ester	1-naphtalene
37	2-methyl ester	cyclohexane
42	2-methyl ester	(5-chloro-2-methyl)phenyl
43	2-methyl ester	(4-methyl-3-chloro)phenyl
50	2-ethyl ester	(2,4-dichloro-5-methyl)phenyl
51	3-ethyl ester	(4-trifluoromethyl)phenyl
52	2-methyl ester	(4-iodo)phenyl
53	3-methyl ester	(4-iodo)phenyl
54	2-ethyl ester	(2-methyl-3-chloro)phenyl
55	3-ethyl ester	(2-methyl-3-chloro)phenyl
56	2-methyl ester	1-(<i>p</i> -tolyl)methane
57	2-methyl ester	2-furan

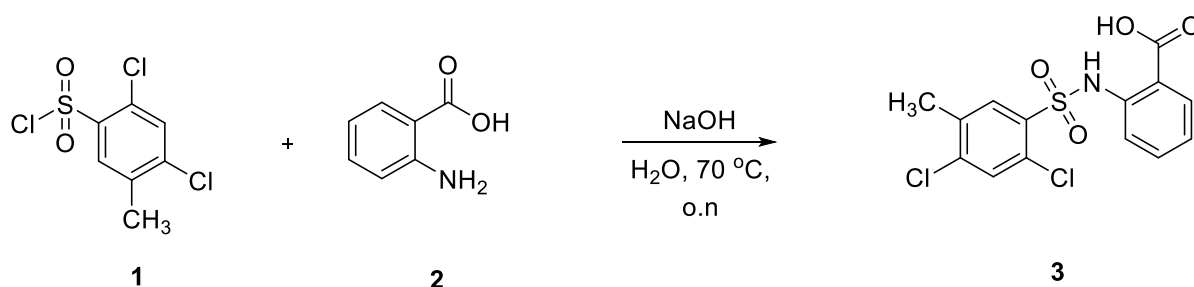
63	2-carboxylic acid	benzene
64	2-carboxylic acid	1-(4-(trifluoromethyl)phenyl)methane
65	2-carboxylic acid	2-thiophene
66	2-carboxylic acid	8-quinoline
67	2-carboxylic acid	3-quinoline
69	2-carboxylic acid	(4-methyl-3-chloro)phenyl
70	2-carboxylic acid	(4-pentafluorosulfanyl)phenyl
71	2-methyl ester	(4-pentafluorosulfanyl)phenyl
72	2-carboxylic acid	3-pyridine
73	2-carboxylic acid	2-naphtalene
74	2-carboxylic acid	1-naphtalene
75	2-carboxylic acid	cyclohexane
76	2-carboxylic acid	2-furan
78	2- isopropyl ester	(2,4-dichloro-5-methyl)phenyl
79	2- isopropyl ester	(4-methyl-3-chloro)phenyl
80	2- <i>tert</i> -butyl ester	(2,4-dichloro-5-methyl)phenyl
81	2- <i>tert</i> -butyl ester	(4-methyl-3-chloro)phenyl
86	4-(1 <i>H</i> -tetrazol)	(2,4-dichloro-5-methyl)phenyl
87	4-(1 <i>H</i> -tetrazol)	(4-methyl-3-chloro)phenyl
88	2-(1 <i>H</i> -tetrazol)	(2,4-dichloro-5-methyl)phenyl
89	2-(1 <i>H</i> -tetrazol)	(4-methyl-3-chloro)phenyl
90	2-(1 <i>H</i> -tetrazol)	(4-trifluoromethyl)phenyl
91	2-(1 <i>H</i> -tetrazol)	2-naphtalene
92	2-(1 <i>H</i> -tetrazol)	8-quinoline
93	2-(1 <i>H</i> -tetrazol)	2-quinoline
97	2-(5-oxo-4,5-dihydro-1,2,4-oxadiazol)	(2,4-dichloro-5-methyl)phenyl
98	2-(5-oxo-4,5-dihydro-1,2,4-oxadiazol)	(4-methyl-3-chloro)phenyl
101	2-N-methyl carboxamide	(4-methyl-3-chloro)phenyl
102	2-N-methyl carboxamide	(2,4-dichloro-5-methyl)phenyl
103	2-N-ethyl carboxamide	(2,4-dichloro-5-methyl)phenyl
104	2-N,N-dimethyl carboxamide	(2,4-dichloro-5-methyl)phenyl
105	2-N-isopropyl carboxamide	(2,4-dichloro-5-methyl)phenyl

106	2-carboxamide	(2,4-dichloro-5-methyl)phenyl
-----	---------------	-------------------------------

Table 3.1: Designed sulfonamide derivatives.

3.2 Synthesis of hit 3

Compound **3** tested in the previous study ⁽²⁾ had been purchased from the SPECS company, therefore in order to confirm the activity demonstrated, the hit compound was resynthesised. Scheme 3.3 shows the reaction scheme.



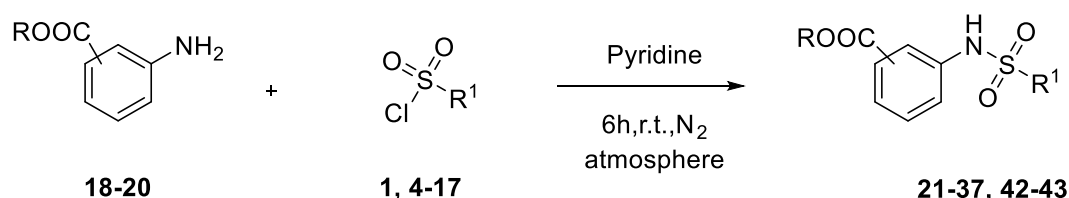
Scheme 3.2: Synthesis of hit 3.

The hit **3** was obtained by the reaction between anthranilic acid and 2,4-dichloro-5-methylsulfonyl chloride. The reaction occurs through nucleophilic attack by amine on the sulfonyl chloride which leads to Cl⁻ elimination. The base NaOH is used to remove the HCl formed during the reaction. The desired product was obtained, and the yield of the reaction was optimised from 28% to 50% increasing the reaction temperature to 70°C instead of 25°C.

3.3 Synthesis of sulfonamide derivatives

3.3.1 Synthesis of methyl(arylsulfonamidobenzoates) (21-37, 42-43)

Given the commercial availability of most of the sulfonyl chlorides required for the synthesis of the new analogues, the one step reaction with methyl aminobenzoates **18-20** was carried out to obtain the analogues **21-37** and **42-43**. The general scheme is shown in scheme 3.3.1.



Scheme 3.3.1: General scheme for the synthesis of compounds 21-37.

The procedure followed is the General Procedure 2 reported in the Experimental Section. The reaction mechanism involves the nucleophilic attack by the amino group of anthranilic ester on the

electrophilic sulfur atom, which is followed by elimination of Cl⁻. The base used is pyridine which removes HCl formed as well as being used as solvent.

Table 3.3.1 shows all the compounds synthesised and the corresponding yields obtained.

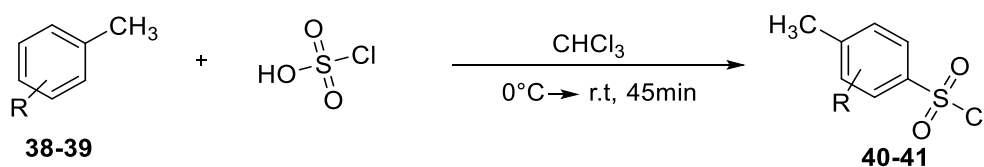
Starting Sulfonyl Chloride	R ¹	R	Product	Yield%
1	(2,4-dichloro-5-methyl)phenyl	2-methyl (18)	21	49%
1	(2,4-dichloro-5-methyl)phenyl	3-methyl (19)	22	56%
1	(2,4-dichloro-5-methyl)phenyl	4-methyl (20)	23	46%
4	(4-trifluoromethyl)phenyl	2-methyl (18)	24	60%
5	(3,4-dimethyl)phenyl	2-methyl (18)	25	29%
6	(3,4-dichloro)phenyl	2-methyl (18)	26	65%
7	(2,4-dichloro)phenyl	2-methyl (18)	27	68%
8	(2,4-dimethyl)phenyl	2-methyl (18)	28	55%
9	(2,5-dimethyl)phenyl	2-methyl (18)	29	47%
10	(2,5-dichloro)phenyl	2-methyl (18)	30	56%
11	(4-tert-butyl)phenyl	2-methyl (18)	31	75%
12	(3,5-bis(trifluoromethyl))phenyl	2-methyl (18)	32	70%
13	1-phenylmethane	2-methyl (18)	33	28%
14	3-pyridine	2-methyl (18)	34	79%
15	2-naphthalene	2-methyl (18)	35	58%
16	1-naphthalene	2-methyl (18)	36	48%
17	Cyclohexane	2-methyl (18)	37	26%

Table 3.3.1: Compounds 21-37.

In general, this reaction worked well for every product, with only compounds **25**, **33** and **37** being obtained with a low yield of 29%, 28% and 26% respectively, due to the loss of the product during the purification process. After the characterisation of each compound by ¹H-NMR, ¹³C-NMR and HPLC, they were subjected to biological evaluation.

3.3.2 Synthesis of methyl(arylsulfonamido)benzoate (42-43)

The synthesis of the last two analogues required the preparation of the two starting sulfonyl chlorides. The reaction scheme used to obtain the two starting materials is shown in scheme 3.3.2.



Scheme 3.3.2: First step for the synthesis of compounds 40-41.

The chlorosulfonation which occurs between chlorosulfonic acid and the two different substituted toluenes complies with the electrophilic aromatic substitution mechanism. Initially, a self-protonation of chlorosulfonic acid occurs to form water. Afterwards, an electron pair of the toluene ring attacks the sulphur atom of the acid, leading to the formation of the aromatic sulfonyl chloride after elimination of water.

Table 3.3.2 illustrates the two starting materials used and corresponding sulfonyl chlorides obtained with the yield of the reactions.

Starting Material	Structure	Sulfonyl Chloride	Structure	Yield
38		40		35%
39		41		19%

Table 3.3.2: Starting materials used and corresponding sulfonyl chlorides obtained.

In order to obtain the selective chlorosulfonation on the desired position, the starting toluenes were chosen analysing the influence of the different substituents on the reactivity. In fact, in this reaction the methyl and chlorine groups act as activating and deactivating substituents respectively and both orientate the substitution at *ortho* and *para* positions. The two starting material structures are shown in figure 3.3.2.1



Fig 3.3.2.1: Starting toluene structures.

Since starting **38** is para-substituted, both substituents can orientate the chlorosulfonation only at the *ortho* positions; however, since the methyl group, which is an activating substituent, has a

stronger influence than the chlorine group, the methyl *ortho*-orientation is the most likely. In **39** both *ortho* and *para* positions are available, however also in this case the methyl effect prevails over the chlorine. Moreover, generally in the chlorosulfonation reaction the percentage of the *para*-substituted product formed is higher than the *ortho* substituted, therefore the sulfonyl chloride expected was the one with the methyl and chlorine at positions *para* and *meta* respectively. The two sulfonyl chloride structures and the corresponding $^1\text{H-NMR}$ spectra are shown in figure 3.3.2.2

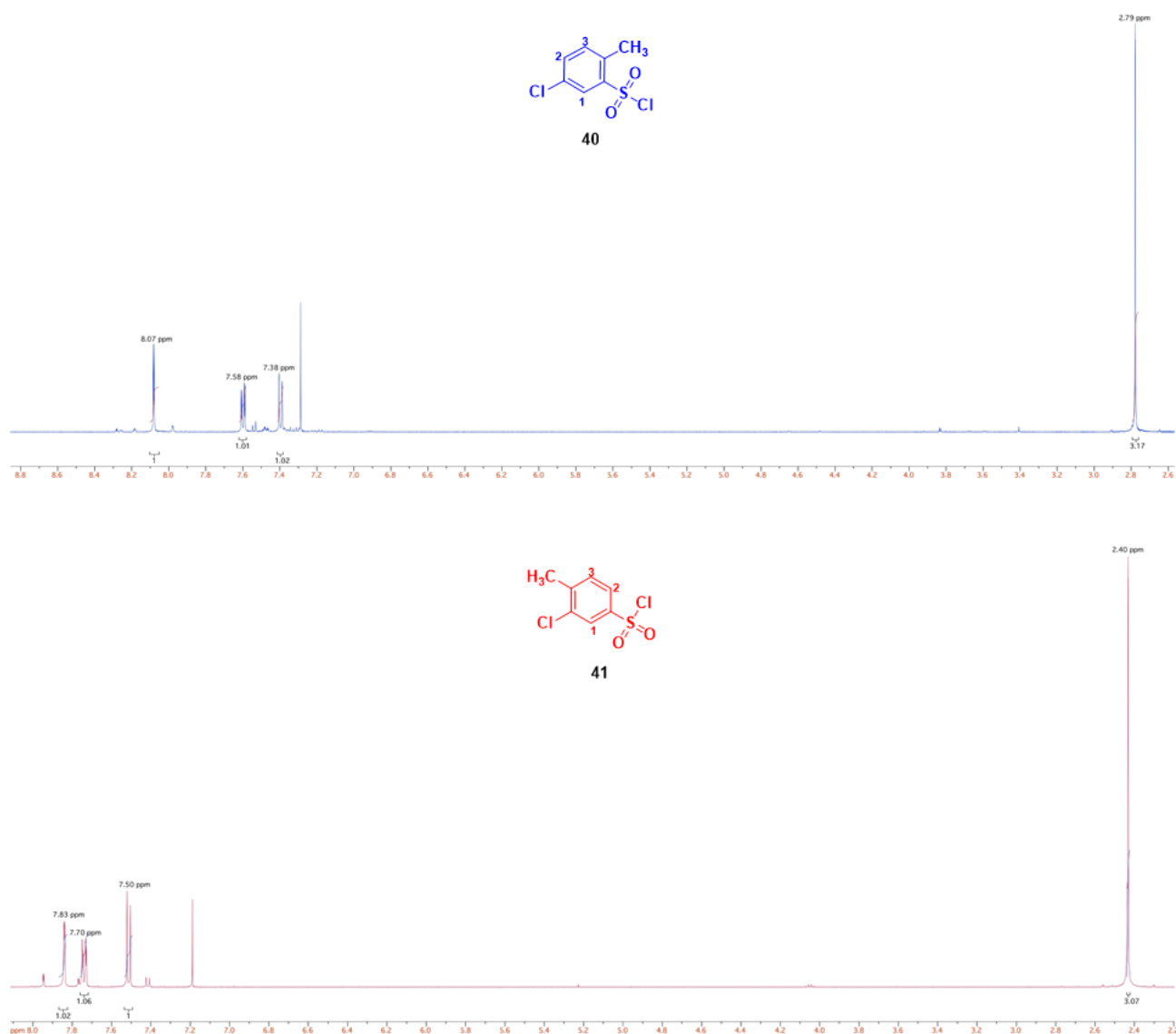
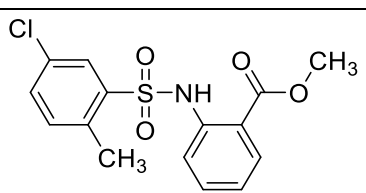
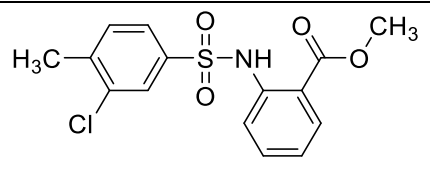


Fig 3.3.2.2: Sulfonyl chloride structures and corresponding $^1\text{H-NMR}$ spectra.

According to $^1\text{H-NMR}$ experiments, both desired sulfonyl chlorides were obtained. The splitting and the ppm values of the signals were crucial for the determination of the compounds structures. In particular, the correspondence between the ppm value and the electron-withdrawing effect on the surrounding protons was evaluated. In both cases, using the splitting of signals and the J coupling values, it was possible to identify all three protons belonging to the aromatic ring. Considering only

these three protons, in the $^1\text{H-NMR}$ spectra of compound **40** the doublet signal corresponding to proton 1 resonance was the most downfield because of the strong electron-withdrawing effect, whilst the low ppm value of the doublet generated by proton 3 was due to the shield of the methyl group. The doublet of doublet representing proton 2 occupied an intermediate position between the other two protons resulting from the electron-withdrawing effect of the chlorine. An analogous situation occurred in the $^1\text{H-NMR}$ spectrum of compound **41**, with the doublet signal of proton 3 which resonated at the lowest ppm value, followed by the doublet of doublet of proton 2, whilst the doublet of proton 1 was the last signal downfield. Therefore, the synthesis of the two desired compounds was confirmed. However, the two reactions exhibited two different trends. In the synthesis of **40**, the desired sulfonyl chloride was the major product of the reaction, thereby it was used for the next step. Nevertheless, small percentages of side products occurred explaining the low yield of the reaction (35%). On the contrary, the second sulfonyl chloride (**41**) was obtained in equal percentage with three different side products, therefore a flash column chromatography was performed in order to isolate the desired compound. Unfortunately, the formation of greater amounts of additional compounds decreased the yield to 19%. Afterwards in order to obtain the corresponding final sulfonamides, compounds **40** and **41** were reacted with the methyl 2-aminobenzoate, using the same reaction shown in the scheme 3.3.1. Products **42** and **43** were obtained and table 3.3.2.2 displays their structures and reaction yields.

Product	Structure	Yield
42		9%
43		24%

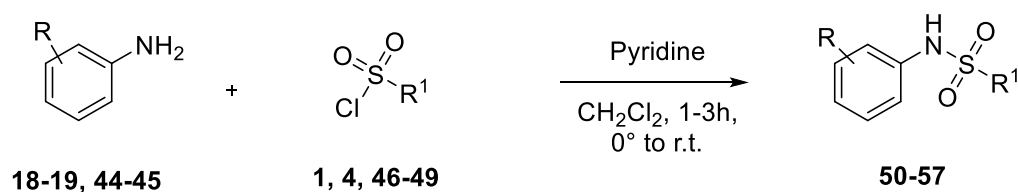
Tab 3.3.2.2: Compounds 42-43.

Despite the fact that both the two final products were obtained, in both cases they were associated with low yields. **42** showed the lowest yield. Two different reasons caused a reduction of the amount of product obtained. The first reason involved the reaction that occurred between the anthranilic ester and the small amounts of impurities coming from the starting material, thus leading to the formation of additional side products. The second reason concerned the purification processes, in fact several recrystallisations were attempted in order to remove the impurities shown by the $^1\text{H-NMR}$

NMR spectrum. However, it was impossible to completely purify the product by recrystallisation only, therefore also a flash column chromatography was performed. All these factors contributed to the decrease of yield. The slightly improved yield in the synthesis of compound **43** was probably due to the cleaner starting material used. However also in this case recrystallisation, followed by flash column chromatography, was performed, thus decreasing the yield obtained (24%).

3.3.3 Synthesis of alkyl(arylsulfonamido)benzoates (50-57)

The general scheme of the reaction used to synthesise analogues **50-57** is shown in scheme 3.3.3, and the reaction follows the same mechanism explained in paragraph 3.3.1.



Scheme 3.3.3: General scheme for the synthesis of compounds 50-57.

Table 3.4.3 lists all the analogues obtained following the General Procedure 4 reported in the Experimental Section.

Starting Sulfonyl Chloride	R ¹	R	Product	Yield%
1	(2,4-dichloro-5-methyl)phenyl	2-ethyl ester (44)	50	43%
4	(4-trifluoromethyl)phenyl	3-ethyl ester (45)	51	65%
46	(4-iodo)phenyl	2-methyl ester (18)	52	25%
46	(4-iodo)phenyl	3-methyl ester (19)	53	12%
47	(2-methyl-3-chloro)phenyl	2-ethyl ester (44)	54	40%
47	(2-methyl-3-chloro)phenyl	3-ethyl ester (45)	55	82%
48	1-(<i>p</i> -tolyl)methane	2-methyl ester (18)	56	15%
49	2-furan	2-methyl ester (18)	57	57%

Table 3.3.3: Compounds 50-57.

Generally, compounds which show the ester group in *ortho* position were obtained in lower yields compared to compounds with the ester group in *meta* position. This might be explained by the bigger steric hindrance around the nitrogen atom that makes the amino group less reactive. Nevertheless, compounds **50**, **51**, **54**, **55** and **57** were obtained in moderate yields. On the other

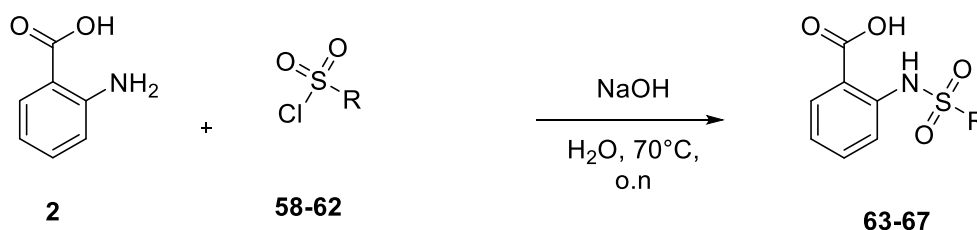
hand, low yields were obtained for compounds **52**, **53** and **56**. In all cases the reaction did not reach completion even after 24 hours, thus explaining the low yields obtained. Moreover, in order to facilitate the formation of **53** the temperature was increased to 40°C. Although this strategy promoted the formation of **53**, an undesired product was also obtained. Unfortunately, considering the highly similar retention factor of the side product, the complete isolation of **53** was not achieved, leading to the 12% yield obtained. Similarly to **53**, different purification processes were required for **56**, thus contributing to the low yield obtained.

3.3.4 Synthesis of (arylsulfonamido)benzoic acids (**63-67**, **69-70**, **72-76**)

As mentioned in section 3.1, some of the designed derivatives retain the carboxylic acid function whilst different modifications are introduced on the hydrophobic ring. The several (arylsulfonamido)benzoic acid derivatives were obtained using different reactions.

3.3.4.1 Synthesis of compounds **63-67**

Analogues **63-67**, shown in table 3.3.4.1, were obtained using the reaction reported in paragraph 3.3 and the reaction scheme is shown in scheme 3.3.4.1.



Scheme 3.3.4.1: General scheme for the synthesis of compound **63-67**.

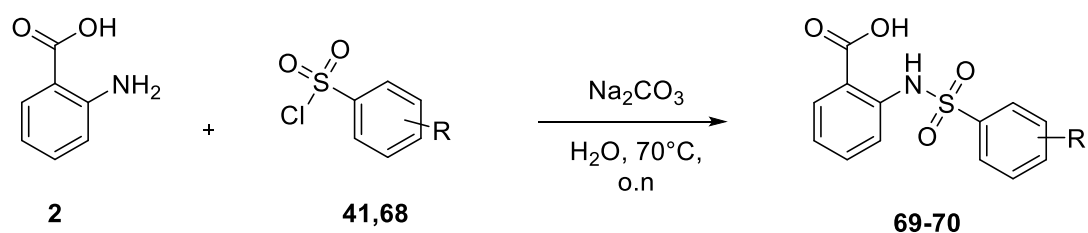
Starting Sulfonyl Chloride	R	Product	Yield%
58	benzene	63	59%
59	1-(4-(trifluoromethyl)phenyl)methane	64	23%
60	2-thiophene	65	22%
61	8-quinoline	66	28%
62	3-quinoline	67	35%

Table 3.3.4.1: Compounds **63-67**.

In general, this reaction worked well with the starting sulphonyl chlorides reacting completely. All the products obtained with this method were purified by recrystallisation and the moderate yields obtained can be explained by the loss of product during this process.

3.3.4.2 Synthesis of compounds 69-70, 71

Analogues **69-70** are characterised by the presence of different substituents on the hydrophobic phenyl ring. The reaction scheme is shown in scheme 3.3.4.2.



Scheme 3.3.4.2: General scheme for the synthesis of compounds 69-70.

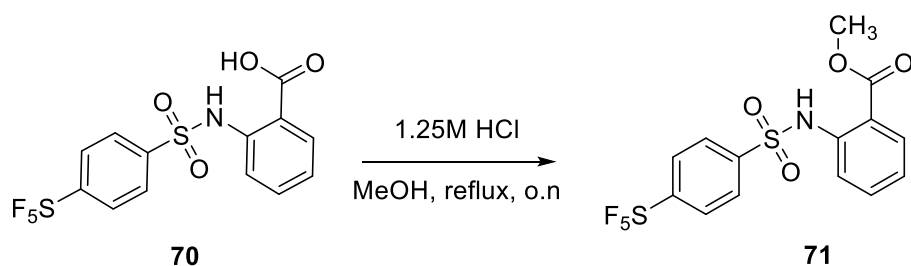
The reaction follows the same mechanism explained in paragraph 3.3, however a different base was used to obtain **69** and **70**. This is due to the fact that when the same reaction was performed using NaOH the yields obtained were extremely low (< 5%). The use of an alternative base, sodium carbonate, allowed optimisation of the yields.

Compounds and corresponding yields obtained are shown in table 3.3.4.2

Starting Sulfonyl Chloride	R	Product	Yield%
41	3-chloro-4-methyl	69	61%
68	4-pentafluorosulfonyl	70	40%

Table 3.3.4.2: Compounds 69-70.

69 was synthesised in order to investigate whether retaining the carboxylic acid moiety may improve the activity of the corresponding methyl ester derivative (**43**). In **70** instead a new hydrophobic substituent was introduced, the 4-pentafluorosulfonyl (SF₅). This group has been reported to impart lipophilicity, chemical resistance, thermal stability and low surface energy to molecules, therefore the synthesis of new analogues containing this moiety was considered.⁽³⁾ Moreover, the methyl ester derivative (**71**) of **70** was also synthesised. The analogue **71** was obtained through a Fischer esterification and the reaction scheme is shown in scheme 3.3.4.2.2.

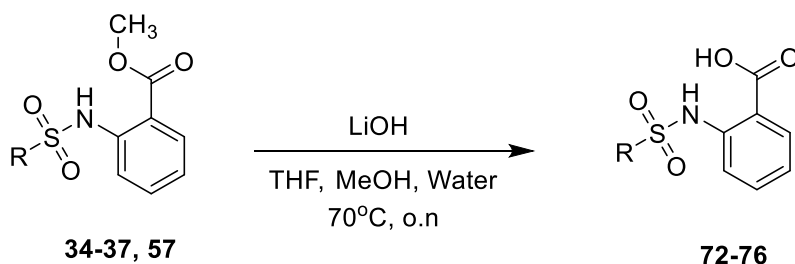


Scheme 3.3.4.2.2: Synthesis of compound 71.

Following the General Procedure 7 reported in the Experimental Section, compound **71** was obtained with 43% yield.

3.3.4.3 Synthesis of compounds 72-76

Derivatives **72-76** were obtained via hydrolysis of the corresponding methyl esters **34-37**, **57**. The structures of the carboxylic acid derivatives are shown in table 3.3.4.3 while scheme 3.3.4.3 reports the general reaction scheme.



Scheme 3.3.4.3: General scheme for the synthesis of compounds 72-76.

Hydrolysis, performed in basic conditions, afforded products **72**, **75**, and **76** in moderate yields and products **73** and **74** in good yields. The General Procedure applied is reported in the Experimental Section.

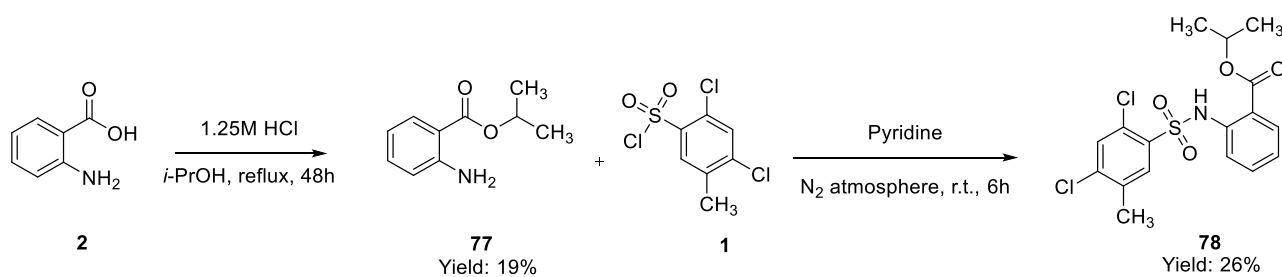
Starting Ester	R	Product	Yield%
34	3-pyridine	72	30%
35	2-naphthalene	73	67%
36	1-naphthalene	74	90%
37	cyclohexane	75	26%
38	2-furan	76	32%

Table 3.3.4.3: Compounds 72-76.

3.3.5 Synthesis of alkyl(arylsulfonamido)benzoates (78, 80-82)

In **78**, **80-82** alternative esters such as the isopropyl ester and the *tert*-butyl ester were considered as substituents instead of the methyl group. These two groups aim to explore whether bigger alkyl groups, which show higher stability to hydrolysis compared to the methyl ester, may influence the activity of the compounds. In order to make a direct comparison between the different alkyl esters, the isopropyl derivative and the *tert*-butyl derivative of **21** and **43** were synthesised.

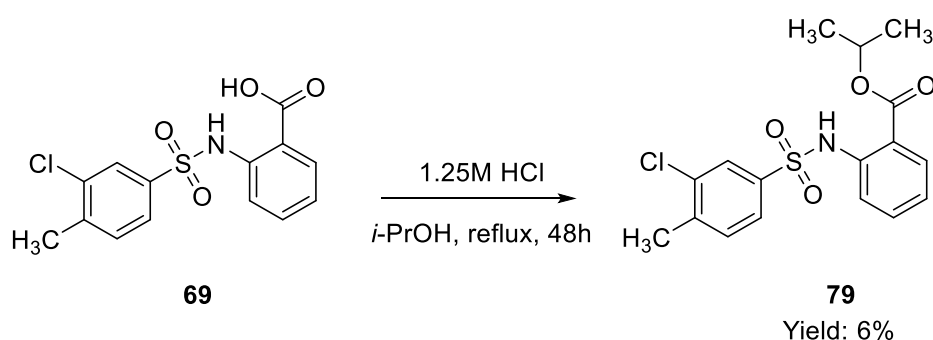
Scheme 3.3.5.1 shows the synthetic strategy applied to obtain **78**, the isopropyl derivative of **21**.



Scheme 3.3.5.1: Synthesis of compound 78.

The isopropyl 2-aminobenzoate was obtained via Fisher esterification of the anthranilic acid. The procedure followed is the General Procedure 7, however in this case the time of the reaction was increased to 48 hours. Nevertheless, only a partial conversion of the starting material into the corresponding isopropyl ester was reached, probably due to the low reactivity of the isopropyl alcohol. Considering the low yield obtained, an alternative strategy which aims to increase the reactivity of the starting acid was also attempted. Consequently, the chlorination of the anthranilic acid by reaction with thionyl chloride and the following reaction with *i*-PrOH was performed. However, this approach was unsuccessful giving an even lower yield (11%). Therefore, the 19% yield obtained through the Fisher esterification was the best result achieved. The following step involves the reaction with sulfonyl chloride **1** to give the final product **78**. The procedure applied is General Procedure 2. In this case, the reaction did not reach completion, probably because of the decreased reactivity of the amino group which is sterically hindered by the isopropyl group, thus explaining the low yield obtained.

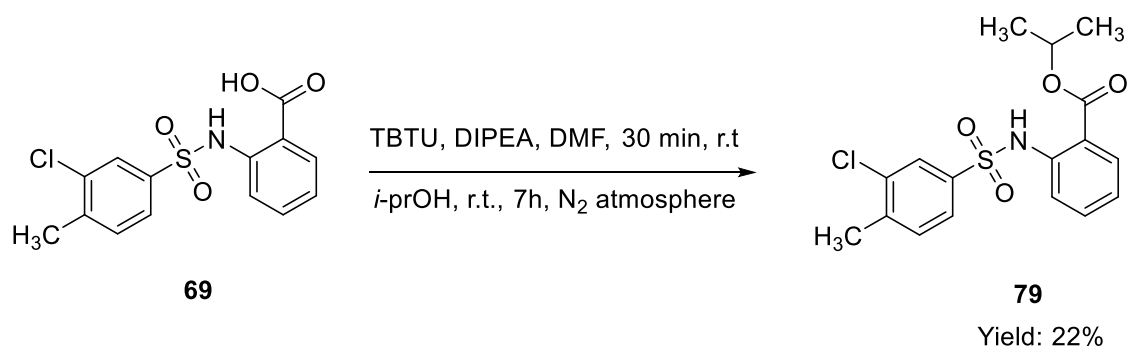
Compound **79**, the isopropyl derivative of **43**, was obtained via esterification of the carboxylic acid derivative **69**. Two different synthetic strategies were applied. The first attempt was the Fisher esterification shown in scheme 3.3.5.2



Scheme 3.3.5.2: Synthesis of compound 79.

Unfortunately, also in this case the conversion to the isopropyl ester was extremely low, and after 48 hours only the 6% of product was formed. An alternative synthetic approach which involves the

use of the coupling agent 2-(1H-benzotriazol-1-yl)-N,N,N',N'-tetramethylamminium tetrafluoroborate (TBTU) was considered. The reaction scheme is shown in scheme 3.3.5.3



Scheme 3.3.5.3: Synthesis of compound 79.

The procedure followed for this reaction is reported in the Experimental Section. The mechanism of the reaction implicates different steps. The first step is the formation of the carboxylate anion which reacts with TBTU. The following decomposition of the resulting tetrahedral intermediate promotes the addition of the benzotriazole derivative to the carbonyl centre generating the activated carbonyl group which reacts with the alcohol, eventually leading to the formation of the corresponding ester and a by-product soluble in water. Figure 3.3.5.1 illustrates the reaction mechanism.

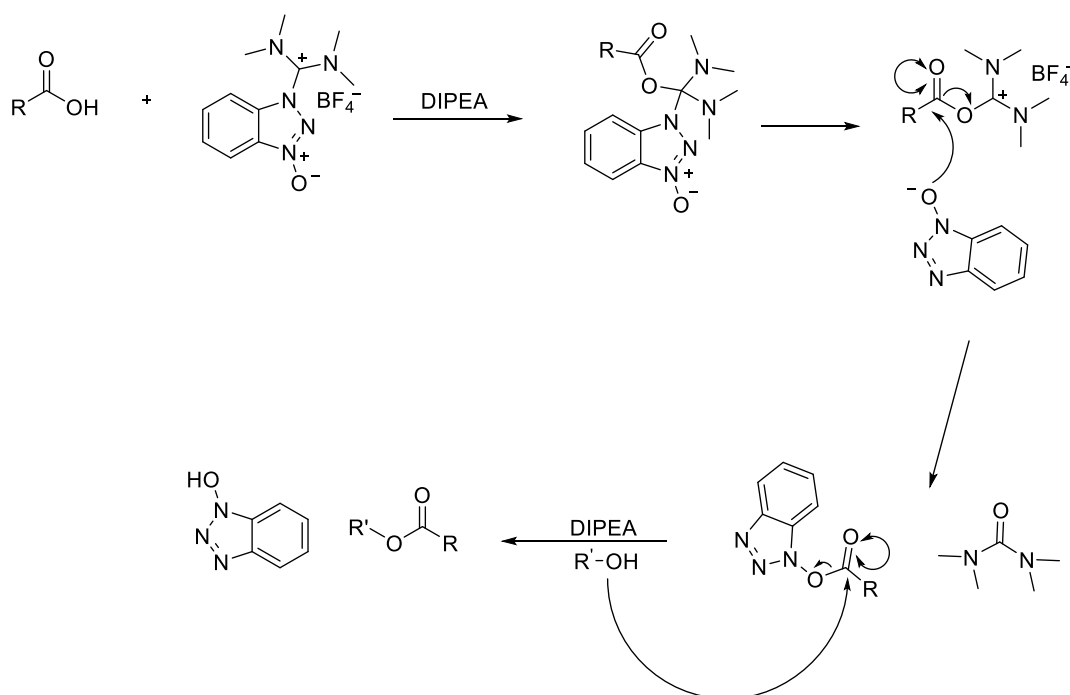
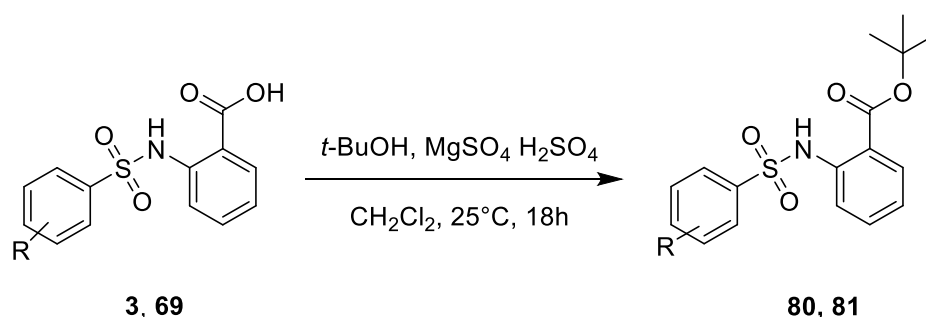


Fig 3.3.5.1: Esterification mechanism using the coupling reagent TBTU.

Although the percentage of product formed was much higher compared to the Fisher esterification, only 22% yield was obtained. This low value is due to the formation of different impurities which did not allow the complete isolation of the pure product, although several purification processes

were performed. However, using this alternative synthetic strategy, a slight optimisation of the yield was achieved.

The *tert*-butyl derivatives **80** and **81** were synthesised following the General Procedure 8 reported in the Experimental Section. The reaction scheme is shown in scheme 3.3.5.4.



Scheme 3.3.5.4: Synthesis of compounds 80-81.

The procedure applied is commonly used for the synthesis of *tert*-butyl esters and it involves the reaction between the carboxylic acid and the tertiary alcohol in the presence of H₂SO₄ absorbed on MgSO₄. Compounds and corresponding yields obtained are shown in table 3.3.5.1.

Product	Structure	Yield
80		20%
81		22%

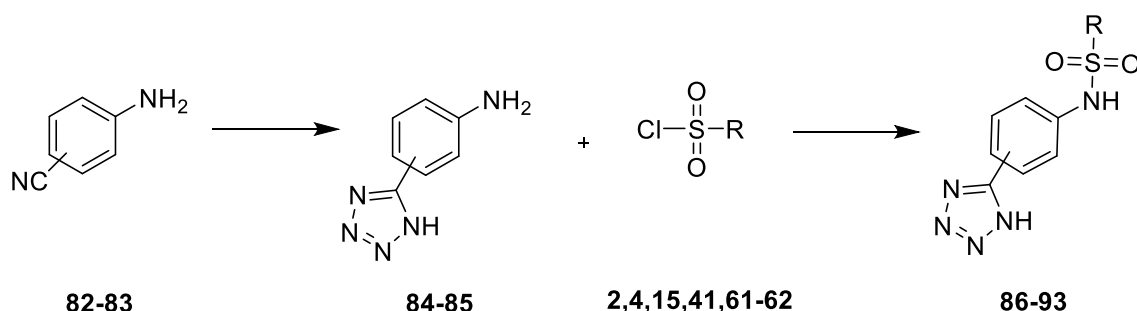
Table 3.3.5.1: Compounds 80-81.

In both reactions, only a partial conversion of the starting material was observed, thus explaining the low yields obtained.

3.3.6 Synthesis of (arylsulfonamido)N-(1H-tetrazol-5-yl)phenyls (86-93)

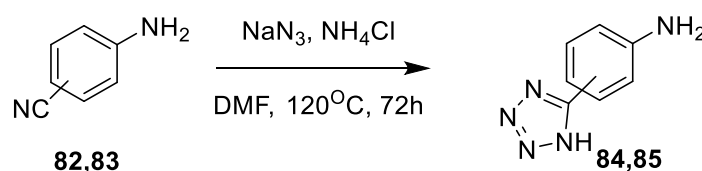
The replacement of the carboxylic acid moiety with a tetrazole group characterises compounds **86-93**. Tetrazoles are the most common carboxylic acid bioisosteres. ⁽¹⁾ Compared to the carboxylic acid groups, tetrazoles show similar planarity and acidity. However, the higher lipophilicity of the tetrazolate anions might result in a better permeability across the cellular membrane. ⁽⁴⁾ Moreover, the metabolic product deriving from the N-glucuronidation of the tetrazole group is less reactive

than the O-glucuronidated derivatives generated from carboxylic acids, thus implying minor cytotoxicity effects. ⁽⁵⁾ Different tetrazole derivatives were synthesised. Scheme 3.3.6.1 shows the synthetic pathway.



Scheme 3.3.6.1: Synthetic pathway applied for the synthesis of the tetrazole derivatives.

The first step involves the synthesis of the *ortho* and *para* substituted (1H-tetrazol-5-yl)anilines. The reaction, carried out in the presence of sodium azide and ammonium chloride, is shown in scheme 3.3.6.2 and General Procedure 9 applied is reported in the Experimental Section.



Scheme 3.3.6.2: Synthesis of compounds 84-85.

The reaction occurs via a concerted 1-3 dipolar cycloaddition where the dipolarophile is represented by the aminobenzonitrile, whilst the azide is the 1-3 dipolar species. The mechanism of reaction is shown in figure 3.3.6.1.

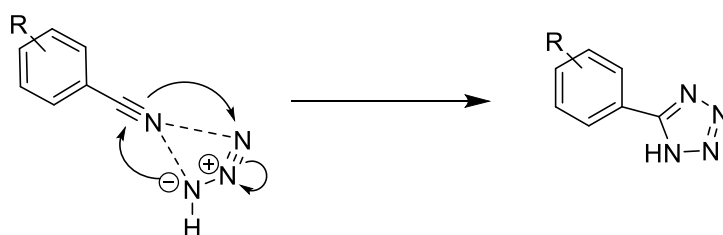
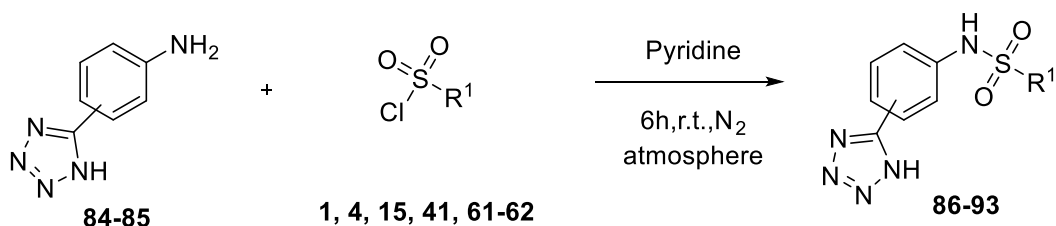


Fig 3.3.6.1: Concerted 1-3 dipolar cycloaddition mechanism.

Following this reaction, the *ortho* (**84**) and *para* (**85**) substituted (1H-tetrazol-5-yl) anilines were obtained with a yield of 53% and 33% respectively. The low yield obtained for 85 is mainly due to the loss of product in the aqueous layer during the extraction process. For 84, an alternative method involving solvent evaporation and purification by column chromatography was attempted and the yield was increased to 53%. The final tetrazole derivatives 86-93 were obtained by reaction of 84 and 85 with the corresponding sulfonyl chlorides, following the reaction described in paragraph

3.4.1. The reaction scheme is shown in scheme 3.3.6.3, while table 3.3.6.1 reports the structure of 86-93 and the corresponding yields obtained.



Scheme 3.3.6.3: Synthesis of compounds 86-93.

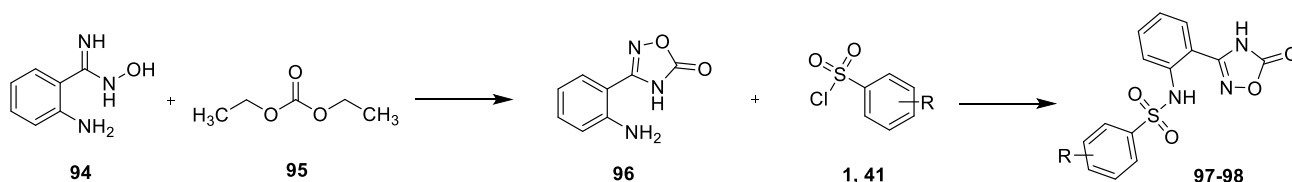
(1H-tetrazol-5yl)aniline	R ¹	Product	Yield%
4-(1H-tetrazol-5yl)aniline (85)	(2,4-dichloro-5-methyl)phenyl (1)	86	46%
4-(1H-tetrazol-5yl)aniline (85)	3-chloro-4-methyl (41)	87	18%
2-(1H-tetrazol-5yl)aniline (84)	(2,4-dichloro-5-methyl)phenyl (1)	88	18%
2-(1H-tetrazol-5yl)aniline (84)	3-chloro-4-methyl (41)	89	16%
2-(1H-tetrazol-5yl)aniline (84)	(4-trifluoromethyl)phenyl (4)	90	42%
2-(1H-tetrazol-5yl)aniline (84)	2-naphthalene (15)	91	38%
2-(1H-tetrazol-5yl)aniline (84)	8-quinoline (62)	92	26%
2-(1H-tetrazol-5yl)aniline (84)	3-quinoline (63)	93	46%

Table 3.3.6.1: Compounds 86-93.

Although this reaction worked well in terms of amount of product formed, some of the derivatives were obtained with poor yields (<20%). This is mostly due to the fact that some derivatives required different recrystallisation steps, which contributed to reduce the amount of product obtained.

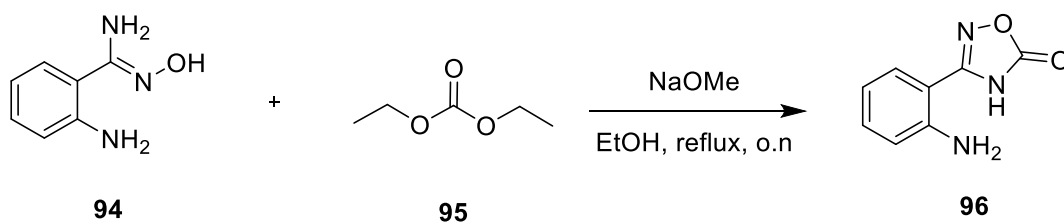
3.3.7 Synthesis of (arylsulfonamido)N-(5-oxo-2,5-dihydro-1,2,4-oxadiazol-3-yl)phenyls (97-98)

In **97-98** the carboxylic acid group was replaced with a 5-oxo-1,2,4-oxadiazole ring. This moiety is characterised by a planar acidic heterocycle and it has been reported to be more lipophilic than the tetrazole ring, representing therefore a good carboxylic acid surrogate. ^(1, 6) In order to explore whether the replacement of the carboxylic acid function with the 5-oxo-1,2,4-oxadiazole ring may improve the cell membrane permeability, the synthesis of the oxadiazole derivatives of **3** and **43** was performed. Scheme 3.3.7.1 shows the reaction scheme for the synthesis of **97-98**.



Scheme 3.3.7.1: Synthetic pathway applied for the synthesis of compounds 97-98.

The 5-oxo-1,2,3-oxadiazole intermediate (**96**) was obtained reacting the 2-aminobenzamidoxime (**94**) with diethyl carbonate (**95**) in basic conditions, as reported in scheme 3.3.7.2, following the procedure reported in the Experimental Section.



Scheme 3.3.7.2: Synthesis of compound 96.

The reaction mechanism, shown in figure 3.3.7.1, involves the initial deprotonation of the -OH group, which is followed by attack of the anion generated at the oxygen atom, on the carbonyl group. The formation of the tetrahedral species and the subsequent loss of EtOH, generate an intermediate which, following the attack of the nitrogen atom on the carbonyl group, and the loss of another molecule of EtOH, cyclises to give the desired product **96**, with a yield of 58%.⁽⁷⁾

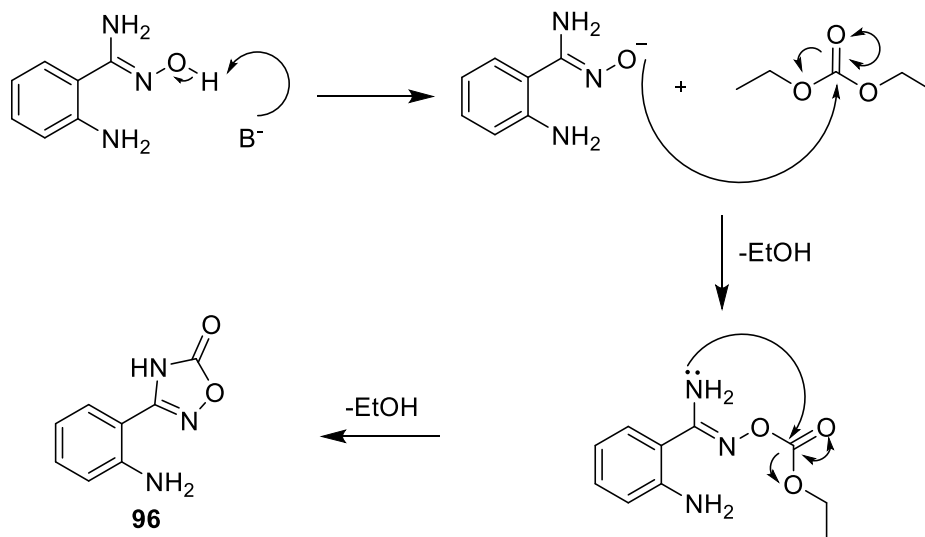
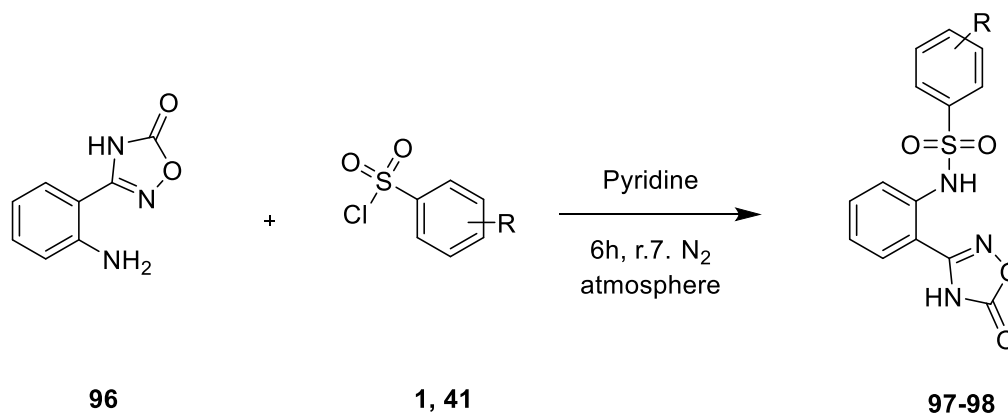


Fig 3.3.7.1: Reaction mechanism for the synthesis of compound 96.

Reaction of **96** with sulfonyl chlorides **1** and **41** was performed in order to obtain the desired final products **97-98**, following the reaction described in paragraph 3.3.1 and reported in scheme 3.3.7.3, while table 3.3.7.1 illustrates the structure of the two 5-oxo-1,2,4-oxadiazole derivatives.

Starting Sulfonyl Chloride	R	Product
1	2,4-dichloro-5-methyl	97
41	3-chloro-4-methyl	98

Table 3.3.7.1: Compounds 97-98.



Scheme 3.3.7.3: Synthesis of compounds 97-98.

When the synthesis of **97** and **98** was attempted, the formation of several by-products was observed. Although, following a series of chromatographic purifications, **97** and **98** were isolated with a yield of 7% and 2% respectively, $^1\text{H-NMR}$, HPLC and mass spectrometry analyses revealed degradation of the 5-oxo-1,2,4-oxadiazole ring. According to the results obtained from the analyses performed, in both cases, the decarboxylation of the 5-oxo-1,2,4-oxadiazole ring occurs, leading to the formation of the corresponding amidine. Degradation of the two products was assessed by repeating $^1\text{H-NMR}$, HPLC and MS analyses of the isolated compounds **97** and **98** after 24 hours. Table 3.3.7.2 summarises the data obtained, and the structure of the degraded products is shown in figure 3.3.7.2.

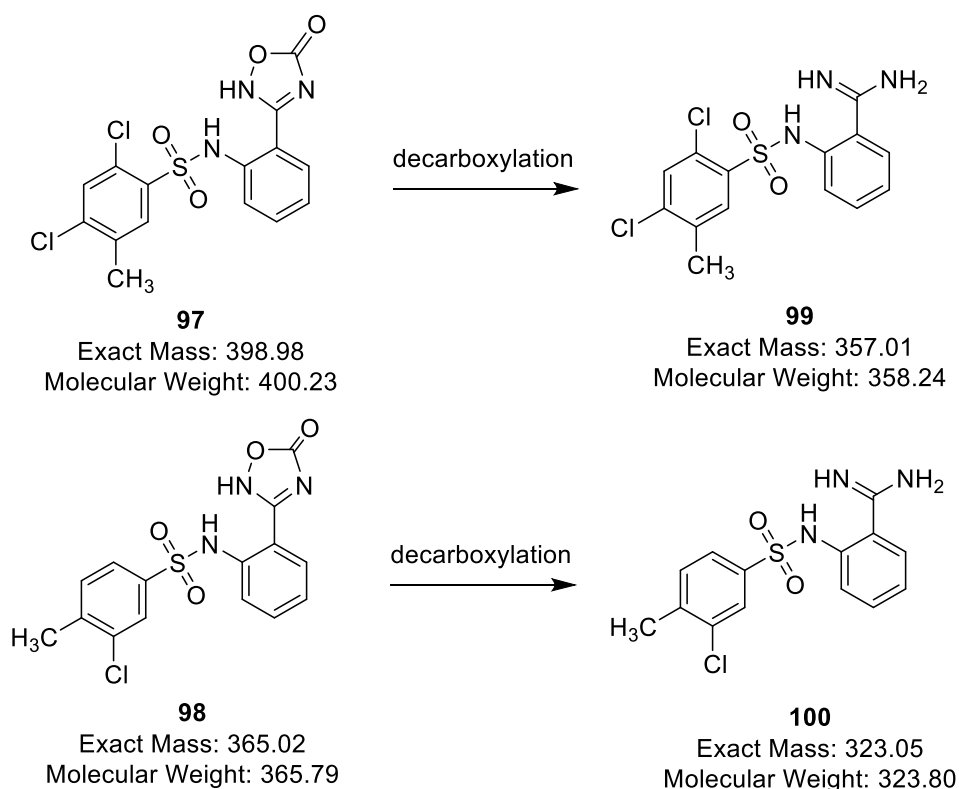


Figure 3.3.7.2: Compounds 97-98 and corresponding amidine species 99-100.

Before 24h	After 24h	
Ratio (%)	Ratio (%)	MS (ESI) ⁺
97 (95.86%): 99 (4.14%)	97 (92.41%): 99 (7.59%)	402.07:358.06
98 (95.96%): 100 (3.30%)	98 (85.72%): 100 (12.94%)	366.18:324.12

Table 3.3.7.2: HPLC and MS analyses.

Interestingly, the decarboxylation of the oxadiazole ring seems to be promoted by the presence of a sulfonamide group, indeed, when the sulphonamide linker was replaced by an amine moiety, which will be discussed in Chapter 4, this phenomenon was not observed. Therefore, considering the stability problems associated with the 5-oxo-1,2,4-oxadiazole ring, this series of derivatives was discarded.

3.3.8 Synthesis of alkyl(arylsulfonamido)benzamides (101-106)

Analogue **101-106** are characterised by the replacement of the methyl ester of compounds **21** and **43** with differently substituted carboxamides in order to increase the hydrolytic stability of these molecules. The synthetic strategy applied to obtain the carboxamide derivatives involves the use of the coupling reagent N-N' carbonyldiimidazole (CDI), which allows the direct amidation of carboxylic acids, and the reaction mechanism is shown in figure 3.3.8.2. Initially the carboxylic acid reacts with CDI generating the acyl carboxy imidazole and imidazole. The two intermediates immediately react

together to form the activated acylimidazole which will be attacked by the nitrogen atom of the amine giving the desired product.

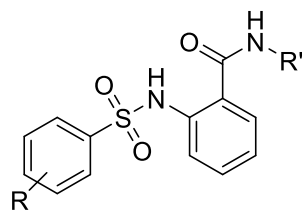


Fig 3.3.8.1: General scaffold of the carboxamide derivatives (101-106).

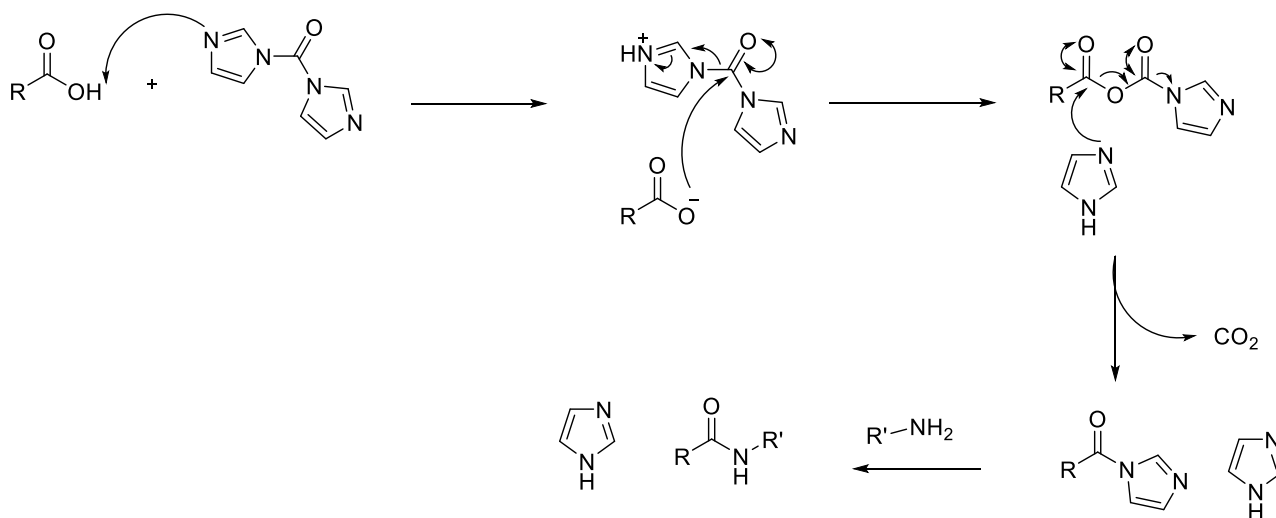
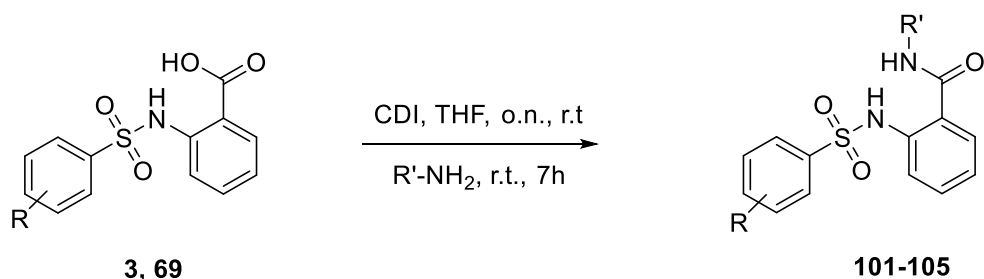


Fig 3.3.8.2: Reaction mechanism for the synthesis of the carboxamide derivatives.

The starting carboxylic acid and CDI were stirred overnight in order to allow the formation of the activated species, and then the desired amine was added following General Procedure 10 reported in the Experimental Section. The scheme of the reaction for the synthesis of the substituted carboxamide derivatives is reported in scheme 3.3.8.1, products obtained and their corresponding yields are shown in table 3.3.8.1.



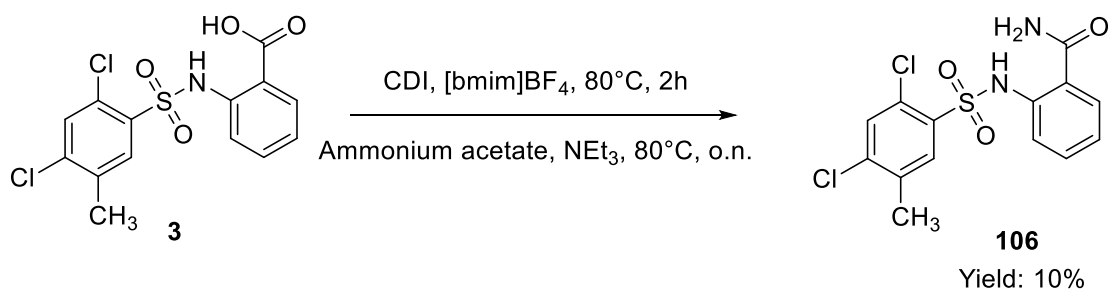
Scheme 3.3.8.1: Synthesis of derivatives 101-105.

Starting carboxylic acid	R	R'	Product	Yield%
69	3-chloro-4-methyl	-methyl	101	30%
3	2,4-dichloro-5-methyl	-methyl	102	49%
3	2,4-dichloro-5-methyl	-ethyl	103	44%
3	2,4-dichloro-5-methyl	-dimethyl	104	35%
3	2,4-dichloro-5-methyl	-isopropyl	105	53%

Table 3.3.8.1: Compounds 101-105.

Generally the reaction worked well, with only two compounds (**101** and **105**) giving poor yields (<40%.) The low yield obtained for **101** can be explained by the loss of product during the different purification techniques (flash column chromatography and recrystallisation) required for the complete purification of the compound. In the case of **104** the reaction was slow and even after stirring the reaction overnight the activated species did not react completely, giving only 35% of the desired product.

In order to obtain the primary carboxamide derivative of **3** the conditions of the reaction were slightly changed. The organic solvent was replaced by the 1-butyl-3-methylimidazolium tetrafluoroborate ([bmim]BF₄) ionic liquid in order to promote the solubility of the ammonium acetate which was used as source of ammonia. The scheme of the reaction is shown in scheme 3.3.8.2, and the procedure applied is reported in the Experimental Section.



Scheme 3.3.8.2: Synthesis of derivative 106.

Although this procedure has been reported as an effective method for the synthesis of the primary carboxamide, ⁽⁸⁾ the product was obtained in a very low yield (10%). Unfortunately, the starting carboxylic acid and the activated acylimidazole were the main species obtained from the reaction, while only a small amount of product, corresponding to the 10 % yield, was formed.

3.4 Conclusions

Starting from the structure of the hit **3**, 60 sulfonamide derivatives were designed, with the aim of obtaining new molecules showing a better pharmacokinetic profile and improved activity compared to hit **3**. Several modifications on the original structure were considered. The carboxylic acid moiety was replaced by different groups such as alkyl esters, tetrazole, oxadiazole and carboxamide groups. On the other side changes on the hydrophobic ring were also explored, including the introduction of various hydrophobic substituents, as well as the replacement with different heterocycles and bigger aromatic rings. Different synthetic strategies were developed, and all the designed derivatives were synthesised. Unfortunately, compounds belonging to the 5-oxo-1,2,4-oxadiazole series showed stability issues, therefore this family was discarded. The newly synthesised derivatives were biologically evaluated in order to assess their ability to sensitise breast cancer cells and breast cancer stem cells to TRAIL. The results obtained will be discussed in the Biological Evaluation chapter.

3.5 References

- 1: Ballatore, C.; Huryn, D. M.; Smith, A. B. Carboxylic acid (bio)isosteres in drug design. *ChemMedChem*. **2013**, *8*, 385-395.
- 2: Hayward, O. Design and Synthesis of Molecular Inhibitors of c-FLIP Activity as a Therapeutic Strategy to Target Breast Cancer Stem Cells. PhD Thesis. **2015**, Cardiff University.
- 3: Savoie, P. R.; Welch, J. T. Preparation and utility of organic pentafluorosulfonyl-containing compounds. *Chem. Rev.* **2015**, *115*, 1130-1190.
- 4: Herr, R. J. 5-Substituted-1H-tetrazoles as carboxylic acid isosteres: medicinal chemistry and synthetic methods. *Bioorg. Med. Chem.* **2002**, *10*, 3379-3393.
- 5: Gardner, I.; Obach, R. S.; Smith, D. A.; Miao, Z.; Alex, A. A.; Beaumont, K.; Kalgutkar, A.; Walker, D.; Dalvie, D.; Prakash, C.; Alf, V. Carboxylic acids and their bioisosteres. In *Metabolism, Pharmacokinetics and Toxicity of Functional Groups: Impact of Chemical Building Blocks on ADMET.*; Smith, D. A, Ed.; RSC Publishing: Cambridge, 2010; pp 99-167.
- 6: Kohara, J.; Kubo, K.; Imamiya, E.; Wada, T.; Inada, Y.; Naka, T. Synthesis and angiotensin II receptor antagonistic activities of benzimidazole derivatives bearing acid heterocycles as novel tetrazole bioisosteres. *J. Med. Chem.* **1996**, *39*, 5228-5235.
- 7: Barros, C. J. P.; De Souza, Z. C.; De Freitas, J. J. R.; Da Silva, P. B. N.; Militao, G. C. G.; Da Silva, T. G.; Freitas, J. C. R.; De Freitas Filho, J. R. A convenient synthesis and cytotoxic activity of 3-aryl-5-pentyl-1,2,4-oxadiazoles from carboxylic acid, esters and arylamidoximes under solvent-free conditions. *J. Chil. Chem. Soc.* **2014**, *59*, no.1.
- 8: Kwan S. L.; Kee D. K. Efficient synthesis of primary amides from carboxylic acid using N,N'-carbonyldiimidazole and ammonium acetate in ionic liquid. *Synth. Comm.* **2011**, *41*, 3497-3500.

Chapter 4

Amine Derivatives

Chapter 4: Amine Derivatives

4.1 Design of amine derivatives

This series of analogues was developed in order to investigate whether the replacement of the sulfonamide linker by an amine group affects the activity of the compounds. The general scaffold of this new series of derivatives, represented by an amine group which links two differently substituted aromatic rings, is shown in figure 4.1. The new amine linker retains the original tetrahedral geometry required for the adjustment of the molecules to the curved-shaped cavity of the c-FLIP pocket, as well as the original distance between the two aromatic rings. However, in order to explore whether increasing the length and the flexibility of the linker might affect the ability of the two rings to occupy the pocket of c-FLIP, molecules showing an elongated linker were also designed. Moreover, with the aim to carry out structure-activity relationships studies, a further modification to the linker, involving the inversion of the -NH group ($R-NH-CH_2-R'$), was considered. All the designed amine derivatives retain the carboxylic acid function in the *ortho* or *meta* position of the original anthranilic ring. However, using the same criteria discussed in chapter 3, the substitution of the carboxylic acid moiety with a methyl ester group, or with the carboxylic acid bioisosteres, tetrazole and oxadiazole rings, was also considered. On the other side, modifications designed for the hydrophobic ring were mostly selected according to the early biological data obtained for the sulfonamide derivatives, which will be discussed in the Biological Evaluation chapter. Those hydrophobic substituents that gave the best biological results were introduced in the amine series. The replacement of the original phenyl ring with bigger aromatic rings such as naphthalene and quinoline, and with the heterocycle pyridine was also explored. Considering the features described above, 33 new derivatives were designed, and they are listed in table 4.1.

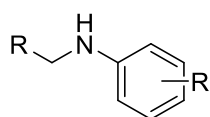


Fig 4.1: Central scaffold of the amino derivatives

Molecule	R	R'
113	(4-trifluoromethyl)phenyl	2-carboxylic acid
114	(4-trifluoromethyl)phenyl	3-carboxylic acid
115	(3,4-dimethyl)phenyl	2-carboxylic acid
116	(3,4-dimethyl)phenyl	3-carboxylic acid
117	(3-chloro-4-methyl)phenyl	2-carboxylic acid

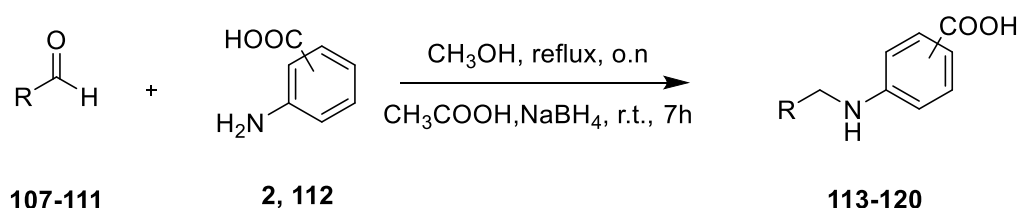
118	(3-chloro-4-methyl)phenyl	3-carboxylic acid
119	8-quinoline	2-carboxylic acid
120	2-quinoline	2-carboxylic acid
121	(4-trifluoromethyl)phenyl	2-methyl ester
122	(4-trifluoromethyl)phenyl	3-methyl ester
123	(3,4-dimethyl)phenyl	2-methyl ester
124	(3,4-dimethyl)phenyl	3-methyl ester
129	(3-chloro-4-methyl)phenyl	2-methyl ester
130	(3-chloro-4-methyl)phenyl	3-methyl ester
131	3-pyridine	2-methyl ester
132	4-pyridine	2-methyl ester
133	2-naphtalene	2-methyl ester
134	1-naphtalene	2-methyl ester
137	benzyl	2-methyl ester
138	(4-trifluoromethyl)phenyl	2-methyl ester
139	3-pyridine	2-carboxylic acid
140	4-pyridine	2-carboxylic acid
141	2-naphtalene	2-carboxylic acid
142	1-naphtalene	2-carboxylic acid
143	(4-trifluoromethyl)phenyl	2-carboxylic acid
144	(4-trifluoromethyl)phenyl	2-(1H-tetrazole)
145	(3-chloro-4-methyl)phenyl	2-(1H-tetrazole)
146	(3-chloro-4-methyl)phenyl	4-(1H-tetrazole)
147	8-quinoline	2-(1H-tetrazole)
148	2-quinoline	2-(1H-tetrazole)
149	2-naphtalene	2-(1H-tetrazole)
150	(3-chloro-4-methyl)phenyl	2-(5-oxo-4,5-dihydro-1,2,4-oxadiazol)
155	2-methylbenzoic acid	3-chloro-4-methyl
156	2-methylbenzoic acid	5-chloro-2-methyl
157	2-methylbenzoic acid	4-(trifluoromethyl)

Table 4.1: Designed amine derivatives.

4.2 Synthesis of amine derivatives

4.2.1: Synthesis of (aryl)amino)benzoic acids (113-120)

Some of the carboxylic acid derivatives of the amine series were obtained via reductive amination of the appropriate aldehyde using *ortho* or *meta* aminobenzoic acid, and sodium borohydride (NaBH_4) as reducing agent. The reaction scheme is shown in scheme 4.2.1, and the mechanism of the reaction is illustrated in figure 4.2.1. Initially, the aldehyde and the aminobenzoic acid react to form a Schiff base intermediate which will be reduced by NaBH_4 in the presence of acetic acid.



Scheme 4.2.1: Synthesis of compounds 113-120.

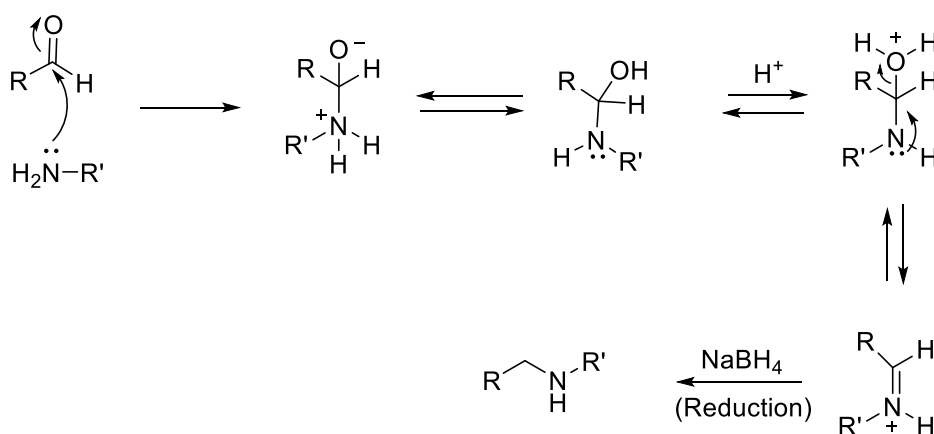


Figure 4.2.1: Reductive amination mechanism.

Following General Procedure 11 reported in the Experimental Section, derivatives **113-120** were obtained. The substituents belonging to each analogue, and the corresponding yields obtained are shown in table 4.2.1.

Starting aldehyde	R	-COOH	Product	Yield
107	4-(trifluoromethyl)phenyl	2-COOH (2)	113	17%
107	4-(trifluoromethyl)phenyl	3-COOH (112)	114	20%
108	(3,4-dimethyl)phenyl	2-COOH (2)	115	52%
108	(3,4-dimethyl)phenyl	3-COOH (112)	116	26%
109	(3-chloro-4-methyl)phenyl	2-COOH (2)	117	21%

109	(3-chloro-4-methyl)phenyl	3-COOH (112)	118	28%
110	8-quinoline	2-COOH (2)	119	43%
111	3-quinoline	2-COOH (2)	120	41%

Table 4.2.1: Compounds 113-120.

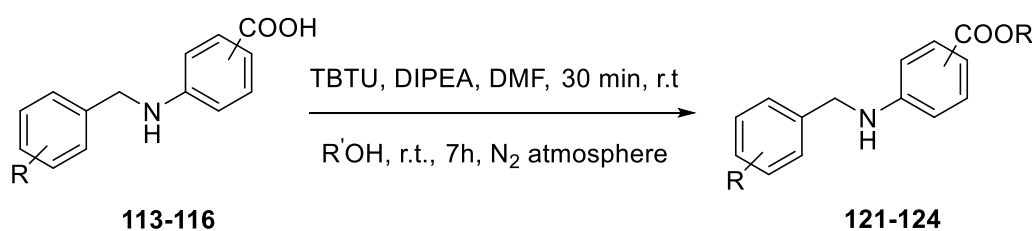
Unfortunately, poor yields were obtained for most of the new compounds. All the derivatives showing a yield less than 30% required at least two flash column chromatography purifications followed by recrystallisation. Therefore, the low yields obtained were mainly due to the loss of product during the several purification processes.

4.2.2 Synthesis of methyl((aryl)amino)benzoates (**121-124**, **129-134**, **137-138**)

Derivatives **121-124** and **129-134** are characterised by the replacement of the carboxylic acid function with a methyl ester group. This modification was carried out with the aim to increase the lipophilicity of the compounds in order to enhance their ability to cross the cellular membrane. Two main reactions were used to obtain the methyl ester derivatives.

4.2.2.1 Synthesis of methyl((aryl)amino)benzoates (**121-124**)

Methyl ester derivatives **121-124** were synthesised via esterification of the corresponding carboxylic acids **113-116**. The procedure used is General Procedure 11 reported in the Experimental Section and it involves the use of the coupling agent TBTU in the presence of DIPEA. The reaction scheme is shown in scheme 4.2.2.1 and the reaction follows the same mechanism explained in paragraph 3.3.5 in Chapter 3.



Scheme 4.2.2.1: Synthesis of derivatives 121-124.

In table 4.2.2.1 are listed the derivatives synthesised and the corresponding yields obtained.

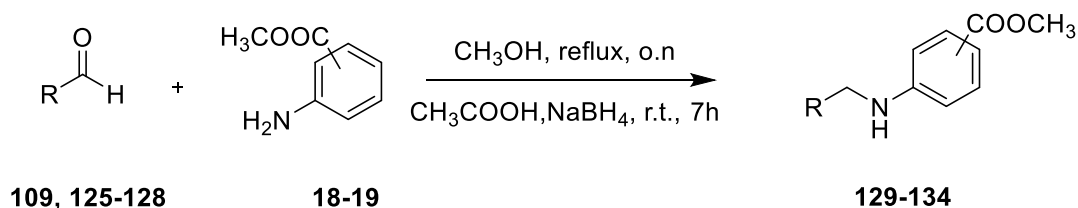
Product	R	R'	Yield
121	4-trifluoromethyl	2-COOCH ₃	44%
122	4-trifluoromethyl	3-COOCH ₃	38%
123	3,4-dimethyl	2-COOCH ₃	13%
124	3,4-dimethyl	3-COOCH ₃	26%

Table 4.2.2.1: Compounds 121-124.

Although all the desired products were obtained, the reaction did not give a complete conversion of the starting carboxylic acids, even after the reaction time was increased from 7 hours to 15 hours. Moreover, the complete purification of **123** and **124** required repeated flash column chromatography, thus contributing to the decrease of the yield to 13% and 26% respectively.

4.2.2.2: Synthesis of methyl((aryl)amino)benzoates (129-134)

Scheme 4.2.2.2. shows the reaction scheme for the synthesis of the derivatives **129-134**, which were obtained via reductive amination of the appropriate aldehydes, following General Procedure 11 and the reaction explained in paragraph 4.2.1.



Scheme 4.2.2.2: Synthesis of derivatives 129-134.

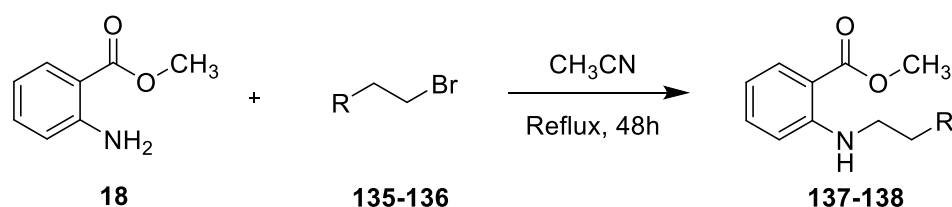
In most cases this reaction worked well and the desired products were obtained in good yields. Only compound **129** was obtained with a yield of 26% due to the different purification processes required.

Starting aldehyde	R	-COOCH ₃	Product	Yield
109	(3-chloro-4-methyl)phenyl	2-COOCH ₃ (18)	129	26%
109	(3-chloro-4-methyl)phenyl	3-COOCH ₃ (19)	130	83%
125	3-pyridine	2-COOCH ₃ (18)	131	96%
126	4-pyridine	2-COOCH ₃ (18)	132	95%
127	2-naphthalene	2-COOCH ₃ (18)	133	76%
128	1-naphthalene	2-COOCH ₃ (18)	134	79%

Table 4.2.2.2: Compounds 129-134.

4.2.2.3 Synthesis of methyl((aryl)amino)benzoates (137-138)

In derivatives **137-138** the amine linker was elongated by adding an additional carbon atom. As shown in scheme 4.2.2.3, these derivatives were obtained via nucleophilic substitution occurring between the methyl-2-amino benzoate and differently substituted bromides, following the procedures reported in the Experimental Section. Table 4.2.2.3. reports the structure of the two compounds obtained and the corresponding yields.



Scheme 4.2.2.3: Synthesis of compounds 137-138.

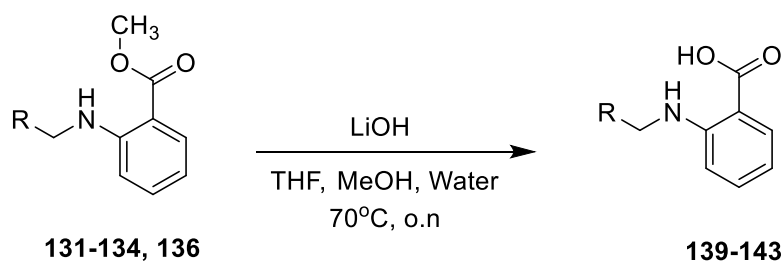
Starting bromide	R	Product	Yield
135	benzyl	137	5%
136	4-(trifluoromethyl)phenyl	138	26%

Table 4.2.2.3: Compounds 137-138.

Compounds **137** and **138** were obtained in low yields. Unfortunately, in both cases, even after the time of the reaction was increased to 48 hours, the T.L.C showed the presence of the two unreacted starting materials with only a small amount of the desired products formed. Therefore, **137** was isolated and obtained in 5% yield, whilst only traces of **138** were collected after the purification process. In order to obtain a higher amount of compound **138**, the same reaction was carried out in basic conditions, which increased the percentage of product formed, giving a yield of 26%.

4.2.3 Synthesis of (aryl)amino)benzoic acids (139-143)

The carboxylic acid derivatives **139-143** were obtained via hydrolysis of the corresponding methyl esters. The reaction scheme is shown in scheme 4.2.3 and the procedure followed is General Procedure 13 in the Experimental Section. The structure of the derivatives obtained and the corresponding yields are reported in table 4.2.3. In the majority of the cases, the hydrolysis of the starting methyl ester reached completion, therefore, the low yields obtained are mainly due to the loss of product during the purification process.



Scheme 4.2.3: Synthesis of compounds 139-143.

Starting aldehyde	R	Product	Yield
131	3-pyridine	139	28%
132	4-pyridine	140	26%
133	2-naphthalene	141	89%
134	1-naphthalene	142	41%
136	(4-trifluoromethyl)benzyl	143	16%

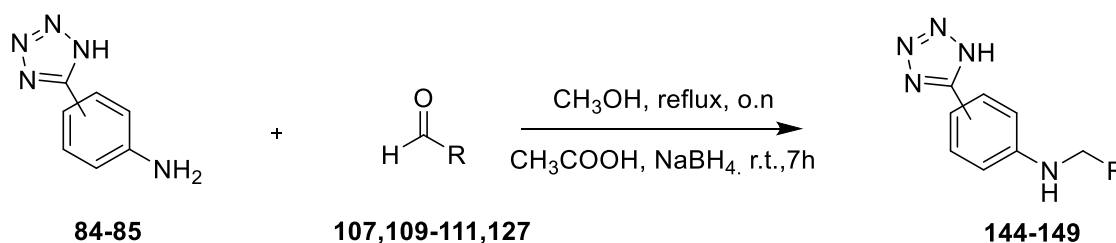
Table 4.2.3: Compounds 139-143.

4.2.4 Synthesis of derivatives 144-149, 150

As discussed in Chapter 3, the advantage of replacing a carboxylic acid with bioisostere groups such as a tetrazole or oxadiazole ring is represented by their higher lipophilicity compared to the carboxylic acid function and the less reactivity of their metabolic products, whilst retaining similar acidity and planarity.⁽¹⁾ A few amine derivatives showing the tetrazole and the oxadiazole group were designed.

4.2.4.1 Synthesis of ((aryl)amino)N-(1H-tetrazol-5-yl)phenyl (144-149)

The tetrazole derivatives were obtained via reductive amination of the appropriate aldehyde with the (1H-tetrazol-5-yl)anilines, previously synthesised and discussed in paragraph 3.3.6, following General Procedure 11. The reaction scheme is shown in scheme 4.3.4.1, while the derivatives obtained are shown in table 4.2.4.1



Scheme 4.2.4.1: Synthesis of compounds 144-149.

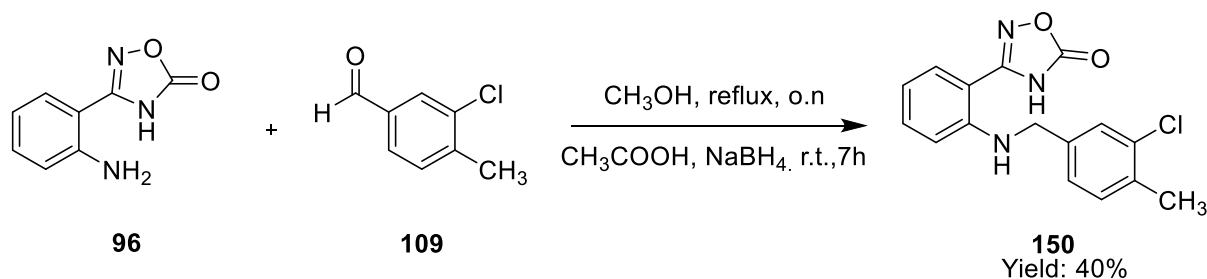
Starting aldehyde	R	(1H-tetrazol-5yl)aniline	Product	Yield
107	4-(trifluoromethyl)phenyl	2-(1H-tetrazol-5yl)aniline (84)	144	32%
109	(3-chloro-4-methyl)phenyl	2-(1H-tetrazol-5yl)aniline (84)	145	25%
109	(3-chloro-4-methyl)phenyl	4-(1H-tetrazol-5yl)aniline (85)	146	15%
110	8-quinoline	2-(1H-tetrazol-5yl)aniline (84)	147	12%
111	2-quinoline	2-(1H-tetrazol-5yl)aniline (84)	148	11%
127	2-naphthalene	2-(1H-tetrazol-5yl)aniline (84)	149	75%

Table 4.2.4.1: Compounds 144-149.

Despite the complete reductive amination of the starting aldehydes **107**, **109-111** and **127**, assessed by T.L.C., different purification processes were required to isolate the final products from the starting anilines **84** and **85**, thus explaining the low yields obtained.

4.2.4.2 Synthesis of (arylamino)N-(5-oxo-2,5-dihydro-1,2,4-oxadiazol-3-yl)phenyl (**150**)

The derivative **150**, which is characterised by the presence of the oxadiazole ring, was obtained via reductive amination of aldehyde **109** with the 3-(2-aminophenyl)-1,2,4-oxadiazol-5(4H)-one (**96**) as shown in scheme 4.2.4.2.

Scheme 4.2.4.2: Synthesis of compound **150**.

Considering the stability issues observed for the corresponding sulfonamide derivatives **97-98**, further $^1\text{H-NMR}$, HPLC and MS analyses were performed in order to assess whether degradation of the oxadiazole ring occurs for compound **150**. Interestingly, according to the results obtained from these analyses, no changes in the structure of **150** was observed after 24 hours and 7 days. These results suggest a potential role of the sulphonamide group in promoting this phenomenon. Therefore, considering the stability of **150**, this derivative was biologically evaluated.

4.2.5: Synthesis of 2-(((aryl)amino)methyl)benzoic acids (**155-157**)

In order to investigate whether changing the disposition of the $-\text{CH}_2\text{-NH}-$ linker may affect the ability of compounds to occupy the cavity of c-FLIP, the inversion of the amine linker was considered.

Therefore, a small series of derivatives showing the -NH group bound to the hydrophobic aromatic ring (figure 4.2.5.1) was designed. Table 4.2.5.1 shows the structure of the designed derivatives.

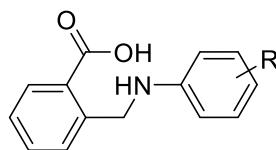
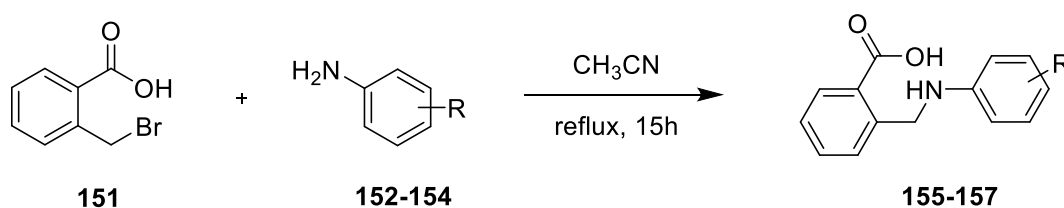


Fig 4.2.5.1: General scaffold of derivatives showing an inverted amine linker.

R	Product
3-chloro-4-methyl	155
5-chloro-2-methyl	156
4-(trifluoromethyl)	157

Table 4.2.5.1: Designed derivatives.

Initially, in order to obtain derivatives **155-157**, a nucleophilic displacement of the 2-(bromomethyl)benzoic acid by differently substituted anilines was attempted, as shown in scheme 4.2.5.1.



Scheme 4.2.5.1: Synthesis of compounds 155-157.

Unfortunately, using these conditions, the synthesis of the desired derivatives was not achieved. Indeed, in all cases, this reaction promoted the formation of a different product, which was analysed by $^1\text{H-NMR}$ and mass spectrometry. The $^1\text{H-NMR}$ data obtained revealed the absence of the two peaks corresponding to the protons belonging to the -OH and -NH groups. With the help of MS analyses, which suggested the loss of a water molecule, the undesired species obtained were identified as the corresponding lactams (figure 4.2.5.2).

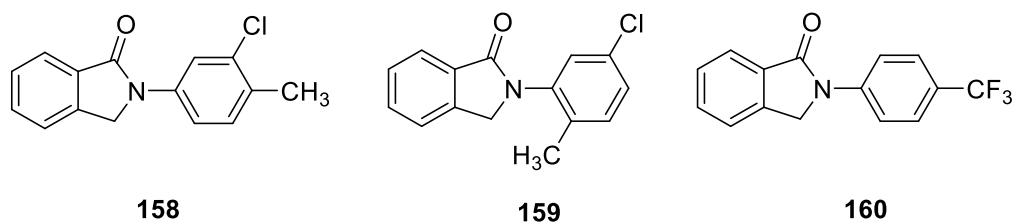
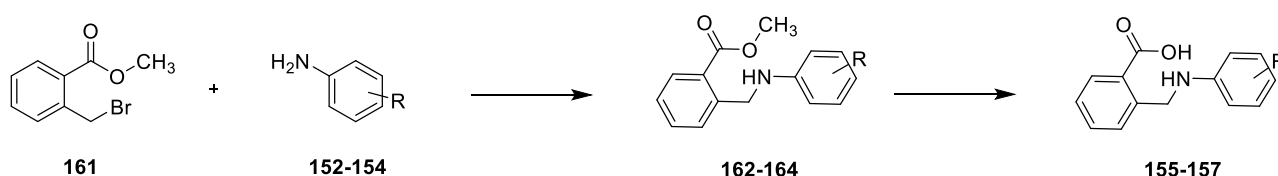


Figure 4.2.5.2: By-products formed.

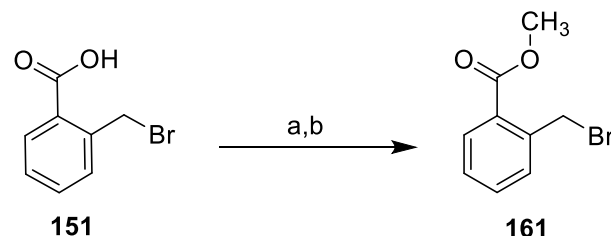
However, although this strategy was unsuccessful for the synthesis of the desired derivatives, the three by-products were conserved in order to investigate whether the lactam scaffold might show biological activity.

On the other side, in order to obtain the desired derivatives, an alternative synthetic pathway was developed as shown in scheme 4.2.5.2. The first step involves a nucleophilic substitution reaction occurring between the methyl 2-(bromomethyl)benzoate (**161**) and the appropriate anilines, with the aim to obtain the ester intermediates, which, following hydrolysis, generate the desired carboxylic acid derivatives.



Scheme 4.2.5.2: Alternative synthetic pathway for the synthesis of derivatives 155-157.

Initially, the synthesis of the starting material methyl 2-(bromomethyl)benzoate (**161**), was attempted through esterification of the corresponding carboxylic acid **151**. Two different reactions were performed, as shown in scheme 4.2.5.3.



a: TBTU, DIPEA, DMF, r.t., 30mins, MeOH, r.t.7h, N₂ atmosphere
 b: 1.25M HCl, MeOH, reflux, overnight

Scheme 4.2.5.3: Synthesis of starting material 161.

The first reaction (a), involves the TBTU-mediated esterification and follows General Procedure 12 in the Experimental Section. Unfortunately, this reaction led to the formation of a single by-product, which, by ¹H-NMR and ¹³C-NMR analyses, was identified as the cyclic ester (figure 4.3.5.3) deriving from the intramolecular reaction between the oxygen of the carboxylic acid and the electrophilic -CH₂. Considering the basic conditions used in reaction (a) which may promote the intramolecular interaction, the acid catalysed Fisher esterification (b) was also attempted. Also in this case, the main product obtained was the undesired lactone. However, using acid conditions, a small amount of desired product, corresponding to the 10% yield, was obtained.

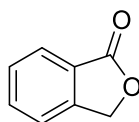
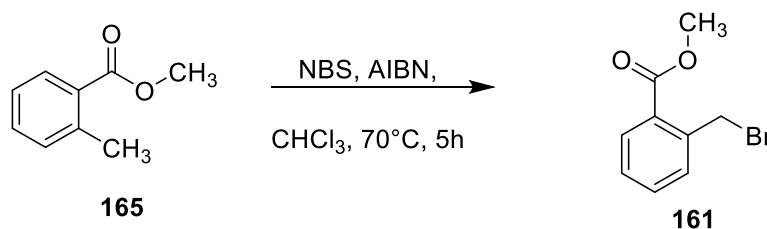


Fig 4.2.5.3: By-product formed during the esterification.

Therefore, an alternative synthetic strategy, involving the benzylic bromination of the starting methyl 2-methylbenzoate, using N-bromosuccinimide (NBS) as a bromine source, in the presence of azobisisobutyronitrile (AIBN) as a radical initiator, was attempted. The procedure followed is reported in the Experimental Section and the mechanism of the reaction is shown in figure 4.2.5.4, while the scheme of the reaction is illustrated in scheme 4.2.5.4. The reaction occurs via a free radical-based bromination. The AIBN acts as the radical initiator and generates the bromine radical which carries out the propagation step. The termination step is represented by the formation of succinimide and bromine.



Scheme 4.2.5.4: Synthesis of the starting material 161.

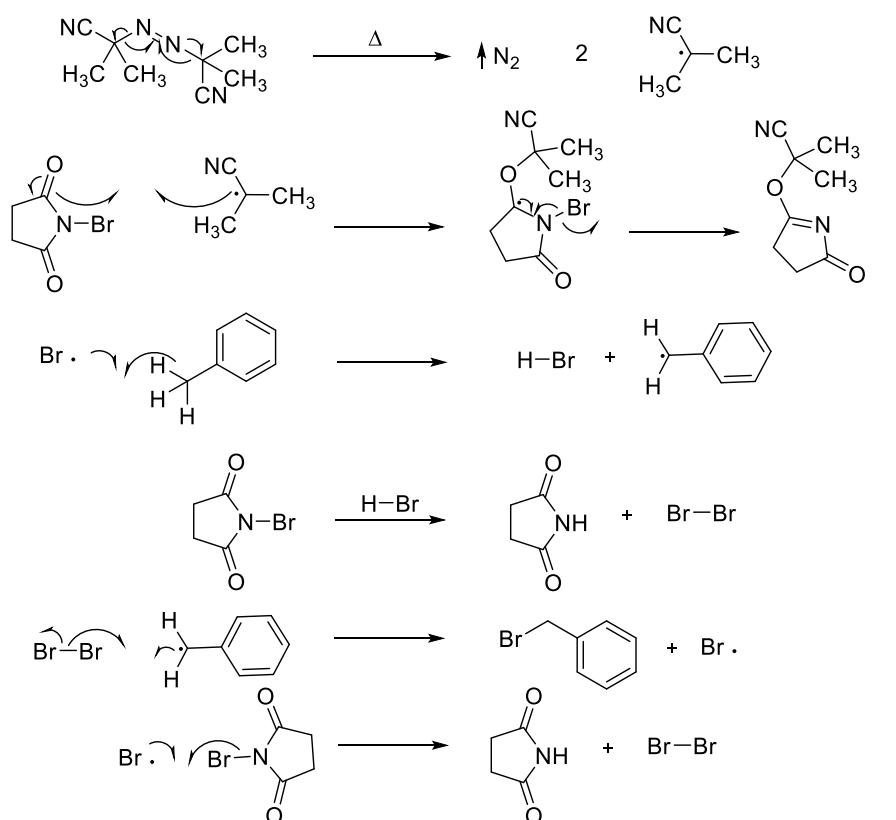
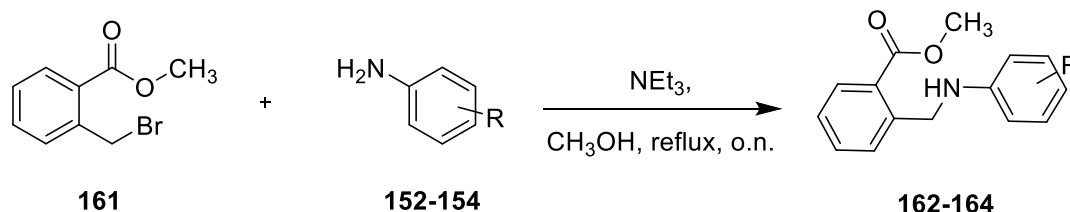


Figure 4.2.5.4: General mechanism of the bromination.

The described strategy was successful, giving the desired product in 83% yield. Once the starting **161** was obtained, the ester intermediates were obtained by reacting **161** with the different anilines, in presence of MeOH and NEt₃, as shown in scheme 4.2.5.5 and reported in General Procedure 14. The derivatives obtained and the corresponding yields are illustrated in table 4.2.5.2.

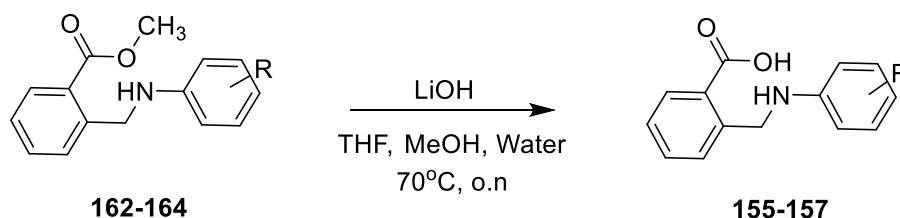


Scheme 4.2.5.5: Synthesis of intermediates 162-164.

Aniline	R	Product	Yield
152	3-chloro-4-methyl	162	74%
153	5-chloro-2-methyl	163	38%
154	4-(trifluoromethyl)	164	43%

Table 4.2.5.2: Intermediates 162-164.

The synthesis of the corresponding acid derivatives was attempted via basic hydrolysis of derivatives **162-164**, as shown in scheme 4.2.5.6.



Scheme 4.2.5.6: Synthesis of derivatives 155-157.

Although this strategy was successful in order to achieve the synthesis of **156**, which was obtained in 53% yield, derivatives **155** and **157** were not obtained due to the formation of the corresponding lactams **158** and **160** as main products of the reaction. The different trend observed for **156** might be determined by the presence of the chlorine atom in *alpha* position to the nitrogen which, creating steric hindrance, may decrease the reactivity of the nitrogen and prevent the cyclisation of the molecule. Stability tests were performed after a period of one week. Interestingly, no stability issues were observed for **156**, whilst the two methyl ester derivatives **162** and **164** showed cyclisation with formation of the corresponding lactams **158** and **160**. Therefore, although the different attempts performed in order to obtain the three designed derivatives **155-157**, only the synthesis of **156** was successful.

4.3 Conclusions

In order to investigate whether the replacement of the original sulfonamide moiety may affect the activity of the compounds, a new series of analogues, characterised by an amine group that links two differently substituted aromatic rings, was designed. 33 new derivatives, characterised by several changes on the hydrophobic ring and different functional groups as replacement of the carboxylic acid moiety, were synthesised. The synthetic strategies applied were successful for most designed derivatives. Unfortunately, for the compounds belonging to the family of 2-(((aryl)amino)methyl)benzoic acids, out of three designed derivatives, only **156** was obtained. Indeed, although different attempts were performed, these compounds showed a tendency to cyclise to form the corresponding lactams. However, the cyclised derivatives obtained were biologically evaluated together with the other amine derivatives and the results obtained will be discussed in the Biological Evaluation chapter.

4.4 References

- 1: Ballatore, C.; Hury, D. M.; Smith, A. B. Carboxylic acid (bio)isosteres in drug design. *ChemMedChem*. **2013**, *8*, 385-395.

Chapter 5

Methylene and Amide Derivatives

Chapter 5: Methylene and Amide Derivatives

5.1 Design of methylene and amide derivatives

With the aim to further explore structure-activity relationships, the role played by the distance between the two aromatic rings, and by the molecular geometry, was investigated with the design of two additional small series of analogues, characterised by the replacement of the original sulfonamide moiety with a methylene and an amide group. The central scaffold of the new series of compounds is represented in figure 5.1A-B. The methylene linker shortens the distance between the two aromatic rings, whilst retaining the desired molecular geometry for the correct arrangement of the molecule in the pocket of c-FLIP. On the contrary, the introduction of an amide linker, induces molecules to acquire a planar conformation, allowing to investigate how changes in the molecular geometry might affect the activity of the compounds. A few derivatives for each series were designed and as shown in table 5.1. The substituents introduced on the hydrophobic ring were selected on the basis of the preliminary data obtained for the sulfonamide analogues, whilst the carboxylic acid moiety and the corresponding alkyl ester groups were inserted in *ortho* and *meta* position of the original anthranilic ring.

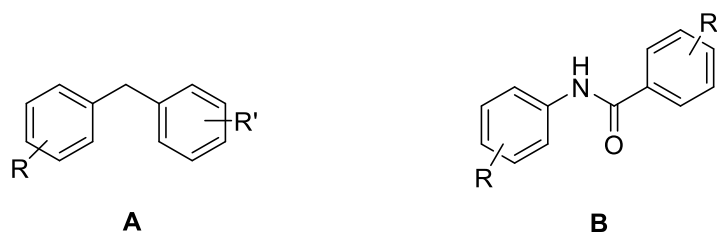


Fig 5.1: Central scaffold of the methylene(A) and amide (B) derivatives.

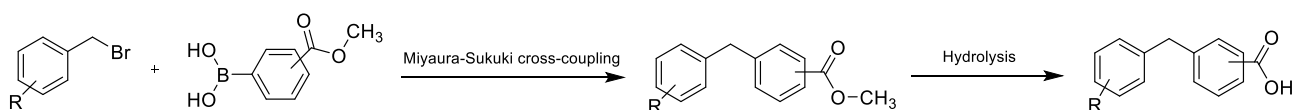
Molecule	Linker	R	R'
169	Methylene	4-trifluoromethyl	2-methyl ester
170	Methylene	3-chloro-4-methyl	3-methyl ester
171	Methylene	3-chloro-4-methyl	2-methyl ester
172	Methylene	3-chloro-4-methyl	3-carboxylic acid
173	Methylene	3-chloro-4-methyl	2-carboxylic acid
178	Amide	4-trifluoromethyl	3-ethyl ester
179	Amide	4-trifluoromethyl	2-methyl ester
180	Amide	4-trifluoromethyl	3-methyl ester
181	Amide	4-iodo	3-ethyl ester
182	Amide	3-chloro-2-methyl	2-methyl ester

183	Amide	3-chloro-2-methyl	3-methyl ester
186	Amide	3-chloro-4-methyl	2-carboxylic acid

Table 5.1.: Different substituents on the methylene derivatives.

5.2 Synthesis of methylene derivatives

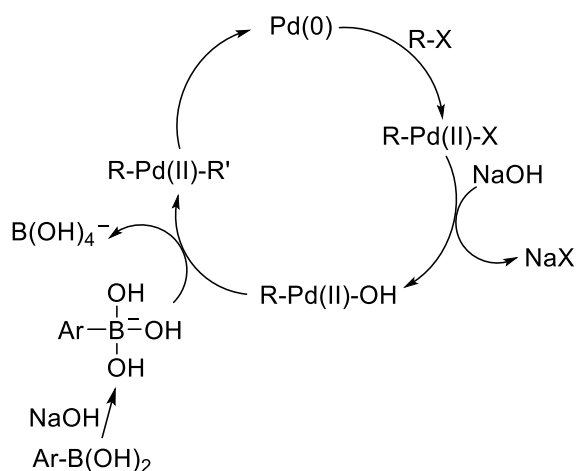
The synthetic strategy applied for the synthesis of the new methylene derivatives is shown in scheme 5.2. The methylene linker was synthesised via a Miyaura-Suzuki cross-coupling reaction between the desired aryl halides and ((methoxycarbonyl)phenyl)boronic acids. The corresponding carboxylic acids were obtained by hydrolysis of the synthesised methyl ester derivatives.



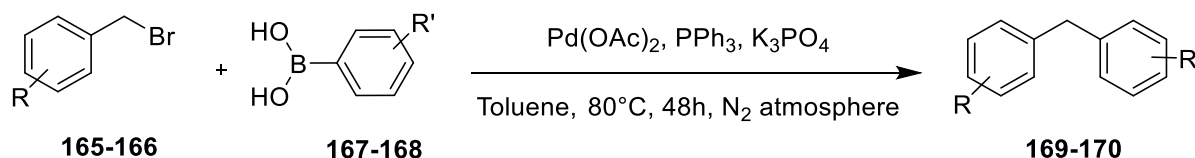
Scheme 5.2.: Synthetic strategy for the synthesis of the methylene derivatives.

5.2.1 Synthesis of methyl(benzyl)benzoates (169-171)

The mechanism of the Miyaura-Suzuki cross-coupling, which allows the formation of the methylene linker between the two aromatic rings, is represented in figure 5.2.1. The reaction is a palladium-catalysed reaction which requires three steps: oxidative addition, transmetalation and reductive elimination. In the oxidative addition the palladium is oxidised from palladium(0) to palladium(II), which forms an organopalladium complex with the aryl halide. The next step, the transmetalation, promotes the transfer of the ligand from the organoboronic acid to the palladium(II) complex. This step requires the presence of the base, represented by NaOH in figure 5.2.1, which activates the boronic species. Reductive elimination leads to the formation of the desired product, and the regeneration of palladium(0).

Fig 5.2.1.: Miyaura-Suzuki cross-coupling mechanism. ⁽¹⁾

Considering the wide range of palladium catalysts available, and additionally several bases and multiple solvent systems which may be used, this reaction was performed following different procedures, in order to find the optimal conditions for the synthesis of this series of analogues. Following General Procedure 15 reported in the Experimental Section, which involves the use of the catalyst Pd(OAc)₂ plus PPh₃ ligand, and the base K₃PO₄, two of the methylene derivatives were synthesised (**169-170**). Scheme 5.2.1.1. illustrates the general scheme of the reaction, while the derivatives obtained, with the corresponding starting materials are listed in table 5.2.1.



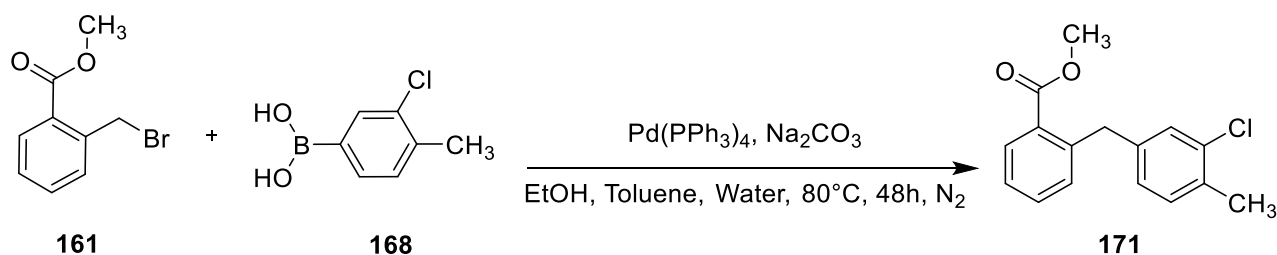
Scheme 5.2.1.1: General scheme for the synthesis of compounds 169-170.

Aryl Bromide	(R)	Boronic Acid	(R')	Product	Yield
165	4-trifluoromethyl	167	2-methylester	169	37%
166	3-methylester	168	3-chloro-4-methyl	170	58%

Table 5.2.1: Compounds 169-170.

The low yield obtained for **169** can be explained by the fact that the starting aryl halide did not react completely, thus leading to a small amount of product formed. Moreover, the complete isolation of the desired compound during the purification process, was not possible because of the highly similar RF shared between the starting bromide **165** and the final product **169**. A better yield was obtained for **170**, mainly because of the easier purification process required for the isolation of the final product.

In order to obtain the derivative **171**, initially, the same reaction between the synthesised bromide **161** (discussed in Chapter 4) and the boronic acid **168** was attempted. Also in this case, the reaction was slow and the starting bromide did not react completely. However, although different purification processes were attempted, the isolation of the desired product from the remaining starting bromide was not possible. Therefore, the conditions of the reaction were changed, in order to investigate whether using a different catalyst the reaction may reach completion. The procedure applied is reported in the Experimental Section. The scheme of the reaction is shown in scheme 5.2.1.2.

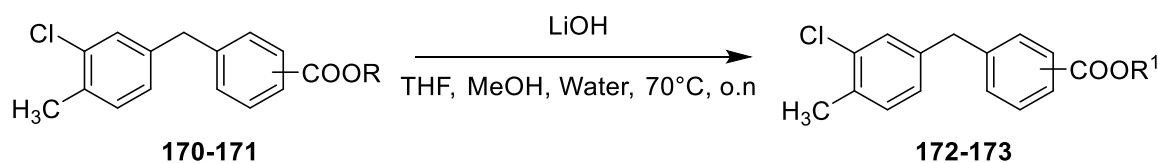


Scheme 5.2.1.2: Synthesis of 171.

Interestingly, changing the catalyst, the base and the solvents system, the starting bromide **161** completely reacted. However, although the desired product was the main species formed, the isolation of the pure product was not possible due to the formation of the by-product 2-ethyl ester derivative, promoted by the presence of EtOH and base at high temperature. Therefore, the mixture of ethyl and methyl esters obtained was used for the next step in order to obtain the carboxylic acid derivative.

5.2.2 Synthesis of benzyl benzoic acids (172-173)

The methylene derivatives showing the carboxylic acid function were obtained via hydrolysis of the corresponding methyl esters, following General Procedure 16 in the Experimental Section. The reaction scheme is shown in scheme 5.2.2.



Scheme 5.2.2: Synthesis of derivatives 172-173.

In general, the reaction worked well giving the two final products **172** and **173** in 74% and 67% yield, respectively. The two methylene derivatives obtained are shown in table 5.2.2.

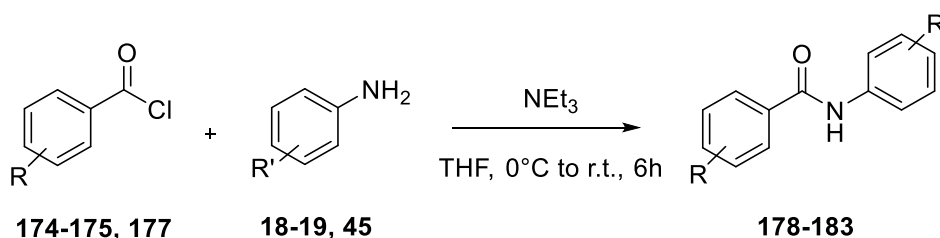
Starting Material	R	Product	R'	Yield
170	3-methylester	172	3-carboxylic acid	74%
171	2-methylester	173	2-carboxylic acid	67%

Table 5.2.2.: Compounds 172-173.

5.3: Synthesis of the amide derivatives

5.3.1: Synthesis of alkyl 2-arylamido benzoates (178-183)

Derivatives **178-183** were obtained through a nucleophilic acyl substitution reaction between the differently substituted benzoyl chlorides and the desired amines. Scheme 5.3.1 illustrates the general reaction scheme.



Scheme 5.3.1.: Synthesis of compounds 178-183.

The procedure followed is General Procedure 17 in the Experimental Section. The reaction mechanism involves the addition of the nucleophilic amine to the carbonyl group yielding a tetrahedral intermediate. The elimination of the leaving group -Cl^- leads to the formation of the desired amide. The base NEt_3 serves to neutralise the HCl formed during the reaction. The amide derivatives obtained and the corresponding yields are shown in table 5.3.1.

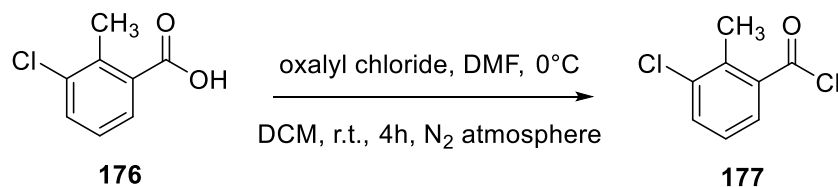
Compound	R	R'	Yield
178	4-trifluoromethyl	3-ethyl ester	45%
179	4-trifluoromethyl	2-methyl ester	35%
180	4-trifluoromethyl	3-methyl ester	90%
181	4-iodo	3-ethyl ester	37%
182	3-chloro-2-methyl	2-methyl ester	28%
183	3-chloro-2-methyl	3-methyl ester	30%

Table 5.3.1: Compounds 178-183.

Most of the time the starting benzoyl chloride reacted completely, therefore the variable yields obtained were mainly due to the loss of product during the work-up or the purification phases.

5.3.2 Synthesis of the 3-chloro-2-methyl benzoyl chloride (177)

In order to obtain derivatives **182** and **183** the synthesis of the starting benzoyl chloride (**177**) was required. The reaction is shown in scheme 5.3.2. and involves the conversion of the corresponding carboxylic acid into the desired chloride using oxalyl chloride and DMF.



Scheme 5.3.2: Synthesis of **177**.

The reaction mechanism involves the initial reaction between the DMF and the oxalyl chloride that generates the by-products CO_2 and CO and a reactive imine intermediate which interacts with the starting carboxylic acid to form the desired acyl chloride as reported in figure 5.3.2.

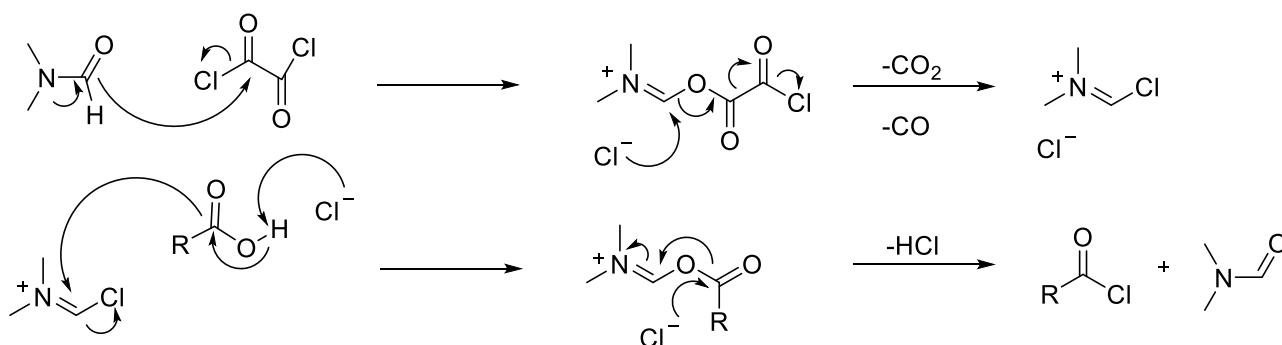
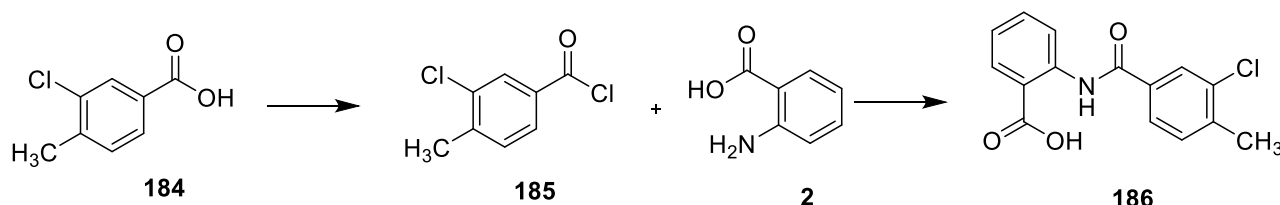


Fig 5.3.2: General mechanism for the conversion of carboxylic acid into acyl chloride.

The reaction gave the desired chloride in 92% yield.

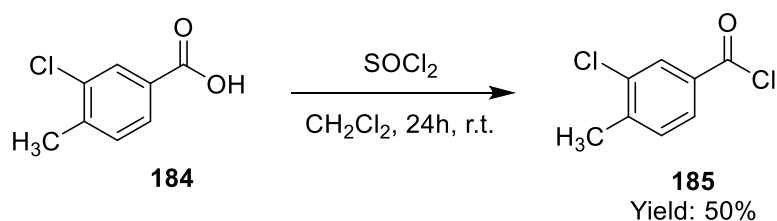
5.3.3: Synthesis of 2-(3-chloro-4-methylbenzamido)benzoic acid (186)

The synthetic pathway applied for the synthesis of the amide derivative showing the carboxylic acid moiety (**186**) is shown in scheme 5.3.3.1.



Scheme 5.3.3.1: Synthetic pathway for the synthesis of compound **186**.

In order to obtain the desired derivative, following the procedure reported in the Experimental Section, the starting benzoyl chloride **185** was synthesised via conversion of the corresponding carboxylic acid **184** using thionyl chloride (SOCl_2) as shown in scheme 5.3.3.2.

Scheme 5.3.3.2: Synthesis of 3-chloro-4-methyl benzoyl chloride **185**.

As shown in figure 5.3.3.1, the reaction involves the initial nucleophilic attack of the oxygen to the sulfur atom, which leads to the addition of the chloride to the carbonyl group. The following [1,2] elimination generates the desired acyl chloride, SO_2 and HCl .

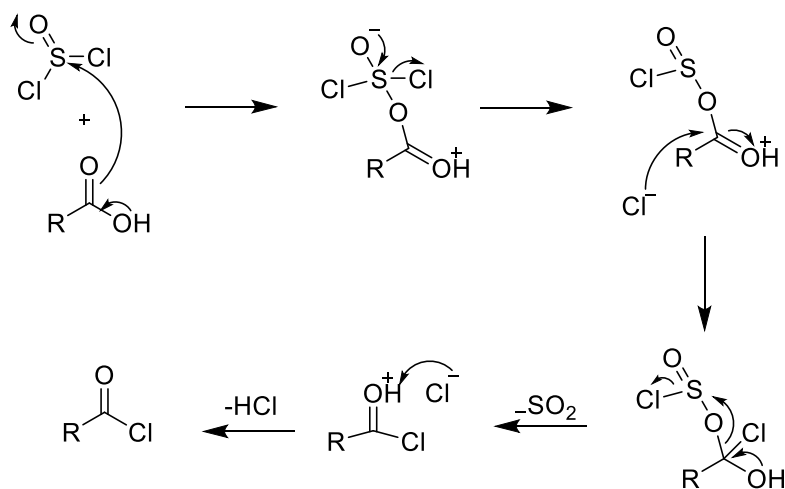
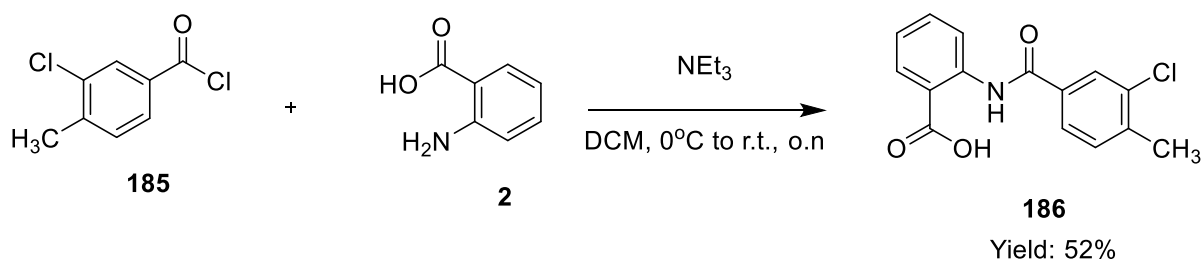


Fig 5.3.3.1: Mechanism for the conversion of the carboxylic acid into the corresponding acyl chloride.

Unfortunately, even after stirring the reaction for 24 hours, the conversion of the starting carboxylic acid was uncompleted, giving the desired benzoyl chloride **185** in 50% yield.

The final product was obtained by reacting benzoyl chloride **185** with anthranilic acid **2**, as shown in scheme 5.3.3.3.

Scheme 5.3.3.3: Synthesis of compound **186**.

Following a nucleophilic attack of the amine group on the carbonyl atom and subsequently elimination of the leaving group chlorine, the desired product **186** was obtained in 52% yield.

5.4 Conclusions

The two small series of methylene and amide derivatives were designed with the aim to investigate whether factors such as the length and the geometry of the molecules may influence the ability of compounds to fit the curved-shaped cavity of the pocket of c-FLIP. The synthetic strategies applied led to the synthesis of 4 methylene derivatives and 7 amide derivatives, which were biologically evaluated and the results obtained will be discussed in the Biological Evaluation chapter.

5.5 References

- 1: Miyaura, N.; Suzuki, A. Palladium-catalysed cross-coupling reactions of organoboron compounds. *Chem. Rev.* **1995**, *95*, 2457-2483.

Chapter 6

Biological Evaluation

Chapter 6: Biological Evaluation

6.1 Introduction

Due to their ability to self-renew, breast cancer stem cells (BCSCs) play a crucial role in the development and the spread of tumour, and in phenomena such as resistance to treatment and recurrence. ^(1, 2) Unfortunately, conventional treatments developed for breast cancer, although acting on the bulk tumour cells and inducing tumour regression, do not affect breast cancer stem cells. ⁽²⁾ Moreover, a further limitation associated with the common chemotherapeutic drugs is represented by the wide range of cytotoxic effects as a result of the lack of selectivity against cancer cells. ⁽³⁾ The development of new selective therapies, targeting both breast cancer stem cells and differentiated cancer cells, while sparing normal cells represents an important need. TRAIL, due to its ability to induce apoptosis selectively in cancer cells, while leaving normal cells unaffected, is considered a promising anticancer agent. ⁽⁴⁾ However, different cancer cell lines and in particular breast cancer cell lines are resistant to TRAIL treatment. ⁽⁵⁾ In the course of previous studies carried out in our research group, new potential therapeutic strategies, aiming to induce TRAIL sensitisation via the inhibition of c-FLIP, were identified. ^(5, 6) These studies have demonstrated that the inhibition of c-FLIP expression, using siRNA, sensitises resistant breast cancer cells and BCSCs to TRAIL treatment. ⁽⁵⁾ Moreover, a new potential c-FLIP small molecule inhibitor (**3**), able to induce TRAIL sensitisation in resistant breast cancer cell lines at a low micromolar concentration, was identified. ⁽⁶⁾ Following these previous studies, a series of analogues of **3** were designed and synthesised with the aim to explore structure-activity relationships and to improve the activity and the pharmacokinetic properties of the original hit compound. Using a specific *in vitro* assay, all the designed derivatives were evaluated for their ability to sensitise both breast cancer cells and breast cancer stem cells to TRAIL.

6.2 Colony Forming Assay (CFA)

All the compounds were tested using the Colony Forming Assay (CFA) or Clonogenic Assay. Generally, this *in vitro* assay is based on the ability of single cells to replicate indefinitely, thus creating "colonies" of cells. ⁽⁷⁾ A colony is composed of 50 cells minimum and each colony is counted as a Colony Forming Unit (CFU). ⁽⁸⁾ In a cancer cell line for instance, when cells are treated with anti-cancer agents, a reduction of the CFU indicates the ability of these agents to reduce cancer cell renewal. An additional important property of the CFA is its applicability to cancer stem cells. Indeed, the single cancer cells generating colonies are deemed to be representative of cancer stem cells, mainly because of the clonogenic activity and the expression of genes such as p63, and BMI-1, which

are associated with properties typically belonging to stem cells such as self-renewal and survival. ^(7, 9, 10)

6.2.1 Compounds evaluation

The protocol used to assess the activity of the compounds is reported in the Experimental Section. In general, cells were pre-treated with the different compounds, before adding TRAIL (soluble human recombinant TRAIL, SuperKiller TRAIL, Enzo Life Sciences). Colonies were left to form for 10 days. After this period the colonies formed were counted. The ability of the test compounds to sensitise cancer cells to TRAIL was measured as reduction of the colony forming units (CFU) and normalised to the DMSO control. **3** was also evaluated, in order to compare the activity of the newly synthesised derivatives with the original hit compound. Additionally, in each experiment, cells were treated with compounds only, in order to assess the lack of cytotoxic or off-target effects. Those compounds inducing a CFU reduction when combined with TRAIL, without affecting colonies formation when administered alone, were of most interest, as they act specifically via the TRAIL-mediated pathway.

6.3 Breast cancer cell line

The TRAIL resistant MCF-7, a human breast adenocarcinoma cancer cell line, was used to evaluate the activity of the synthesised compounds. Originally, this cell line was isolated in 1970 from a Caucasian woman with metastatic breast cancer and it is representative of ER positive cancer cells. ⁽¹¹⁾ This cell line was chosen on the basis of the results obtained in previous studies carried out in our research group. ^(5, 6) These studies assessed the TRAIL resistance of the MCF-7 cell line and the ability to induce TRAIL sensitisation by inhibiting c-FLIP expression via siRNA. ⁽⁵⁾ Consecutively, a similar sensitising effect was observed after treatment of MCF-7 cells with hit **3**, which was able to increase TRAIL sensitisation in different biological assays (Cell Viability assay, Mammosphere Assay and Colony Forming Assay). ⁽⁶⁾ Interestingly, according to the results obtained in these previous studies, while MCF-7 cells were completely resistant to TRAIL in the Cell Viability Assay, TRAIL alone was able to reduce the number of colonies formed in the Colony Forming Assay. ⁽⁶⁾ However, when MCF-7 cells were treated with the combination TRAIL/hit **3**, the number of colonies formed was significantly lower, thus demonstrating the ability of hit **3** to increase TRAIL sensitisation in the MCF-7 cancer cells. ⁽⁶⁾ Following these studies, all the new derivatives synthesised in this work were evaluated for their ability to increase MCF-7 cells TRAIL sensitisation in the Colony Forming Assay.

6.4 Biological Results

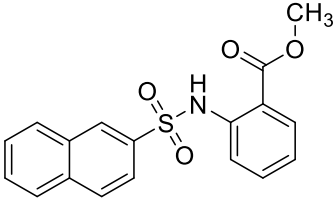
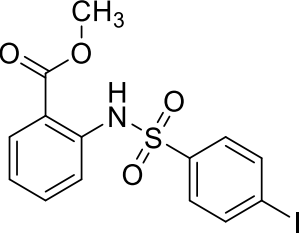
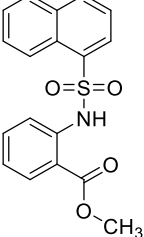
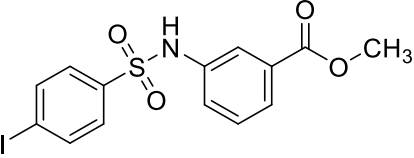
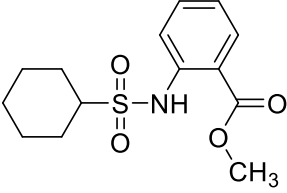
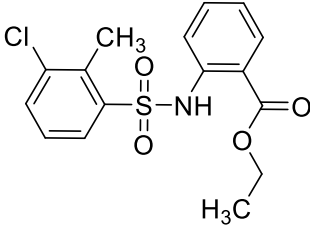
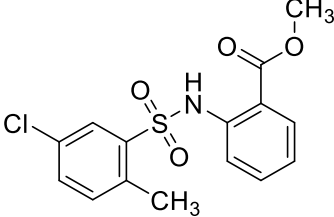
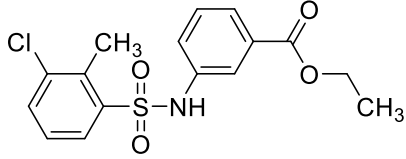
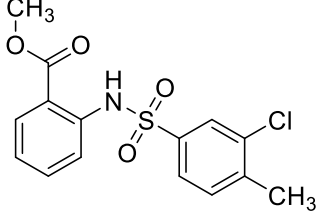
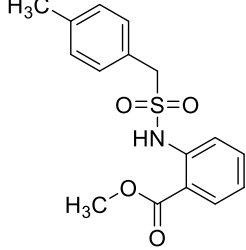
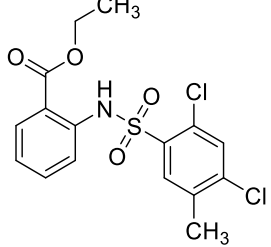
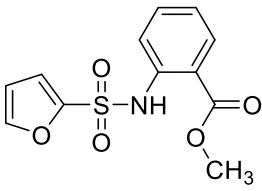
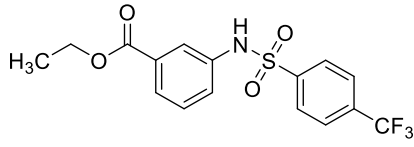
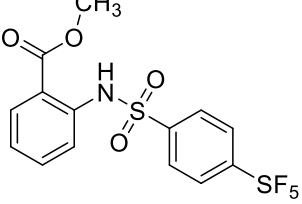
All the following data are the combined results of at least three independent repetitions for each compound. Data were analysed using GraphPad Prism version 7.03 for Windows.⁽¹²⁾ Each compound was tested alone (“minus TRAIL” graph) and in combination with TRAIL (“plus TRAIL” graph). In accordance with the data obtained in the previous study,⁽⁶⁾ TRAIL alone, tested at a fixed concentration of 20ng/ml, induced a reduction of the colony forming units (CFU) of approximately 80%. Generally, the activity of the compounds was measured as the ability to reduce the number of colonies formed (CFU) compared to TRAIL. A reduction in colonies formation when the compounds were administered in the absence of TRAIL was considered as an indication of potential cytotoxic or off-target effects.

6.4.1 Sulfonamide Derivatives

6.4.1.1 Alkyl(arylsulfonamido)benzoates (21-37, 42-43, 50-57, 71, 78-81)

The first set of compounds tested is characterised by analogues showing several modifications on the hydrophobic ring, as well as the replacement of the original carboxylic acid moiety with different alkyl ester groups. Table 6.4.1.1 reports the structure of the compounds tested, while the results obtained are shown in Graph 6.4.1.1.

Molecule	Structure	Molecule	Structure
21		28	
22		29	
23		30	
24		31	
25		32	
26		33	
27		34	

35		52	
36		53	
37		54	
42		55	
43		56	
50		57	
51		71	

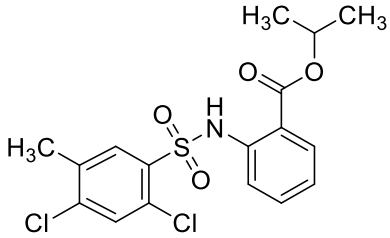
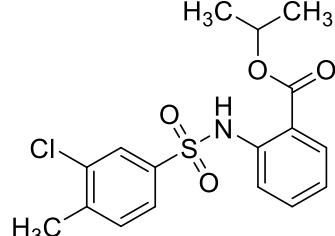
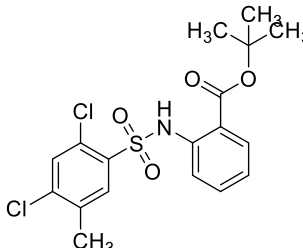
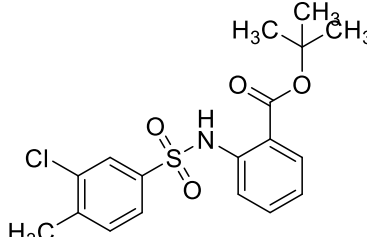
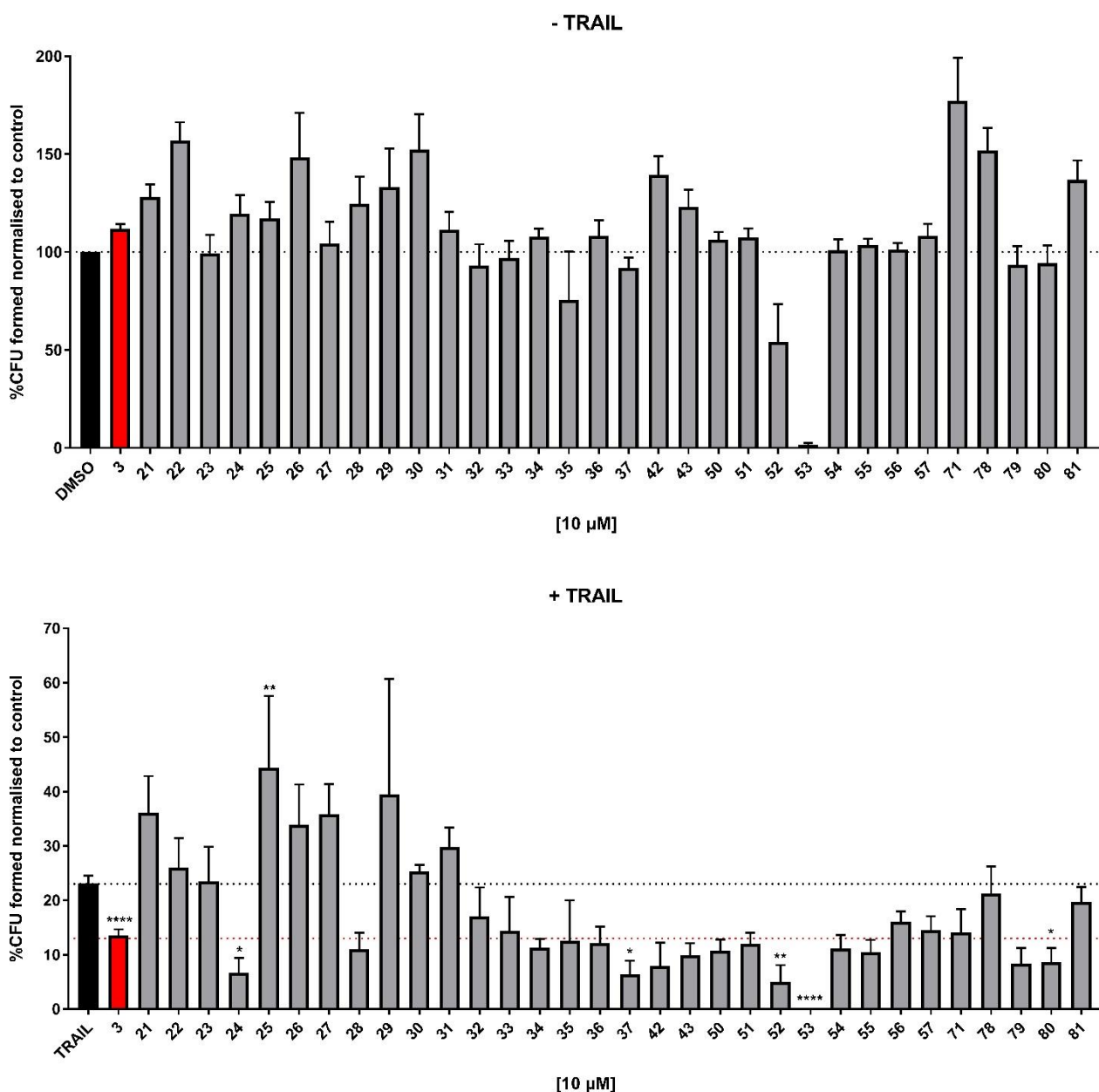
78	 <chem>CC(=O)Oc1ccc(NC(=O)c2cc(Cl)c(C)c(Cl)c2)cc1</chem>
79	 <chem>CC(=O)Oc1ccc(NC(=O)c2ccc(Cl)c(C)c2)cc1</chem>
80	 <chem>CC(=O)Oc1ccc(NC(=O)c2cc(Cl)c(C)c(Cl)c2)cc1</chem>
81	 <chem>CC(=O)Oc1ccc(NC(=O)c2ccc(Cl)c(C)c2)cc1</chem>

Table 6.4.4.1: Alkyl(arylsulfonamido)benzoates.



Graph 6.4.4.1: MCF-7 cells were treated with compounds at 10 μ M, alone or in combination with TRAIL (20ng/ml). Colonies were counted after 10 days. %CFU was calculated from the number of cells plated and normalised to control (DMSO). Data shown is representative of at least 3 experiments \pm SEM. * $p < 0.05$, ** $p < 0.005$, *** $p < 0.0005$, **** $p < 0.0001$ One-way ANOVA compared to TRAIL. Black and red dashed lines represent the effect of TRAIL and compound 3 in the presence of TRAIL respectively.

Compounds **21**, **22**, **23**, **78**, **80**, **50** retain the original 2,4-dichloro-5-methylphenyl ring of **3**, while different alkyl esters were introduced to replace the carboxylic acid moiety. According to the results obtained, analogues showing an ethyl ester in *ortho* position (**50**), as well as a *tert*-butyl ester group (**80**), retained the ability to increase TRAIL sensitisation, demonstrating a similar activity compared to hit **3**. Contrarily, the introduction of an isopropyl ester (**78**) induced a reduction of activity, whilst the analogues showing a methyl ester in *ortho*, *meta* and *para* position (**21**, **22** and **23**) lost their ability to increase TRAIL sensitisation. Among the derivatives exhibiting a different hydrophobic ring while maintaining the methyl ester group in the *ortho* position, a few compounds, showing two

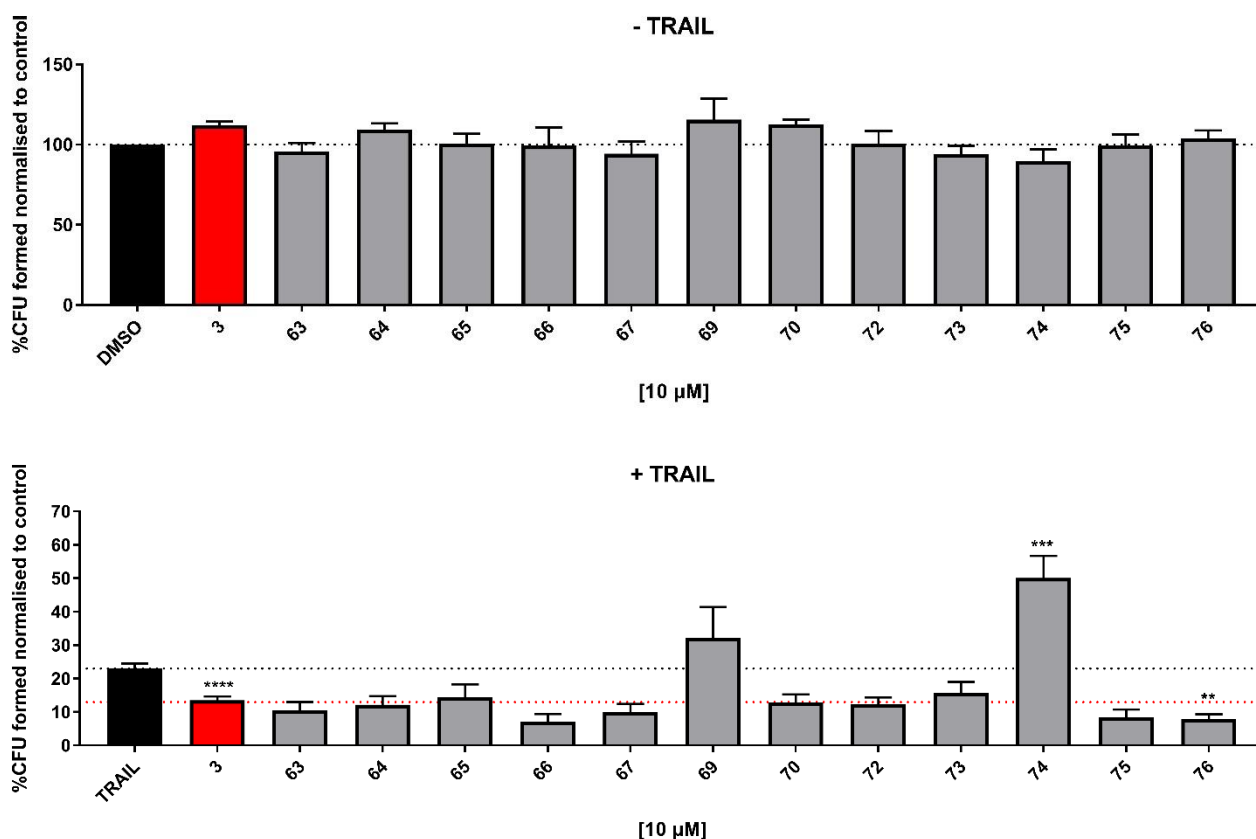
methyl or two chlorine groups at different positions of the ring and a *para tert*-butyl substituted derivative, did not show any sensitising effect (**21**, **25**, **26**, **27**, **29**, **30** and **31**). Interestingly, the number of CFU observed in the presence of these specific derivatives was higher compared to TRAIL, thus implying a non-specific mechanism of action of these compounds. Nevertheless, the majority of the newly designed derivatives were able to increase TRAIL sensitisation. The replacement of the phenyl ring with a 3-pyridine (**34**) and a furan (**57**) ring, as well as the introduction of the -SF₅ group (**71**) and of an additional -CH₂ on the sulfonamide linker (**33** and **56**), were associated with a CFU reduction similar to **3**. **36** and **35**, both characterised by the presence of a naphthalene ring, retained the ability to increase TRAIL sensitisation; however, **35**, the 2-naphthalene ring derivative, showed a potential off-target effect, causing a reduction in the number of colonies formed also in the absence of TRAIL. Compounds **24**, which shows a trifluoromethyl group as hydrophobic substituent, **42** and **43**, showing a methyl and a chlorine group at positions *ortho,para* and *para,meta*, respectively, and **37**, characterised by the replacement of the phenyl ring with a cyclohexane, gave the best results, inducing a higher reduction of CFU compared to **3**. Moreover, the isopropyl and *tert*-butyl ester derivatives of **43**, **79** and **81**, respectively, retained the activity, with compound **79** giving better results than the corresponding *tert*-butyl ester derivative. Generally, all compounds characterised by the presence of an ethyl ester group in position *ortho* or *meta* (**51**, **54** and **55**) demonstrated a comparable activity with **3**. Interesting results were obtained for **52** and **53**, both showing an iodine group as hydrophobic substituent of the phenyl ring, which caused a reduction of the CFU even in the absence of TRAIL, thus suggesting potential cytotoxic or off-target effects.

6.4.1.2 (Arylsulfonamido)benzoic acids (63-70, 72-76)

The structures of the sulfonamide derivatives retaining the carboxylic acid group and the corresponding biological data obtained are reported in Table 6.4.1.2 and Graph 6.4.1.2.

Molecule	Structure	Molecule	Structure
63		70	
64		72	
65		73	
66		74	
67		75	
69		76	

Table 6.4.1.2: (Arylsulfonamido)benzoic acids.



Graph 6.4.1.2: MCF-7 cells were treated with compounds at 10 μ M, alone or in combination with TRAIL (20ng/ml). Colonies were counted after 10 days. %CFU was calculated from the number of cells plated and normalised to control (DMSO). Data shown is representative of at least 3 experiments \pm SEM. * $p < 0.05$, ** $p < 0.005$, *** $p < 0.0005$, **** $p < 0.0001$ One-way ANOVA compared to TRAIL. Black and red dashed lines represent the effect of TRAIL and compound 3 in the presence of TRAIL respectively.

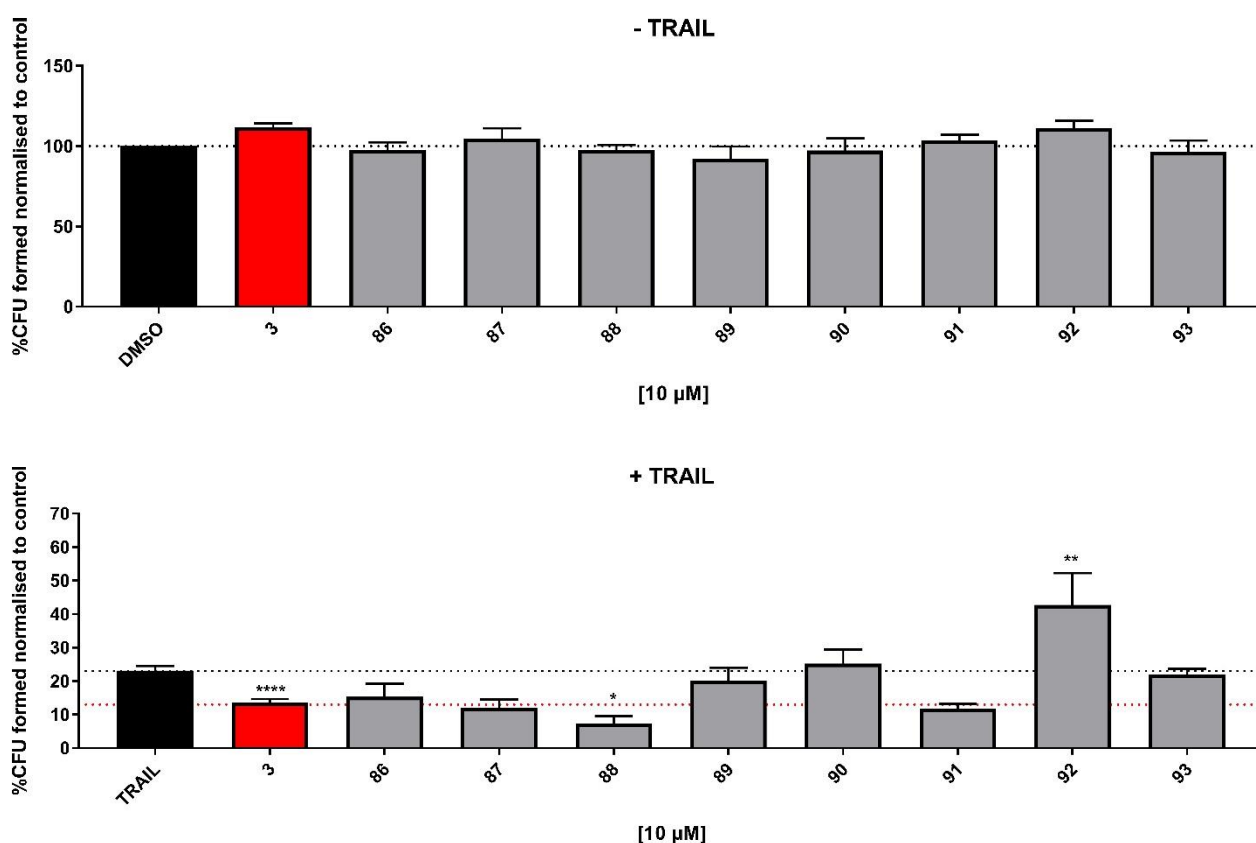
Most derivatives retaining the carboxylic acid function maintained the ability to increase TRAIL sensitisation. In accordance with the results obtained for the corresponding methyl ester derivatives, compounds characterised by an elongated sulfonamide linker (**64**), or by the presence of a cyclohexane (**75**), a pyridine (**72**) and a furan (**76**) ring, as well as the $-SF_5$ substituted derivative (**70**), showed similar or slightly improved activity compared to **3**. Additional modifications were explored, such as the introduction of a thiophene (**65**) or a benzyl ring (**63**). Both derivatives were able to retain the ability to increase TRAIL sensitisation. Interestingly, the two naphthalene compounds **73** and **74** showed a different behaviour compared to the corresponding methyl esters. In fact, whilst the 2-naphthalene derivative **73** maintained a moderate sensitising effect, the 1-naphthalene **74** not only lost its activity, but it also induced an increase in the number of CFU compared to TRAIL. Contrary to the naphthalene derivatives, the two quinoline compounds, **66** and **67**, gave similar results, both showing a slightly improved activity compared to **3**. Interesting results were obtained for **69**, the carboxylic acid derivative of **43**, which induced an increase of the CFU compared to TRAIL, losing the sensitising effect observed with the corresponding methyl ester derivative (**43**).

6.4.1.3 (Arylsulfonamido)N-(1H-tetrazol-5-yl)phenyls (86-93)

Compounds **86-93** are characterised by the presence of a 1H-tetrazole ring as substituent of the carboxylic acid moiety. The biological results obtained for these derivatives are shown in Graph 6.4.1.3 and Table 6.4.1.3 reports their chemical structures.

Molecule	Structure	Molecule	Structure
86		91	
87		92	
88		93	
89			
90			

Table 6.4.1.3: (Arylsulfonamido)N-(1H-tetrazol-5-yl)aryls.



Graph 6.4.1.3: MCF-7 cells were treated with compounds at 10 μ M, alone or in combination with TRAIL (20ng/ml). Colonies were counted after 10 days. %CFU was calculated from the number of cells plated and normalised to control (DMSO). Data shown is representative of at least 3 experiments \pm SEM. * $p < 0.05$, ** $p < 0.005$, *** $p < 0.0005$, **** $p < 0.0001$ One-way ANOVA compared to TRAIL. Black and red dashed lines represent the effect of TRAIL and compound 3 in the presence of TRAIL respectively.

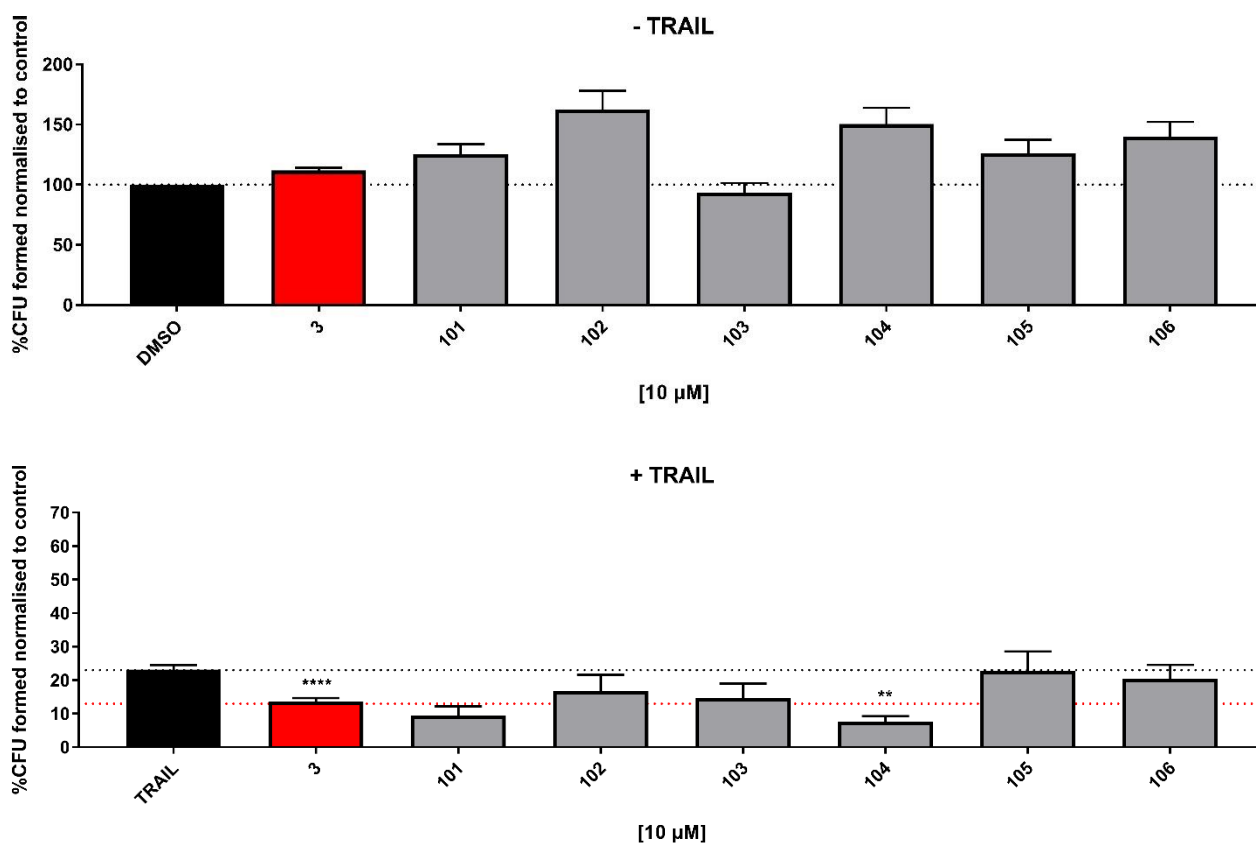
Compounds **86** and **88**, which retain the 2,4-dichloro-5-methyl phenyl ring, differ in the position of the tetrazole group, which is in position *para* and *ortho*, respectively. Both derivatives retained the ability to increase TRAIL sensitisation, however the 2-(1*H*-tetrazol) analogue **88** showed a slightly improved activity compared to **3**. In contrast with these data, analogues **87** and **89**, the *para* and *ortho* derivatives of **43**, respectively, gave different results, with **87** showing similar activity compared to **3**, while a decrease in the TRAIL-sensitisation effect was observed for the 2-(1*H*-tetrazol) derivative **89**. Among the other tetrazole analogues, **91**, characterised by the presence of a 2-naphthalene ring, showed similar activity compared to the 2-methyl ester and the carboxylic acid derivatives (**35** and **73**), whilst **90**, showing a trifluoromethyl group as hydrophobic substituent, lost the ability to sensitise cells to TRAIL compared to the methyl ester derivative **24**. Similar results were obtained for the two quinoline compounds, **92** and **93**, where the replacement of the carboxylic acid group with a tetrazole ring was associated with loss of activity.

6.4.1.4 Alkyl(arylsulfonamido)benzamides (101-106)

Table 6.4.1.4 and graph 6.4.1.4 show the structures of the carboxamide derivatives and the corresponding biological results obtained.

Molecule	Structure
101	
102	
103	
104	
105	
106	

Table 6.4.1.4: Alkyl(arylsulfonamido)benzamides.



Graph 6.4.1.4: MCF-7 cells were treated with compounds at 10 μ M, alone or in combination with TRAIL (20ng/ml). Colonies were counted after 10 days. %CFU was calculated from the number of cells plated and normalised to control (DMSO). Data shown is representative of at least 3 experiments \pm SEM. * $p < 0.05$, ** $p < 0.005$, *** $p < 0.0005$, **** $p < 0.0001$ One-way ANOVA compared to TRAIL. Black and red dashed lines represent the effect of TRAIL and compound 3 in the presence of TRAIL respectively.

In order to evaluate whether the introduction of a carboxamide moiety may affect the activity of the compounds, a few derivatives retaining the original 2,4-dichloro-5-methyl phenyl ring while showing different N-alkyl carboxamide groups were synthesised. Generally, the free carboxamide group (**106**) was associated with a decrease in activity compared to **3**, as well as the differently substituted carboxamide derivatives, **102**, **103**, **105**. However, the N,N-dimethyl carboxamide **104**, and the methyl carboxamide derivative of **43** (**101**), showed an ability to increase TRAIL sensitisation similar to **3**.

6.4.1.5 Structure-activity relationships

Taking into consideration all the biological data obtained for the sulfonamide derivatives, an analysis of the potential structure-activity relationships was performed. Molecules retaining the original hydrophobic ring of **3**, lost their activity when the carboxylic acid in *ortho* position of the anthranilic ring was replaced by a methyl ester in *ortho*, *meta* or *para* position. A reduction in activity was observed when an isopropyl ester or differently substituted carboxamide groups, including the free carboxamide, were introduced. However, derivative **104**, which shows a N,N-dimethyl carboxamide

group, induced a slightly higher reduction of CFU compared to **3**. Groups such as ethyl and *tert*-butyl esters, and the tetrazole group in the *para* position of the original anthranilic ring, retained a similar activity compared to **3**, while the introduction of the tetrazole ring in *ortho* position (**88**) induced a slightly improved ability to increase TRAIL sensitisation. For all the other derivatives, changes in both aromatic rings were explored. In general, the replacement of the hydrophobic phenyl ring with heterocycles such as furan, thiophen and pyridine was associated with activity retention in both carboxylic acid and methyl ester derivatives. The introduction of a cyclohexane ring (**37** and **75**) induced a slight improvement in activity compared to **3**. Interesting results were obtained for the naphthalene derivatives. In the presence of a methyl ester group, both derivatives **35** and **36** showed a comparable activity to **3**. The 2-naphthalene derivative retained the activity in the presence of a carboxylic acid (**73**) or of a tetrazole ring (**91**), while **74**, the carboxylic acid 1-naphthalene derivative, completely lost its sensitising effect. The introduction of a 8-quinoline or 2-quinoline was associated with a slight improvement in activity in the presence of the carboxylic acid group (**66** and **67**), whereas both quinoline derivatives in the presence of the tetrazole ring (**92** and **93**) lost their activity. All the derivatives showing an elongated sulfonamide linker (**33**, **56** and **64**) demonstrated a comparable activity to **3**. A similar activity was also observed with the introduction of an unsubstituted phenyl ring (**63**). The different hydrophobic substituents introduced on the phenyl ring gave interesting results. The two iodine derivatives **52** and **53** were considered as potentially cytotoxic, due to the significant reduction of CFU caused in the absence of TRAIL. On the contrary, groups such as the 4-trifluoromethyl (**24**), 5-chloro-3-methyl (**42**), 3-chloro-4-methyl (**43**) and the 4-SF₅ group (**71**), in the presence of a methyl ester, retained a similar or a slightly improved activity compared to **3**. The carboxylic acid derivative of **71**, **70**, gave similar results, showing activity retention. The introduction of a tetrazole ring in the 4-trifluoromethyl derivative (**90**) induced a complete loss of activity. Interesting results were obtained for the different derivatives of **43** synthesised. In contrast with the data obtained for hit **3**, the introduction of a carboxylic acid group (**69**) or a *tert*-butyl ester (**81**) or a tetrazole ring in *ortho* position (**89**) was associated with loss or reduction of activity. On the contrary, the isopropyl ester derivative (**79**), the *para*-tetrazole derivative (**87**) and the methyl carboxamide derivative (**101**) retained a similar activity compared to **43** and hit **3**. The conflicting data obtained for **3** and **43**, in addition with all the results discussed above, suggest that the difference in activity observed for the synthesised derivatives is not related to a single modification or to a particular group, but it seems to be associated with a combination of the changes at both aromatic rings.

6.4.2 Amine Derivatives

6.4.2.1 (Aryl)amino)benzoic acids (113-120, 139-143, 156)

The structures of the amine derivatives retaining a carboxylic acid group are shown in table 6.4.2.1 and the biological results obtained are reported in graph 6.4.2.1.

Molecule	Structure	Molecule	Structure
113		118	
114		119	
115		120	
116		139	
117		140	

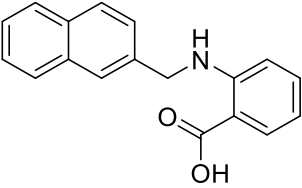
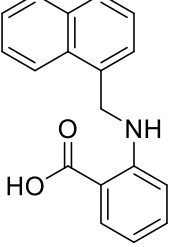
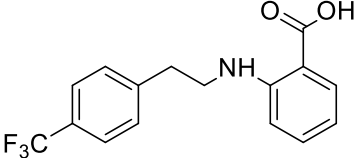
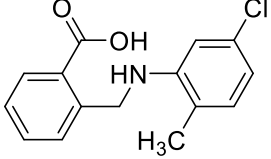
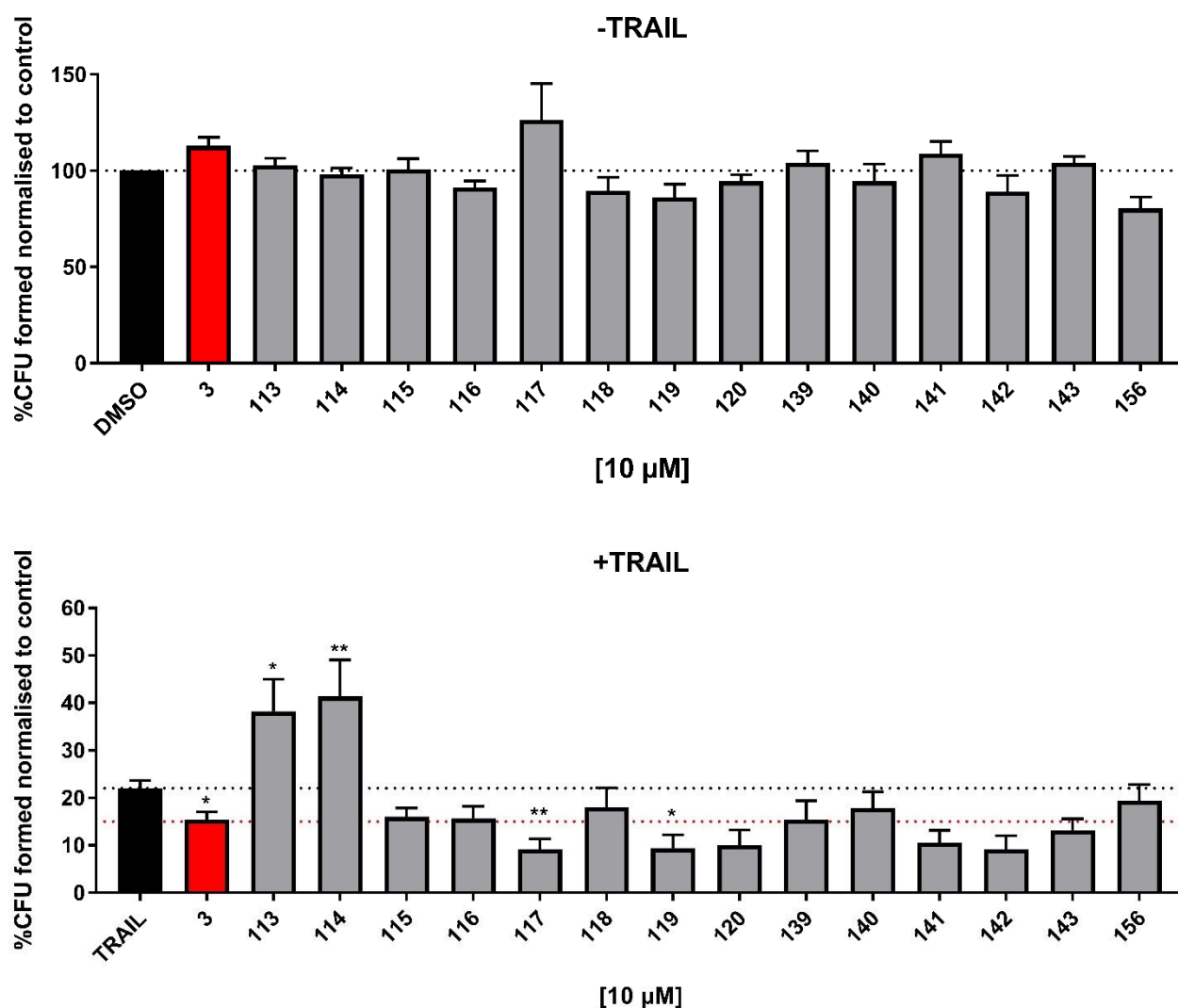
141	 <p>Chemical structure of 2-(2-(naphthalen-1-ylmethylamino)phenyl)acetic acid. It features a naphthalene ring system connected via a methylene group to the nitrogen of an amine group, which is further attached to a phenyl ring. A carboxylic acid group is attached to the ortho position of this phenyl ring.</p>
142	 <p>Chemical structure of 2-(2-(naphthalen-1-ylmethylamino)phenyl)acetic acid. It features a naphthalene ring system connected via a methylene group to the nitrogen of an amine group, which is further attached to a phenyl ring. A carboxylic acid group is attached to the ortho position of this phenyl ring.</p>
143	 <p>Chemical structure of 2-(4-(trifluoromethyl)phenyl)ethan-1-amine. It consists of a benzene ring with a trifluoromethyl group (F_3C) at the para position, connected via a two-carbon ethyl chain to the nitrogen of an amine group. The amine group is attached to a phenyl ring with a carboxylic acid group at the ortho position.</p>
156	 <p>Chemical structure of 2-(2-(4-chloro-3-methylphenyl)amino)phenylacetic acid. It features a phenyl ring with a carboxylic acid group at the ortho position, connected via a methylene group to the nitrogen of an amine group. The amine group is further attached to a phenyl ring with a chlorine atom at the para position and a methyl group (H_3C) at the meta position.</p>

Table 6.4.2.1: (Aryl)amino)benzoic acids.



Graph 6.4.2.1: MCF-7 cells were treated with compounds at 10 μM , alone or in combination with TRAIL (20ng/ml). Colonies were counted after 10 days. %CFU was calculated from the number of cells plated and normalised to control (DMSO). Data shown is representative of at least 3 experiments \pm SEM. * $p < 0.05$, ** $p < 0.005$, *** $p < 0.0005$, **** $p < 0.0001$ One-way ANOVA compared to TRAIL. Black and red dashed lines represent the effect of TRAIL and compound 3 in the presence of TRAIL respectively.

The majority of the amine derivatives showing a carboxylic acid group on the anthranilic ring retained the ability to increase TRAIL sensitisation. Only **113** and **114**, both characterised by a trifluoromethyl group as hydrophobic substituent and the carboxylic acid moiety in position *ortho* and *meta*, respectively, significantly increased the number of colonies formed compared to TRAIL, thus suggesting potential off-target effects. Interestingly, different results were obtained for **143**, which shows an elongated amine linker while maintaining the $-\text{CF}_3$ group. In this case, the ability to increase TRAIL sensitisation was similar to the original hit **3**. Similar results were obtained for all the other derivatives. Substituents such as 3,4-dimethyl groups (**115** and **116**), or 3-chloro-4-methyl groups (**117** and **118**) were associated with activity retention. The replacement of the phenyl ring by a 3-pyridine (**139**) or a 4-pyridine (**140**) ring, as well as the introduction of bigger hydrophobic rings such as the 2- and 1-naphthalenes (**141** and **142**) or the 2- and 8-quinolines (**120** and **119**),

induced an increase of TRAIL sensitisation. However, derivatives **142** and **119** induced a slight reduction of the CFU even in the absence of TRAIL, thus suggesting potential cytotoxic or off-target effects. Similarly, a sensitising effect was observed for **156**, characterised by an inverted amine linker, although this derivative also induced a 20% reduction of colonies formation when administered without TRAIL.

6.4.2.2 Methyl((aryl)amino)benzoates (121-124, 129-134, 137-138)

Biological results obtained for the amine derivatives showing a methyl ester group in position *ortho* or *meta* of the original anthranilic acid are shown in Graph 6.4.2.2 and their chemical structures are reported in Table 6.4.2.2.

Molecule	Structure	Molecule	Structure
121		129	
122		130	
123		131	
124		132	

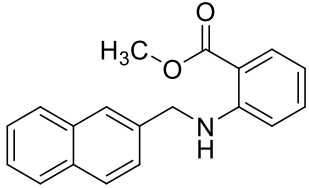
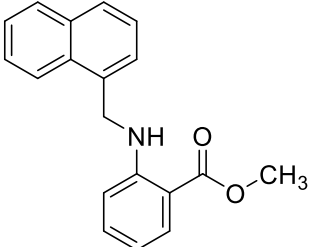
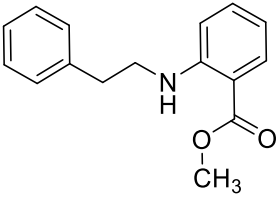
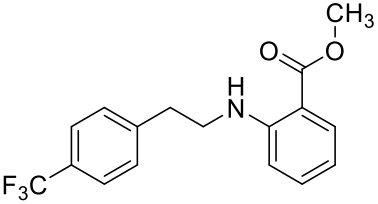
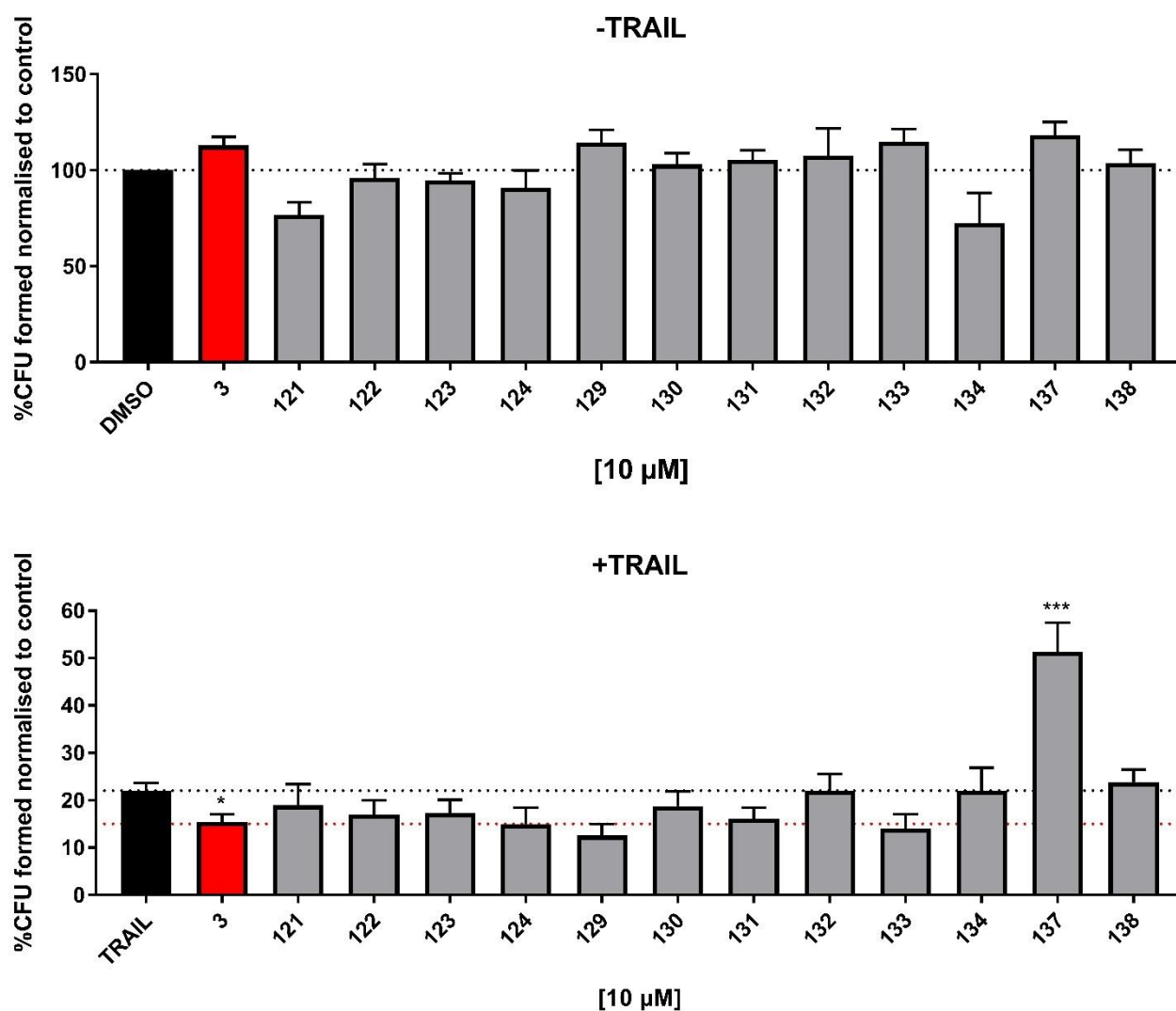
133	
134	
137	
138	

Table 6.4.2.2: Methyl((aryl)amino)benzoates.



Graph 6.4.2.2: MCF-7 cells were treated with compounds at 10 μM , alone or in combination with TRAIL (20ng/ml). Colonies were counted after 10 days. %CFU was calculated from the number of cells plated and normalised to control (DMSO). Data shown is representative of at least 3 experiments \pm SEM. * $p < 0.05$, ** $p < 0.005$, *** $p < 0.0005$, **** $p < 0.0001$ One-way ANOVA compared to TRAIL. Black and red dashed lines represent the effect of TRAIL and compound 3 in the presence of TRAIL respectively.

In most cases, the replacement of the carboxylic acid moiety with a methyl ester group was associated with activity retention. Analogues **123**, **124**, **129**, **130**, **131** and **133**, the corresponding methyl ester derivatives of **115**, **116**, **124**, **118**, **139** and **141**, showed an ability to increase TRAIL sensitisation similar to the one observed for the corresponding carboxylic acid derivatives. Controversial results were obtained instead for the two analogues showing the trifluoromethyl substituent on the phenyl ring, **121** and **122**. Contrarily to the corresponding carboxylic acids (**113** and **114**), both *ortho* (**121**) and *meta* (**122**) methyl ester derivatives increased TRAIL sensitisation. However, the effect of **121** might also be associated with cytotoxic or off-target effects, due to its ability to reduce colonies formation in the absence of TRAIL. In comparison with the corresponding carboxylic acids, the introduction of the methyl ester group in **132** and **134**, showing a 4-pyridine ring and 1-naphthalene ring, respectively, induced loss of activity. Interestingly, **134**, induced CFU

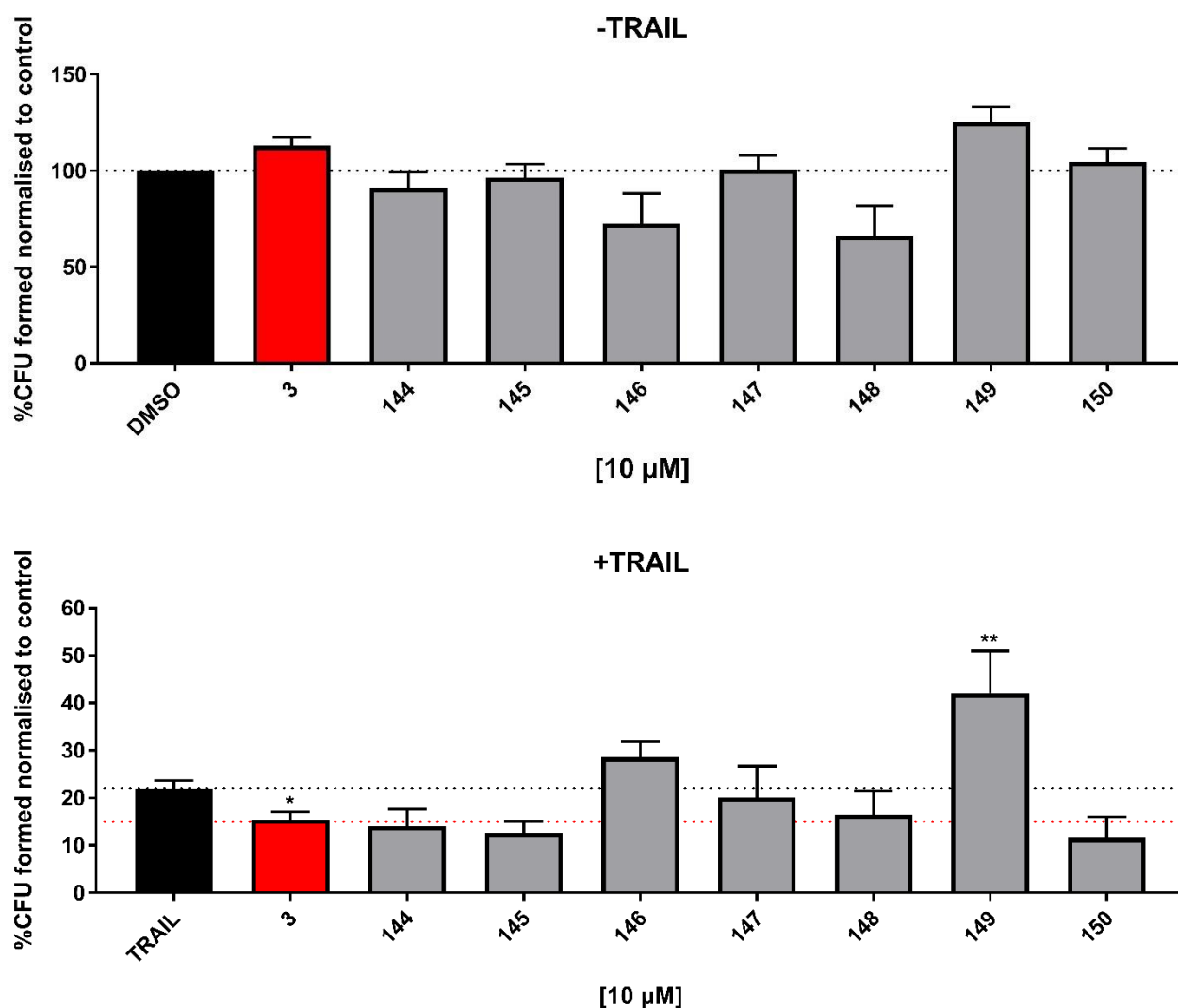
reduction even in the absence of TRAIL, in accordance with its carboxylic acid derivative, **142**. The loss of activity induced by the introduction of a methyl ester group was also observed for **138**, the methyl ester derivative of **143**, characterised by an elongated amine linker. The same negative results were obtained also for **137**, showing an unsubstituted phenyl ring and a longer linker, which increased the number of CFU compared to TRAIL, thus indicating a non-specific mechanism of action.

6.4.2.3 ((Aryl)amino)N-(1H-tetrazol-5-yl)phenyls and (arylamino)N-(5-oxo-2,5-dihydro-1,2,4-oxadiazol-3-yl)phenyls (144-150)

The chemical structures of compounds showing the tetrazole and oxadiazole rings are shown in Table 6.4.2.3 and their biological activity is reported in Graph 6.4.2.3.

Molecule	Structure	Molecule	Structure
144		148	
145		149	
146		150	
147			

Table 6.4.2.3: ((Aryl)amino)N-(1H-tetrazol-5-yl)phenyls and (arylamino)N-(5-oxo-2,5-dihydro-1,2,4-oxadiazol-3-yl)phenyl.



Graph 6.4.2.3: MCF-7 cells were treated with compounds at 10 μ M, alone or in combination with TRAIL (20ng/ml). Colonies were counted after 10 days. %CFU was calculated from the number of cells plated and normalised to control (DMSO). Data shown is representative of at least 3 experiments \pm SEM. * $p < 0.05$, ** $p < 0.005$, *** $p < 0.0005$, **** $p < 0.0001$ One-way ANOVA compared to TRAIL. Black and red dashed lines represent the effect of TRAIL and compound 3 in the presence of TRAIL respectively.

Compounds **145** and **146** are respectively the *ortho* and *para* tetrazole derivatives of **117** and **129**. Interestingly, according to the results obtained, while **145** showed similar activity compared to the previous carboxylic acid (**117**) and methyl ester (**129**) derivatives, the introduction of the tetrazole ring in *para* position (**146**) is associated with potential off-target effects, as shown by the reduction in CFU induced in the absence of TRAIL and at the same time the slightly increase of colonies formed compared to TRAIL. A similar potential off-target effect was observed with **149**, the 2-naphthalene tetrazole derivative, which increased the number of CFU compared to TRAIL alone. The introduction of a tetrazole ring to the 8-quinoline (**147**) and 3-quinoline (**148**) derivatives, although retaining the TRAIL sensitisation effect, did not improve the activity compared to the corresponding carboxylic acid derivatives or to hit **3**. Moreover, the activity of **148** might be correlated to potential off-target effects, due to its ability to reduce the CFU number even in the absence of TRAIL. On the contrary,

positive results were obtained for **144**, which is the $-CF_3$ substituted tetrazole derivative, which, controversially to the corresponding carboxylic acid, showed an ability to increase TRAIL sensitisation similar to **3**. Retention of activity was also observed with the oxadiazole derivative of **145**, compound **150**.

6.4.2.4 2-(alkyl)isoindolin-1-ones (158-159)

As mentioned in Chapter 4, the undesired lactam by-products obtained during the synthesis of 2-(((aryl)amino)methyl)benzoic acids **158-159**, were also biologically evaluated. The results obtained are shown in Graph 6.4.2.4 and the structures of the two lactam derivatives tested are reported in Figure 6.4.2.4.

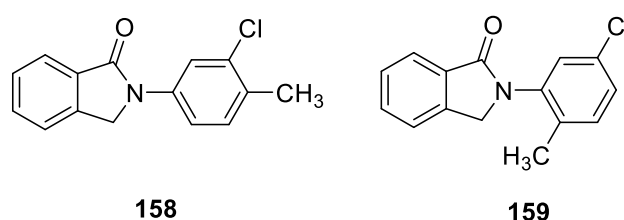
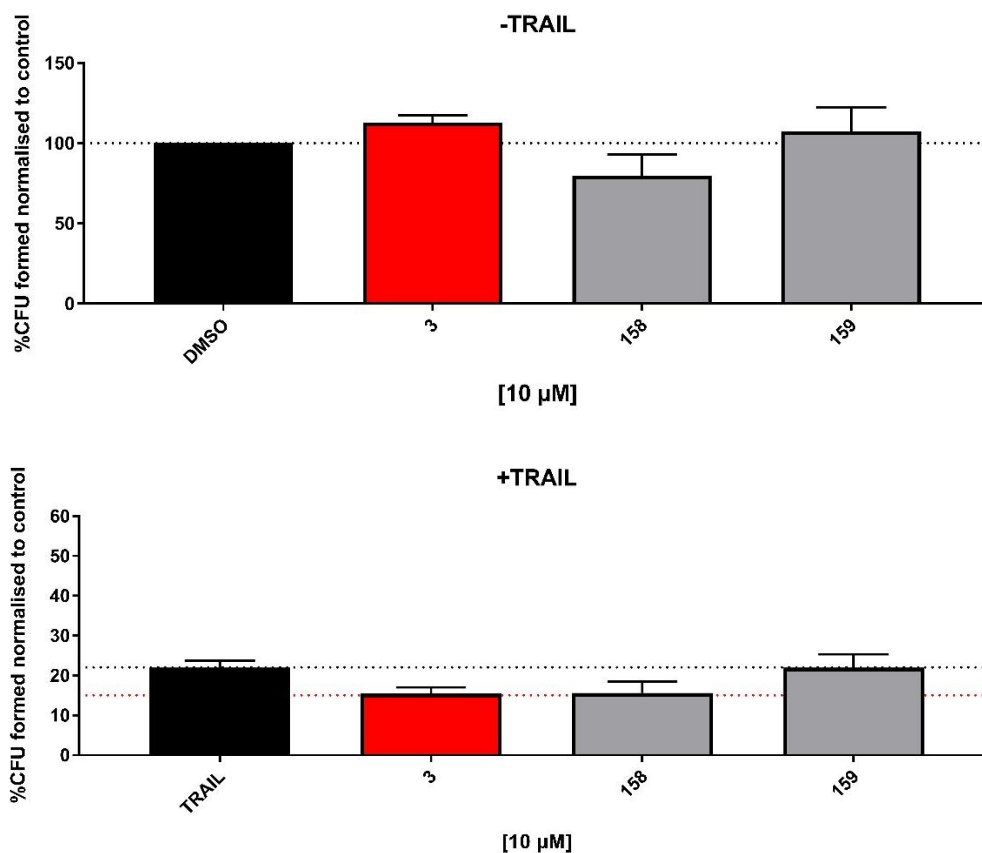


Fig 6.4.2.4: 2-(alkyl)isoindolin-1-ones.



Graph 6.4.2.4: MCF-7 cells were treated with compounds at 10 μ M, alone or in combination with TRAIL (20ng/ml). Colonies were counted after 10 days. %CFU was calculated from the number of cells plated and normalised to control (DMSO). Data shown is representative of at least 3 experiments \pm SEM. * $p < 0.05$, ** $p < 0.005$, *** $p < 0.0005$, **** $p < 0.0001$ One-way ANOVA compared to TRAIL. Black and red dashed lines represent the effect of TRAIL and compound 3 in the presence of TRAIL respectively.

One of the two derivatives, **159**, did not show any sensitising effect, whilst **158** revealed potential cytotoxicity or off-target effects by inducing a reduction in CFU even in the absence of TRAIL.

6.4.2.5 Structure-activity relationships

In accordance with the data obtained for the sulfonamide derivatives, the different biological activity of the amine derivatives seems to be correlated with modifications on both aromatic rings. **129**, the amine derivative of **43**, which shows a 3-chloro-4-methyl phenyl ring and a methyl ester in *ortho* position of the original anthranilic ring, retained similar activity compared to the original sulfonamide compound and to **3**. Interestingly, in contrast with the data obtained for the corresponding sulfonamide derivative (**69**), the introduction of a carboxylic acid group in **117** was associated with a slight improvement of activity compared to **3**. Also, the 3-methyl ester and the 3-carboxylic acid derivatives, **118** and **130**, respectively, retained the ability to increase TRAIL sensitisation, although showing a decrease in activity compared to **3**. Moreover, contrary to the results obtained for the corresponding sulfonamide derivative, the introduction of the tetrazole ring in *para* position (**146**) induced loss of activity, while a slightly higher reduction of CFU compared to **3** was observed with the *ortho* tetrazole derivative **145** and the oxadiazole derivative **150**. The introduction of a pyridine ring was associated with activity retention in the presence of a carboxylic acid group (**139** and **140**). The corresponding methyl esters, however, gave opposite results, with the 3-pyridine **131** retaining the activity, whereas the 4-pyridine **132** lost its sensitising effect. The naphthalene derivatives, as well as the quinoline derivatives, in the presence of a carboxylic acid group showed a similar activity compared to **3**, although a slight reduction of the CFU was observed for the 1-naphthalene (**142**) and the 8-quinoline (**119**) derivatives even in the absence of TRAIL. Interestingly, in the presence of a methyl ester, while the 2-naphthalene **133** retained the activity, the 1-naphthalene **134** completely lost its sensitising effect, increasing instead its ability to induce a reduction of CFU in the absence of TRAIL. Moreover, in contrast with the corresponding sulfonamide derivatives (**91** and **93**), the introduction of a tetrazole ring in the 2-naphthalene derivative (**149**) induced a significant decrease in the ability to increase TRAIL sensitisation, whilst for the 2-quinoline derivative (**148**) the presence of a tetrazole ring was associated with a higher ability to induce a reduction of CFU in the absence of TRAIL. The amine analogue of **24**, characterised by a 4-trifluoromethyl phenyl ring and a 2-methyl ester (**121**), although retaining a similar activity compared to **3**, also induced a reduction of the CFU formed in the absence of TRAIL, indicating potential additional off-target effects. Interestingly, while the replacement of the methyl ester with a carboxylic acid group (**113**, **114**) was associated with loss of activity, the introduction of a tetrazole

ring in **144** induced a reduction of the CFU comparable to **3**, contrarily to the results obtained for the corresponding sulfonamide derivative (**90**). Controversial results were obtained also for the 4-trifluoromethyl derivatives showing a longer amine linker, with the carboxylic acid derivative **143** showing a similar activity compared to **3**, while the corresponding methyl ester **138**, as well as the unsubstituted phenyl ring (**137**), did not show any sensitising effect. Similarly, the inversion of the amine linker in **156** only showed a small sensitising effect, associated with a reduction of the CFU even in the absence of TRAIL.

6.4.3 Methylene and Amide Derivatives

6.4.3.1 Methylene Derivatives (169-170, 172-173)

Compounds belonging to the small series of methylene derivatives synthesised are reported in table 6.4.3.1 and the corresponding biological results are shown in graph 6.4.3.1.

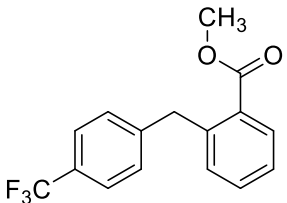
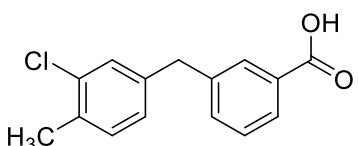
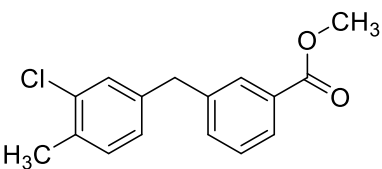
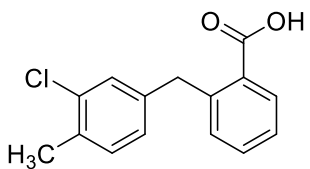
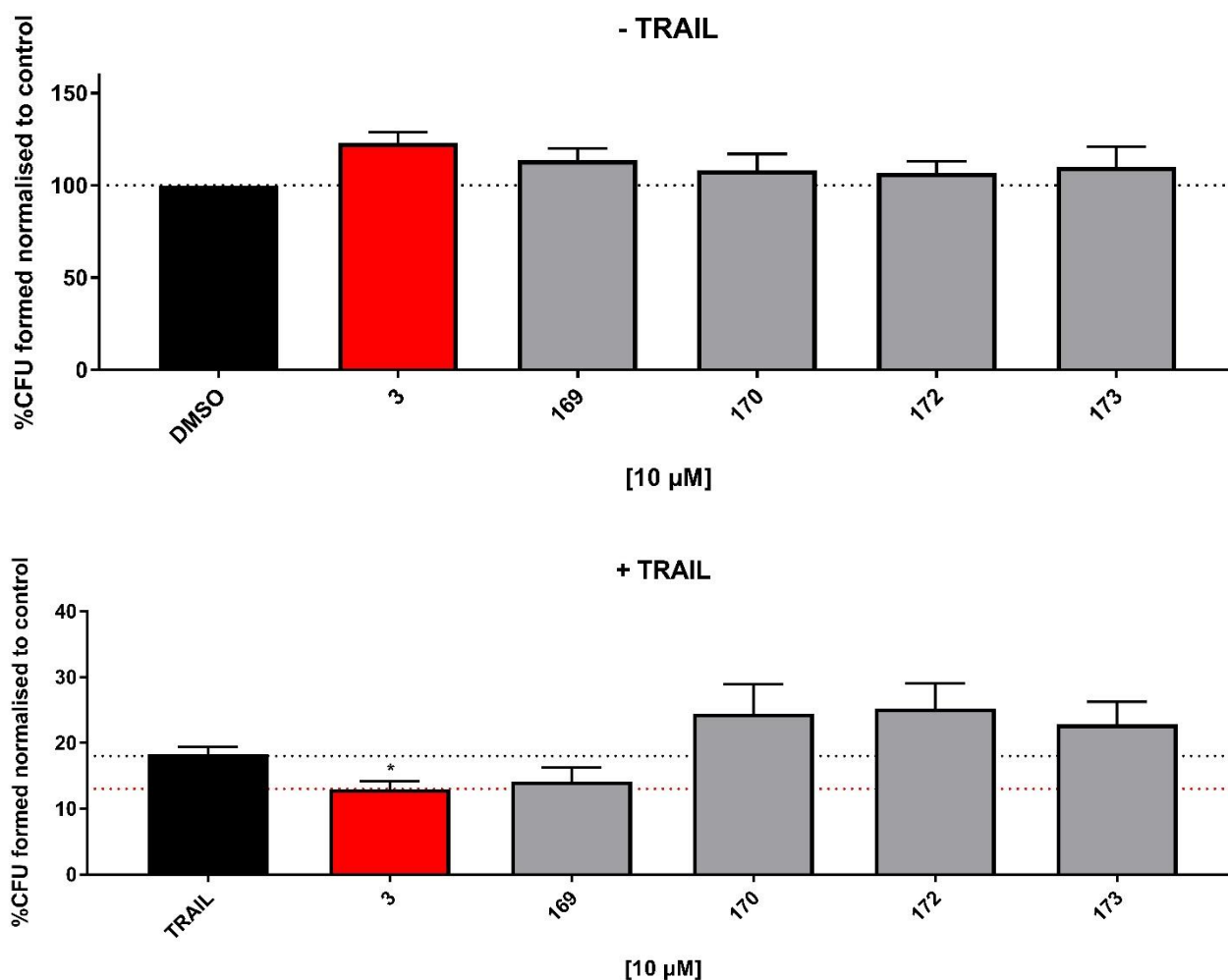
Molecule	Structure	Molecule	Structure
169		172	
170		173	

Table 6.4.3.1: Methylene Derivatives.



Graph 6.4.3.1: MCF-7 cells were treated with compounds at 10 μM , alone or in combination with TRAIL (20ng/ml). Colonies were counted after 10 days. %CFU was calculated from the number of cells plated and normalised to control (DMSO). Data shown is representative of at least 3 experiments \pm SEM. * $p < 0.05$, ** $p < 0.005$, *** $p < 0.0005$, **** $p < 0.0001$ One-way ANOVA compared to TRAIL. Black and red dashed lines represent the effect of TRAIL and compound 3 in the presence of TRAIL respectively.

The methylene derivatives **173**, **172** and **170** retain the 3-chloro-4-methyl phenyl ring of compound **43**. According to the results obtained, the introduction of a methylene linker in the carboxylic acid (**172** and **173**) and the methyl ester (**170**) derivatives was associated with loss of activity. On the contrary, **169**, showing a *para* trifluoromethyl phenyl and a 2-methyl ester group as R^1 , retained the ability to increase TRAIL sensitisation.

6.4.3.2: Amide Derivatives (**178-183**, **186**)

A small series of amide derivatives was synthesised in order to explore whether changes in the molecular geometry affected the activity of the compounds. Table 6.4.3.2 shows the structure of the amide derivatives, while the biological results obtained are reported in Graph 6.4.3.2.

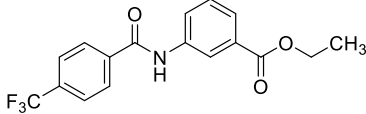
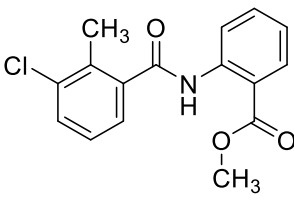
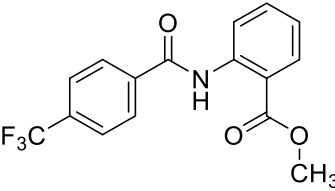
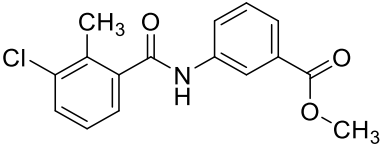
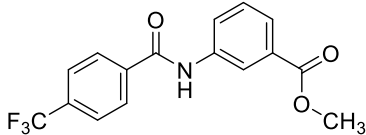
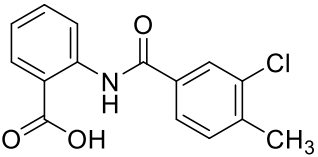
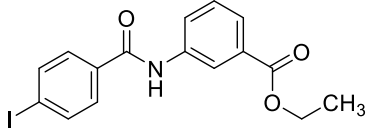
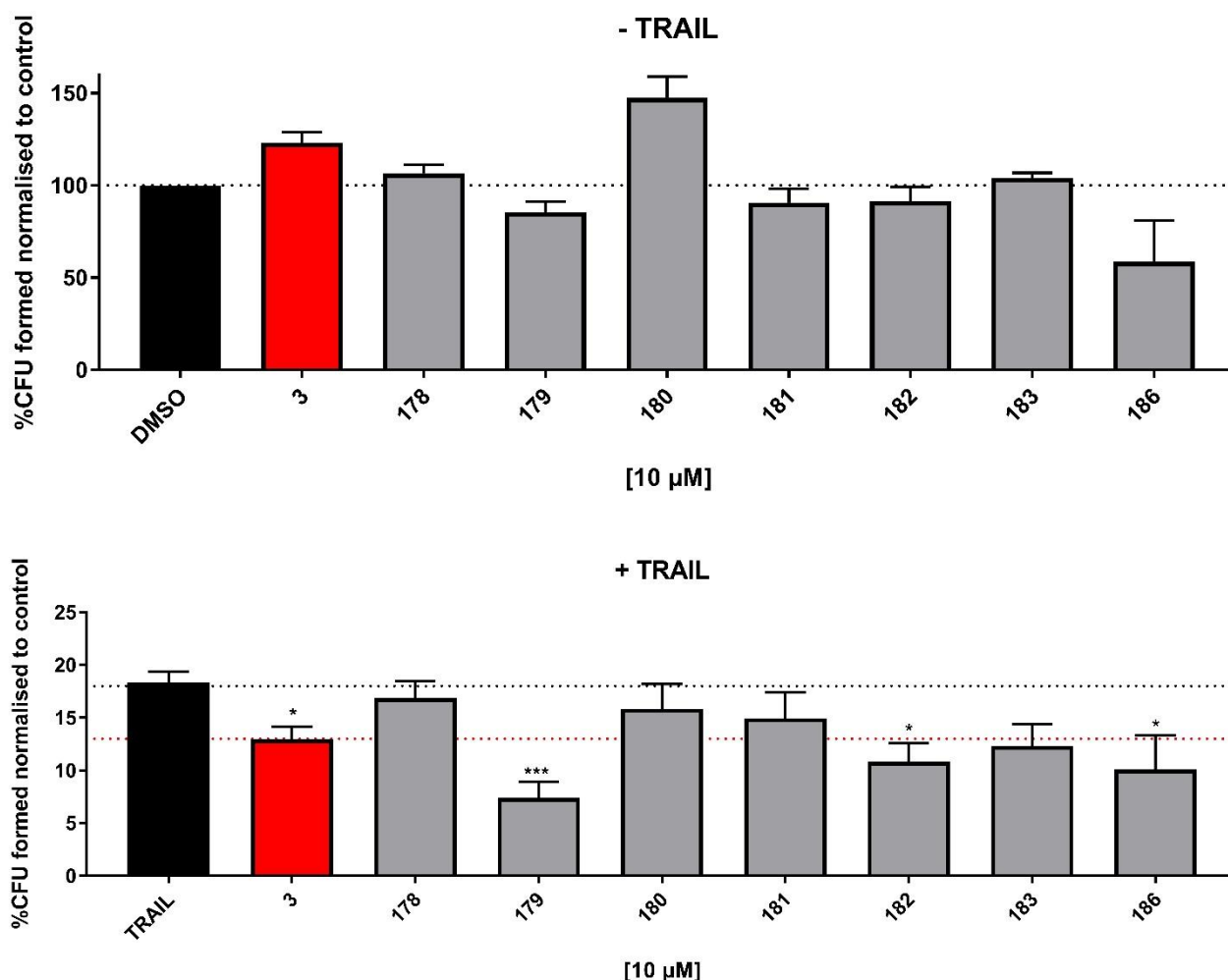
Molecule	Structure	Molecule	Structure
178		182	
179		183	
180		186	
181			

Table 6.4.3.2: Amide Derivatives.



Graph 6.4.3.2: MCF-7 cells were treated with compounds at 10 μM , alone or in combination with TRAIL (20ng/ml). Colonies were counted after 10 days. %CFU was calculated from the number of cells plated and normalised to control (DMSO). Data shown is representative of at least 3 experiments \pm SEM. * $p < 0.05$, ** $p < 0.005$, *** $p < 0.0005$, **** $p < 0.0001$ One-way ANOVA compared to TRAIL. Black and red dashed lines represent the effect of TRAIL and compound 3 in the presence of TRAIL respectively.

Only compound **183**, which shows a 2-methyl-3-chloro phenyl ring and a methyl ester in the *meta* position of the original anthranilic ring, increased TRAIL sensitisation with similar activity compared to **3**. Derivatives **179**, amide analogue of **24**, and **186**, amide analogue of **69**, although increasing TRAIL sensitisation, also promoted a reduction of the CFU in the absence of TRAIL. A slight ability to induce a reduction of colonies formation in the absence of TRAIL was also observed for **182** and the iodine derivative **181**, suggesting a potential off-target or cytotoxic effect associated with this series of derivatives. On the contrary, **178** and **180**, both showing a trifluoromethyl substituent on the phenyl ring, and an ethyl (**178**) and a methyl (**180**) ester in *meta* position, did not show ability to increase TRAIL sensitisation.

6.4.3.3 Structure-activity relationships

The introduction of a methylene linker in derivatives showing a 3-chloro-4-methyl phenyl ring (**173**, **170** and **172**) was associated with loss of activity compared to the corresponding sulfonamide and

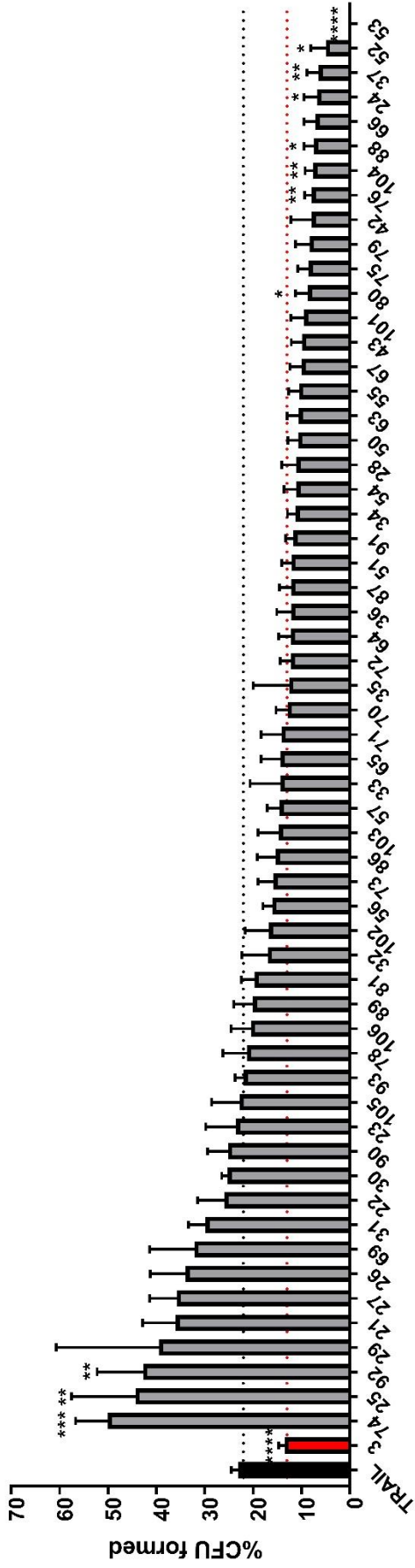
amine derivatives. On the contrary, the 4-trifluoromethyl phenyl methylene derivative **169** retained a similar activity compared to **3**. Controversial results were obtained for the amide derivatives. A decrease in activity was observed for the 4-trifluoromethyl phenyl derivatives showing a 3-ethyl and 3-methyl ester, **178** and **180**, respectively, while the 2-methyl ester **179**, although showing an increased activity compared to **3**, also induced a reduction of the CFU in the absence of TRAIL. A similar effect was observed for the 3-chloro-4-methyl phenyl derivative, **186**.

6.4.4 Conclusions

The ability of all the newly synthesised compounds to increase TRAIL sensitisation in the MCF-7 cells was evaluated and compared to the original hit **3**. Although a clear identification of the features required for the activity was not possible due to the variable results obtained among all the compounds, several new derivatives were found to increase TRAIL sensitisation by reducing colonies formation with a similar or slightly improved activity compared to **3**. The active compounds belong to all four series of derivatives and they show different chemical features, thus suggesting that multiple factors determine the ability of the compounds to stimulate the response to TRAIL. Graph 6.4.4.A-D summarises the results obtained for all the tested compounds when administered in combination with TRAIL. Among the derivatives retaining the sulfonamide linker, some of the best compounds were identified in **24**, **42** and **43**, all showing the methyl ester group in *ortho* position on the original anthranilic ring and a 4-trifluoromethyl phenyl (**24**), 5-chloro-2-methyl phenyl (**42**) and 3-chloro-4-methyl phenyl (**43**) on the hydrophobic side of the molecule. The two compounds characterised by the presence of a cyclohexane ring, methyl ester **37** and carboxylic acid **75**, also showed a slightly improved ability to reduce the CFU number compared to **3**. Additional modifications such as the introduction of a furan ring (**76**), or a 8-quinoline (**66**) and a 3-quinoline (**67**), while retaining the carboxylic acid moiety, also resulted in a slightly greater ability to increase TRAIL sensitisation. The *tert*-butyl ester derivative (**80**), the tetrazole derivative (**88**) and the N,N-dimethyl carboxamide derivative (**104**) of **3**, all induced a slightly higher reduction of CFU compared to **3**. The introduction of an amine linker was associated with activity retention in **129**, **117** and **145**, the amine derivatives of **43**, **69**, **89**, respectively, as well as in the presence of an oxadiazole group (**150**). Compounds characterised by the presence of a naphthalene (**141** and **142**) and a quinoline (**119** and **120**) ring also retained a similar activity compared to hit **3**. On the contrary, amine derivatives showing a 4-trifluoromethyl phenyl ring demonstrated interesting activity only in the presence of a tetrazole group (**144**). Among the small series of methylene derivatives synthesised, **169**, showing a 4-trifluoromethyl phenyl ring, was the only compound demonstrating ability to

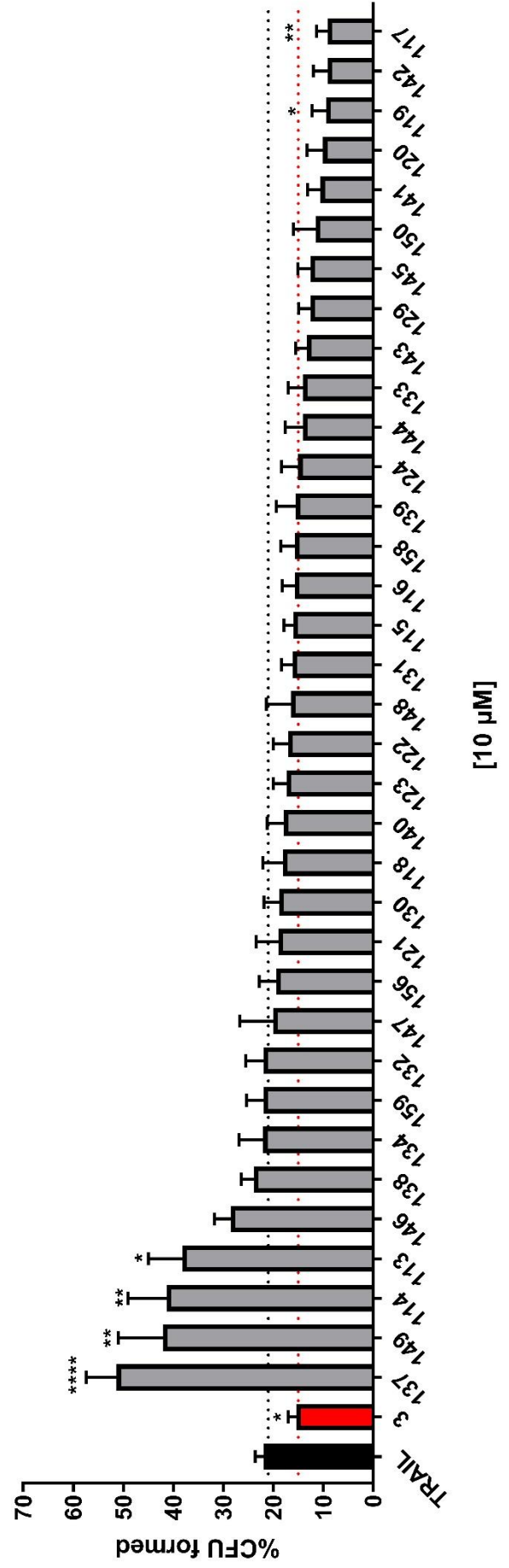
increase TRAIL sensitisation. A few amide derivatives induced a higher TRAIL sensitisation compared to **3**, however these compounds were also associated with a reduction of colonies formation when tested alone, suggesting potential cytotoxic or off-target effects.

A

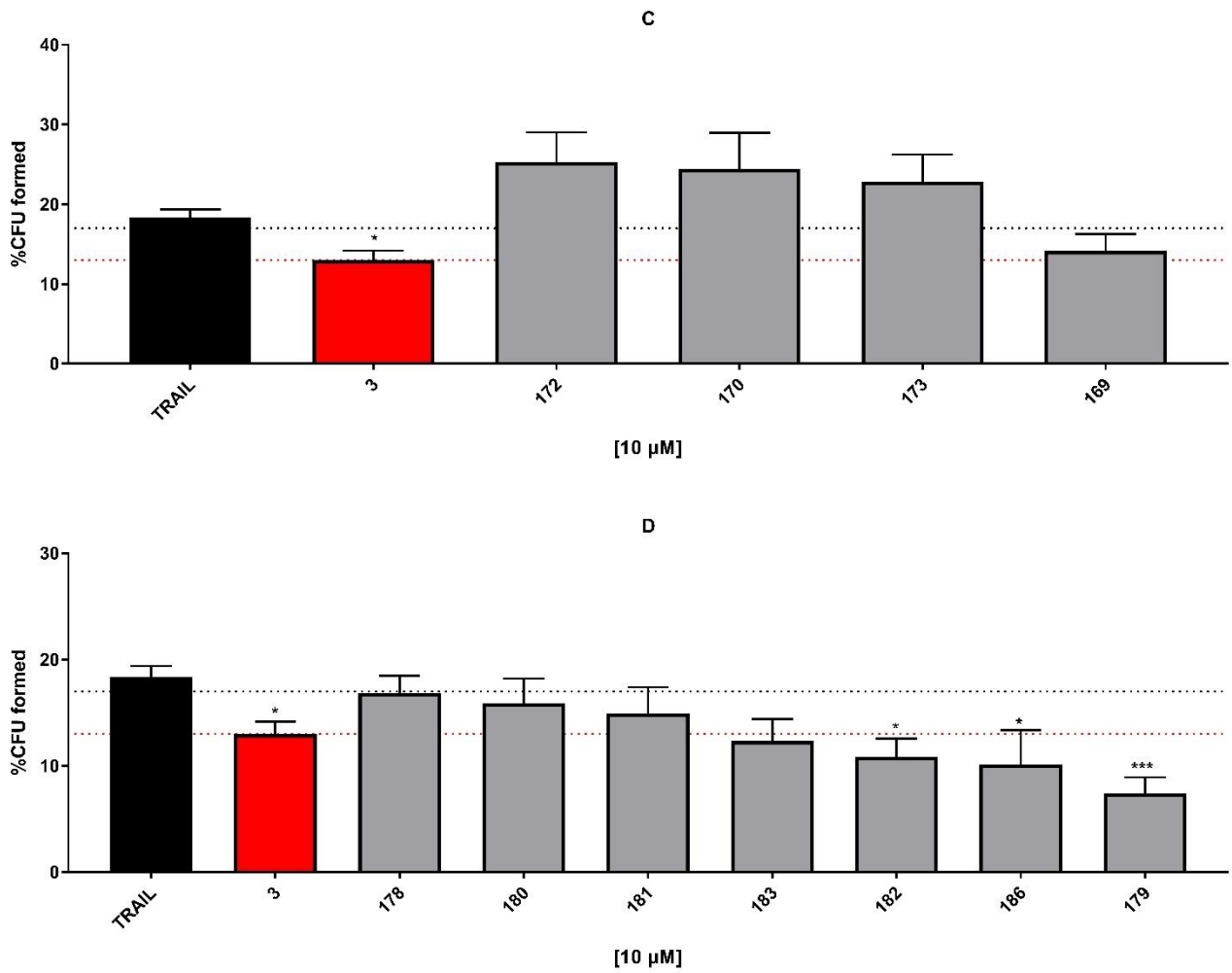


[10 µM]

B



[10 µM]



Graph 6.4.4A-D: Summary of the results obtained for all the test compounds when administered in combination with TRAIL. A:sulfonamide derivatives; B:amine derivatives; C:methylene derivatives; D:amide derivatives.

6.5 *In vitro* pharmacokinetic studies

In order to investigate how the newly designed chemical modifications affected the pharmacokinetic properties of the compounds, some of the synthesised derivatives were subjected to preliminary *in vitro* pharmacokinetic studies. These studies were performed by Cyprotex Ltd and they include metabolic stability, Caco2 cell permeability and hERG inhibition. The metabolic stability was evaluated using the microsomal stability assay which measures the *in vitro* intrinsic clearance. ⁽¹³⁾ The Caco2 cell permeability assay ⁽¹⁴⁾ estimates the intestinal permeability of the compounds and finally the hERG inhibition assay ⁽¹⁵⁾ evaluates their potential cardiotoxicity. Data obtained are reported in Tables 6.5.1, 6.5.2 and 6.5.3.

Compound	CL _{int} (µl/min/mg protein)	Standard Error CL _{int}	t1/2 (min)
3	15.1	3.14	91.8
24	Nd	Nd	Nd
79	79.5	12.7	17.4
117	35.6	2.85	39.0
141	35.6	2.90	39.0
88	10.4	1.33	134
150	92.3	3.33	15.0

Table 6.5.1: Microsomal Stability Assay Results.

Compound	Mean % recovery (A2B)	Mean % recovery (B2A)	Efflux Ratio
3	86.3	95.6	0.660
24	Nd	nd	Nd
79	Nd	nd	Nd
117	66.2	77.2	0.622
141	61.3	73.5	0.881
88	66.7	67.2	6.43
150	23.1	51.7	0.768

Table 6.5.2: Caco2 Cell Permeability Assay Results.

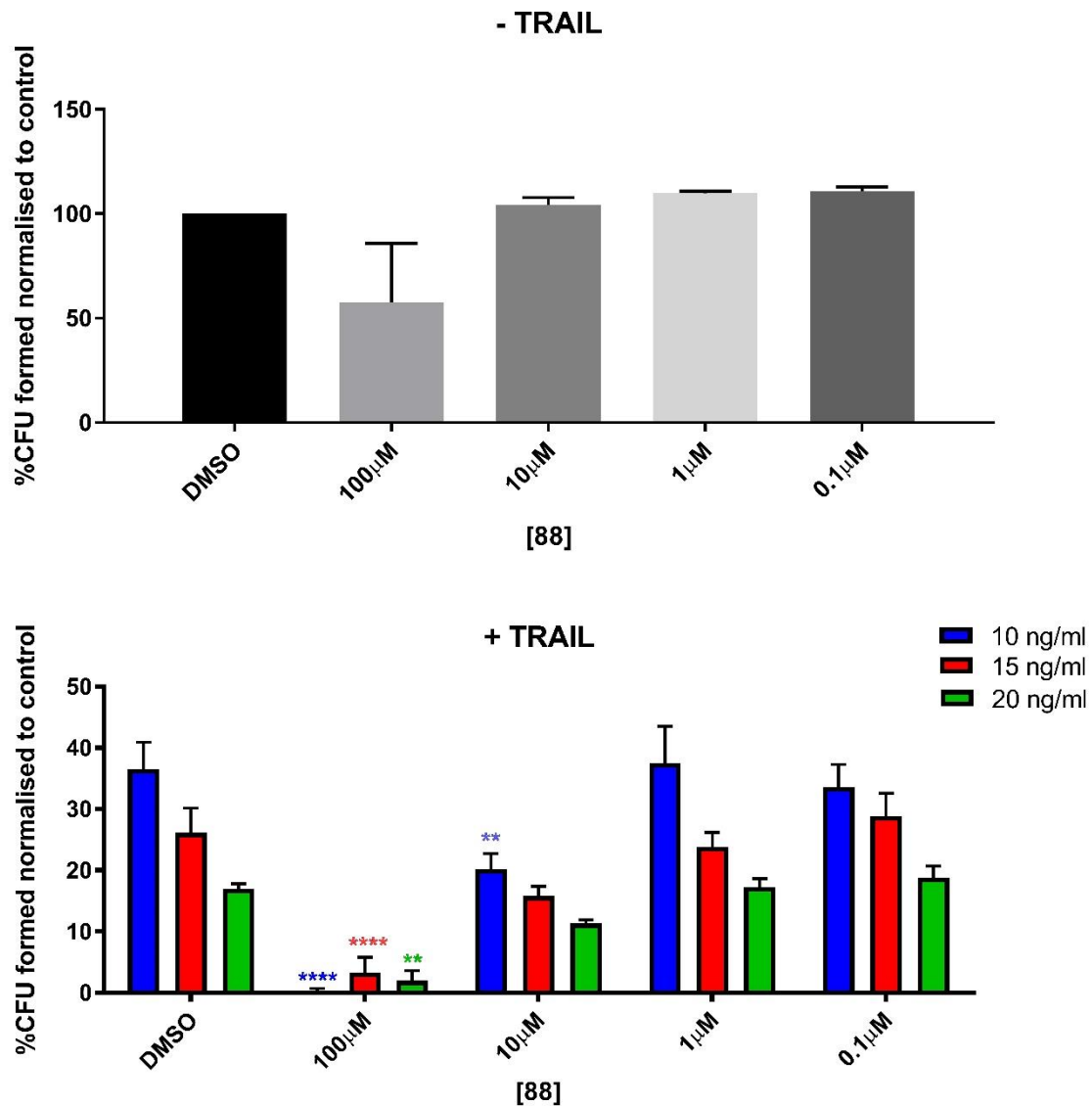
Compound	IC ₅₀ (μM)
3	>25
24	23.6
79	>25
117	>25
141	>25
88	>25
150	92.3

Table 6.5.3: hERG Inhibition Assay Results.

In general, all the compounds tested did not show any significant ability to inhibit hERG channels, thus suggesting lack of cardiotoxic effects. Good permeability in both directions across the Caco2 cells was observed for all compounds, indicating a predicted oral absorption potential. In terms of microsomal stability, most of the compounds showed a higher clearance and a shorter half-life time compared to **3**, whilst **88**, the *ortho* tetrazole derivative of **3**, was found to be more metabolically stable, increasing the half-life time of **3** from approximately 92 mins to 134 mins.

6.6 Dose-response studies

In order to further evaluate the activity of the compounds showing the best ability to increase TRAIL sensitisation at 10 μM concentration, dose-response studies were performed. Unfortunately, due to the time required for this assay to be performed, only a few compounds were selected. Compound **88**, the *ortho* tetrazole derivative of **3**, was the initial compound tested, mainly because of the slightly improved ability to reduce the number of CFU compared to **3**, and the positive pharmacokinetic profile showed in the preliminary *in vitro* ADME studies. This compound was tested at four different concentrations (100 μM, 10 μM, 1 μM and 0.1 μM). At the same time, a dose-response study for TRAIL was performed in order to evaluate whether the different concentration of TRAIL might influence the activity of the compound. Results are shown in Graph 6.6.1.



Graph 6.6.1: MCF-7 cells were treated with 88 at 100 µM, 10 µM, 1 µM, 0.1 µM, alone or in combination with TRAIL at 20 ng/ml, 15 ng/ml, 10 ng/ml. Colonies were counted after 10 days. %CFU was calculated from the number of cells plated and normalised to control (DMSO). Data shown is representative of at least 3 experiments \pm SEM. * $p < 0.05$, ** $p < 0.005$, *** $p < 0.0005$, **** $p < 0.0001$ Two-way ANOVA compared to TRAIL.

The dose-response curve, as well as the IC_{50} values calculated for the different concentrations of TRAIL used, is reported in Figure 6.6.1.

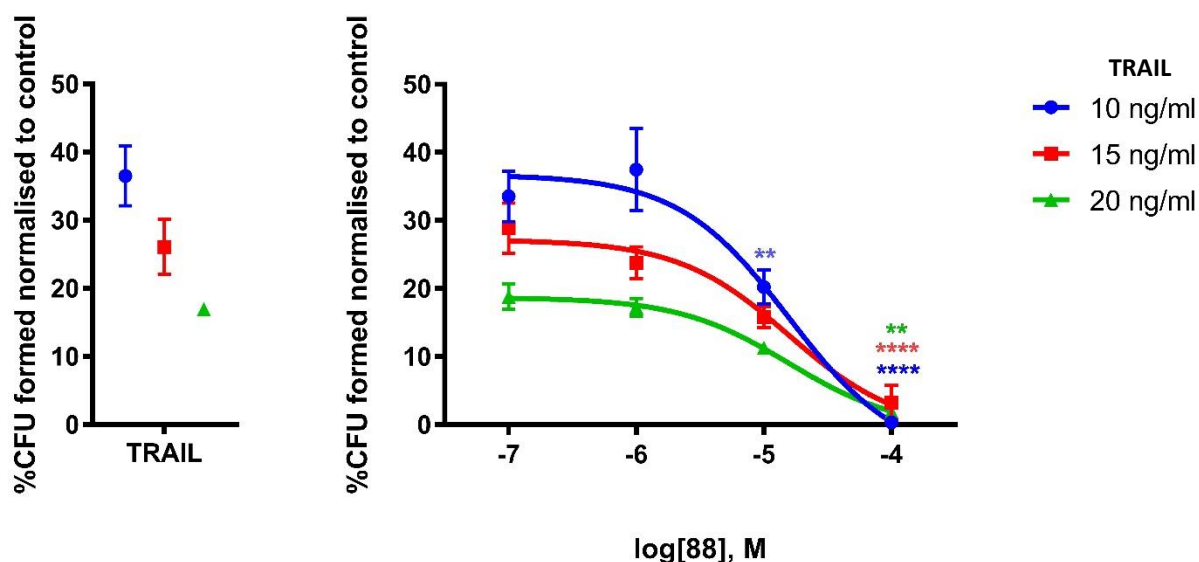
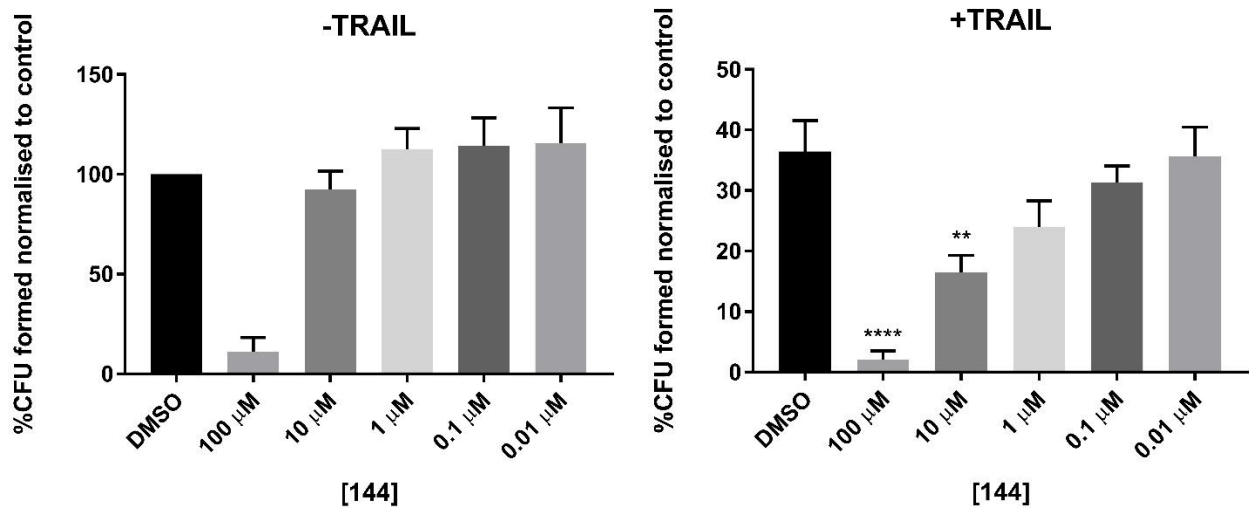


Fig 6.6.1: Dose-response curve and IC₅₀ values for compound **88**. IC₅₀ was calculated using GraphPad Prism 7.03, log(inhibitor) vs response (three parameters).

According to the results obtained, at the highest concentration of 100 μM, a reduction of CFU was observed even in the absence of TRAIL, thus indicating potential cytotoxic or non-specific effects at higher concentrations. Nevertheless, **88** increased TRAIL sensitisation in a dose-dependent manner, with an IC₅₀ value in the range of 15-19 μM. As shown in Figure 6.6.1, the effect of TRAIL alone (left graph) was dose-dependent, inducing a reduction of approximately 80% when tested at 20 ng/ml and 60% at the lowest concentration of 10 ng/ml. However, as demonstrated by the similar IC₅₀ values calculated, **88** retained a similar ability to increase TRAIL sensitisation independently of the TRAIL concentration, thus indicating that the concentration of TRAIL does not affect the activity of the compound.

A dose-response study was performed also for **144**, belonging to the amine series of derivatives. When tested at 10 μM concentration, **144** demonstrated a similar ability to increase TRAIL sensitisation compared to **3**. Taking into consideration the TRAIL concentration study performed for **88**, **144** was tested alone and in combination with TRAIL at 10 ng/ml. Similarly to **88**, **144** increased TRAIL sensitisation in a dose-dependent manner with an IC₅₀ value of 8.09 μM. The results obtained are shown in Graph 6.6.2 and the dose-response curve is illustrated in Figure 6.6.2.



Graph 6.6.2: MCF-7 cells were treated with 144 at 100 μM, 10 μM, 1 μM, 0.1 μM, 0.01 μM alone or in combination with TRAIL at 10 ng/ml. Colonies were counted after 10 days. %CFU was calculated from the number of cells plated and normalised to control (DMSO). Data shown is representative of at least 3 experiments ± SEM. * p<0.05, **p<0.005, ***p<0.0005, ****p<0.0001 One-way ANOVA compared to TRAIL.

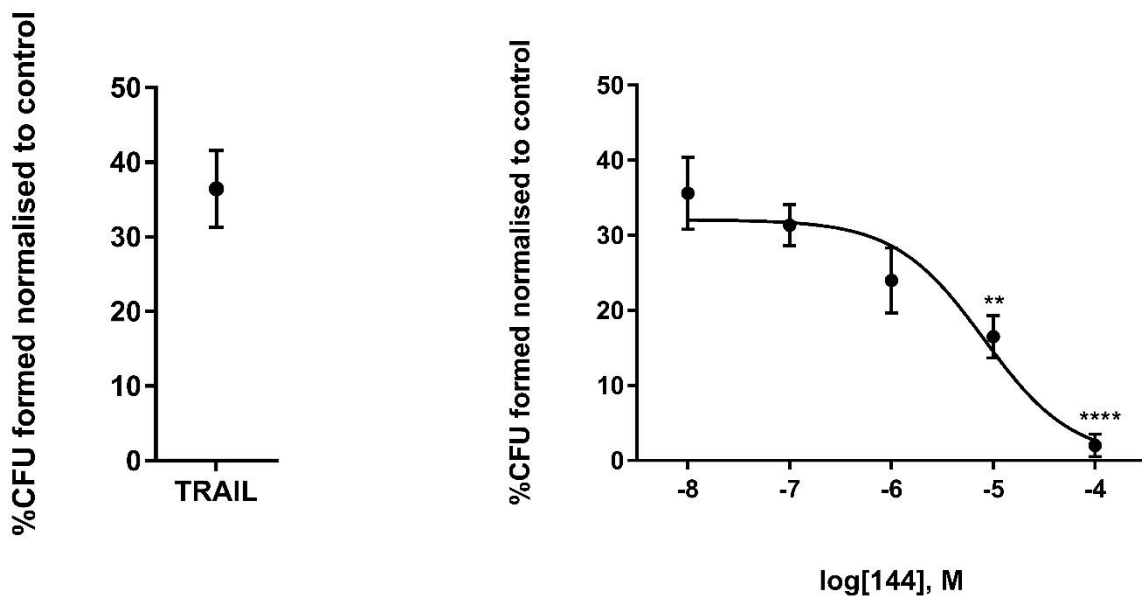


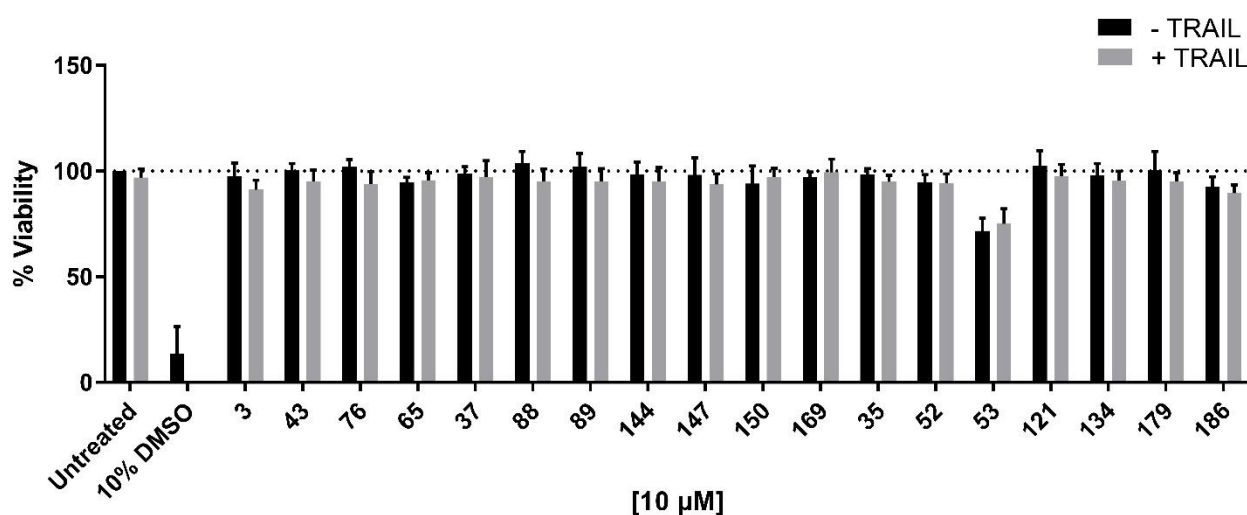
Fig 6.6.2: Dose-response curve and IC₅₀ values for compound 144. IC₅₀ was calculated using GraphPad Prism 7.03, log(inhibitor) vs response (three parameters).

6.7 Cytotoxicity Studies

As discussed in the previous paragraphs, several compounds demonstrated the ability to increase TRAIL sensitisation showing an activity similar or slightly improved compared to hit **3**. Cytotoxicity studies were performed for some of the best compounds in order to assess the lack of cytotoxic effects on non-cancerous cells. Moreover, those compounds inducing a reduction of the number of colonies formed in the absence of TRAIL, suggesting potential cytotoxic or off-target effects, were also investigated.

6.7.1 Cell Viability Assay

Cytotoxicity studies were performed using the CellTiter-Blue Cell Viability Assay. ⁽¹⁶⁾ The assay is based on the ability to measure the number of viable cells after treatment with different compounds, in order to evaluate the effects on cell proliferation and the ability to induce cell death. The number of viable cells is calculated according to their ability to convert resazurin into the highly fluorescent metabolite resofurin, which will emit a fluorescent signal. The fluorescence will be then measured to give the number of viable cells. ⁽¹⁶⁾ The assay was performed on human embryonic kidney cells (HEK293), which are representative of non-tumorigenic cells. ⁽¹⁷⁾ The protocol applied is reported in the Experimental Section. In general, cells were treated with the different compounds, alone and in combination with TRAIL at 20 ng/ml. After 24 hours viable cells were counted. The cytotoxicity of the compounds was measured as reduction of cell viability compared to the control, represented by untreated cells (minus TRAIL). The experiment was performed in the presence of a positive control represented by 10% DMSO. Graph 6.7.1 shows the results obtained.



Graph 6.7.1: Cell Viability Assay. HEK293 cells were treated with compounds at 10 μ M concentration, alone or in combination with TRAIL at 20 ng/ml. After 24 hours treatment the percentage of viable cells was calculated and normalised to the control (Untreated -TRAIL). 10% DMSO represents the positive control. Data shown is representative of at least 3 experiments \pm SEM.

All the compounds showing ability to increase TRAIL sensitisation in the Colony Forming Assay (**43**, **76**, **65**, **37**, **88**, **89**, **144**, **147**, **150** and **169**) did not induce a reduction of cell viability compared to the control, demonstrating lack of cytotoxic effects. Compounds **35**, **52**, **53**, **121**, **134**, **170** and **186** were also investigated due to their ability to induce a reduction of colonies formation in the absence of TRAIL. However, only **53** was found to be cytotoxic, inducing approximately 30% of cell death. Moreover, the non-toxicity of the original hit **3** was also confirmed, as well as the inability of TRAIL to induce cell death in non-cancerous cells.

6.8 Conclusions

The ability of compounds to sensitise TRAIL resistant MCF-7 cells to TRAIL was evaluated using the Colony Forming Assay. This assay is based on the ability of cancer cells, in particular of cancer stem cells, to proliferate, forming colonies of cells. The ability of the different compounds to increase TRAIL sensitisation was measured as the ability to reduce the number of colonies formed compared to TRAIL. Initially, a screening of all the newly synthesised compounds was performed testing all derivatives at 10 μM concentration. Several compounds revealed a similar ability to increase TRAIL sensitisation compared to hit **3**, while a few analogues were able to slightly increase the reduction of the CFU number. With the aim to investigate how the chemical changes introduced on the original hit structure affected the pharmacokinetic properties, preliminary *in vitro* ADME studies were performed on some of the compounds. Among the derivatives tested, **88** showed a greater metabolic stability and a higher half-life time compared to **3**. **88** was further evaluated with dose-response studies. These studies confirmed the ability of **88** to act in a dose-dependent manner, with an IC_{50} value that varies between approximately 15-19 μM . Contemporarily, a dose-response study of TRAIL was also performed. The results obtained indicated that, although the effect of TRAIL on MCF-7 cells was dose-dependent, the activity of the compound to increase TRAIL sensitisation was not influenced by the different concentrations of TRAIL. A dose-response study was performed also for **144**, which belongs to the amine series of derivatives and, similarly to **88**, shows a tetrazole moiety. **144** was found to be able to increase TRAIL sensitisation with an IC_{50} of 8.09 μM . Additionally, these two compounds, together with other analogues showing a good efficacy in increasing TRAIL sensitisation, were evaluated in a cytotoxicity assay on non-cancerous cells. The results obtained confirmed the lack of cytotoxic effects of the tested compounds. Taking into consideration the better pharmacokinetic profile and the slightly improved activity compared to **3**, **88** was identified as a new promising hit and additional studies will be performed with the aim to further demonstrate the ability of **88** to increase TRAIL sensitisation in breast cancer stem cells and

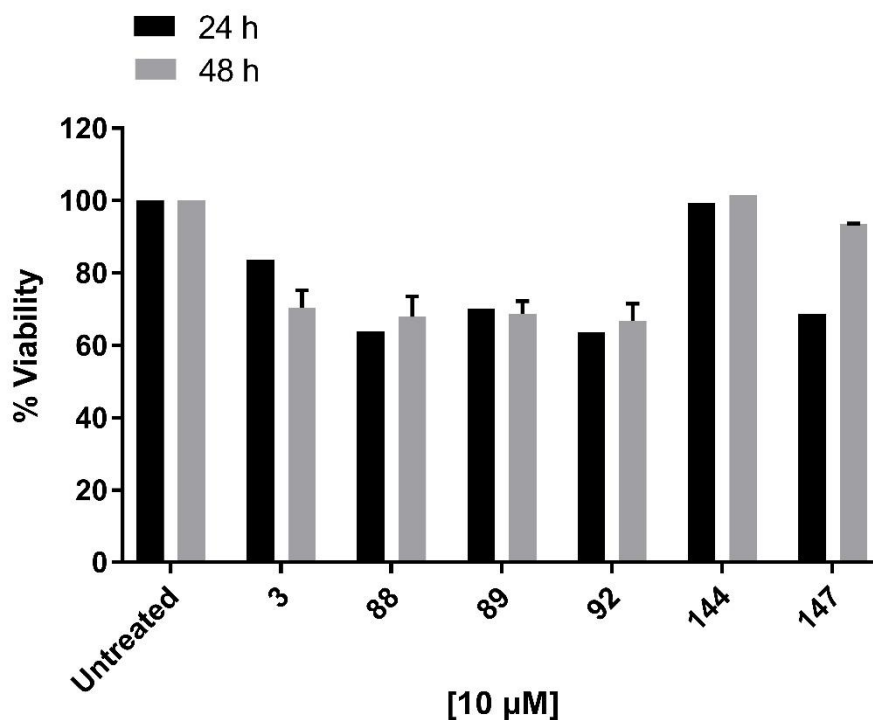
to confirm the role of **88** as a c-FLIP inhibitor. A description of the future assays will be discussed in the Conclusion chapter. At the same time, dose-response studies will be performed for all the other derivatives that showed an ability to increase TRAIL sensitisation similarly or slightly improved compared to **3**.

6.9 Pancreatic Studies

As part of a project carried in our research group, some of the newly synthesised derivatives were also evaluated for their ability to induce apoptosis in a pancreatic cancer cell line (TKCC-07). This project followed the results obtained in a previous work, which demonstrated the ability of TRAIL to promote proliferation and migration of pancreatic *KRAS*-mutated cancer via TRAIL-R2 mediated activation of the RAc1/PI3K signalling pathway. ⁽¹⁸⁾ The project undertaken in our research group aimed to investigate whether c-FLIP, via blocking the activation of the apoptotic pathway, might indirectly contribute to the stimulation of the proliferative pathway. Preliminary results obtained from this study, performed by Dr Aleksandra Gruca, showed that inhibition of c-FLIP, using siRNA increased cell death in different pancreatic cancer cell lines in the cell viability assay. Moreover, treatment of cells with hit **3** at 10 μ M concentration and TRAIL, induced a reduction in cell viability of approximately 60-70% after 19 hours treatment. Interestingly hit **3**, when administered alone, showed a reduction in cell viability of approximately 30% after 19 hours treatment, which was increased to approximately 40% prolonging the treatment with hit **3** to 48 hours. Therefore, according to the preliminary data obtained in this study, a promising ability of hit **3** to induce activation of the apoptotic pathway even in the absence of TRAIL was suggested. Following these studies, some of the newly designed derivatives were also investigated.

6.9.1 Cell Viability Assay

At the time when this experiment was performed, only preliminary data had been obtained from the colony forming assay, therefore the selected derivatives for the pancreatic studies do not necessarily correspond to the compounds showing the best ability to increase TRAIL sensitisation in the MCF-7 cells. Compounds were tested at 10 μ M concentration for their ability to reduce cell viability of the pancreatic cancer cells after 24 and 48 hours treatment. The preliminary results obtained are shown in Graph 6.9.1.



Graph 6.9.1: TKCC-07 cells were treated with different compounds at 10 μ M concentration for 24 hours (black bars) and 48 hours (grey bars). After this time, the viable cells were counted and the %viability was calculated and normalised to the control (Untreated). N=1 for 24h treatment, N=2 for 48h treatment (144 N=1).

Compared to the data obtained in the previous experiments performed in our research group, hit **3** showed a similar potency in reducing cell viability. **88**, **89** and **92** gave the best results, showing approximately a 40% of reduction in cell viability after 24 hours and 48 hours of treatment. On the contrary, **144** did not affect the number of viable cells, which was comparable to the control. Controversial results were obtained for **147**, which induced a higher percentage of cell death after 24 hours than the 48 hours treatment. Although more repetitions are needed in order to confirm these results, the positive preliminary data obtained might be used as a starting point for further evaluations aiming to investigate a potential application of **3** and its derivatives in the treatment of pancreatic cancer.

6.10 References

- 1: Velasco-Velazquez, M. A.; Homsí, N.; De La Fuente, M.; Pestell, R. G. Breast cancer stem cells. *Int. J. Biochem. Cell Biol.* **2012**, *44*, 573-577.
- 2: Smalley, M.; Piggott, L.; Clarkson, R. Breast cancer stem cells: obstacles to therapy. *Cancer Lett.* **2013**, *338*, 57-62.
- 3: Chari R. V. J. Targeted cancer therapy: conferring specificity to cytotoxic drugs. *Acc. Chem. Res.* **2008**, *41*, 98-107.
- 4: Koschny, R.; Walczak, H.; Ganten, T.M. The promise of TRAIL-potential and risk of a novel anticancer therapy. *J. Mol. Med.* **2007**, *85*, 923-935.
- 5: Piggott, L.; Omidivar, N.; Pérez, S.M.; Eberl, M.; Clarkson, R. W. E. Suppression of apoptosis inhibitor c-FLIP selectively eliminates breast cancer stem cell activity in response to the anti-cancer agent, TRAIL. *Breast Cancer Res.* **2011**, *13*, S88.
- 6: Hayward, O. Design and Synthesis of Molecular Inhibitors of c-FLIP Activity as a Therapeutic Strategy to Target Breast Cancer Stem Cells. PhD Thesis. **2015**, Cardiff University.
- 7: Rajendran, V.; Jain, V. M. In vitro tumorigenic assay: colony forming assay for cancer stem cells. *Methods Mol. Bio.* **2018**, *1735*, 1984-2018.
- 8: Franken, N. A.; Rodermond, H. M.; Stap, J.; Haveman, J.; Van Bree, C. Clonogenic assay of cells in vitro. *Nat. Protoc.* **2006**, *1*, 2315-2319.
- 9: Pellegrini, G.; Dellambra, E.; Golisano, O.; Martinelli, E.; Fantozzi, I; Bondanza, S.; Ponzin, D.; McKeon, F.; De Luca, M. p63 identifies keratinocyte stem cells. *Proc. Nat. Acad. Sci.* **2001**, *98*, 3156-3161
- 10: Claudinot, S.; Nicolas, M.; Oshima, H.; Rochat, A; Barrandon, Y. Long-term renewal of hair follicles from clonogenic multipotent stem cells. *Proc. Nat. Acad. Sci.* **2005**, *102*, 14677-14682.
- 11: MCF-7 Cells. <http://www.mcf7.com> (accessed October 13, 2017).
- 12: GraphPad Software, La Jolla California USA, www.graphpad.com.
- 13: Microsomal Stability Assay. <http://www.cyprotex.com> (accessed January 13, 2018).

- 14:** Caco-2 Permeability Assay. <http://www.cyprotex.com> (accessed January 13, 2018).
- 15:** hERG Safety Assay. <http://www.cyprotex.com> (accessed January 13, 2018).
- 16:** Riss, L. T.; Moravec, R. A.; Niles, A. L.; Duellman, S.; Benink, H. A.; Worzella, T. J.; Minor, L. Cell viability assays. In *Assay guidance manual*, 1st ed.; Sittampalam, G. S.; Coussens, N. P.; Nelson, H.; Arkin, M.; Auld, D.; Austin, C.; Bejcek, B.; Glicksman, M.; Inglese, J.; Iversen, P. W.; Li, Z.; McGee, J., McManus, O.; Minor, L.; Napper, A., Peltier, J. M.; Riss, T.; Trask, O. J.; Weidner, J. Eds.; Bethesda (MD): Eli Lilly & Company and the National Center for Advancing Translational Sciences, 2013. Available from: <http://www.ncbi.nlm.nih.gov/books/NBK53196/>.
- 17:** HEK293. <http://www.hek293.com/> (accessed November 21, 2017).
- 18:** Von Karstedt, S.; Conti, A.; Nobis, M.; Montinaro, A.; Hartwig, T.; Lemke, J.; Legler, K.; Annewanter, F.; Campbell, A. D.; Taraborrelli, L.; Grosse-Wilde, A.; Coy, J. F.; El-Bahrawy, M. A.; Bergmann, F.; Koschny, R.; Werner, J.; Ganten, T. M.; Schweiger, T.; Hoetzenecker, K.; Kenessey, I.; Hegedüs, B.; Bergmann, M.; Hauser, C.; Egberts, J. H.; Becker, T.; Röcken, C.; Kalthoff, H.; Trauzold, A.; Anderson, K. I.; Sansom, O. J.; Walczak, H. Cancer cell-autonomous TRAIL-R signaling promotes KRAS-driven cancer progression, invasion, and metastasis. *Cancer Cell*. **2015**, *27*, 561-573.

Chapter 7

Molecular Docking Studies

Chapter 7: Molecular Docking Studies

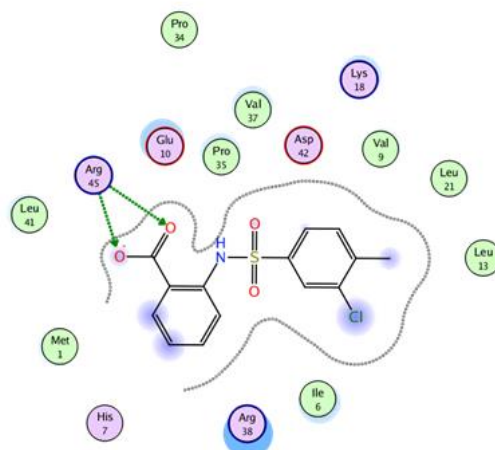
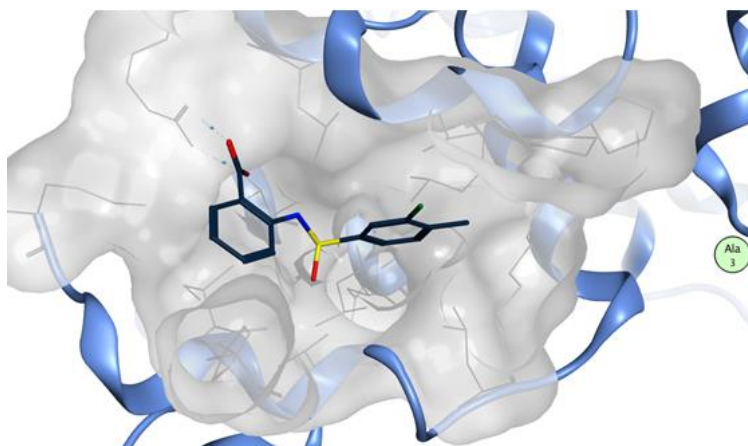
7.1 Molecular Docking Studies

Following the biological evaluation, molecular docking studies were performed in order to investigate the predicted binding mode of the newly designed derivatives within the c-FLIP pocket and potentially explain the differences in activity observed between the derivatives. All molecular docking analyses were performed using Glide SP ⁽¹⁾ and the methodology applied is reported in the Experimental Section.

7.1.2 Sulfonamide derivatives

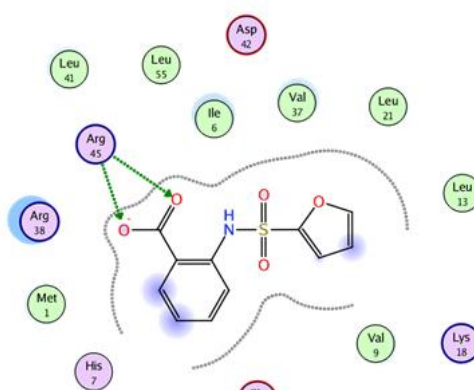
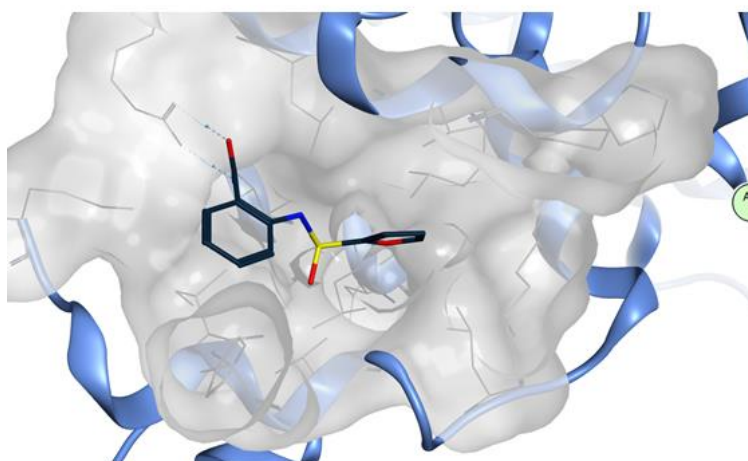
According to the docking results, the majority of the sulfonamide derivatives occupy the hydrophobic c-FLIP pocket with a binding mode which is similar to the one predicted for hit **3**. In general, the sulfonamide group is located behind the residues Arg38 and Glu10 and it allows the two aromatic rings to fit the pocket. The hydrophobic ring of the different derivatives, which in most molecules is represented by a phenyl ring showing different hydrophobic substituents, or in some cases replaced by heterocycles such as furan or thiophene, or in bigger hydrophobic rings such as naphthalene and quinoline rings, always occupies the deepest part of the cavity. On the contrary, the “hydrophilic” ring remains on the external side due to the interactions occurring between the carboxylic acid moiety and Arg45. These interactions are maintained in the derivatives where the carboxylic acid group is replaced by bioisosteres such as tetrazole and oxadiazole. On the contrary, different results were obtained for the carboxamide derivatives. According to the docking results, the introduction of the carboxamide group leads to the loss of the interaction with Arg45, while a new hydrogen bond is formed between the carboxyl group and Lys18, thus causing a shift of the aromatic ring position to the opposite site of the c-FLIP pocket. Figure 7.1.2 (A-F) shows the predicted binding mode for representative structures of the different chemical modifications mentioned above.

A



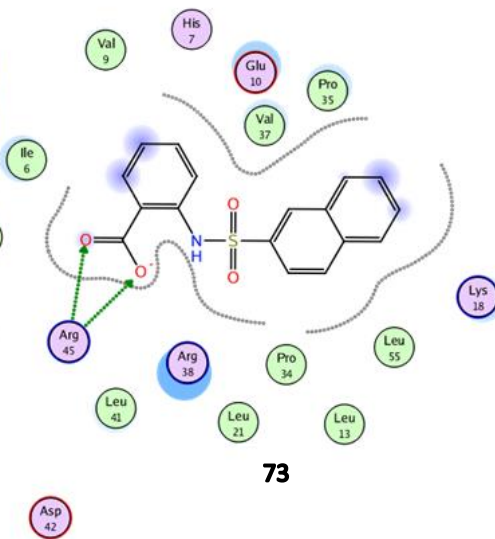
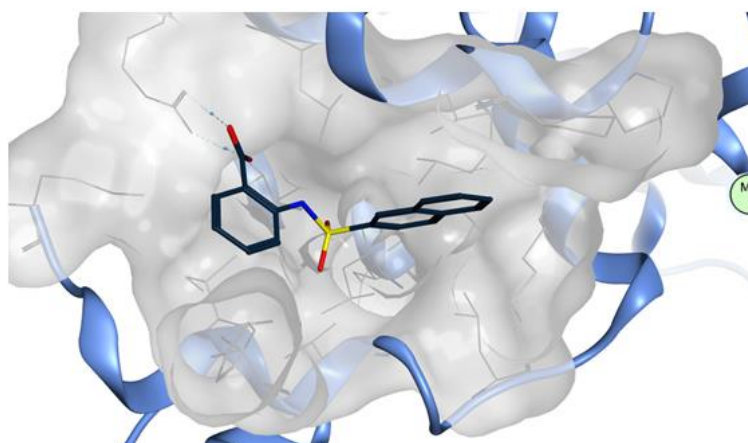
43

B



76

C



73

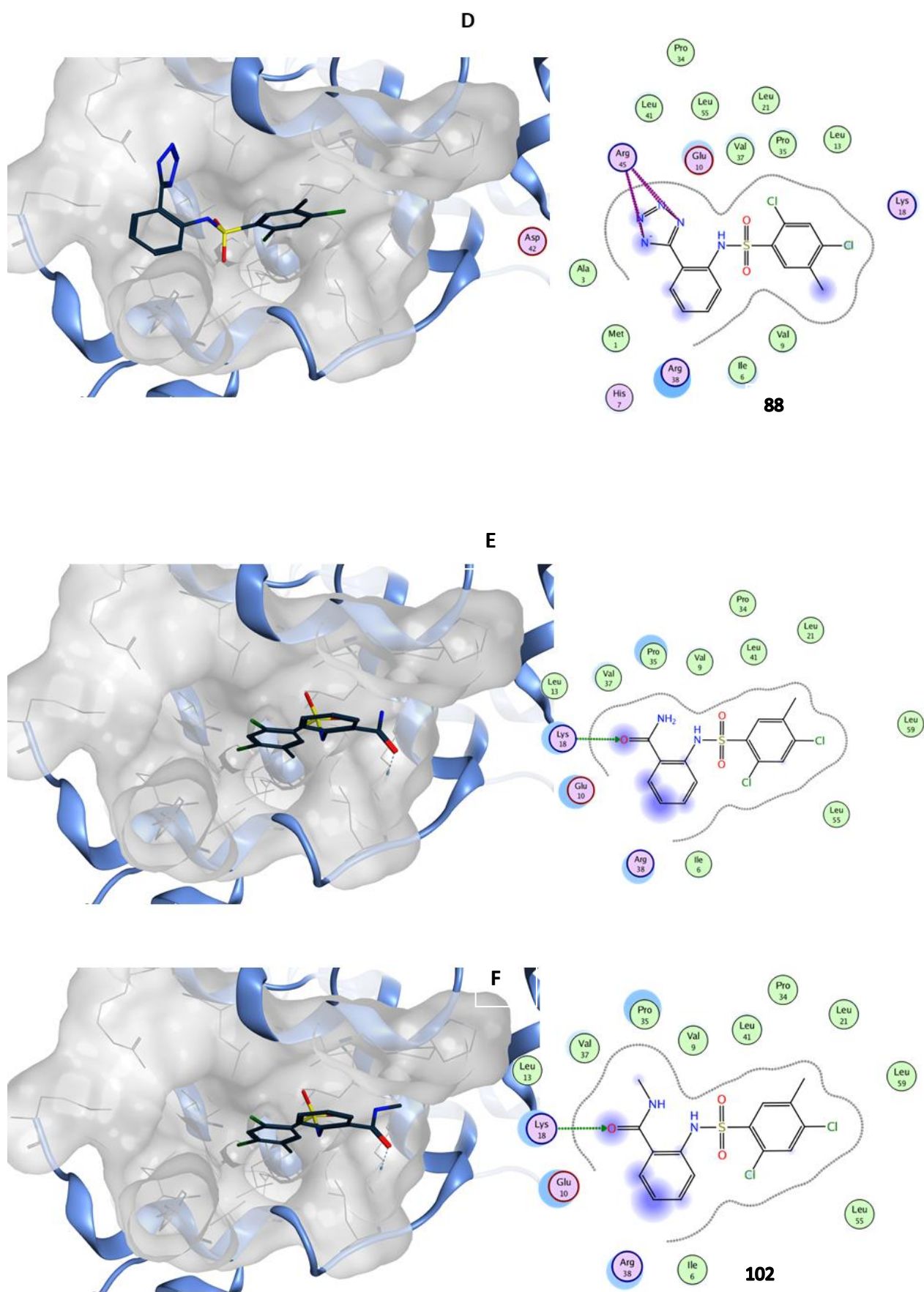


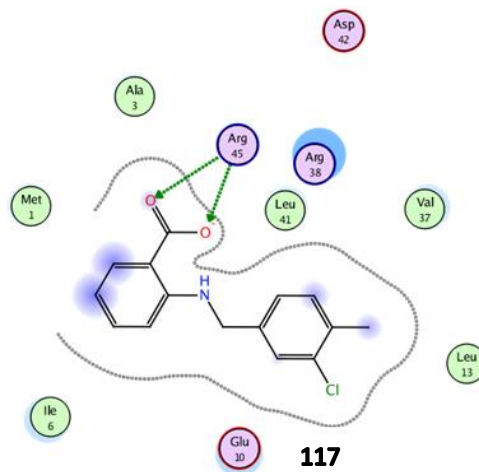
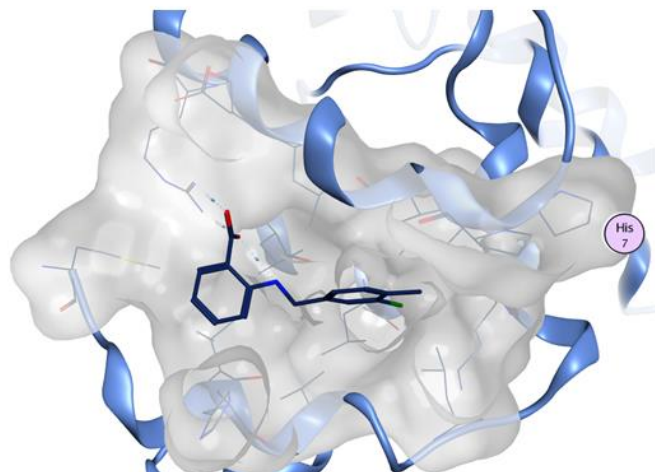
Fig 7.1.2: Predicted binding mode and ligand interactions for compounds A:43, B:76, C:73, D:88, E:106, F:102. These compounds (dark blue) are representative of the general binding mode. On the right are shown the interactions which occur with the amino acid residues.

Taking into consideration the general scaffold of the synthesised sulfonamide derivatives, all characterised by the presence of two aromatic rings linked by a sulfonamide group, a similar binding mode was predicted for the majority of the different analogues, therefore these results cannot be used for explaining the different biological activity observed among the compounds. Moreover, the biological results obtained for the derivatives showing a carboxamide group, which, although showing a decrease in activity, retained the ability to increase TRAIL sensitisation, is in contrast with the predicted poor ability to fit the hydrophobic cavity of c-FLIP. In conclusion, a correlation between the docking results and the biological activity cannot be clearly identified.

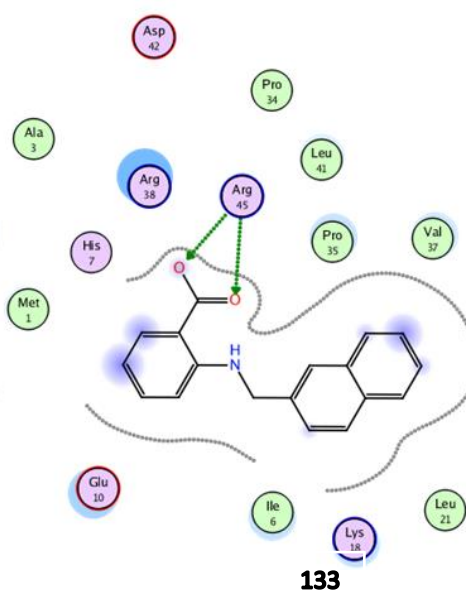
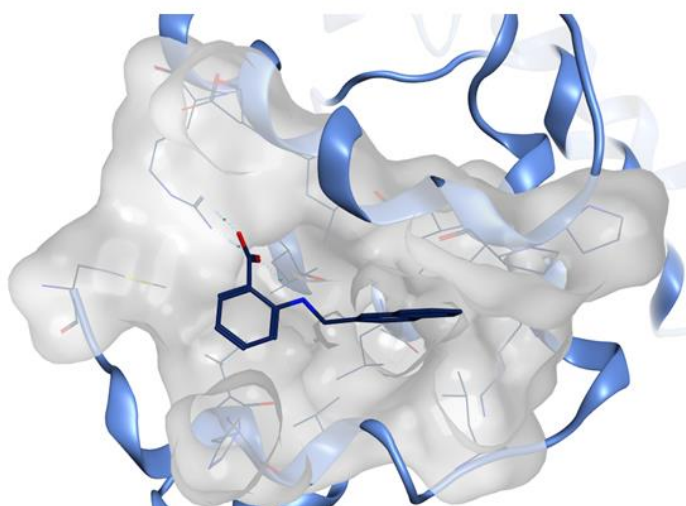
7.1.3 Amine Derivatives

The docking results obtained for the amine derivatives are shown in figure 7.1.3(A-E). The amine linker, fitting the area behind the residues Glu10 and Arg38, allows the hydrophobic rings to reach the deepest part of the pocket, while the anthranilic rings are located in proximity of the residue Arg45, which forms a H-bond with the carboxylic acid group (A-B). Derivatives showing a longer or inverted amine linker seem to retain the general binding mode described above (C-D), as well as the derivatives where the carboxylic acid group is replaced by a tetrazole ring (E).

A



B



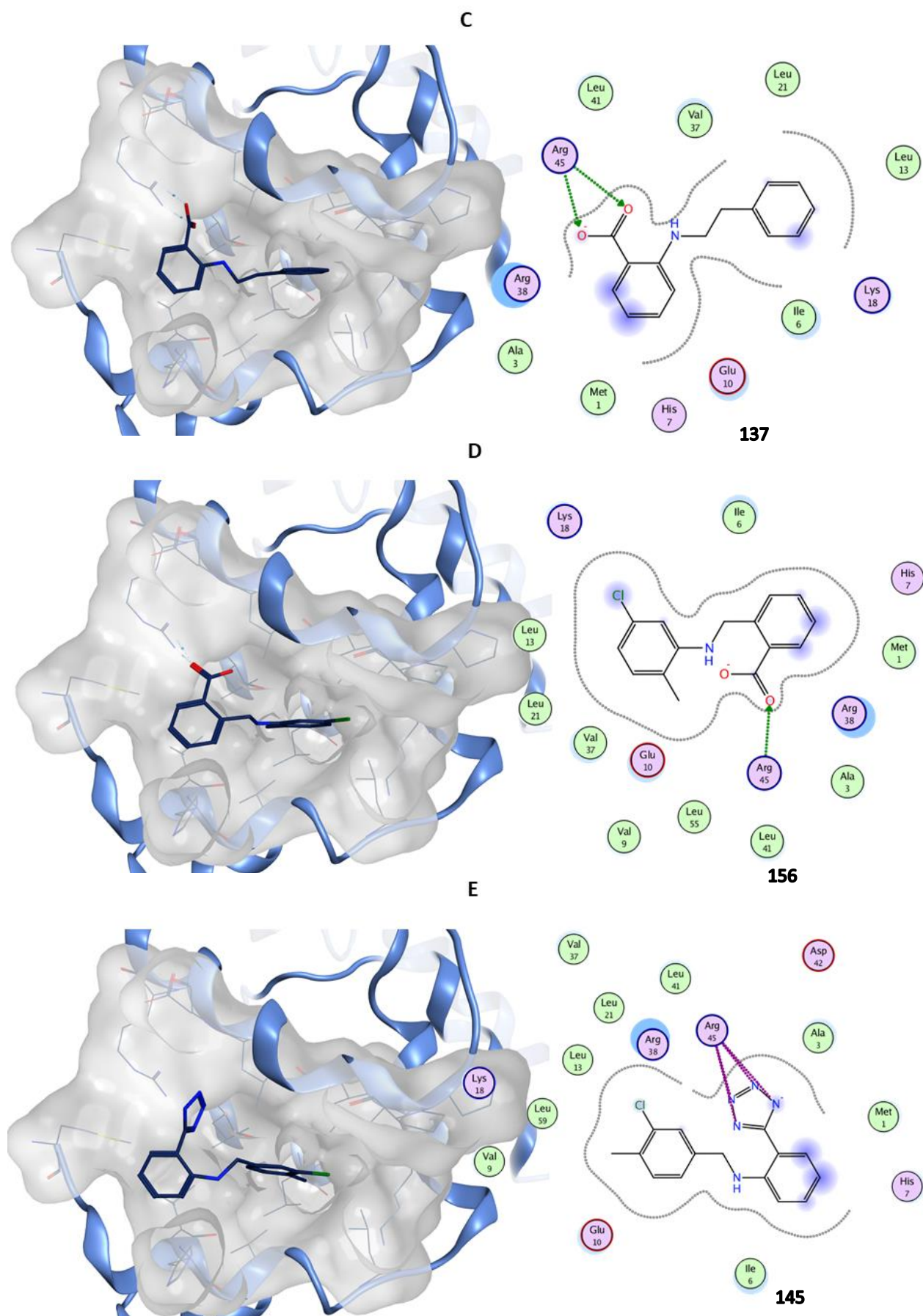


Fig 7.1.3: Predicted binding mode for the compounds A:117, B:133, C:137, D:156, E:145. These compounds (dark blue) are representative of the general binding mode. On the right are shown the interactions which occur with the amino acid residues.

Similarly to the sulfonamide derivatives, all the amine analogues were predicted to fit the c-FLIP pocket with the general binding mode described above. Therefore, unfortunately, the docking results cannot be used to explain the differences in biological activity observed for the amine derivatives.

7.1.3 Methylene and amide derivatives

The general predicted binding mode for the methylene and amide derivatives within the pocket of c-FLIP is similar to the one described for the sulfonamide and amine series and it is shown in Figures 7.1.3.1. and 7.1.3.2.

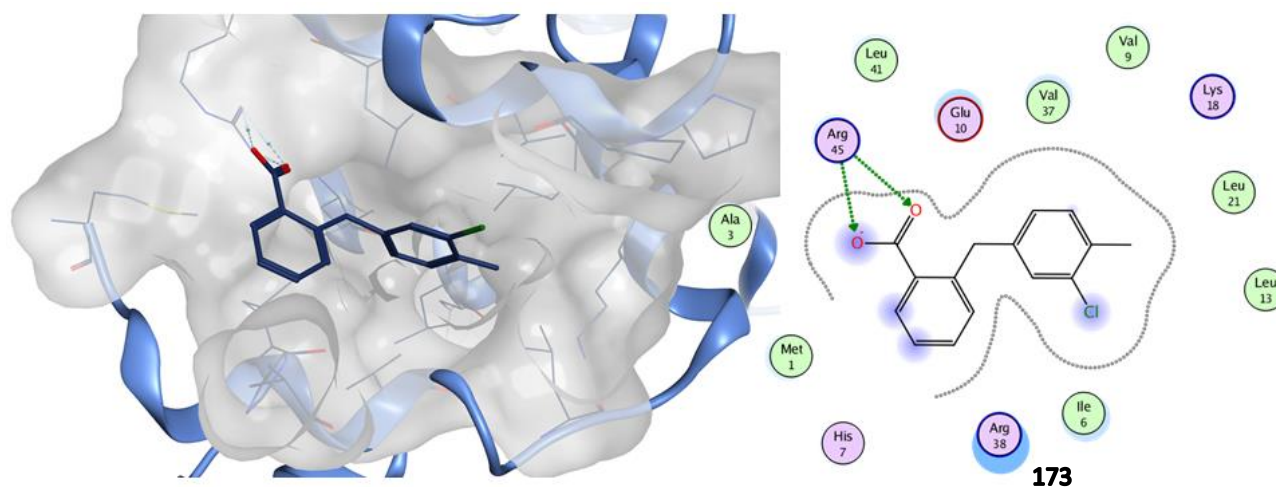


Figure 7.1.3.1: Predicted binding mode for compound 173. This compound (dark blue) is representative of the general binding mode of the methylene derivatives. On the right are shown the interactions which occur with the amino acid residues.

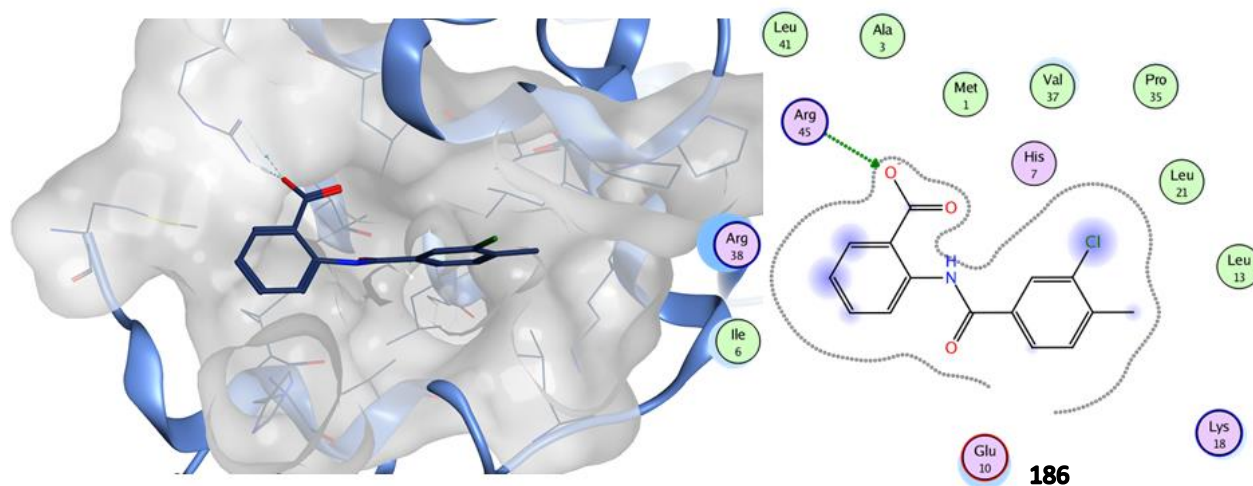


Figure 7.1.3.2.: Predicted binding mode for compound 186. This compound (dark blue) is representative of the general binding mode of the amide derivatives. On the right are shown the interactions which occur with the amino acid residues.

For the methylene derivatives, despite the shorter distance between aryl groups, the two aromatic rings are predicted to retain their ability to occupy the c-FLIP pocket. The $-CH_2$ linker is located in proximity of the residues Arg38 and Glu10, allowing the hydrophobic substituted ring to ease into

the internal part of the pocket, whilst, on the other side, the carboxylic acid moiety on the anthranilic ring forms a H-bond with Arg45. Despite the positive docking results obtained, three of the four methylene derivatives evaluated did not show biological activity. Moreover, according to the docking results for the amide derivatives, the planar geometry does not affect the ability of the amide linker to occupy the curved-shaped cavity, thus promoting the arrangement of the hydrophobic ring in the internal hydrophobic area of the pocket, whilst leaving the carboxylic acid moiety to interact with Arg45 (Figure 7.1.3.2). Although this general predicted binding mode does not allow explanation of the differences in biological activity observed for the amide derivatives, the predicted ability of molecules showing a planar conformation to fit the pocket of c-FLIP might correlate with the ability observed for some of the amide derivatives to increase TRAIL sensitisation.

7.2 Conclusions

All the newly synthesised derivatives show a common scaffold which can be divided into three different parts: a hydrophobic region represented by different aromatic rings, a more hydrophilic area characterised by a phenyl ring substituted with several carboxylic acid-based functional groups, and a short linker which connects the two aromatic rings. Taking into consideration this general structure, the predicted binding mode generated from the molecular docking analyses was highly similar among all the derivatives, with the different linkers occupying the central area of the curved-shaped cavity of c-FLIP, the hydrophobic ring reaching the deepest part of the pocket and the different functional groups on the other side interacting with Arg45. Although these positive docking results might confirm the ability of this class of molecules to occupy the c-FLIP pocket, considering the generalised results obtained, a potential correlation between molecular docking predictions and the differences observed in the biological activity could not be clearly identified.

7.3 References

1: Schrödinger, Cambridge, MA. www.schrodinger.com (accessed December 21, 2017).

Chapter 8

Conclusion and Future Perspectives

Chapter 8: Conclusion and Future Perspectives

8.1 Conclusion

This study aimed to develop novel and selective c-FLIP inhibitors in order to sensitise resistant breast cancer cells and breast cancer stem cells to TRAIL treatment. During previous work performed in our research group, molecular modelling techniques had been used to explore the features involved in the binding between c-FLIP and FADD, and a targetable pocket in the structure of c-FLIP had been identified. Virtual screening studies had been performed leading to the identification of one potential c-FLIP inhibitor, **3**, active at micromolar concentrations. ⁽¹⁾ In this work, molecular modelling studies were performed in order to analyse the features required for the binding between the potential inhibitors and the pocket of c-FLIP. Taking into consideration these studies, several analogues of the original hit compound were designed with the aim to develop novel small-molecule c-FLIP inhibitors showing improved pharmacokinetic profiles and a greater activity compared to **3**. Four different series of derivatives were designed and they are summarised in Table 8.1. In general, the central scaffold of each series shows a hydrophobic region (R), which is connected to a substituted phenyl ring by different linkers.

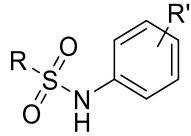
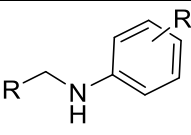
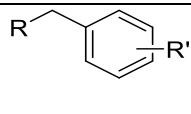
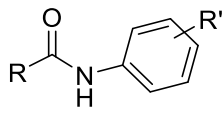
Sulfonamide derivatives	
Amine derivatives	
Methylene derivatives	
Amide derivatives	

Table 8.1: Central scaffold of the different series of derivatives.

In each series different modifications were explored in order to investigate structure-activity relationships. Different synthetic strategies were applied and all the designed derivatives were successfully synthesised. The newly synthesised small molecules were biologically evaluated for their ability to induce TRAIL sensitisation in the TRAIL-resistant MCF-7 breast cancer cell line using the *in vitro* Colony Forming Assay. This assay is based on the ability of cancer cells, in particular cancer stem cells, to proliferate forming colonies of cells, counted as colony forming units (CFU).

The activity of the compounds was measured as the ability to reduce the number of CFU when administered in association with TRAIL. Most derivatives demonstrated the ability to increase TRAIL sensitisation when tested at 10 μ M concentration, showing a similar activity compared to hit **3**. Moreover, some of the compounds slightly increase the reduction of CFU compared to **3**. Among these compounds, **88**, the tetrazole derivative of **3**, also demonstrated greater metabolic stability and longer half-life (when incubated with microsomes) compared to **3**. Dose-response studies confirmed the ability of **88** to increase TRAIL sensitisation in a dose-dependent manner, with an IC_{50} value in the range of 15-19 μ M. A dose-dependent TRAIL sensitising effect was observed also for **144**, which showed an IC_{50} value of 8.09 μ M. Additional dose-response studies for compounds which gave the best results in the initial 10 μ M CFA will be performed in the future. Cytotoxicity studies on non-cancerous cells confirmed the lack of cytotoxic effects for the majority of the compounds evaluated. Taking into consideration all these data, together with the results obtained from the molecular docking studies which suggested the ability of the synthesised derivatives to occupy the pocket of c-FLIP, a series of novel potential c-FLIP inhibitors showing ability to increase TRAIL sensitisation in breast cancer stem cells was developed. A novel hit, **88**, was identified and future studies will be performed to investigate its role as a c-FLIP inhibitor. Moreover, as part of a project undertaken in our research group, some of the synthesised derivatives were evaluated for their ability to activate the TRAIL-apoptotic pathway in a pancreatic cancer cell line. Although further confirmations are needed, positive preliminary results were obtained and they might represent the starting point for additional investigations of potential applications of the synthesised compounds in the treatment of pancreatic cancer.

8.2 Future Perspectives

In order to confirm the role of the synthesised derivatives as novel c-FLIP inhibitors, a series of different biological assays will be performed.

8.2.1 Biological Evaluation

8.2.1.1 Mammosphere Assay

The mammosphere formation assay is an *in vitro* assay based on the ability of cancer stem cells to form cluster of cells, termed “mammospheres”.⁽²⁾ This assay is the most reliable *in vitro* assay for the identification of cancer stem cells. Practically, the cancer cell line will be plated in suspension in non-adherent conditions, using particular media and culture plates. Only cancer stem cells will be able to survive in these conditions, while all the other cells will die by anoikis.⁽³⁾ The mammospheres formed in the first passage are consequently broken-up and treated in the same conditions described above. The new mammospheres formed in the second passage will be representative of the cancer stem cells self-renewal ability.⁽³⁾ A reduction of the number of mammospheres will indicate the compounds to hit cancer stem cells.

8.2.1.2 *In Vivo* Studies

In Vivo studies will be necessary to confirm the ability of the combined TRAIL/compounds therapy to reduce tumour growth and to prevent reoccurrence of the tumour, as well as to provide information about potential toxicity and undesired effects.

8.2.2 Mechanism Of Action Studies

8.2.2.1 Caspase-8 Activity Assay

The caspase-8 activity assay measures the protease activity using specific kits containing a luminogenic caspase-8 substrate.⁽⁴⁾ The assay will be performed to measure the increase of caspase-8 activity in presence of the combined treatment using TRAIL and test compounds, in order to prove that the compounds are acting via the caspase-8 pathway.

8.2.2.2 Co-immunoprecipitation

Co-immunoprecipitation (Co-IP) is a technique used to identify protein-protein interactions.⁽⁵⁾ The assay is based on the ability to precipitate the complex formed by the two interacting proteins from a cell lysate. Practically, the incubation of the cell lysate with an antibody against one of the two interacting proteins forms an immune complex. This complex is then precipitated using an antibody-binding protein attached to a beaded support. The precipitate, constituted by the antibody bound

to the complex protein-protein interaction, is then fractionated by SDS-PAGE and then analysed by Western Blot. ⁽⁵⁾ The interaction between c-FLIP and FADD will be explored using this technique. Moreover, the assay will be performed treating the cells with those compounds which showed the most promising activity in the cellular assays, in order to demonstrate that the mechanism of action of the synthesised molecules effectively involves the disruption of the interaction c-FLIP:FADD.

8.2.2.3 Fluorescence Resonance Energy Transfer (FRET)

The Fluorescence Resonance Energy Transfer (FRET) is an additional method to investigate protein-protein interactions. ⁽⁶⁾ The two proteins are labelled with two fluorophores, one acting as donor and the other acting as acceptor. When there is a physical interaction between the proteins, the donor, in an excited electronic state, is able to transfer energy to the acceptor. Using the appropriate microscope, it is possible to detect the energy transfer expressed by the increment of the acceptor fluorescence emission. Therefore, labelling c-FLIP, caspase-8 and FADD with donor and acceptor fluorophores in the presence of the compounds will enable confirmation of the selective binding between the compounds and c-FLIP, and the resulting interaction between caspase-8 and FADD which leads to apoptosis.

The biological experiments described in this section will be performed by Dr Richard Clarkson's research group (European Cancer Stem Cells Research Institute, Hadyn Ellis Building, Cardiff University).

8.3 References

- 1: Hayward, O. Design and Synthesis of Molecular Inhibitors of c-FLIP Activity as a Therapeutic Strategy to Target Breast Cancer Stem Cells. PhD Thesis. **2015**, Cardiff University.
- 2: Dontu, G.; Al-Hajj, M.; Abdallah, W. M.; Clarke, M. F.; Wicha, M. S. Stem cells in normal breast development and breast cancer. *Cell Prolif.* **2003**, *36*, 59-72.
- 3: Iglesias, J. M.; Beloqui, I.; Garcia-Garcia, F.; Leis, O.; Vazquez-Martin, A.; Eguiara, A.; Cufi, S.; Pavon, A.; Menendez, J. A.; Dopazo, J.; Martin, A. G. Mammosphere formation in breast Carcinoma cell lines depends upon expression of e-cadherin. *PLoS One.* **2013**, *8*: e77281.
- 4: Caspase-Glo® 8 Assay Systems. <https://www.promega.co.uk> (accessed January 28, 2018).
- 5: Co-immunoprecipitation (co-IP). <https://www.thermofisher.com> (accessed January 28, 2018).
- 6: Kenworthy, K. A.; Imaging protein-protein interactions using fluorescence resonance energy transfer microscopy. *Methods.* **2001**, *24*, 289-296.

Chapter 9

Experimental

Chapter 9: Experimental

9.1 General Information

9.1.1 Chemistry

All chemicals, reagents and solvents were purchased from commercial sources, and were used without further purification. TLC was performed on silica gel plates (Merck Kieselgel 60F₂₅₄) and was developed by the ascending method. After solvent evaporation, compounds were visualised by irradiation with UV light at 254 nm and 366 nm. Flash column chromatography was performed using the Biotage Isolera One system. ¹H and ¹³C NMR spectra were recorded on a Bruker AVANCE DPX500 spectrometer (500 MHz and 75 MHz respectively) and auto-calibrated to the deuterated solvent reference peak. Chemical shifts are given in δ relative to tetramethylsilane (TMS); the coupling constants (J) are given in Hertz. TMS was used as an internal standard ($\delta = 0$) for ¹H- NMR and CDCl₃ served as an internal standard ($\delta = 77.0$) for ¹³C- NMR. Purity and mass of compounds were determined by UPLC-MS analyses, performed on a Waters UPLC system provided with Diode Array detector and Electrospray (positive and negative ion) MS detector. Stationary phase: Waters Acquity UPLC BEH C18 1.7 μ m 2.1 \times 50 mm column. Mobile phase: H₂O containing 0.1% Formic acid (A) and MeCN containing 0.1% Formic acid (B). Column temperature: 40 °C. Samples were prepared in acetonitrile at 1 μ g/mL concentration. Injection volume: 2 μ L. A linear gradient standard method (A) was used: 90% A (0.1 min), 90–0% A (2.6 min), 0% A (0.3 min), 90% A (0.1 min); flow rate 0.5 mL/min. Purity of the compounds tested in biological assays was >95%.

9.1.2 Biology

9.1.2.1 Cell Lines

Human MCF-7 cells ⁽¹⁾ were cultured in RPMI-1640 medium (Invitrogen) supplemented with 10% v/v heat inactivated fetal bovine serum (FBS), 2mM L-glutamine (Invitrogen) and 50 units/mL penicillin-streptomycin. TKCC-07 cells ⁽²⁾ were cultured in M199/F12 medium (Life Technologies) supplemented with 15 mM HEPES (Life Technologies), 2mM glutamine (Life Technologies), 20ng/mL EGF (Life Technologies), 40 ng/mL hydrocortisone (Sigma), 5 μ g/mL apo-transferrin (Sigma), 0.2IU/mL insulin ActRapid (Life Technologies), 0.06% glucose solution (10%) (Sigma), 7.50 % fetal bovine serum (FBS), 0.5 pg/mL tri-iodotyronine (Sigma), MEM vitamins (100x) (Life Technologies), 2 μ g/mL o-phosphoryl ethanolamine (Sigma), 1% penicillin-streptomycin and 0.05% gentamicin. Human HEK-293 cells ⁽³⁾ were cultured in Dulbecco's modified eagle medium with nutrient mixture F12 (DMEM/F12) (Gibco), supplemented with 10% v/v heat inactivated FBS and 50 units/mL penicillin-streptomycin.

9.1.2.2 Cell Culture Maintenance

Cells were kept in a logarithmic growth phase in 25cm² cell culture flasks (T25) (Nunc) at 37°C in a sterile incubator with a humidified atmosphere of 5% CO₂ and 95% air by passaging or refreshing media when required. Passaging was performed by removing the culture medium and adding 2mL of 0.05% trypsin/EDTA (Invitrogen) for MCF-7 and HEK-293 cells and 0.1 mM EDTA (Sigma) for TKCC-07 cells. Cells were incubated at 37°C for 5-10 mins. When all cells were detached, culture medium was added according to the appropriate passage ratio. MCF-7 and HEK-293 cells were kept to a passage number of around 35, TKCC-07 cells were kept to a passage number of around 10.

9.1.2.3 Cell Storage

Cells were frozen at low passage number and cryo-stored in liquid nitrogen. To prepare cells for storage, cells were trypsinised and pelleted. Pellets were resuspended in 1mL normal media with 10% DMSO-D6 (Sigma) in 1.5mL cryo-tubes (Nunc). Cryo-tubes were left overnight at -80°C in an isopropanol cell freezing container, after which tubes were transferred to long term storage in liquid nitrogen container. To revive cells, tubes were defrosted rapidly in a 37°C water bath and spun at 1100rpm to obtain a cell pellet which was resuspended in 5mL growth medium and cultured in a T25 flask.

9.1.2.4 Cell-Based Assays

9.1.2.4.1 Cell Counting

Cells were detached as described in section 9.1.2.2. Cells were moved to a 15 ml Falcon Tube (Nunc) and resuspended in culture media. Following centrifugation at 1100 RPMI for 5 mins, the pellet was resuspended in culture media and 10 µL of the resulting suspension were loaded into the Fastread 10-chamber counting grid (Immune Systems). The average of the number of cells in four counting squares was measure and multiplied by 10,000 to obtain the number of cells/mL.

9.1.2.4.2 Colony Forming Assay ⁽⁴⁾

Cells were plated in a 12 well plate at a density of 184.8 cells/mL and left to attach overnight, after which media was refreshed with appropriate control or test medium. Colonies were left to form for 10 days, after which, medium was removed and cells were gently washed with 1X PBS for 5 minutes. Crystal violet was then added for 15 minutes, followed by 3 x PBS washes for 5 minutes each. Colonies were then visualised and photographed under white light. Colonies showing a minimum diameter of 200 µm were counted using the GelCount plate reader (Oxford Optronix) setting threshold values of 200-1000 µm.

9.1.2.4.3 CellTiter Blue Viability Assay ⁽⁵⁾

Cells were plated in 96 well plate at a density of 100,000 cells/mL and left to attach overnight. When cells reached a confluence of approximately 70%, medium was refreshed with appropriate control or test medium. After 24 or 48 hours, 20 μ L of CellTiter Blue reagent was added to each well (100 μ L culture media) and incubated for at 37°C with 5% CO₂ for 2 hours. Following this period, fluorescence was measured using a FluoStar Optima plate reader (BMG Labtech) setting excitation/emission wavelengths to 560/590 nm.

9.1.3 Molecular Modelling

9.1.3.1 Molecular Docking

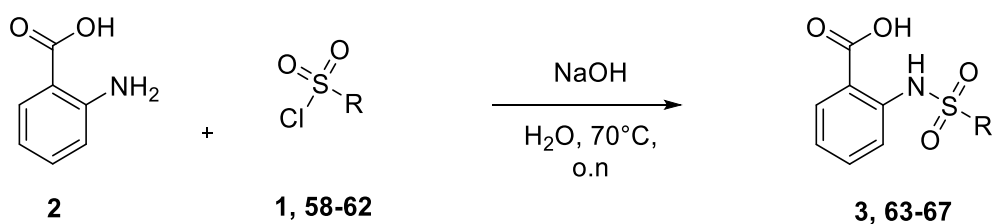
All molecular docking studies were performed on a Intel Xeon (R) CPU 5150 @ 2.66 GHz x 4, running Ubuntu 12.04 (precise) 32-bit. Molecular Operating Environment (MOE) 2015 ⁽⁶⁾ and Glide SP-Maestro (Shrödinger Release 2017-1) ⁽⁷⁾ were used to perform the docking analyses. MOE was initially used to build a database containing all synthesised compounds in their energy minimised status. Maestro was used to prepare the model of c-FLIP was using the Protein Preparation Wizard tool which allowed the assignment of bond orders, the additions of hydrogens and finally a restrained energy minimization of the hydrogens using OPLS_2005 force field. The receptor grid was generated by selecting the predicted position occupied by hit **3** as binding site, and a maximum length of 12Å from this site was selected to dock the compounds. Before running the molecular docking analyses, the database of compounds previously generated was prepared using the LigPrep tool in Maestro. Molecular docking analyses were performed using Glide SP precision retaining the default parameters and including 15 poses for each compound in the post-docking minimization. The docking results were exported in MOE and then visually inspected. The interactions between compounds and the amino acid residues were predicted using the Ligand Interaction tool in MOE.

9.1.3.2 Molecular Dynamics (MD)

DESMOND ⁽⁸⁾ was used with OPLS2005 force field for the molecular dynamics (MD) simulation. The two interacting proteins were placed in a cubic box filled with TIP 3P water. The energy of the system was minimised using a steepest descent minimisation algorithm. Consequently, the simulation time was set up at 100 ns, and the simulation was performed at NTP conditions: constant number of atoms (N), constant temperature of (300K) (T) and constant pressure (1atm) (P), saving the trajectory and energy values every 40 ps. The results were analysed using Maestro ⁽⁷⁾ and then exported and visually inspected using MOE ⁽⁶⁾. The MD simulation was monitored with C-alpha RMSD evaluation in order to analyse the stability of the system.

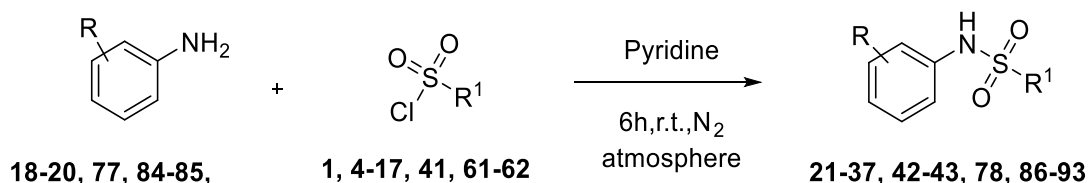
9.2 Synthesis of sulfonamide derivatives

General Procedure 1: arylsulfonamido benzoic acids (3, 63-67) ⁽⁹⁾



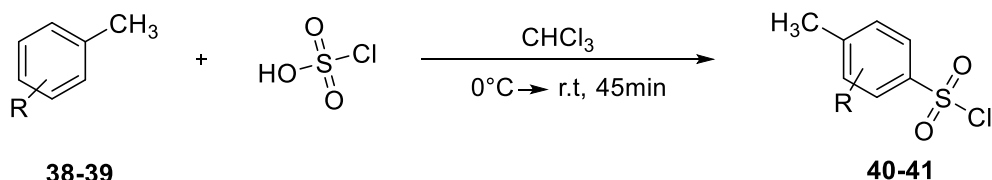
2-Aminobenzoic acid (1 eq), the appropriate arylsulfonyl chloride (1 eq) and NaOH (1 eq) were stirred in water (10 mL/mmol) at 70°C overnight. The product was filtered, washed with water, dried and purified by recrystallisation or flash column chromatography.

General Procedure 2: methyl(arylsulfonamidobenzoates) (21-37, 42-43, 78, 86-93) ⁽¹⁰⁾



To a stirred solution of the differently substituted aniline (1 eq) in anhydrous pyridine (4 mL/mmol) was added the appropriate arylsulfonyl chloride (1.2 eq) under an atmosphere of nitrogen. The reaction mixture was stirred at room temperature for 6h and was then quenched by addition of water (10 mL/mmol). The aqueous layer was extracted with ethyl acetate (20 mL/mmol) and the organic layer was then dried over anhydrous sodium sulfate. The solvent was removed under vacuum, and the crude product was purified by recrystallisation or flash column chromatography.

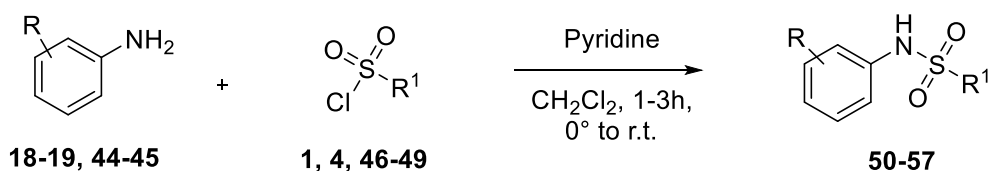
General Procedure 3: arylsulfonyl chlorides (40-41) ⁽¹¹⁾



To a cooled (0°) mixture of the appropriated substituted benzene (1eq) in chloroform (4 mL/mmol), chlorosulfonic acid (2.5 eq) was added dropwise. The reaction mixture was magnetically stirred at 0° C and the chlorosulfonic acid was added at such a rate that the temperature of the reaction mixture did not exceed 5°C. After the complete addition of chlorosulfonic acid, the reaction mixture was stirred for another 45 mins at room temperature and the mixture was poured into crushed ice.

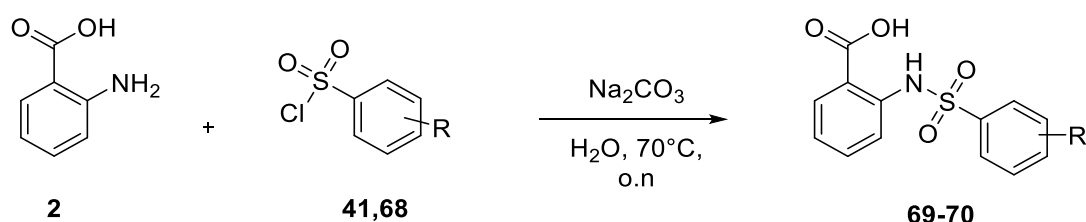
The product was extracted with chloroform (20 mL/mmol) and dried over anhydrous sodium sulfate. Chloroform was removed under vacuum. The crude product was directly used for the next step or purified by flash column chromatography.

General Procedure 4: alkyl(arylsulfonamido)benzoates (50-57) ⁽¹²⁾

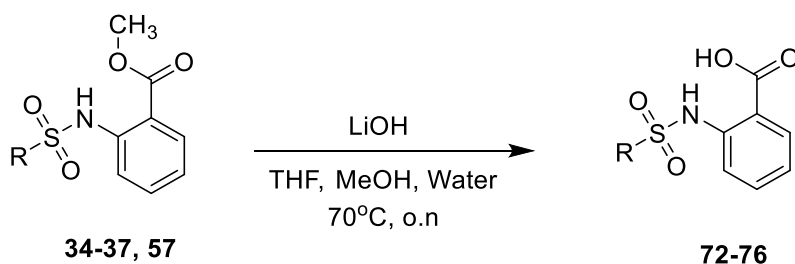


To a cooled (0°) stirring solution of alkyl anthranilate (1 eq) in CH_2Cl_2 (4 mL/mmol) was added pyridine (7.5 eq). The appropriate arylsulfonyl chlorides (1.2 eq) was then added slowly. The solution was allowed to warm to room temperature and stirred for 1-3 hours. The reaction was poured into saturated NaHCO_3 solution (14 mL/mmol), extracted with CH_2Cl_2 (3 x 5 mL/mmol), and washed with 1M HCl (15 mL/mmol). The combined organic phases were dried over MgSO_4 and concentrated *in vacuo*. The desired products were purified by recrystallization or flash column chromatography.

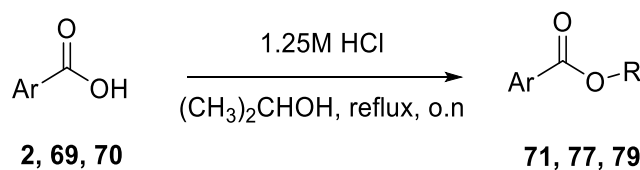
General Procedure 5: arylsulfonamido benzoic acids (69-70) ⁽¹³⁾



A solution of Na_2CO_3 (2.4 eq) in H_2O (4.5 mL/mmol) was heated to 60°C , treated with anthranilic acid and stirred for 5 min. The appropriate arylsulfonyl chloride was added in portions, the temperature was raised to 70°C and the mixture stirred overnight. The temperature was raised to 85°C and the mixture was vacuum filtered. The resulting filtrate was treated with 6 M HCl (5 mL/mmol) and cooled down to room temperature. The resulting precipitate was isolated by vacuum filtration, washed with 1M HCl and water. The desired products were purified by recrystallisation or flash column chromatography.

General Procedure 6: arylsulfonamido benzoic acids (72-76) ⁽¹⁴⁾

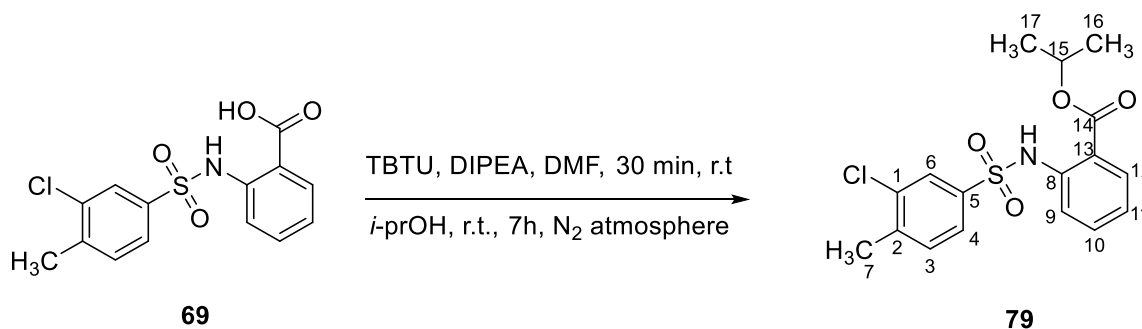
To a solution of the appropriate methyl-(arylsulfonamido) benzoate (1 eq) in THF (7 mL/mmol), H₂O (3.5 mL/mmol), MeOH (3.5 mL/mmol) was added LiOH (3 eq). The reaction was stirred at 70°C overnight. After the reaction was allowed to cool to room temperature, the reaction mixture was acidified with 2M HCl. The product was extracted with ethyl acetate (3x10 mL/mmol). The organic layer was dried over MgSO₄ and evaporated under reduced pressure. The product was purified by flash column chromatography or recrystallisation.

General Procedure 7: alkyl(aryl)esters (71, 77, 79) ⁽¹⁵⁾

To a solution of the appropriate aryl acid (1 eq) in isopropanol (1.9 mL/mmol) was added 1.25 M HCl in isopropanol solution (1.9 mL/mmol). The reaction was refluxed overnight. The solution was then cooled to room temperature and concentrated in vacuum. The residue was partitioned between sat. aq. NaHCO₃ solution (30mL/mmol) and ethylacetate (3x25 mL/mmol). The combined organic layers were washed with sat. aq. NaHCO₃ solution (25 mL/mmol) and water (10 mL/mmol), dried over MgSO₄ and concentrated under vacuum to give the alkyl esters. The desired products were purified by flash column chromatography.

Synthesis of Isopropyl 2-((3-chloro-4-methylphenyl)sulfonamido)benzoate (79) ⁽¹⁶⁾

(C₁₇H₁₈ClNO₄S; M.W. = 367.84)



2-((3-chloro-4-methylphenyl)sulfonamido)benzoic acid (0.100 g, 0.3 mmol), TBTU (0.09 g, 0.3 mmol) and DIPEA (0.08 g, 0.6 mmol) were stirred in anhydrous DMF (1 mL), and the resulting mixture was stirred at room temperature for 30 min, under N₂ atmosphere. Isopropyl alcohol (0.02 g, 0.3 mmol) was then injected into the reaction mixture via syringe and stirring was continued at room temperature until completion of the reaction. The reaction mixture was diluted with DCM (10 mL) and the resulting mixture was extracted with sat.aq NH₄Cl (10 mL) and sat.aq NaHCO₃ (10 mL). The organic layer was dried over MgSO₄ and the solvent was evaporated under vacuum. The desired product was purified by flash column chromatography.

Colourless oil;

T.L.C. System: *n*-hexane-EtOAc 7:3 v/v, R_f: 0.60;

Purification1: Biotage Isolera One automated flash column chromatography (cartridge: ZIP KP SIL 10g, *n*-hexane-EtOAc 100:0 increasing to *n*-hexane-EtOAc 70:30 in 10 CV);

Purification2: Biotage Isolera One automated flash column chromatography (cartridge: ZIP KP SIL 10g, *n*-hexane-EtOAc 100:0 increasing to *n*-hexane-EtOAc 70:30 in 15 CV);

Purification3: Biotage Isolera One automated flash column chromatography (cartridge: ZIP KP SIL 5g, *n*-hexane-DCM 100:0 increasing to *n*-hexane-DCM 0:100 in 11 CV);

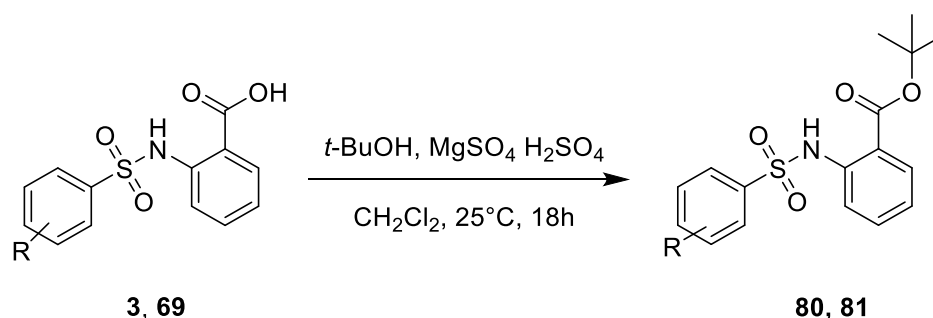
Yield: 0.024 g (22%);

¹H-NMR (CDCl₃), δ: 1.26 (d, J = 6.2 Hz, 6H, H-16,17), 2.30 (s, 3H, H-7), 5.11-5.14 (m, 1H, H-15), 6.97-7.00 (m, 1H, H-aromatic), 7.17-7.19 (m, 1H, H-aromatic), 7.37-7.41 (m, 1H, H-aromatic), 7.52 (dd, J₁ = 7.8 Hz, J₂ = 1.9 Hz, 1H, H-aromatic), 7.59 (dd, J₁ = 8.3 Hz, J₂ = 1.0 Hz, 1H, H-aromatic), 7.74-7.76 (m, 1H, H-aromatic), 7.85 (m, 1H, H-aromatic), 10.68 (bs, 1H, NH) ppm.

$^{13}\text{C-NMR}$ (CDCl_3), δ : 20.2 (CH_3 , C-7), 21.7 ($2\times\text{CH}_3$, C-16,17), 69.5 (CH , C-15), 119.4, 123.2, 125.3, 127.7, 131.1, 131.3, 134.3 (CH , C-aromatic), 116.9, 135.1, 138.3, 140.1, 141.8 (C , C-aromatic), 167.3 (C , C-14).

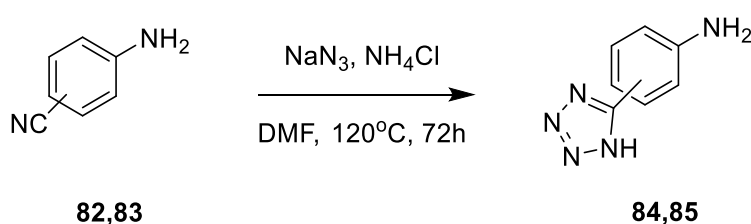
UPLC-MS: Rt 2.77 (100%) **MS (ESI) $^+$:** 368.8 [$\text{M}+\text{H}$] $^+$.

General Procedure 8: *tert*-Butyl(arylsulfonamido) benzoate (80-81) ⁽¹⁷⁾

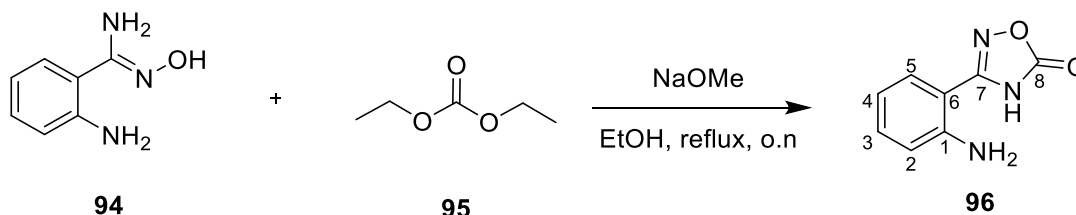


Concentrated sulfuric acid (1eq) was added to a vigorously stirred suspension of anhydrous magnesium sulfate (4eq) in DCM (4mL/mmol). The mixture was stirred for 15 minutes, after which the appropriate carboxylic acid (1eq) was added. *Tert*-Butyl alcohol (5eq) was added last. The mixture was stoppered tightly and stirred at 25°C for 18h. The reaction mixture was then quenched with sat.aq. NaHCO_3 solution and stirred until all the MgSO_4 was dissolved. The solvent phase was separated, washed with brine, dried over MgSO_4 and concentrated to afford the crude *tert*-butyl ester, which was purified by flash column chromatography.

General Procedure 9: (1H-tetrazol-5yl) anilines (84-85) ⁽¹⁸⁾



The appropriate aminobenzonitrile (1 eq), sodium azide (1.2 eq), ammonium chloride (1.2 eq) and DMF (0.6 mL/mmol) were mixed and heated at 120° C for 72 hours. The solvent was evaporated under reduced pressure. The desired products were purified by flash column chromatography.

Synthesis of 3-(2-aminophenyl)-1,2,4-oxadiazol-5(4H)-one (96) ⁽¹⁹⁾**(C₈H₇N₃O₂; M.W.= 177.16)**

Sodium methoxide (25wt% in MeOH, 0.534 g, 9.9 mmol) was added to a stirred solution of 2-amino-N-hydroxy-benzamidinium (0.500 g, 3.3 mmol) in ethanol (10 mL) at room temperature. The mixture was vigorously stirred and diethyl carbonate (1.563 g, 13.2 mmol) was added. The reaction mixture was refluxed overnight and then allowed to cool to room temperature. The solvent was removed under reduced pressure and the residue was diluted with water (5 mL). The basic solution was neutralised to pH 7 with 1M HCl at 0°C. The resulting precipitate was filtered under reduced pressure, washed with water and dissolved in ethyl acetate. The organic phase was dried over MgSO₄, filtered and evaporated in vacuum. The crude product was used without further purification.

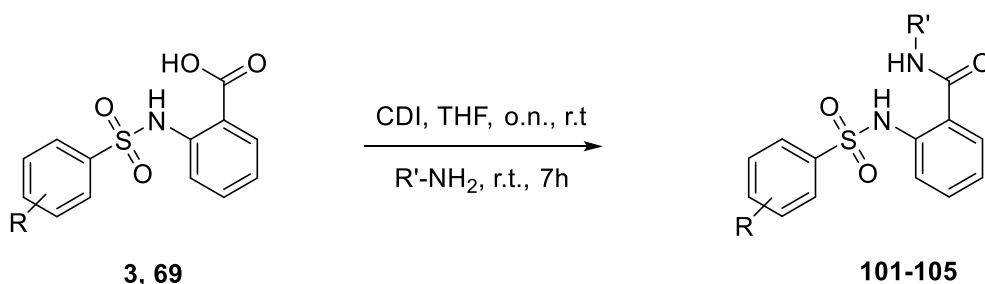
Yellow Solid;

T.L.C. System: N-hexane-EtOAc 6:4 v/v, R_f: 0.85;

Yield: 0.279 g (48%);

¹H-NMR (DMSO-D₆), δ: 6.63-6.66 (m, 1H, H-aromatic), 6.85 (dd, J₁= 8.3 Hz, J₂= 0.7 Hz, 1H, H-aromatic), 7.22-7.25 (m, 1H, H-aromatic), 7.47 (dd, J₁= 7.9 Hz, J₂= 1.4 Hz, 1H, H-aromatic), 8.54 (bs, 1H, NH).

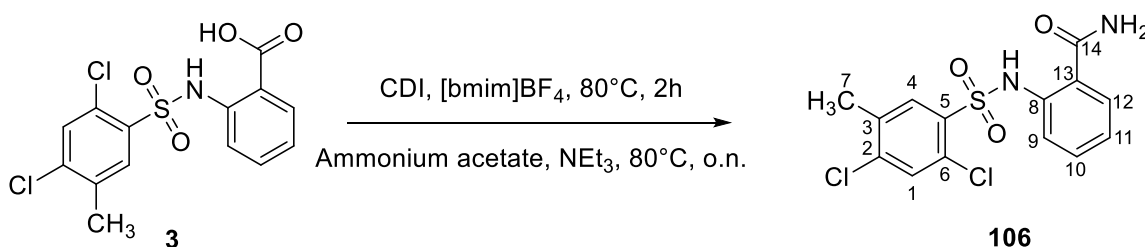
¹³C-NMR (DMSO-D₆), δ: 115.8, 116.6, 128.3, 132.6 (CH, C-aromatic), 104.6, 148.0, 159.3 (C, C-aromatic), 160.4 (C, C-8).

General Procedure 10: alkyl(arylsulfonamido) carboxamide (101-105) ⁽²⁰⁾

A suspension of CDI (1.2eq) and the appropriate carboxylic acid (1eq) in THF (6 mL/mmol) was stirred at room temperature overnight. A 2N solution of alkylamine in THF (1.5eq) was then added and the resulting solution was stirred at room temperature for 6 hours. The solvent was evaporated and the residue dissolved in ethyl acetate (10mL/mmol). The solution was washed sequentially with water and brine. The organic layer was dried over MgSO₄ and then evaporated. The desired product was purified by column chromatography or recrystallisation.

Synthesis of 2-((2,4-Dichloro-5-methylphenyl)sulfonamido) benzamide (106) ⁽²¹⁾

(C₁₄H₁₂Cl₂N₂O₃S; M.W.= 359.22)



N,N'-carbonyldiimidazole (0.050 g, 0.33 mmol) was added to a solution of 2-((2,4-dichloro-5-methylphenyl)sulfonamido)benzoic acid (0.100 g, 0.27 mmol) in [bmim]BF₄ (1 mL). The resulting mixture was stirred at 80°C for 2h. Ammonium acetate (0.083 g, 1.08 mmol) and triethylamine (0.082 g, 0.81 mmol) were added to the reaction mixture. The reaction was heated at 80°C for 3h. After completion of the reaction, the product was extracted with ethyl acetate (10 mL), washed with 0.01N solution of HCl (15 mL), and dried over anhydrous MgSO₄. The solvent was evaporated in vacuo, and the crude product was purified by flash column chromatography.

Grey solid;

T.L.C. System: *n*-hexane-EtOAc 3:7 v/v, R_f: 0.60;

Purification: Biotage Isolera One automated flash column chromatography (cartridge: SNAP KP SIL 25g, *n*-hexane:EtOAc 100:0 increasing to *n*-hexane-EtOAc 0:100 in 14CV);

Yield: 0.010 g (10%);

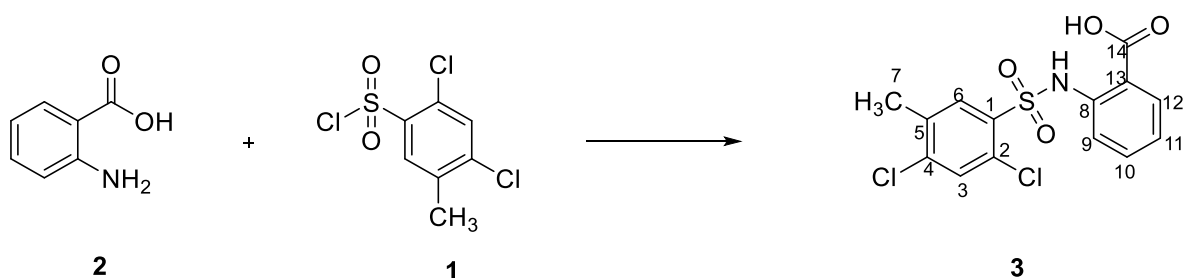
¹H-NMR (CDCl₃), δ: 2.32 (s, 3H, H-7), 5.87 (bs, 2H, NH₂), 6.94-6.98 (m, 1H, H-aromatic), 7.29-7.32 (m, 1H, H-aromatic), 7.36 (s, 1H, H-4), 7.39-7.41 (m, 1H, H-aromatic), 7.48-7.51 (m, 1H, H-aromatic), 7.97 (s, 1H, H-1), 11.50 (bs, 1H, NH).

¹³C-NMR (CDCl₃), δ: 19.6 (CH₃, C-7), 118.3, 122.7, 127.8, 131.8, 133.4, 133.5 (CH, C-aromatic), 118.4, 130.0, 135.1, 135.5, 138.9, 139.8 (C, C-aromatic), 170.4 (C, C-14).

UPLC-MS: Rt 2.13 (>98%) MS (ESI)⁺: 381.9 [M+Na]⁺.

9.2.1: Arylsulfonamido benzoic acids (3, 63-67)

2-((2,4-Dichloro-5-methylphenyl)sulfonamido) benzoic acid (3)

(C₁₄H₁₁Cl₂NO₄S; M.W.= 360.21)Reagent: 2-Aminobenzoic acid (**2**) (0.79 g, 5.78 mmol);Reagent: 2,4-dichloro-5-methylbenzenesulfonyl chloride (**1**) (1.50 g, 5.78 mmol);

General Procedure 1;

White solid;

T.L.C. System: *n*-hexane-EtOAc 5:5 v/v, R_f: 0.48;

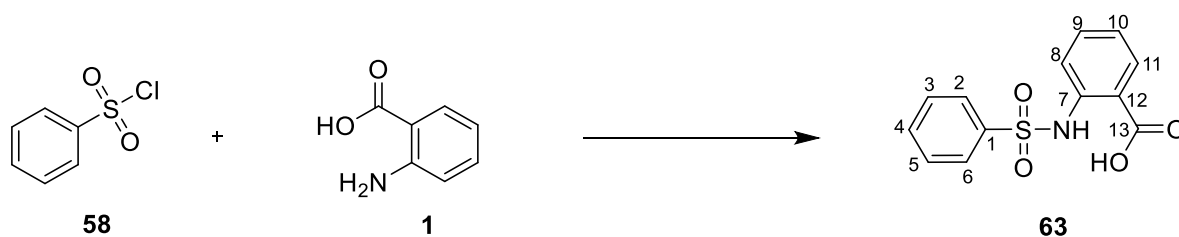
Purification: recrystallisation from EtOH;

Yield: 1.04 g (50%);

¹H-NMR (CDCl₃), δ: 2.40 (s, 3H, H-7), 7.09-7.13 (m, 1H, H-aromatic), 7.41-7.43 (m, 1H, H-aromatic), 7.49-7.53 (m, 1H, H-aromatic), 7.84 (s, 1H, H-6), 7.95-7.97 (m, 1H, H-aromatic), 8.23 (s, 1H, H-3), 11.71 (bs, 1H, NH), 14.15 (bs, 1H, OH).

¹³C-NMR (CDCl₃), δ: 19.5 (CH₃, C-7), 116.9, 123.5, 132.1, 132.2, 134.3, 135.2 (CH, C-aromatic), 116.1, 128.9, 134.4, 136.7, 139.5, 140.0 (C, C-aromatic), 170.3 (C, C-14).

UPLC-MS: Rt 2.03 (98%) MS (ESI)⁺: 360.9 [M+H]⁺.

2-(Phenylsulfonamido)benzoic acid (63) ⁽²²⁾**(C₁₃H₁₁NO₄S; M.W.= 277.29)**Reagent: benzenesulfonyl chloride (**58**) (0.1 g, 0.56 mmol);Reagent: 2-aminobenzoic acid (**1**) (0.078 g, 0.56 mmol);

General Procedure 1;

White Solid;

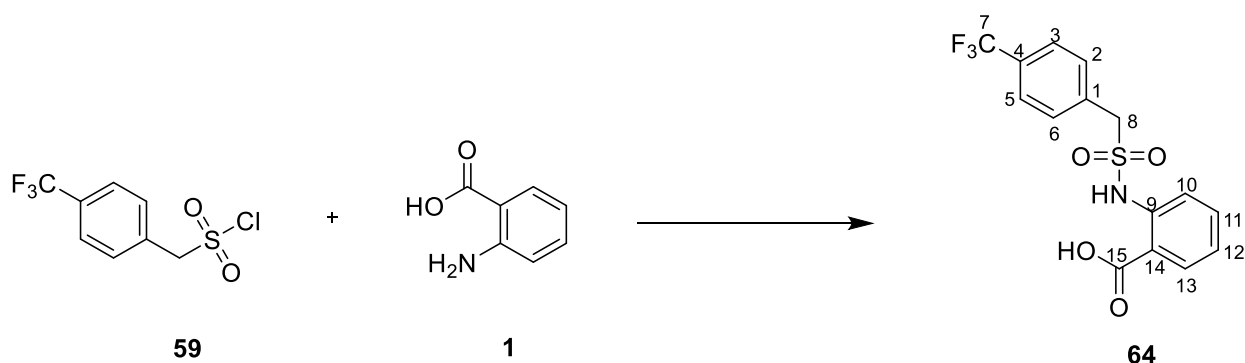
T.L.C. System: DCM:MeOH 98:2 v/v, R_f: 0.25;Purification: Recrystallisation from DCM/*n*-hexane;

Yield: 0.053 g (59%);

¹H-NMR (DMSO-D₆), δ: 7.11-7.14 (m, 1H, H-aromatic), 7.51-7.58 (m, 4H, H-aromatic), 7.63-7.67 (m, 1H, H-aromatic), 7.81-7.83 (m, 2H, H-aromatic), 7.89-7.91 (m, 1H, H-aromatic), 11.16 (bs, 1H, NH), 14.01 (bs, 1H, OH).

¹³C-NMR (DMSO-D₆), δ: 118.97, 123.87, 127.31, 130.00, 132.00, 134.05, 134.98 (CH, C-aromatic), 117.28, 139.05, 140.24 (C-aromatic), 170.22 (C, C- 13).

UPLC-MS: Rt 1.91 (100%) **MS (ESI)⁺:** 278.0 [M+H]⁺.

2-(((4-(Trifluoromethyl)phenyl)methyl)sulfonamido)benzoic acid (64)**(C₁₅H₁₂F₃NO₄S; M.W.= 359.32)**

Reagent: (4-(trifluoromethyl)phenyl)methanesulfonyl chloride (**59**) (0.150 g, 0.58 mmol);

Reagent: 2-aminobenzoic acid (**1**) (0.080 g, 0.58 mmol);

General Procedure 1;

White Solid;

T.L.C. System: DCM-MeOH 98:2 v/v, R_f: 0.26;

Purification: Recrystallisation from EtOH;

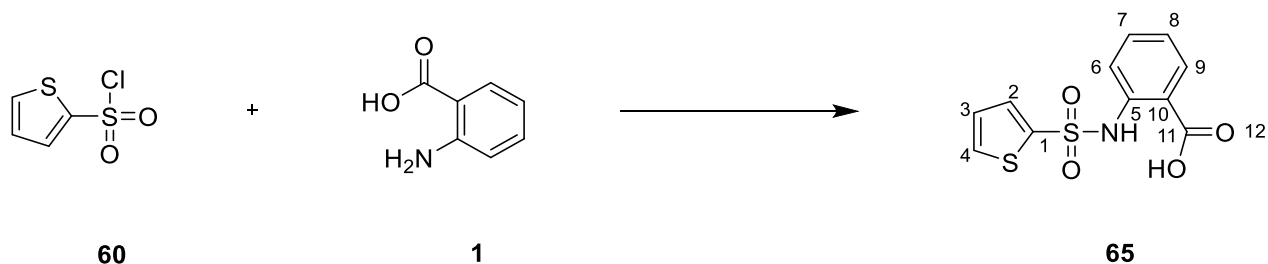
Yield: 0.034 g (23%);

¹H-NMR (DMSO-D₆), δ: 4.86 (s, 2H, H-8), 7.16-7.19 (m, 1H, H-aromatic), 7.47 (d, J= 8.0 Hz, 2H, H-aromatic), 7.55-7.60 (m, 2H, H-aromatic), 7.70 (d, J= 8.0 Hz, 2H, H-aromatic), 7.99-8.01 (m, 1H, H-aromatic), 10.83 (bs, 1H, NH), 13.92 (bs, 1H, OH).

¹³C-NMR (DMSO-D₆), δ: 57.3 (CH₂, C-8), 117.8, 123.1, 125.7, 132.0, 132.1, 135.1 (CH, C-aromatic), 129.3 (d, J= 32.2 Hz, C) 116.0, 132.4, 134.2, 141.0 (C-aromatic), 170.2 (C, C-15).

¹⁹F-NMR (DMSO-D₆), δ: -61.04 (s, 3F).

UPLC-MS: Rt 2.12 (>98%) MS (ESI)⁻: 358.1 [M-H]⁻.

2-(Thiophene-2-sulfonamido)benzoic acid (65)**(C₁₁H₉NO₄S₂; M.W.= 283.32)**Reagent: thiophene-2-sulfonyl chloride (**60**) (0.2 g, 1.09 mmol);Reagent: 2-aminobenzoic acid (**1**) (0.150 g, 1.09 mmol);

General Procedure 1;

Grey Solid;

T.L.C. System: *n*-hexane-EtOAc 6:4 v/v, R_f: 0.25;

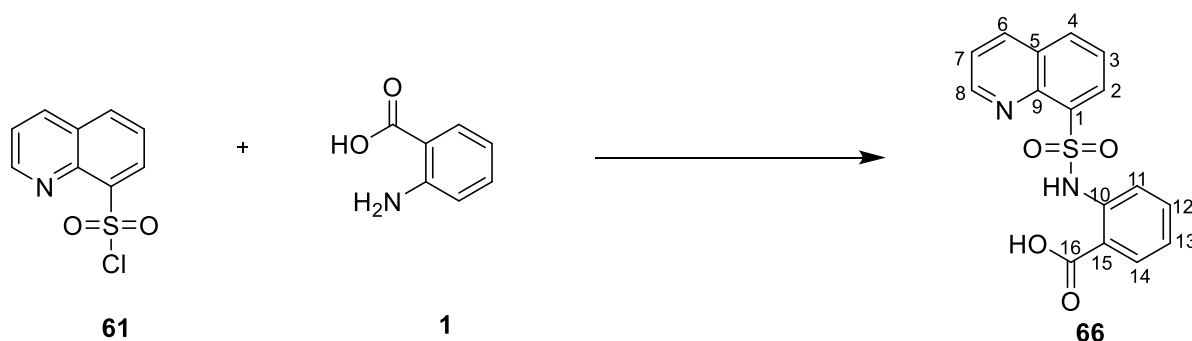
Purification: Recrystallisation from EtOH;

Yield: 0.067 g (22%);

¹H-NMR (DMSO-*D*₆), δ: 7.13-7.15 (m, 1H, H-aromatic), 7.17-7.21 (m, 1H, H-aromatic), 7.60-7.64 (m, 2H, H-aromatic), 7.67 (dd, *J*₁= 3.7 Hz, *J*₂= 1.3 Hz, 1H, H-aromatic), 7.91-7.94 (m, 1H, H-aromatic), 7.96 (dd, *J*₁= 4.9 Hz, *J*₂= 1.3 Hz, 1H, H-aromatic), 11.23 (bs, 1H, NH), 14.09 (bs, 1H, OH).

¹³C-NMR (DMSO-*D*₆), δ: 119.3, 124.2, 128.3, 132.0, 134.0, 134.9, 135.0 (CH. C-aromatic), 117.6, 139.2, 139.9 (C, C-aromatic), 170.2 (C, C- 11).

UPLC-MS: Rt 1.89 (99%) MS (ESI)⁺: 283.9 [M+H]⁺.

2-(Quinoline-8-sulfonamido)benzoic acid (66)**(C₁₆H₁₂N₂O₄S; M.W.= 328.34)**Reagent: quinoline-8-sulfonyl chloride (**61**) (0.100 g, 0.44 mmol);Reagent: 2-aminobenzoic acid (**1**) (0.040 g, 0.44 mmol);

General Procedure 1;

White Solid;

T.L.C. System: DCM-MeOH 98:2 v/v, R_f: 0.10;

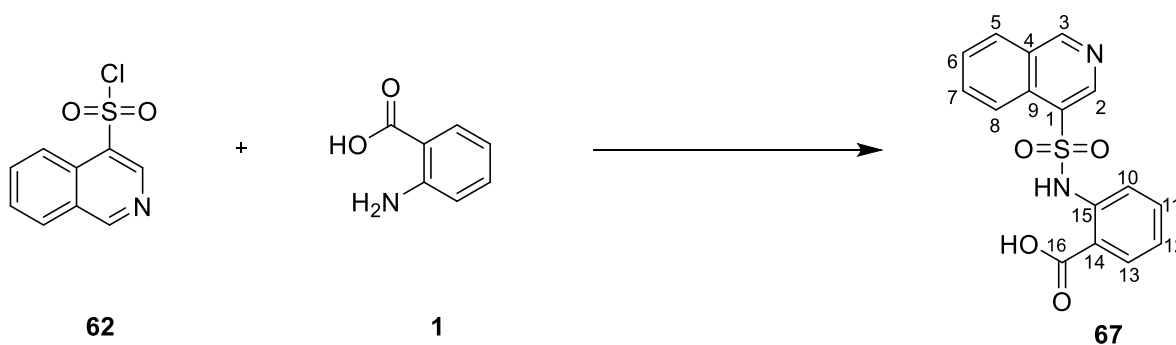
Purification: Recrystallisation from EtOH;

Yield: 0.040 g (28%);

¹H-NMR (DMSO-D₆), δ: 6.93-6.96 (m, 1H, H-aromatic), 7.38-7.41 (m, 1H, H-aromatic), 7.62 (dd, J₁= 8.4 Hz, J₂= 0.7 Hz, 1H, H-aromatic), 7.69 (dd, J₁= 8.3 Hz, J₂= 4.2 Hz, 1H, H-aromatic), 7.73-7.78 (m, 2H, H-aromatic), 8.30 (dd, J₁= 8.3 Hz, J₂= 1.3 Hz, 1H, H-aromatic), 8.49 (dd, J₁= 8.4 Hz, J₂= 1.7 Hz, 1H, H-aromatic), 8.52 (dd, J₁= 7.3 Hz, J₂= 1.3 Hz, 1H, H-aromatic), 8.95 (dd, J₁= 4.2 Hz, J₂= 1.7 Hz, 1H, H-aromatic), 11.55 (bs, 1H, NH), 13.74 (bs, 1H, OH).

¹³C-NMR (DMSO-D₆), δ: 117.1, 122.9, 123.2, 126.1, 131.8, 133.1, 134.6, 135.3, 137.5, 151.9 (CH, C-aromatic), 117.0, 128.8, 140.2, 142.8, 153.6 (C, C-aromatic), 169.41 (C, C-16).

UPLC-MS: Rt 1.87 (99%) MS (ESI)⁺: 329.1 [M+H]⁺.

2-(Isoquinoline-4-sulfonamido)benzoic acid (67)**(C₁₆H₁₂N₂O₄S; M.W.= 328.34)**Reagent: isoquinoline-4-sulfonyl chloride (**62**) (0.100 g, 0.44 mmol);Reagent: 2-aminobenzoic acid (**1**) (0.060 g, 0.44 mmol);

General Procedure 1;

White Solid;

T.L.C. System: DCM-MeOH 98:2 v/v, R_f: 0.34;

Purification: Recrystallisation from EtOH;

Yield: 0.050 g (35%);

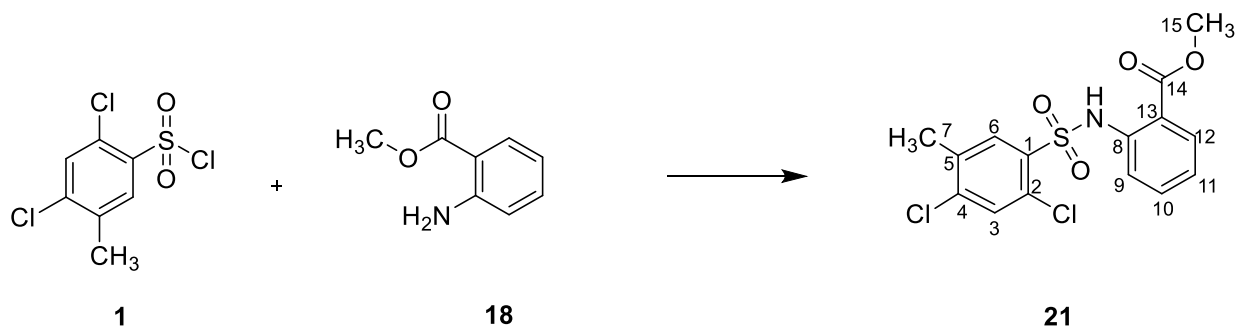
¹H-NMR (DMSO-D₆), δ: 7.13-7.16 (m, 1H, H-aromatic), 7.54-7.59 (m, 2H, H-aromatic), 7.75-7.78 (m, 1H, H-aromatic), 7.85-7.87 (m, 1H, H-aromatic), 7.95-7.98 (m, 1H, H-aromatic), 8.09-8.11 (m, 1H, H-aromatic), 8.23 (dd, J₁= 8.5 Hz, J₂= 1.1 Hz, 1H, H-aromatic), 9.04-9.07 (m, 1H, H-aromatic), 9.14 (d, J= 2.3 Hz, 1H, H-aromatic), 11.29 (bs, 1H, NH), 13.72 (bs, 1H, OH).

¹³C-NMR (DMSO-D₆), δ: 119.8, 124.4, 128.9, 129.3, 130.2, 132.0, 133.5, 135.0, 137.4, 146.5 (CH, C-aromatic), 118.2, 126.3, 132.2, 139.4, 148.9 (C, C-aromatic), 169.9 (C, C-16).

UPLC-MS: Rt 1.93 (99%) MS (ESI)⁺: 329.1 [M+H]⁺.

9.2.2: Methyl(arylsulfonamidobenzoates) (21-37, 42-43, 78, 86-93)

Methyl 2-((2,4-dichloro-5-methylphenyl)sulfonamido)benzoate (21)

(C₁₅H₁₃Cl₂NO₄S; M.W.=374.2)Reagent: 2,4-dichloro-5-methylbenzenesulfonyl chloride (**1**) (0.3 g, 1.15 mmol);Reagent: methyl anthranilate (**18**) (0.14 g, 0.98 mmol);

General procedure 2;

White solid;

T.L.C. System: *n*-hexane-EtOAc 8:2 v/v, R_f: 0.64;

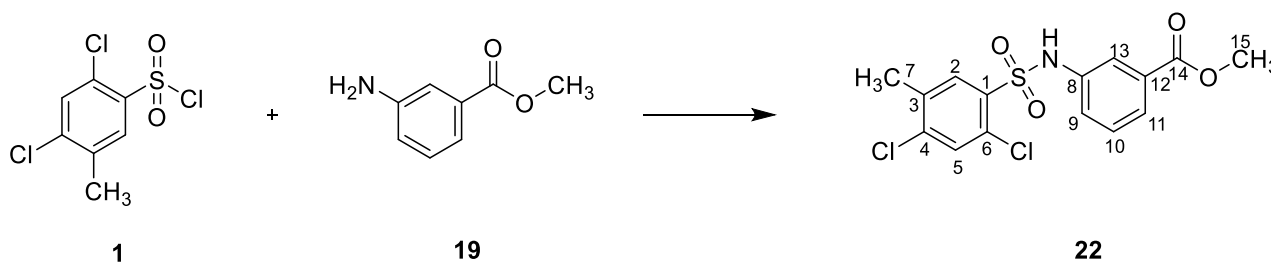
Purification: Recrystallisation from EtOH;

Yield: 0.176 g (49%);

¹H-NMR (CDCl₃), δ: 2.33 (s, 3H, H-7), 3.86 (s, 3H, H-15), 6.93-6.96 (m, 1H, H-aromatic), 7.30-7.34 (m, 1H, H-aromatic), 7.35 (s, 1H, H-aromatic), 7.46 (dd, J₁= 8.4 Hz, J₂= 0.8 Hz, 1H, H-aromatic), 7.90 (dd, J₁= 8.0 Hz, J₂= 1.4 Hz, 1H, H-aromatic), 7.99 (s, 1H, H-aromatic), 11.12 (bs, 1H, NH).

¹³C-NMR (CDCl₃), δ: 19.6 (CH₃, C-7), 52.5 (CH₃, C-15), 116.9, 122.5, 131.4, 131.9, 134.5, 135.6 (CH, C-aromatic), 115.2, 115.9, 129.9, 133.5, 139.7, 140.0 (C, C-aromatic), 168.1 (C, C-14).

UPLC-MS: Rt 2.59 (100%) MS (ESI)⁺: 376.1 [M+H]⁺.

Methyl 3-((2,4-dichloro-5-methylphenyl)sulfonamido)benzoate (22)**(C₁₅H₁₃Cl₂NO₄S; M.W.=374.2)**Reagent: 2,4-dichloro-5-methylbenzenesulfonyl chloride (**1**) (0.3 g, 1.15 mmol);Reagent: methyl-3-aminobenzoate (**19**) (0.145 g, 0.96 mmol);

General Procedure 2;

White solid;

T.L.C. System: *n*-hexane-EtOAc 8:2 v/v, R_f: 0.40;

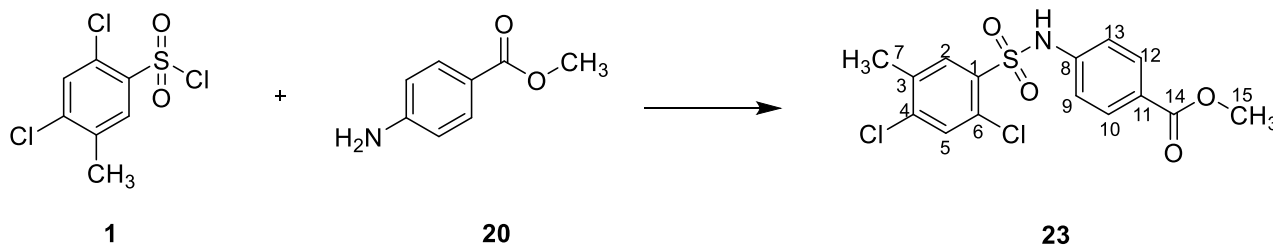
Purification: Recrystallisation from EtOH;

Yield: 0.203 g (56%);

¹H-NMR (CDCl₃), δ: 2.36 (s, 3H, H-7), 3.96 (s, 3H, H-15), 7.33-7.37 (m, 1H, H-aromatic), 7.39-7.42 (m, 1H, H-aromatic), 7.51 (s, 1H, H-aromatic), 7.76-7.77 (m, 1H, H-aromatic), 7.80-7.82 (m, 1H, H-aromatic), 7.89 (s, 1H, H-aromatic), 11.20 (bs, 1H, NH).

¹³C-NMR (CDCl₃), δ: 19.5 (CH₃, C-7), 52.3 (CH₃, C-15), 122.4, 125.6, 126.9, 129.6, 131.6, 133.5 (CH, C-aromatic), 120.5, 128.4, 135.9, 135.9, 136.1, 156.6 (C, C-aromatic), 160.6 (C, C-14).

UPLC-MS: Rt 2.30 (100%) MS (ESI)⁻: 372.1 [M-H]⁻.

Methyl 4-((2,4-dichloro-5-methylphenyl)sulfonamido)benzoate (23)**(C₁₅H₁₃Cl₂NO₄S; M.W.=374.2)**Reagent: 2,4-dichloro-5-methylbenzenesulfonyl chloride (**1**) (0.3 g, 1.15 mmol);Reagent: methyl-4-aminobenzoate (**20**) (0.14 g, 0.96 mmol);

General procedure 2;

Yellow powder;

T.L.C. System: *n*-hexane-EtOAc 8:2 v/v, R_f: 0.40;

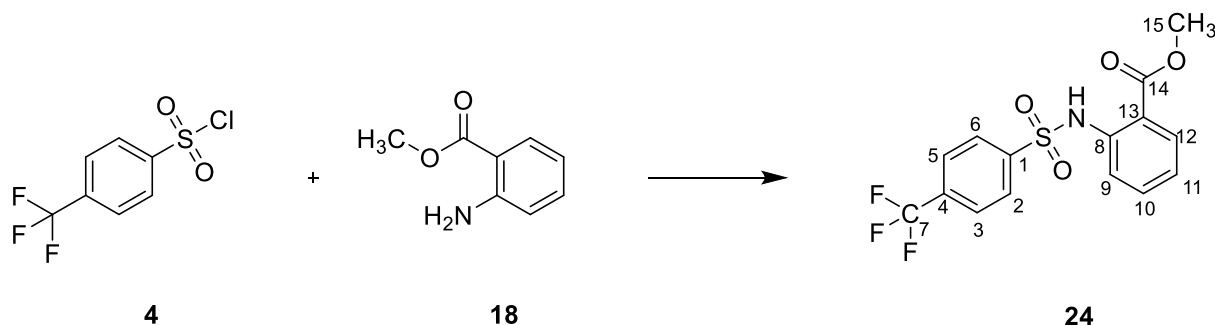
Purification: Recrystallisation from MeOH/DCM;

Yield: 0.166 g (46%);

¹H-NMR (DMSO-*d*₆), δ: 2.39 (s, 3H, H-7), 3.78 (s, 3H, H-15), 7.19-7.22 (m, 2H, H-aromatic), 7.80 (s, 1H, H-aromatic), 7.81-7.84 (m, 2H, H-aromatic), 8.13 (s, 1H, H-aromatic), 11.23 (bs, 1H, NH).

¹³C-NMR (DMSO-*D*₆), δ: 19.0 (CH₃, C-7), 51.8 (CH₃, C-15), 117.1, 130.6, 131.5, 133.5 (CH, C-aromatic), 124.4, 128.7, 134.7, 136.0, 139.0, 141.4 (C, C-aromatic), 165.5 (C, C-14).

UPLC-MS: Rt 2.29 (100%) MS (ESI): 372.1 [M-H]⁻.

Methyl 2-((4-(trifluoromethyl)phenyl)sulfonamido)benzoate (24)**(C₁₅H₁₂F₃NO₄S; M.W.=359.32)**Reagent: 4-(trifluoromethyl)benzenesulfonyl chloride (**4**) (0.3 g, 1.22 mmol);Reagent: methyl anthranilate (**18**) (0.15 g, 1.02 mmol);

General procedure 2;

White solid;

T.L.C. System: *n*-hexane-EtOAc 8:2 v/v, R_f: 0.46;

Purification: Recrystallisation from EtOH;

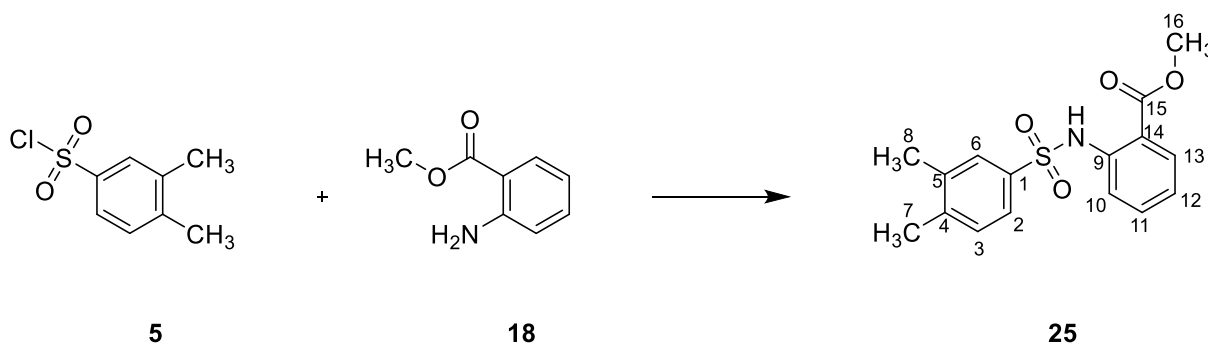
Yield: 0.220 g (60%);

¹H-NMR (CDCl₃), δ: 3.89 (s, 3H, H-15), 7.10-7.13 (m, 1H, H-aromatic), 7.71-7.72 (m, 1H, H-aromatic), 7.73-7.75 (m, 2H, H-aromatic), 7.95-7.97 (m, 1H, H-aromatic), 7.98-8.00 (m, 2H, H-aromatic), 10.76 (bs, 1H, NH).

¹³C-NMR (CDCl₃), δ: 52.6 (CH₃, C-15), 119.3, 123.6, 126.2, 127.7, 131.3, 134.5 (CH, C-aromatic), 116.2, 134.7, 139.8, 142.8 (C, C-aromatic), 168.3 (C, C-14).

¹⁹F-NMR (CDCl₃), δ: -63.19, (s, 3F).

UPLC-MS: Rt 2.39 (100%) **MS (ESI)⁺:** 360.1 [M+H]⁺.

Methyl 2-((3,4-dimethylphenyl)sulfonamido)benzoate (25)**(C₁₆H₁₇NO₄S, M.W.=319.4)**Reagent: 3,4-dimethylbenzenesulfonyl chloride (**5**) (0.3 g, 1.46 mmol);Reagent: methyl anthranilate (**18**) (0.18 g, 1.22 mmol);

General procedure 2;

White solid;

T.L.C. System: *n*-hexane-EtOAc 8:2, v/v, R_f: 0.42;

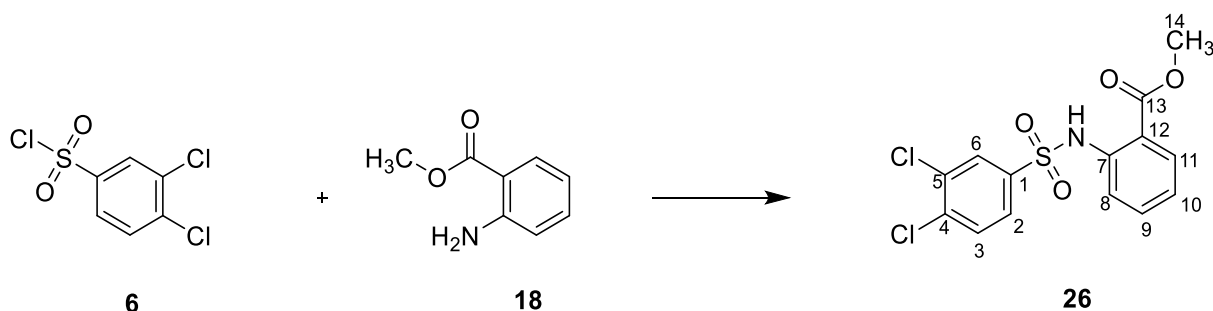
Purification: Recrystallisation from EtOH;

Yield: 0.024 g (29%);

¹H-NMR (DMSO-*D*₆), δ: 2.25 (s, 6H, 2xCH₃, H-7,8), 3.83 (s, 3H, H-16), 7.14-7.18 (m, 1H, H-aromatic), 7.31 (d, J=7.8 Hz, 1H, H-aromatic), 7.45-7.48 (m, 1H, H-aromatic), 7.52 (dd, J₁= 8.0 Hz, J₂= 1.7 Hz, 1H, H-aromatic), 7.55-7.58 (m, 1H, H-aromatic), 7.59-7.61 (m, 1H, H-aromatic), 7.85 (d, J= 7.8 Hz, 1H, H-aromatic), 10.43 (bs, 1H, NH).

¹³C-NMR (DMSO-*D*₆), δ: 19.7, 19.9 (2xCH₃, C-7,8), 53.1 (CH₃, C-16), 119.9, 124.1, 124.9, 127.8, 130.6, 131.4, 134.9 (CH, C-aromatic), 117.8, 136.4, 138.4, 139.3, 143.4 (C, C-aromatic), 168.1 (C, C-15).

UPLC-MS: Rt 2.35 (100%) MS (ESI)⁺: 320.1 [M+H]⁺.

Methyl-2-((3,4-dichlorophenyl)sulfonamido)benzoate (26)**(C₁₄H₁₁Cl₂NO₄S; M.W.=360.2)**Reagent: 3,4-dichlorobenzoyl chloride (**6**) (0.3 g, 1.22 mmol);Reagent: methyl anthranilate (**18**) (0.15 g, 1.01 mmol);

General procedure 2;

White solid;

T.L.C. System: *n*-hexane-EtOAc 8:2 v/v, R_f: 0.33;

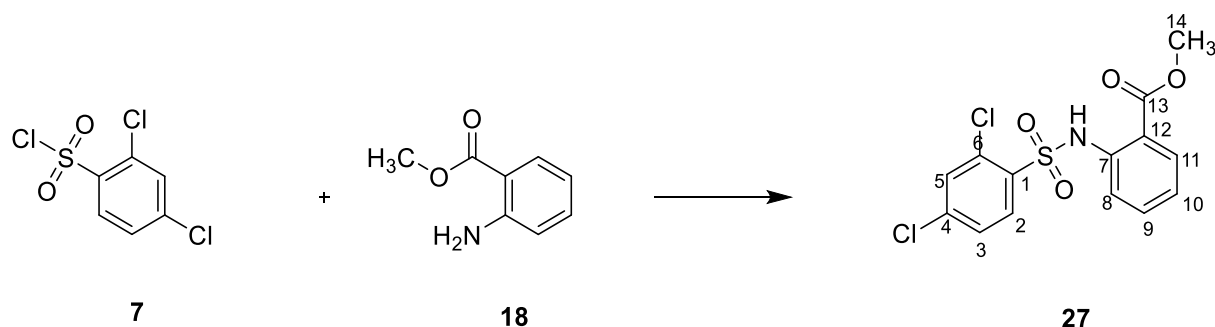
Purification: Recrystallisation from EtOH;

Yield: 0.238 g (65%);

¹H-NMR (DMSO-D₆), δ: 3.88 (s, 3H, H-14), 7.16-7.20 (m, 1H, H-aromatic), 7.38 (d, J= 8.5 Hz, 1H, H-aromatic), 7.52-7.56 (m, 1H, H-aromatic), 7.67-7.70 (m, 1H, H-aromatic), 7.91 (s, 1H, H-6), 7.92-7.94 (m, 1H, H-aromatic), 8.17 (d, J= 8.5 Hz, 1H, H-aromatic), 11.07 (bs, 1H, NH).

¹³C-NMR (DMSO-D₆), δ: 53.3 (CH₃, C-14), 118.5, 124.2, 128.6, 131.7, 132.1, 133.7, 135.2 (CH, C-aromatic), 127.1, 132.3, 135.0, 138.5, 139.8 (C, C-aromatic), 168.2 (C, C-13).

UPLC-MS: Rt 2.46 (100%) MS (ESI)⁺: 362.1 [M+H]⁺.

Methyl 2-((2,4-dichlorophenyl)sulfonamido)benzoate (27)**(C₁₄H₁₁Cl₂NO₄S; M.W.=360.2)**Reagent: 2,4-dichlorobenzoyl chloride (**7**) (0.3 g, 1.22 mmol);Reagent: methyl anthranilate (**18**) (0.15 g, 1.01 mmol);

General procedure 2;

White solid;

T.L.C. System: *n*-hexane-EtOAc 7:3 v/v, R_f: 0.40;

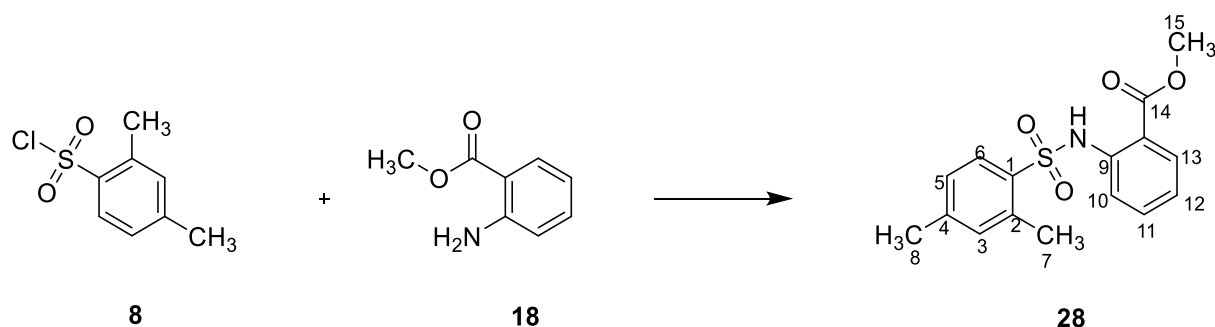
Purification: Recrystallisation from EtOH;

Yield: 0.247 g (68%);

¹H-NMR (DMSO-D₆), δ: 3.88 (s, 3H, H-14), 7.15-7.20 (m, 1H, H-aromatic), 7.38 (d, J= 8.2 Hz, 1H, H-aromatic), 7.52-7.56 (m, 1H, H-aromatic), 7.68 (dd, J₁= 8.5 Hz, J₂= 1.9 Hz, 1H, H-aromatic), 7.90-7.91 (m, 1H, H-aromatic), 7.93 (d, J= 8.2 Hz, 1H, H-aromatic), 8.17 (d, J= 8.5 Hz, 1H, H-aromatic), 11.07 (bs, 1H, NH).

¹³C-NMR (DMSO-D₆), δ: 53.3 (CH₃, C-14), 118.1, 124.2, 128.6, 131.7, 132.1, 133.7, 135.3 (CH, C-aromatic), 118.5, 132.3, 135.2, 138.5, 139.8 (C, C-aromatic), 168.1 (C, C-13).

UPLC-MS: Rt 2.46 (>99%) MS (ESI)⁺: 362.1 [M+H]⁺.

Methyl 2-((2,4,-dimethylphenyl)sulfonamido)benzoate (28)**(C₁₆H₁₇NO₄S; M.W.= 319.4)**Reagent: 2,4-dimethylbenzenesulfonyl chloride (**8**) (0.3 g, 1.46 mmol);Reagent: methyl anthranilate (**18**) (0.18 g, 1.22 mmol);

General procedure 2;

White solid;

T.L.C. System: *n*-hexane-EtOAc 7:3 v/v, R_f: 0.48;

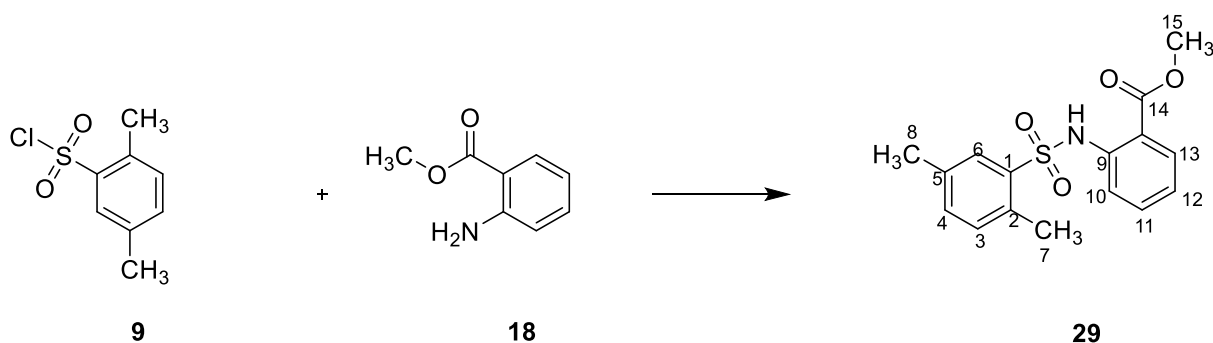
Purification: Recrystallisation from EtOH;

Yield: 0.215 g (55%);

¹H-NMR (DMSO-D₆), δ: 2.30 (s, 3H, H-8), 2.51 (s, 3H, H-7), 3.87 (s, 3H, H-15), 7.09-7.14 (m, 1H, H-aromatic), 7.20-7.23 (m, 2H, H-aromatic), 7.31 (d, J= 8.3 Hz, 1H, H-aromatic), 7.50-7.55 (m, 1H, H-aromatic), 7.78 (d, J= 8.3 Hz, 1H, H-aromatic), 7.89-7.91 (m, 1H, H-aromatic), 10.73 (bs, 1H, NH).

¹³C-NMR (DMSO-D₆), δ: 19.7 (CH₃, C-8), 21.2 (CH₃, C-7), 53.2 (CH₃, C-15), 118.3, 123.5, 127.4, 130.3, 131.6, 133.9, 135.1 (CH, C-aromatic), 116.2, 134.2, 137.0, 139.5, 144.6 (C, C-aromatic), 168.4 (C, C-14).

UPLC-MS: Rt 2.39 (100%) MS (ESI)⁺: 320.2 [M+H]⁺.

Methyl 2-((2,5-dimethylphenyl)sulfonamido)benzoate (29)**(C₁₆H₁₇NO₄S; M.W.= 319.4)**Reagent: 2,5-dimethylbenzenesulfonyl chloride (**9**) (0.3 g, 1.46 mmol);Reagent: methyl anthranilate (**18**) (0.18 g, 1.22 mmol);

General procedure 2;

White solid;

T.L.C. System: *n*-hexane-EtOAc 7:3 v/v, R_f: 0.51;

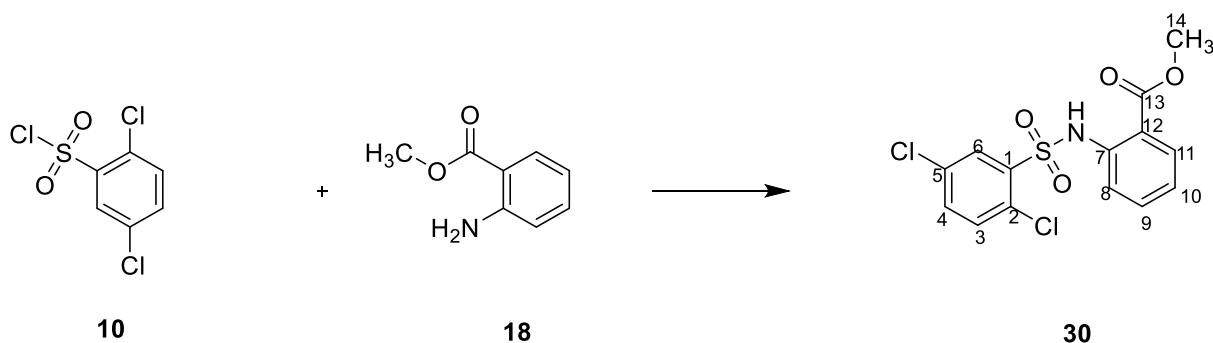
Purification: Recrystallisation from EtOH;

Yield: 0.183 g (47%);

¹H-NMR (DMSO-D₆), δ: 2.33 (s, 3H, H-8), 2.49 (s, 3H, H-7), 3.87 (s, 3H, H-15), 7.11-7.15 (m, 1H, H-aromatic), 7.28 (d, J= 7.7 Hz, 1H, H-aromatic), 7.33 (d, J= 7.7 Hz, 1H, H-aromatic), 7.39-7.40 (m, 1H, H-aromatic), 7.52-7.56 (m, 1H, H-aromatic), 7.81 (s, 1H, H-6), 7.89-7.92 (m, 1H, H-aromatic), 10.71 (bs, 1H, NH).

¹³C-NMR (DMSO-D₆), δ: 19.4 (CH₃, C-8), 20.7 (CH₃, C-7), 53.2 (CH₃, C-15), 118.5, 123.6, 130.3, 131.59, 133.2, 134.7, 135.2 (CH, C-aromatic), 116.4, 134.0, 136.5, 136.9, 139.4 (C, C-aromatic), 168.4 (C, C-14).

UPLC-MS: Rt 2.39 (100%) MS (ESI)⁺: 342.1 [M+Na]⁺.

Methyl 2-(2,5-dichlorophenyl)sulfonamido)benzoate (30)**(C₁₄H₁₁Cl₂NO₄S; M.W.= 360.2)**Reagent: 2,5-dichlorobenzoyl chloride (**10**) (0.3 g, 1.22 mmol);Reagent: methyl anthranilate (**18**) (0.15 g, 1.01 mmol);

General procedure 2;

White solid;

T.L.C. System: *n*-hexane-EtOAc 8:2 v/v, R_f: 0.45;

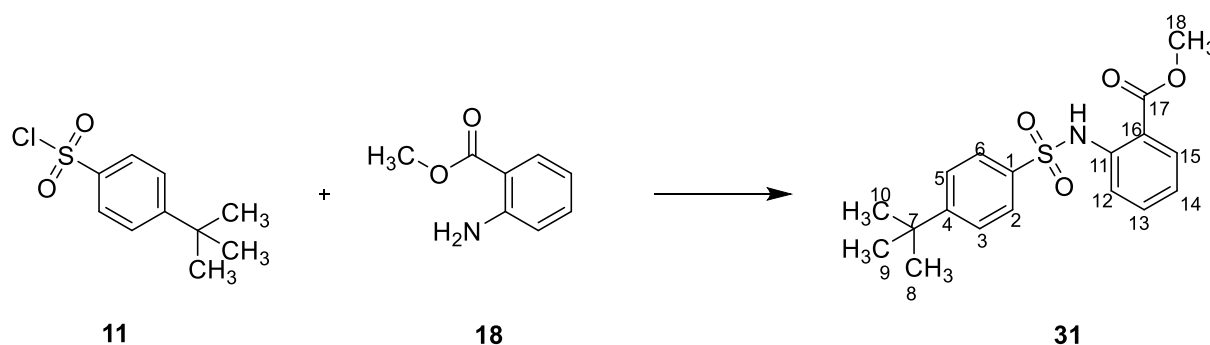
Purification: Recrystallisation from EtOH;

Yield: 0.205 g (56%);

¹H-NMR (DMSO-D₆), δ: 3.88 (s, 3H, H-14), 7.15-7.20 (m, 1H, H-aromatic), 7.42 (d, J= 8.1 Hz, 1H, H-aromatic), 7.55-7.59 (m, 1H, H-aromatic), 7.71 (d, J= 8.5 Hz, 1H, H-3), 7.78 (dd, J₁= 8.5 Hz, J₂= 2.4 Hz, 1H, H-4), 7.91-7.94 (m, 1H, H-aromatic), 8.14 (d, J= 2.4 Hz, 1H, H-6), 11.08 (bs, 1H, NH).

¹³C-NMR (DMSO-D₆), δ: 53.3 (CH₃, C-14), 119.0, 124.4, 131.4, 131.7, 134.3, 135.3, 135.5 (CH, C-aromatic), 117.5, 129.8, 132.9, 137.7, 138.2 (C, C-aromatic), 168.1 (C, C-13).

UPLC-MS: Rt 2.43 (100%) MS (ESI)⁻: 358.0 [M-H]⁻.

Methyl 2-((4-(*tert*-butyl)phenyl)sulfonamido)benzoate (31**)****(C₁₈H₂₁NO₄S; M.W.= 347.4)**Reagent: 4-(*tert*-butyl) benzenesulfonyl chloride (**11**) (0.3 g, 1.26 mmol);Reagent: methyl anthranilate (**18**) (0.16 g, 1.05 mmol);

General procedure 2;

White solid;

T.L.C. System: *n*-hexane-EtOAc 8:2 v/v, R_f: 0.45;

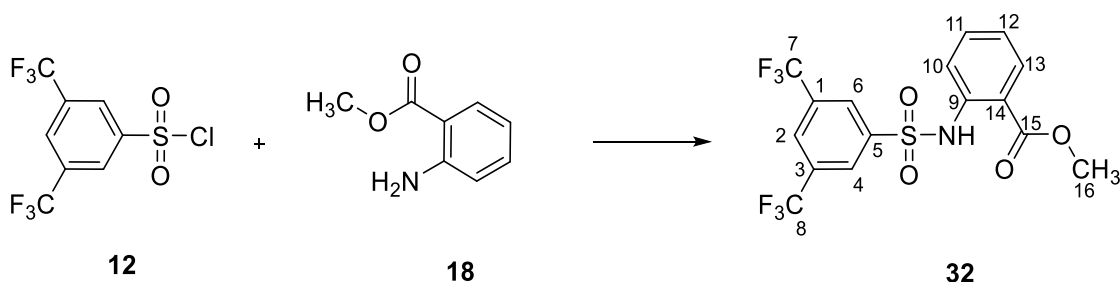
Purification: Recrystallisation from EtOH;

Yield: 0.270 g (74%);

¹H-NMR (DMSO-*D*₆), δ: 1.26 (s, 9H, 3xCH₃, H-8,9,10), 3.81 (s, 3H, H-18), 7.16-7.20 (m, 1H, H-aromatic), 7.50 (m, 1H, H-aromatic), 7.56-7.70 (m, 3H, H-aromatic), 7.73 (m, 2H, H-aromatic), 7.85 (dd, J₁= 7.9 Hz, J₂= 1.3 Hz, 1H, H-aromatic), 10.43 (bs, 1H, NH).

¹³C-NMR (DMSO-*D*₆), δ: 31.1 (3xCH₃, C-8,9,10), 53.1 (CH₃, C-18), 120.2, 124.2, 126.7, 127.2, 131.4, 134.9 (CH, C-aromatic), 35.4 (C, C-7), 118.1, 136.4, 139.2, 157.0 (C, C-aromatic), 168.0 (C, C-17).

UPLC-MS: Rt 2.53 (100%) MS (ESI)⁺: 348.2 [M+H]⁺.

Methyl 2-((3,5-bis(trifluoromethyl)phenyl)sulfonamide)benzoate (32)**(C₁₆H₁₁F₆NO₄S; M.W.= 427.32)**Reagent: 3,5-bis(trifluoromethyl)benzenesulfonyl chloride (**12**) (0.1 g, 0.32 mmol);Reagent: methyl anthranilate (**18**) (0.04 g, 0.26 mmol);

General procedure 2;

White solid;

T.L.C. System: *n*-hexane-EtOAc 8:2 v/v, R_f: 0.39;Purification: Biotage Isolera One automated flash column chromatography (cartridge: SNAP KP SIL 25g, *n*-hexane-DCM 100:0 increasing to *n*-hexane-DCM 20:80 in 15CV);

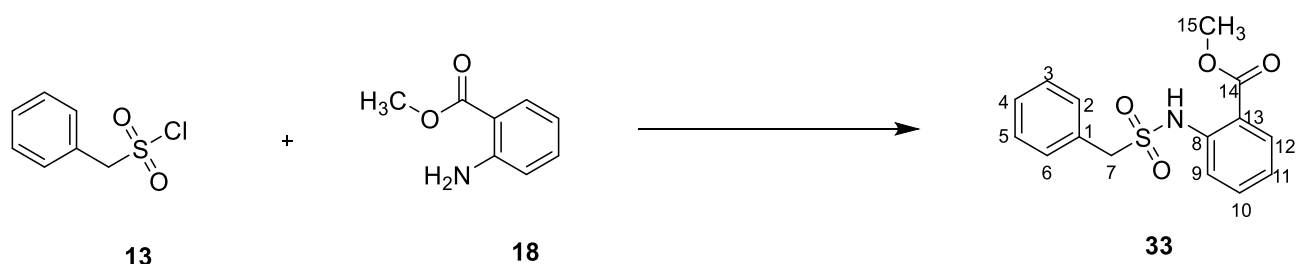
Yield: 0.096 g (70%);

¹H-NMR (CDCl₃), δ: 3.88 (s, 3H, H-16), 7.16-7.19 (m, 1H, H-aromatic), 7.55-7.19 (m, 1H, H-aromatic), 7.75 (dd, J₁= 8.3 Hz, J₂= 1.0 Hz, 1H, H-aromatic), 7.94-7.06 (m, 1H, H-aromatic), 8.00-8.03 (m, 1H, H-aromatic), 8.25-8.27 (m, 2H, H-aromatic), 10.74 (bs, 1H, NH).

¹³C-NMR (CDCl₃), δ: 52.7 (CH₃, C-16), 120.5, 124.5, 126.4, 127.5, 131.4, 132.6, 134.8 (CH, C-aromatic), 117.0, 120.5, 124.5, 127.4, 131.4, 139.1, 141.9 (C, C-aromatic), 168.2 (C, C-15).

¹⁹F-NMR (CDCl₃), δ: -63.02, (s, 2x3F).

UPLC-MS: Rt 2.53 (>98%) MS (ESI)⁻: 426.2 [M-H]⁻.

Methyl 2-((phenylmethyl)sulfonamido)benzoate (33)**(C₁₅H₁₅NO₄S; M.W.= 305.35)**Reagent: phenylmethanesulfonyl chloride (**13**) (0.200 g, 1.04 mmol);Reagent: methyl 2-aminobenzoate (**18**) (0.132 g, 0.88 mmol);

General Procedure 2;

White Solid;

T.L.C. System: *n*-hexane-EtOAc 7:3 v/v, R_f: 0.42;

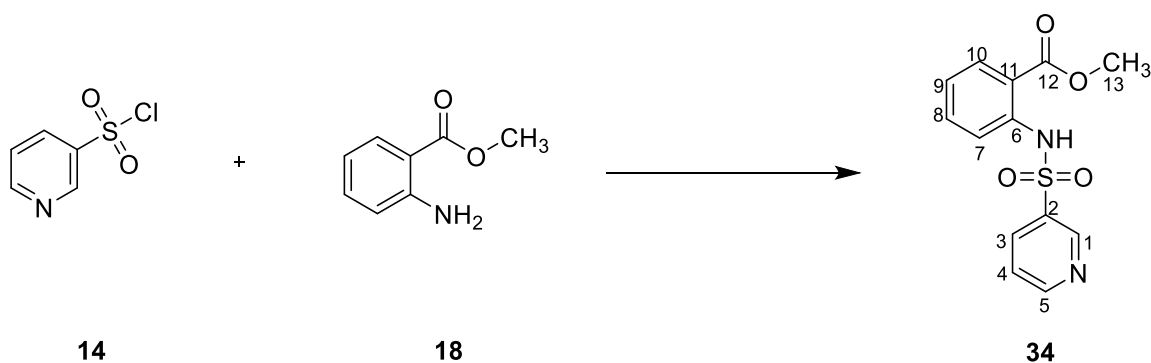
Purification: Recrystallisation from EtOH;

Yield: 0.075 g (28%)

¹H-NMR (DMSO-D₆), δ: 3.82 (s, 3H, H-15), 4.69 (s, 2H, H-7), 7.19-7.22 (m, 3H, H-aromatic), 7.29-7.33 (m, 2H, H-aromatic), 7.34-7.36 (m, 1H, H-aromatic), 7.56-7.58 (m, 1H, H-aromatic), 7.60-7.74 (m, 1H, H-aromatic), 7.95 (dd, J₁= 7.9 Hz, J₂= 1.3 Hz, 1H, H-aromatic), 10.11 (bs, 1H, NH).

¹³C-NMR (DMSO-D₆), δ: 40.5 (CH₃, C-15), 57.9 (CH₂, C-7), 118.8, 123.4, 128.8, 128.9, 131.2, 131.5, 135.2 (CH, C-aromatic), 116.2, 129.3, 140.5 (C, C-aromatic), 168.1 (C, C-14).

UPLC-MS: Rt 2.23 (>98%) MS (ESI): 304.1 [M-H]⁻.

Methyl 2-(pyridine-3-sulfonamido)benzoate (34)**(C₁₃H₁₂N₂O₄S; M.W.= 292.31)**Reagent: pyridine-3-sulfonyl chloride (**14**) (0.200 g, 1.12 mmol);Reagent: methyl 2-aminobenzoate (**18**) (0.141 g, 0.93 mmol);

General Procedure 2;

White Solid;

T.L.C. System: *n*-hexane-EtOAc 7:3 v/v, R_f: 0.20;

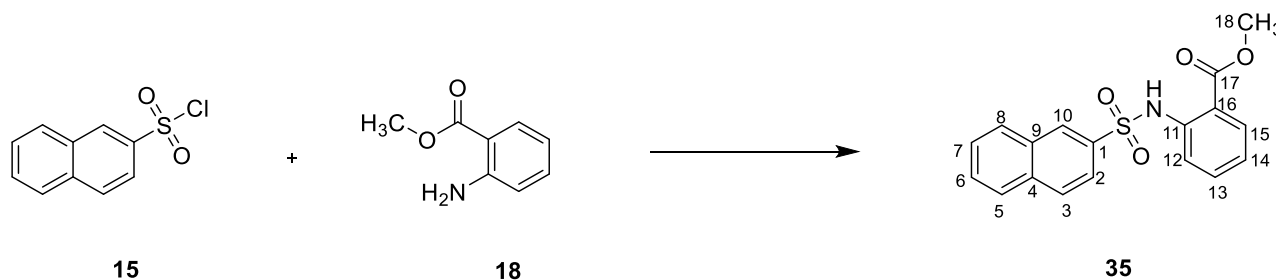
Purification: Recrystallisation from EtOH;

Yield: 0.217 g (79%);

¹H-NMR (DMSO-D₆), δ: 3.80 (s, 3H, H-13), 7.00-7.04 (m, 2H, H-aromatic), 7.29-7.33 (m, 1H, H-aromatic), 7.40-7.45 (m, 1H, H-aromatic), 7.66 (dd, J₁= 8.4 Hz, J₂= 0.9 Hz, 1H, H-aromatic), 7.86 (dd, J₁= 8.0 Hz, J₂= 1.5 Hz, 1H, H-aromatic), 8.03-8.07 (m, 1H, H-aromatic), 8.65-8.68 (m, 1H, H-aromatic), 8.98 (s, 1H, H-2), 10.71 (bs, 1H, NH).

¹³C-NMR (DMSO-D₆), δ: 52.6 (CH₃, C-13), 119.4, 123.6, 123.7, 131.3, 134.7, 134.9, 148.1, 153.5 (CH, C-aromatic), 116.3, 136.0, 139.7 (C, C-aromatic), 168.3 (C, C-12).

UPLC-MS: Rt 2.06 (>98%) MS (ESI)⁺: 293.0 [M+H]⁺.

Methyl 2-(naphthalene-2-sulfonamido)benzoate (35)**(C₁₈H₁₅NO₄S; M.W.= 341.38)**Reagent: naphthalene-2-sulfonyl chloride (**15**) (0.200 g, 0.89 mmol);Reagent: methyl 2-aminobenzoate (**18**) (0.113 g, 0.74 mmol);

General Procedure 2;

Pink Solid;

T.L.C. System: *n*-hexane-EtOAc 8:2 v/v, R_f: 0.38;

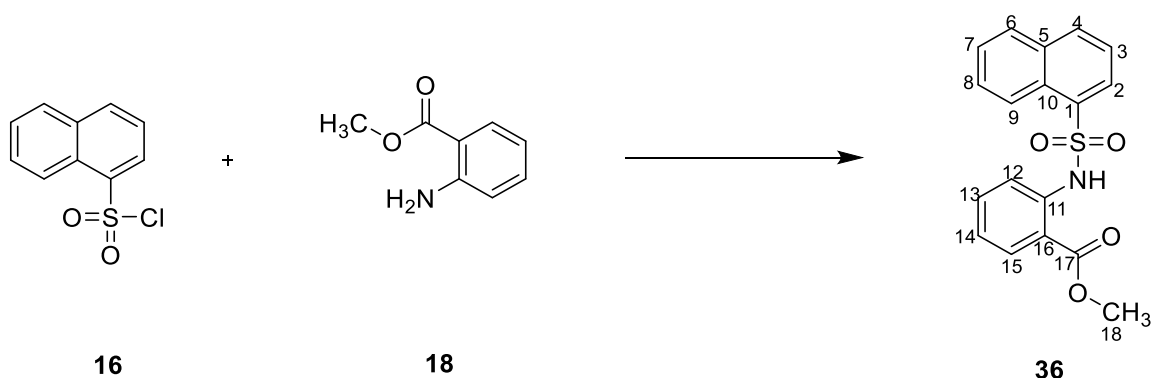
Purification: Recrystallisation from EtOH;

Yield: 0.171 g (68%);

¹H-NMR (CDCl₃), δ: 3.86 (s, 3H, H-18), 7.01-7.04 (m, 1H, H-aromatic), 7.44-7.48 (m, 1H, H-aromatic), 7.59-7.65 (m, 2H, H-aromatic), 7.72 (dd, J₁= 8.5 Hz, J₂= 0.7 Hz, 1H, H-aromatic), 7.83 (dd, J₁= 8.6 Hz, J₂= 1.8 Hz, 1H, H-aromatic), 7.87 (d, J= 8.1 Hz, 1H, H-aromatic), 7.89-7.91 (m, 2H, H-aromatic), 7.95 (d, J= 8.1 Hz, 1H, H-aromatic), 8.48 (s, 1H, H-10), 10.80 (bs, 1H, NH).

¹³C-NMR (CDCl₃), δ: 52.4 (CH₃, C-18), 119.0, 122.2, 122.9, 127.5, 128.8, 128.92, 128.95, 129.3, 129.4, 131.1, 134.5 (CH, C-aromatic), 115.9, 132.0, 134.9, 136.3, 140.42 (C, C-aromatic), 168.32 (C, C-17).

UPLC-MS: Rt 2.37 (100%) MS (ESI)⁺: 342.23 [M+H]⁺.

Methyl 2-(naphthalene-1-sulfonamido)benzoate (36)**(C₁₈H₁₅NO₄S; M.W.= 341.38)**Reagent: naphthalene-1-sulfonyl chloride (**16**) (0.200 g, 0.88 mmol);Reagent: methyl 2-aminobenzoate (**18**) (0.111 g, 0.73 mmol);

General Procedure 2;

White Solid;

T.L.C. System: *n*-hexane-EtOAc 8:2 v/v, R_f: 0.36;

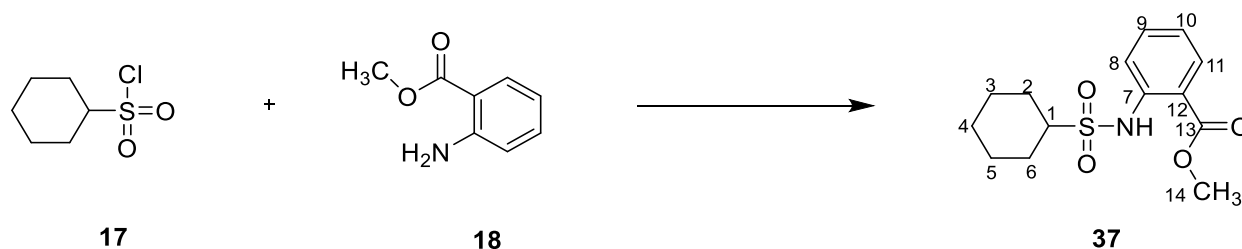
Purification: Recrystallisation from EtOH;

Yield: 0.144 g (48%);

¹H-NMR (CDCl₃), δ: 3.85 (s, 3H, H-18), 6.94-6.97 (m, 1H, H-aromatic), 7.37-7.40 (m, 1H, H-aromatic), 7.50-7.54 (m, 1H, H-aromatic), 7.57-7.61 (m, 1H, H-aromatic), 7.63 (dd, J₁= 8.4 Hz, J₂= 0.8 Hz, 1H, H-aromatic), 7.69-7.72 (m, 1H, H-aromatic), 7.84 (dd, J₁= 8.0 Hz, J₂= 1.4 Hz, 1H, H-aromatic), 7.91 (d, J= 8.4 Hz, 1H, H-aromatic), 8.04 (d, J= 8.0 Hz, 1H, H-aromatic), 8.37 (dd, J₁= 7.4 Hz, J₂= 1.4 Hz, 1H, H-aromatic), 8.74-8.76 (m, 1H, H-aromatic), 11.10 (bs, 1H, NH).

¹³C-NMR (CDCl₃), δ: 52.4 (CH₃, C-18), 118.0, 122.4, 123.9, 124.5, 126.9, 128.4, 128.9, 130.3, 131.0, 134.3, 134.7 (CH, C-aromatic), 115.3, 128.0, 134.2, 140.4 (C, C-aromatic), 168.3 (C, C-17).

UPLC-MS: Rt 2.37 (100%) MS (ESI)⁺: 342.2 [M+H]⁺.

Methyl 2-(cyclohexanesulfonamido)benzoate (37)**(C₁₄H₁₉NO₄S; M.W.= 297.37)**Reagent: cyclohexanesulfonyl chloride (**17**) (0.2 g, 1.09 mmol);Reagent: methyl 2-aminobenzoate (**18**) (0.137 g, 0.91mmol);

General Procedure 2;

Colourless oil;

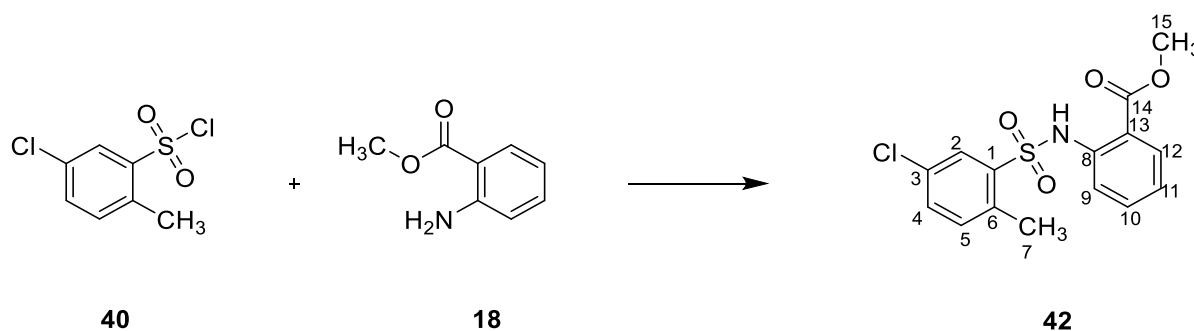
T.L.C. System: *n*-hexane-EtOAc 7:3 v/v, R_f: 0.48;Purification: Biotage Isolera One automated flash column chromatography (cartridge: SNAP KP SIL 10g, *n*-hexane-DCM 100:0 increasing to *n*-hexane-DCM 50:50 in 11CV);

Yield: 0.070 g (26%);

¹H-NMR (DMSO-D₆), δ: 1.08-1.13 (m, 2H, H-cyclohexane), 1.15-1.18 (m, 1H, H-cyclohexane), 1.50-1.57 (m, 2H, H-cyclohexane), 1.58-1.60 (m, 1H, H-cyclohexane), 1.78-1.81 (m, 2H, H-cyclohexane), 2.06-2.08 (m, 2H, H-cyclohexane), 2.98 (tt, J₁= 12.1 Hz, J₂= 3.4 Hz, 1H, H-1), 3.86 (s, 3H, H-14), 6.98-7.01 (m, 1H, H-aromatic), 7.52-7.55 (m, 1H, H-aromatic), 7.73 (dd, J₁= 8.4 Hz, J₂= 0.5 Hz, 1H, H-aromatic), 7.95-7.97 (m, 1H, H-aromatic), 10.31 (bs, 1H, NH).

¹³C-NMR (DMSO-D₆), δ: 52.5 (CH₃, C-14), 25.0, 25.1, 26.2 (CH₂, C-cyclohexane), 61.1 (CH, C-1), 117.6, 122.1, 131.4, 134.8 (CH, C-aromatic), 114.6, 141.6 (C, C-aromatic), 168.4 (C, C-13).

UPLC-MS: Rt 2.35 (99%) MS (ESI)⁻: 296.2 [M-H]⁻.

Methyl 2-((2-chloro-5-methylphenyl)sulfonamido)benzoate (42)**(C₁₅H₁₄ClNO₄S; M.W.= 339.8)**Reagent: 5-chloro-2-methylbenzenesulfonyl chloride (**40**) (0.6 g, 2.66 mmol);Reagent: methyl anthranilate (**18**) (0.33 g, 2.22 mmol);

General procedure 2;

White solid;

T.L.C. System: *n*-hexane-EtOAc 8:2 v/v, R_f: 0.40;

Purification1: Recrystallisation from EtOH;

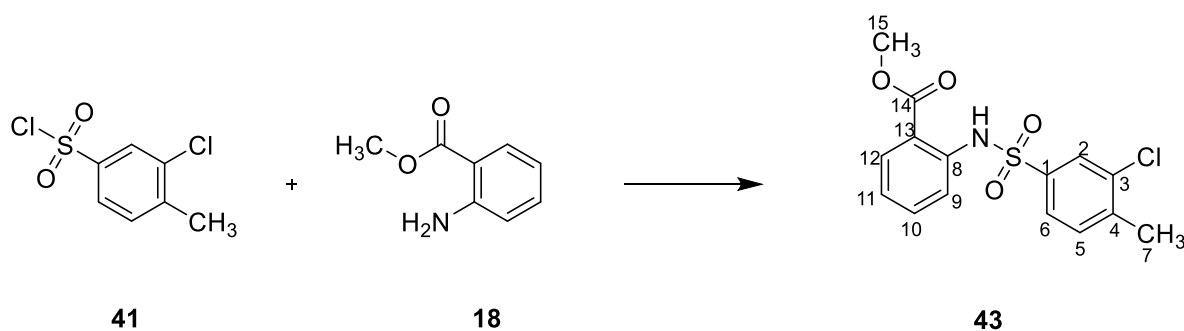
Purification 2: Flash column chromatography (*n*-hexane:EtOAc 100:0 v/v increasing to *n*-hexane:EtOAc 95:5 v/v);

Yield: 0.071 g (9%);

¹H-NMR (DMSO-D₆), δ: 2.51 (s, 3H, CH₃, H-7), 3.84 (s, 3H, H-15), 7.18-7.21 (m, 1H, H-aromatic), 7.38-7.41 (m, 1H, H-aromatic), 7.45 (d, J = 8.2 Hz, 1H, H-5), 7.56-7.60 (m, 1H, H-aromatic), 7.64 (dd, J₁ = 8.2 Hz, J₂ = 2.2 Hz, 1H, H-4), 7.83-7.88 (m, 1H, H-aromatic), 7.89 (d, J = 2.2 Hz, 1H, H-2), 10.71 (bs, 1H, NH).

¹³C-NMR (DMSO-D₆), δ: 19.4 (CH₃, C-7), 53.2 (CH₃, C-15), 120.1, 124.5, 129.1, 131.3, 133.8, 135.0, 135.2 (CH, C-aromatic), 110.1, 131.6, 134.7, 140.3, 147.9 (C, C-aromatic), 168.1 (C, C-14).

UPLC-MS: R_t 2.49 (99%) **MS (ESI):** 338.0 [M-H]⁻.

Methyl 2-((3-chloro-4-methylphenyl)sulfonamido)benzoate (43)**(C₁₅H₁₄ClNO₄S; M.W.= 339.8)**Reagent: 3-chloro-4-methylbenzenesulfonyl chloride (**41**) (0.33 g, 1.33 mmol);Reagent: methyl anthranilate (**18**) (0.17 g, 1.11 mmol);

General Procedure 2;

White solid;

T.L.C. System: *n*-hexane-EtOAc 8:2 v/v, R_f: 0.40;

Purification1: Recrystallisation from EtOH;

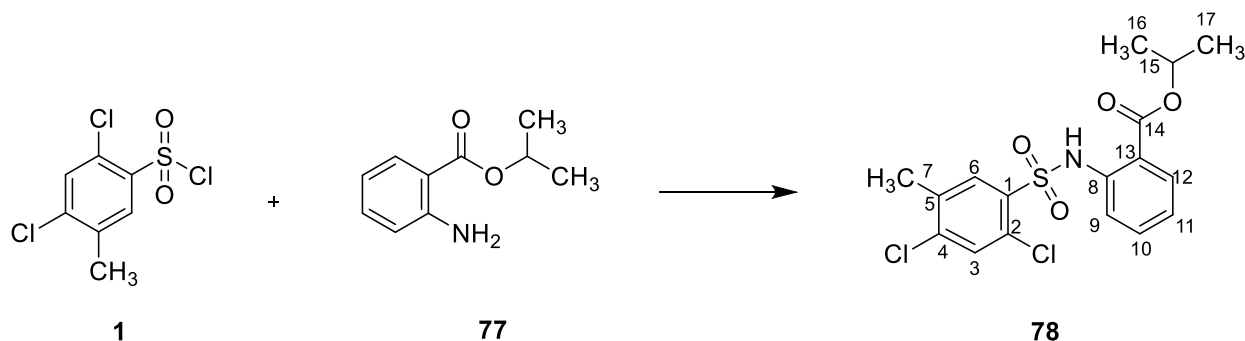
Purification 2: Flash column chromatography (*n*-hexane:EtOAc 100:0 v/v increasing to *n*-hexane:EtOAc 9:1 v/v);

Yield: 0.091 g (24%);

¹H-NMR (DMSO-*D*₆), δ: 2.36 (s, 3H, CH₃, H-7), 3.82 (s, 3H, H-15), 7.19-7.23 (m, 1H, H-aromatic), 7.44 (dd, *J*₁= 8.3 Hz, *J*₂= 1.0 Hz, 1H, H-aromatic), 7.56-7.60 (m, 1H, H-aromatic), 7.61-7.62 (m, 2H, H-aromatics), 7.81-7.82 (m, 1H, H-aromatic), 7.84-7.86 (m, 1H, H-aromatic), 10.42 (bs, 1H, NH).

¹³C-NMR (DMSO-*D*₆), δ: 19.9 (CH₃, C-7), 53.0 (CH₃, C-15), 121.0, 124.7, 126.5, 129.7, 130.3, 131.5, 134.8 (CH, C-aromatic), 119.1, 137.8, 138.0, 138.5, 139.0 (C, C-aromatic), 167.8 (C, C-14).

UPLC-MS: Rt 2.45 (100%) MS (ESI)⁺: 340.1 [M+H]⁺.

Isopropyl 2-((2,4-dichloro-5-methylphenyl)sulfonamido)benzoate (**78**)(C₁₇H₁₇Cl₂NO₄S; M.W.= 402.29)Reagent: 2,4-dichloro-5-methylbenzenesulfonyl chloride (**1**) (0.650 g, 2.50 mmol);Reagent: isopropyl 2-aminobenzoate (**77**) (0.374 g, 2.08 mmol);

General Procedure 2;

White solid;

T.L.C. System: *n*-hexane-EtOAc 7:3 v/v, R_f: 0.6;

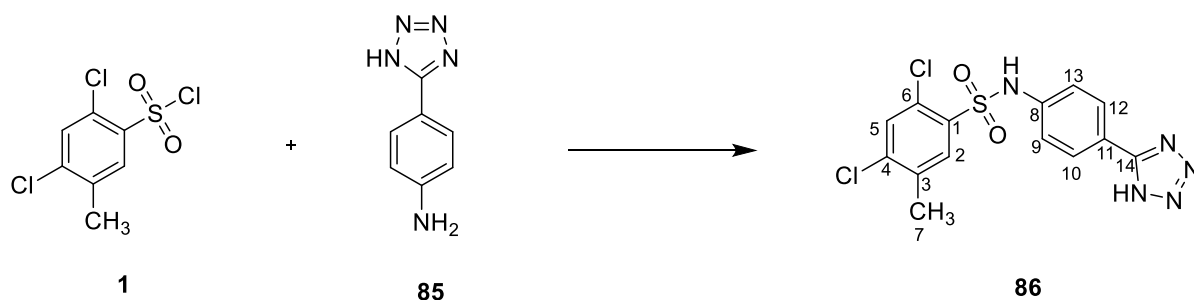
Purification: Recrystallisation from EtOH;

Yield: 0.148 g (26%);

¹H-NMR (CDCl₃), δ: 1.40 (d, J= 6.3Hz, 6H, H-16,17), 2.43 (s, 3H, H-7), 5.27-5.29 (m, 1H, H-15), 7.01-7.05 (m, 1H, H-aromatic), 7.38-7.42 (m, 1H, H-aromatic), 7.44 (s, 1H, H-6), 7.53-7.56 (m, 1H, H-aromatic), 7.99 (dd, J₁= 8.0 Hz, J₂= 1.5 Hz, 1H, H-aromatic), 8.09 (s, 1H, H-3), 11.35 (bs, 1H, NH).

¹³C-NMR (CDCl₃), δ: 19.6 (CH₃, C-7), 21.8 (2xCH₃, C-16,17), 69.6 (CH, C-15), 116.9, 122.4, 131.4, 131.8, 133.5, 134.2 (CH, C-aromatic), 115.9, 129.9, 134.9, 135.5, 139.6, 139.9 (C, C-aromatic), 167.2 (C, C-14).

UPLC-MS: Rt 2.78 (100%) MS (ESI)⁻: 400.1 [M-H]⁻.

N*-(4-(1*H*-Tetrazol-5-yl)phenyl)-2,4-dichloro-5-methylbenzenesulfonamide (**86**)*(C₁₄H₁₁Cl₂N₅O₂S; M.W.= 383.24)**Reagent: 2,4-dichloro-5-methylbenzenesulfonyl chloride (**1**) (0.193 g, 0.74 mmol);Reagent: 4-(1*H*-tetrazol-5-yl)aniline (**85**) (0.100 g, 0.62 mmol);

General Procedure 2;

Pink Solid;

T.L.C. System: *n*-hexane-EtOAc 6:4 v/v, R_f: 0.35;

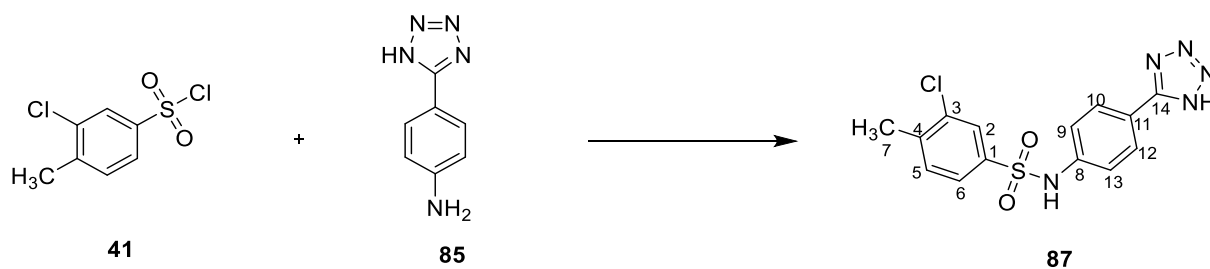
Purification: Recrystallisation from EtOH/Water;

Yield: 0.110 g (46%);

¹H-NMR (DMSO-*D*₆), δ: 2.39 (s, 3H, H-7), 7.30 (d, J= 8.6 Hz, 2H, H-aromatic), 7.81 (s, 1H, H-2), 7.90 (d, J= 8.6 Hz, 2H, H-aromatic), 8.15 (s, 1H, H-5), 11.15 (bs, 1H, NH).

¹³C-NMR (DMSO-*D*₆), δ: 14.4 (CH₃, C-7), 119.3, 128.7, 132.0, 134.0 (CH, C-aromatic), 114.8, 129.2, 135.2, 136.5, 139.5, 139.9 (C, C-aromatic).

UPLC-MS: Rt 1.96 (>99%) **MS (ESI)⁺:** 384.1 [M+H]⁺.

N*-4-(1*H*-Tetrazol-5-yl)phenyl)-3-chloro-4-methylbenzenesulfonamide (**87**)*(C₁₄H₁₂ClN₅O₂S; M.W.= 349.79)**Reagent: 3-chloro-4-methylbenzenesulfonyl chloride (**41**) (0.167 g, 0.74 mmol);Reagent: 4-(1*H*-tetrazol-5-yl)aniline (**85**) (0.100 g, 0.62 mmol);

General Procedure 2;

White Solid;

T.L.C. System: DCM-MeOH 95:5 v/v, R_f: 0.37;

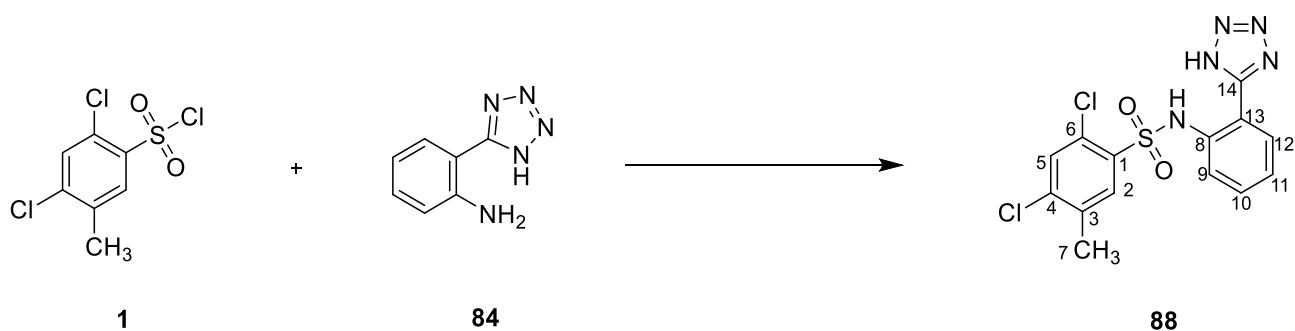
Purification: Recrystallisation from EtOH;

Yield: 0.040 g (28%);

¹H-NMR (DMSO-*D*₆), δ : 2.36 (s, 3H, H-7), 7.32 (d, 2H, J = 8.3 Hz, H-aromatic), 7.56 (d, J = 7.6 Hz, 1H, H-5), 7.68 (d, J = 7.6 Hz, 1H, H-6), 7.82 (s, 1H, H-2), 7.92 (d, J = 8.3 Hz, 2H, H-aromatic), 10.82 (bs, 1H, NH).

¹³C-NMR (DMSO-*D*₆), δ : 20.1 (CH₃, C-7), 120.2, 125.8, 127.1, 128.7, 132.6 (CH, C-aromatic), 131.5, 134.4, 138.8, 140.4, 142.0 (C, C-aromatic), 175.9 (C, C-14).

UPLC-MS: R_t 1.86 (>99%) MS (ESI)⁺: 350.1 [M+H]⁺.

N*-(2-(1*H*-tetrazol-5-yl)phenyl)-2,4-dichloro-5-methylbenzenesulfonamide (**88**)*(C₁₄H₁₁Cl₂N₅O₂S; M.W. = 384.24)**Reagent: 2,4-dichloro-5-methylbenzenesulfonyl chloride (**1**) (0.193 g, 0.74 mmol);Reagent: 2-(1*H*-tetrazol-5-yl)aniline (**84**) (0.100 g, 0.62 mmol);

General Procedure 2;

Off-White Solid;

T.L.C. System: *n*-hexane-EtOAc 7:3 v/v, R_f: 0.29;

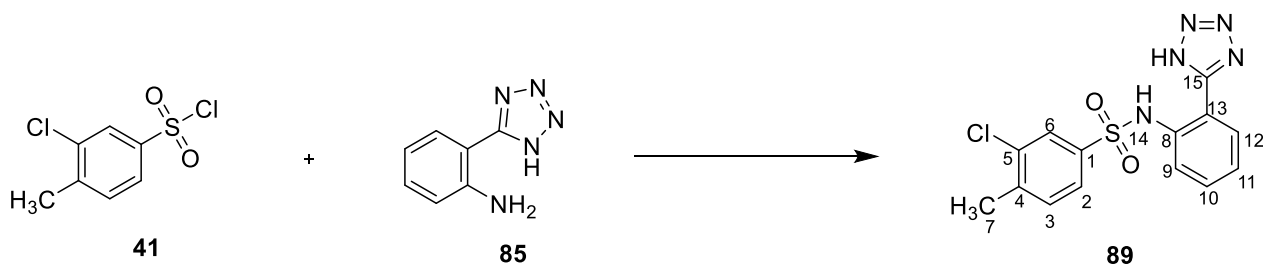
Purification: Recrystallisation from EtOH;

Yield: 0.042 g (18%);

¹H-NMR (DMSO-*D*₆), δ: 2.39 (s, 3H, H-7), 7.28-7.32 (m, 1H, H-aromatic), 7.48-7.51 (m, 2H, H-aromatic), 7.78 (s, 1H, H-2), 7.94-7.98 (m, 1H, H-aromatic), 8.16 (s, 1H, H-5), 11.37 (bs, 1H, NH).

¹³C-NMR (DMSO-*D*₆), δ: 19.5 (CH₃, C-7), 119.2, 124.8, 129.5, 132.1, 132.7, 134.0 (CH, C-aromatic), 113.5, 129.1, 134.7, 135.5, 136.6, 136.8 (C, C-aromatic), 172.3 (C, C-14).

UPLC-MS: Rt 2.26 (>97%) MS (ESI)⁺: 386.1 [M+H]⁺.

N*-(2-(1*H*-tetrazol-5-yl)phenyl)-3-chloro-4-methylbenzenesulfonamide (**89**)*(C₁₄H₁₂ClN₅O₂S; M.W.= 349.79)**Reagent: 3-chloro-4-methylbenzenesulfonyl chloride (**41**) (0.167 g, 0.74 mmol);Reagent: 2-(1*H*-tetrazol-5-yl)aniline (**85**) (0.100 g, 0.62 mmol);

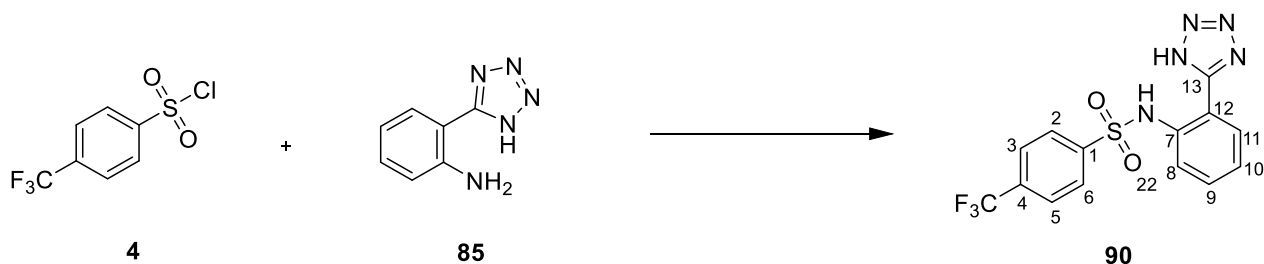
General Procedure 2;

White Solid;

T.L.C. System: *n*-hexane-EtOAc 7:3 v/v, R_f: 0.29;Purification: Biotage Isolera One automated flash column chromatography (cartridge: ZIP KP 10g, *n*-hexane-EtOAc 100:0 increasing to *n*-hexane-EtOAc 0:100 in 15CV);

Yield: 0.034 g (16%);

¹H-NMR (DMSO-*D*₆), δ: 2.33 (s, 3H, H-7), 7.33-7.36 (m, 1H, H-aromatic), 7.45-7.48 (m, 2H, H-aromatic), 7.51-7.55 (m, 2H, H-aromatic), 7.66-7.68 (m, 1H, H-aromatic), 7.86-7.88 (m, 1H, H-aromatic), 10.67 (bs, 1H, NH).**¹³C-NMR (DMSO-*D*₆), δ:** 20.1 (CH₃, C-7), 122.3, 125.8, 125.9, 127.3, 129.7, 132.3, 132.4 (CH, C-aromatic), 116.6, 134.6, 135.6, 138.2, 142.1 (C, C-aromatic), 179.4 (C, C-15).**UPLC-MS: R_t 2.15 (>99%) MS (ESI)⁺: 350.3 [M+H]⁺.**

N*-[2-(1*H*-tetrazol-5-yl)phenyl]-4-(trifluoromethyl)benzenesulfonamide (**90**)*(C₁₄H₁₀F₃N₅O₂S; M.W.= 369.32)**Reagent: 4-(trifluoromethyl)benzenesulfonyl chloride (**4**) (0.182 g, 0.74 mmol);Reagent: 2-(1*H*-tetrazol-5-yl)aniline (**85**) (0.100 g, 0.62 mmol);

General Procedure 2;

White Solid;

T.L.C. System: DCM-MeOH 98:2 v/v, R_f: 0.45;

Purification: Recrystallisation from EtOH/Water;

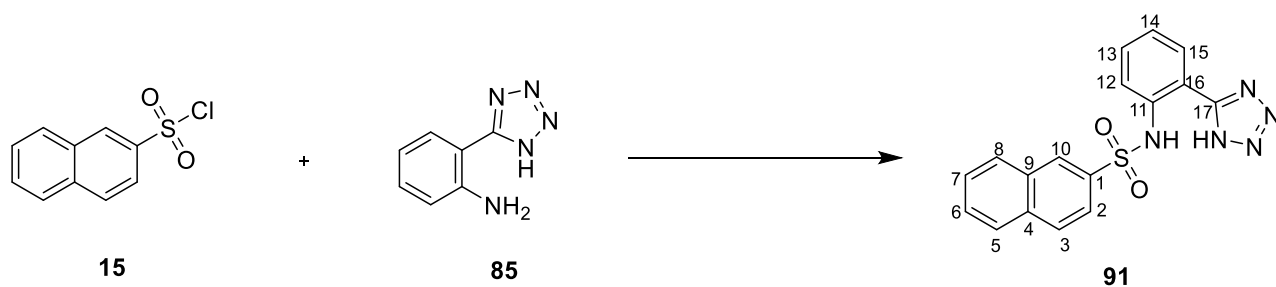
Yield: 0.095 g (42%);

¹H-NMR (DMSO-D₆), δ: 7.36-6.39 (m, 1H, H-aromatic), 7.44 (dd; J₁= 8.1 Hz, J₂= 1.0 Hz, 1H, H-aromatic), 7.52-7.55 (m, 1H, H-aromatic), 7.85 (dd, J₁= 7.8 Hz, J₂= 1.4 Hz, 1H, H-aromatic), 7.88-7.91 (m, 4H, H-aromatic), 10-73 (bs, 1H, NH).

¹³C-NMR (DMSO-D₆), δ: 123.0, 126.2, 126.9, 128.3, 129.9, 132.5 (CH, C-aromatic), 133.2 (d, J= 37.7 Hz, C) 117.0, 122.6, 124.8, 135.3, 143.0 (C-aromatic).

¹⁹F-NMR (DMSO-D₆), δ: -61.76 (s, 3F).

UPLC-MS: Rt 1.81 (100%) **MS (ESI)⁺:** 370.1 [M+H]⁺.

N*-(2-(1*H*-tetrazol-5-yl)phenyl)naphthalene-2-sulfonamide (**91**)*(C₁₇H₁₃N₅O₂S; M.W.= 351.38)**Reagent: naphthalene-2-sulfonyl chloride (**15**) (0.169 g, 0.74 mmol);Reagent: 2-(1*H*-tetrazol-5-yl)aniline (**85**) (0.100 g, 0.62 mmol);

General Procedure 2;

White Solid;

T.L.C. System: *n*-hexane-EtOAc 5:5 v/v, R_f: 0.17;

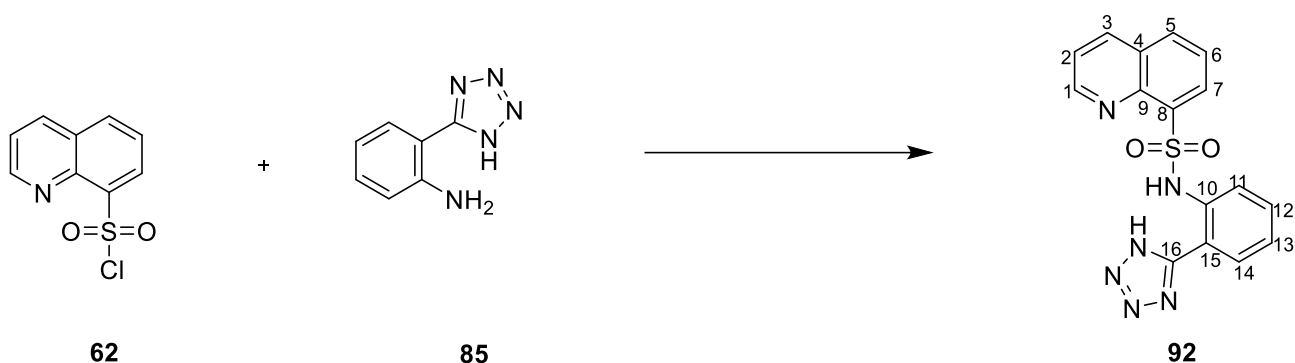
Purification: Recrystallisation from EtOH;

Yield: 0.083 g (38%);

¹H-NMR (DMSO-*D*₆), δ: 7.26-7.29 (m, 1H, H-aromatic), 7.47-7.50 (m, 1H, H-aromatic), 7.54 (d, J=8.1 Hz, 1H, H-aromatic), 7.63-7.66 (m, 1H, H-aromatic), 7.68-7.71 (m, 2H, H-aromatic), 7.82-7.84 (m, 1H, H-aromatic), 7.97-8.02 (m, 2H, H-aromatic), 8.10 (d, J= 8.1 Hz, 1H, H-aromatic), 8.47 (s, 1H, H-10), 10.78 (bs, 1H, NH).

¹³C-NMR (DMSO-*D*₆), δ: 121.5, 122.2, 125.4, 128.26, 128.29, 128.9, 129.6, 129.73, 129.78, 129.9, 134.8 (CH, C-aromatic), 115.2, 131.9, 132.5, 136.0, 136.1(C, C-aromatic).

UPLC-MS: R_t 2.07 (100%) MS (ESI)⁺: 352.1 [M+H]⁺.

N*-[2-(1*H*-tetrazol-5-yl)phenyl]quinoline-8-sulfonamide (**92**)*(C₁₆H₁₂N₆O₂S; M.W. = 352.37)**Reagent: quinoline-8-sulfonyl chloride (**62**) (0.170 g, 0.74 mmol);Reagent: 2-(1*H*-tetrazol-5-yl)aniline (**85**) (0.100 g, 0.62 mmol);

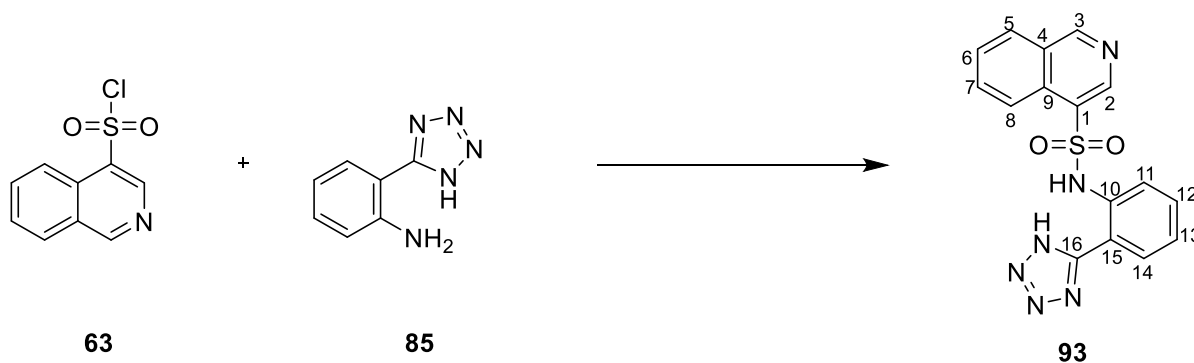
General Procedure 2;

Off-White Solid;

T.L.C. System: *n*-hexane-EtOAc 5:5 v/v, R_f: 0.63;Purification: Biotage Isolera One automated flash column chromatography (cartridge: SNAP KP 25g, *n*-hexane-EtOAc 0:100 increasing to *n*-hexane-EtOAc 50:50 in 15CV);

Yield: 0.056 g (26%);

¹H-NMR (DMSO-*D*₆), δ: 7.11-7.14 (m, 1H, H-aromatic), 7.39-7.42 (m, 1H, H-aromatic), 7.55-7.58 (m, 1H, H-aromatic), 7.72-7.76 (m, 3H, H-aromatic), 8.26-8.28 (m, 1H, H-aromatic), 8.41-8.44 (m, 2H, H-aromatic), 8.48-8.49 (m, 1H, H-aromatic), 11.23 (bs, 1H, NH).¹³C-NMR (DMSO-*D*₆), δ: 112.9, 118.6, 123.1, 124.1, 128.3, 129.3, 132.4, 134.4, 136.5, 151.3 (CH, C-aromatic), 126.1, 134.4, 137.4, 142.6 (C, C-aromatic).UPLC-MS: Rt 1.65 (>96%) MS (ESI)⁺: 353.3 [M+H]⁺.

N*-2-(1*H*-tetrazol-5-yl)phenyl)isoquinoline-4-sulfonamide (**93**)*(C₁₆H₁₂N₆O₂S; M.W.= 352.37)**Reagent: quinoline-3-sulfonyl chloride (**63**) (0.100 g, 0.43 mmol);Reagent: 2-(1*H*-tetrazol-5-yl)aniline (**85**) (0.069 g, 0.43 mmol);

General Procedure 2;

Brown Solid;

T.L.C. System: DCM-MeOH 98:2 v/v, R_f: 0.15;

Purification: Biotage Isolera One automated flash column chromatography (cartridge: SNAP KP SIL 25g, DCM-MeOH 100:0 increasing to DCM-MeOH 95:5 in 10CV);

Yield: 0.069 g (46%);

¹H-NMR (DMSO-*D*₆), δ: 7.05-7.08 (m, 1H, H-aromatic), 7.21-7.25 (m, 1H, H-aromatic), 7.64 (d, *J*= 8.2 Hz, 1H, H-aromatic), 7.69-7.72 (m, 1H, H-aromatic), 7.88-7.91 (m, 1H, H-aromatic), 8.01 (d, *J*= 8.5 Hz, 1H, H-aromatic), 8.03-8.05 (m, 1H, H-aromatic), 8.09-8.11 (m, 1H, H-aromatic), 8.89 (s, 1H, H-3), 8.97 (s, 1H, H-2), 13.23 (bs, 1H, NH).

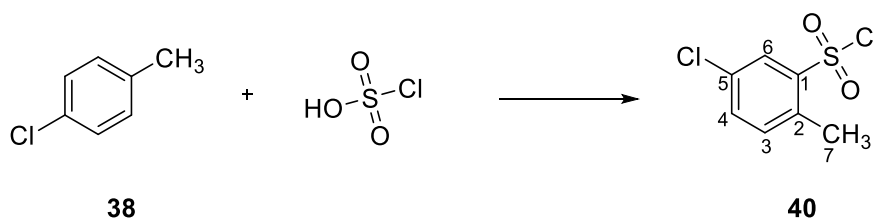
¹³C-NMR (DMSO-*D*₆), δ: 118.8, 124.3, 127.7, 128.6, 128.8, 129.2, 130.0, 133.2, 137.0, 146.4 (CH, C-aromatic), 120.5, 126.2, 134.9, 146.4, 148.7 (C, C-aromatic), 159.6 (C, C-16).

UPLC-MS: R_t 1.85 (100%) MS (ESI)⁺: 353.1 [M+H]⁺.

9.2.3 Arylsulfonyl chlorides (40-41)

5-Chloro-2-methylbenzenesulfonyl chloride (40) ⁽²³⁾

(C₇H₆Cl₂O₂S; M.W.= 225.1)



Reagent: 4-chlorotoluene (**38**) (1.0 g, 8.1 mmol);

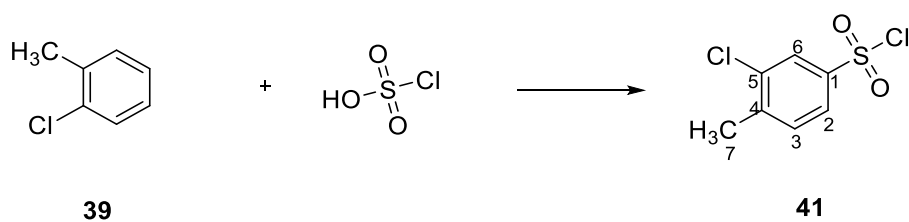
General Procedure 3;

Pink oil;

T.L.C. System: *n*-hexane-EtOAc 8:2 v/v, R_f: 0.52;

Yield: 0.640 g (35%);

¹H-NMR (CDCl₃), δ: 2.58 (s, 3H, CH₃, H-7), 7.39 (d, J= 8.2 Hz, 1H, H-3), 7.52 (dd, J₁= 8.2 Hz, J₂= 2.1 Hz, 1H, H-4), 8.09 (d, J= 2.1 Hz, 1H, H-6).

3-Chloro-4-methylbenzenesulfonyl chloride (41) ⁽²⁴⁾**(C₇H₆Cl₂O₂S; M.W.= 225.1)**Reagent: 2-chlorotoluene (**39**) (1.0 g, 8.1 mmol);

General Procedure 2;

White Solid;

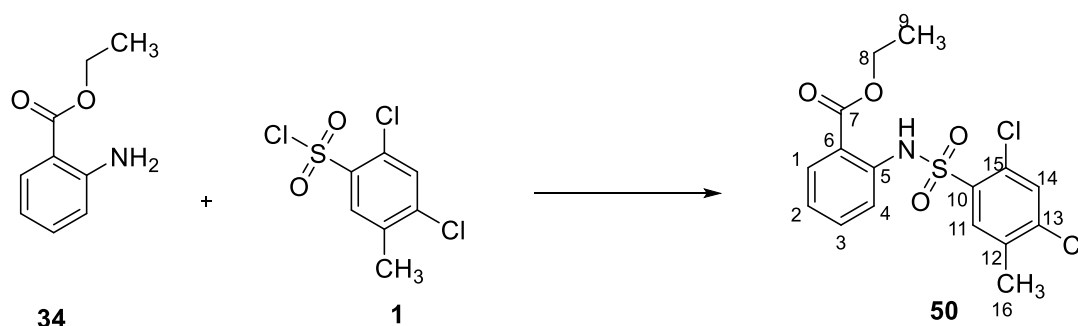
T.L.C. System: *n*-hexane-EtOAcg 8:2 v/v, R_f: 0.57;

Yield: 0.351 g (19%);

¹H-NMR (CDCl₃), δ: 2.43 (s, 3H, CH₃, H-7), 7.51 (d, J= 8.5 Hz, 1H, H-3), 7.73 (dd, J₁= 8.5 Hz, J₂= 2.2 Hz, 1H, H-2), 7.83 (d, J= 2.2 Hz, 1H, H-6).

9.2.4 Alkyl(arylsulfonamido)benzoates (50-57)

Ethyl 2-((2,4-dichloro-5-methylphenyl)sulfonamido)benzoate (50)

(C₁₆H₁₅Cl₂NO₄S; M.W.= 388.26)Reagent: ethyl 2-aminobenzoate (**44**) (0.2 g, 0.77 mmol);Reagent: 2,4-dichloro-5-methylbenzenesulfonyl chloride (**50**) (0.106 g, 0.642 mmol);

General Procedure 4;

Pink solid;

T.L.C. System: *n*-hexane-EtOAc 8:2 v/v, R_f: 0.75;

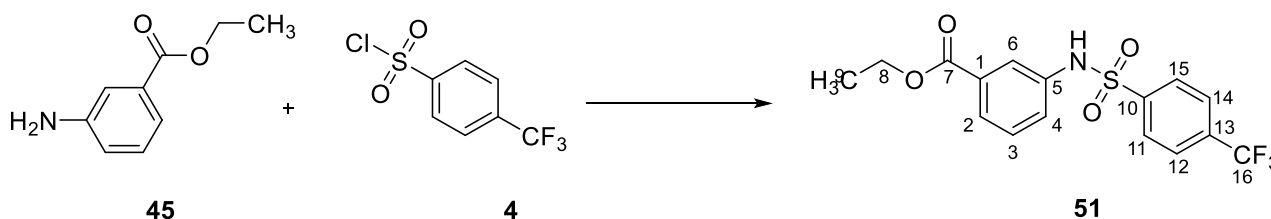
Purification: Recrystallisation from EtOH;

Yield: 0.106 g (43%);

¹H-NMR (DMSO-D₆), δ: 1.33 (t, J= 7.1 Hz, 3H, H-9), 2.39 (s, 3H, H-16), 4.36 (q, J= 7.1 Hz, 2H, H-8), 7.14-7.18 (m, 1H, H-aromatic), 7.40-7.42 (m, 1H, H-aromatic), 7.52-7.56 (m, 1H, H-aromatic), 7.83 (s, 1H, H-aromatic), 7.95 (dd, J₁= 7.0 Hz, J₂= 1.0 Hz, 1H, H-aromatic), 8.19 (s, 1H, H-aromatic), 11.10 (bs, 1H, NH).

¹³C-NMR (DMSO-D₆), δ: 14.3 (CH₃), 19.5 (CH₃), 62.3 (CH₂, C-8), 118.0, 124.0, 131.7, 132.1, 134.1, 134.5 (CH, C-aromatic), 116.7, 129.0, 135.3, 136.7, 138.7, 140.0 (C, C-aromatic), 167.8 (C, C-7) ppm.

UPLC-MS: Rt 2.69 (100%) **MS (ESI):** 386.2 [M-H]⁻.

Ethyl 3-((4-(trifluoromethyl)phenyl)sulfonamido)benzoate (51)**(C₁₆H₁₄F₃NO₄S; M.W.= 373.35)**Reagent: ethyl 3-aminobenzoate (**45**) (0.150 g, 0.91 mmol);Reagent: 4-(trifluoromethyl)benzenesulfonyl chloride (**4**) (0.269 g, 1.1 mmol);

General Procedure 4;

Beige solid;

T.L.C. System: *n*-hexane-EtOAc 8:2 v/v, R_f: 0.3;

Purification: Recrystallisation from EtOH;

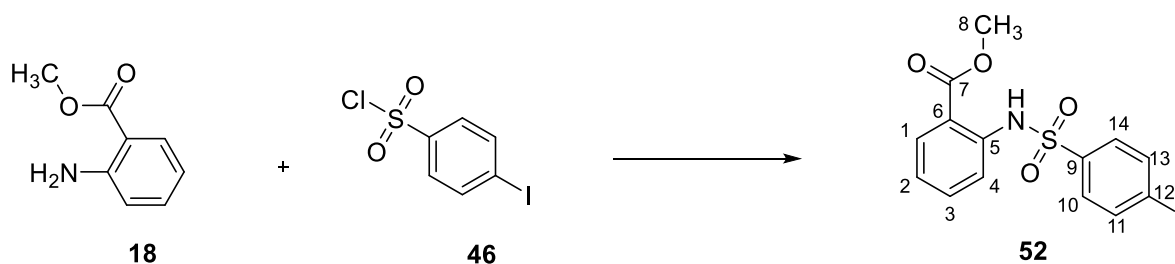
Yield: 0.222 g (65%);

¹H-NMR (DMSO-D₆), δ: 1.29 (t, J= 7,1 Hz, 3H, H-9), 4.28 (q, J= 7.1Hz, 2H, H-8), 7.37-7.44, (m, 2H, H-aromatic), 7.64-7.67 (m, 1H, H-aromatic), 7.69-7.70 (m, 1H, H-aromatic), 7.95-7.99 (m, 4H, H-aromatic), 10.77 (bs, 1H, NH).

¹³C-NMR (DMSO-D₆), δ: 14.5 (CH₃, C-9), 61.4 (CH₂, C-8), 121.1, 125.3, 125.6, 127.16, 127.18, 128.1 (CH, C-aromatic), 130.3, 131.4, 133.0, 138.0, 143.5 (C, C-aromatic), 165.5 (C, C-7).

¹⁹F-NMR (DMSO-D₆), δ: -61.72 (s, 3F).

UPLC-MS: Rt 2.26 (100%) **MS (ESI)⁻:** 372.1 [M-H]⁻.

Methyl 2-((4-iodophenyl)sulfonamido)benzoate (52)**(C₁₄H₁₂INO₄S; M.W.= 417.22)**Reagent: methyl 3-aminobenzoate (**18**) (0.360 g, 1.19 mmol);Reagent: 4-iodobenzenesulfonyl chloride (**46**) (0.150 g, 0.99 mmol);

General Procedure 4;

Beige solid;

T.L.C. System: *n*-hexane-EtOAc 8:2 v/v, R_f: 0.55;

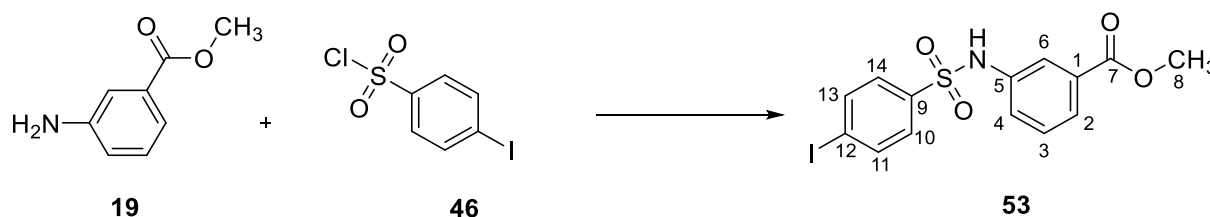
Purification: Recrystallisation from EtOH;

Yield: 0.104 g (25%);

¹H-NMR (DMSO-D₆), δ: 3.81 (s, 3H, H-8), 7.20-7.24 (m, 1H, H-aromatic), 7.42-7.44 (m, 1H, H-aromatic), 7.53 (d, J= 8.6 Hz, 2H, H-aromatic), 7.68-7.60 (m, 1H, H-aromatic), 7.85 (dd, J₁= 6.5 Hz, J₂= 1.5 Hz, 1H, H-aromatic), 7.95 (d, J= 8.6 Hz, 2H, H-aromatic), 10.41 (bs, 1H, NH).

¹³C-NMR (DMSO-D₆), δ: 53.1 (CH₃, C-8), 121.2, 124.9, 128.9, 131.5, 134.8, 138.8 (CH, C-aromatic), 102.4, 119.4, 138.3, 138.9 (C, C-aromatic), 167.8 (C, C-7).

UPLC-MS: Rt 2.39 (100%) MS (ESI)⁺: 418.1 [M+H]⁺.

Methyl 3-((4-iodophenyl)sulfonamido)benzoate (53)**(C₁₄H₁₂INO₄S; M.W.= 417.22)**Reagent: methyl 2-aminobenzoate (**19**) (0.062 g, 0.41 mmol);Reagent: 4-iodobenzenesulfonyl chloride (**46**) (0.150 g, 0.50 mmol);

General Procedure 4;

White solid;

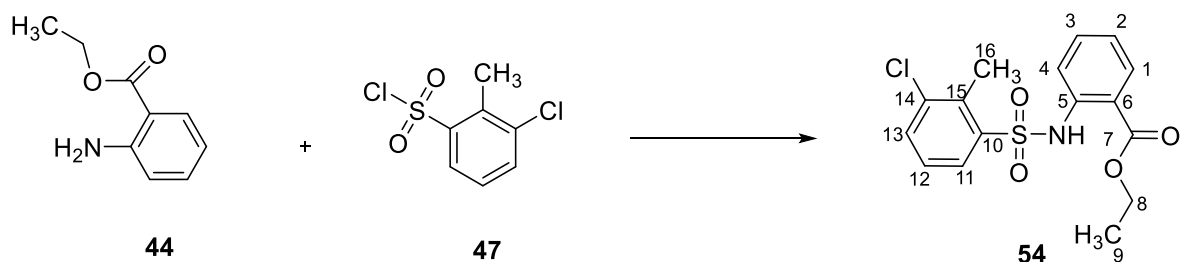
T.L.C. System: *n*-hexane-EtOAc 8:2 v/v, R_f: 0.44;Purification: Biotage Isolera One automated flash column chromatography (cartridge: SNAP KP SIL 25g, *n*-hexane-EtOAc 100:0 increasing to *n*-hexane-EtOAc 60:40 in 10CV);

Yield: 0.02 g (12%);

¹H-NMR (CDCl₃), δ: 3.84 (s, 3H, H-8), 6.79 (bs, 1H, NH), 7.27-7.30 (m, 1H, H-aromatic), 7.31-7.33 (m, 1H, H-aromatic), 7.40 (d, J= 8.5 Hz, 2H, H-aromatic), 7.61-7.62 (m, 1H, H-aromatic), 7.72 (d, J= 8.5 Hz 2H, H-aromatic), 7.73-7.75 (m, 1H, H-aromatic).

¹³C-NMR (CDCl₃), δ: 52.5 (CH₃, C-8), 125.7, 126.7, 128.5, 128.8, 129.6, 138.4 (CH, C-aromatic), 100.9, 131.5, 136.5, 138.5 (C, C-aromatic), 166.2 (C, C-7).

UPLC-MS: Rt 2.16 (>99%) MS (ESI)⁺: 418.1 [M+H]⁺.

Ethyl 2-((3-chloro-2-methylphenyl)sulfonamido)benzoate (**54**)(C₁₆H₁₆ClNO₄S; M.W.= 353.82)Reagent: ethyl 2-aminobenzoate (**44**) (0.150 g, 0.66 mmol);Reagent: 3-chloro-2-methylbenzenesulfonyl chloride (**47**) (0.092 g, 0.55 mmol);

General Procedure 4;

White solid;

T.L.C. System: *n*-hexane-EtOAc 8:2 v/v, R_f: 0.58;Purification1: Biotage Isolera One automated flash column chromatography (cartridge: SNAP KP SIL 25g, *n*-hexane-EtOAc 100:0 increasing to *n*-hexane-EtOAc 60:40 in 10CV);

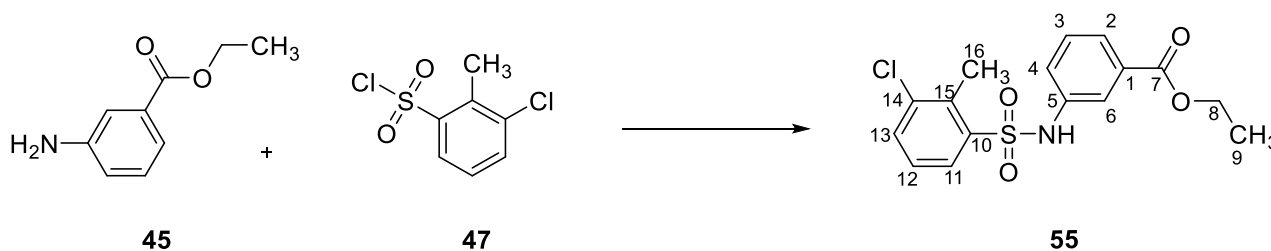
Purification2: Recrystallisation from EtOH

Yield: 0.076 g (40%);

¹H-NMR (DMSO-D₆), δ: 1.31 (t, J = 7.1 Hz, 3H, H-9), 2.60 (s, 3H, H-16), 4.32 (q, J = 7.1 Hz, 2H, H-8), 7.16-7.20 (m, 1H, H-aromatic), 7.35-7.37 (m, 1H, H-aromatic), 7.41-7.45 (m, 1H, H-aromatic), 7.52-7.56 (m, 1H, H-aromatic), 7.75-7.77 (m, 1H, H-aromatic), 7.90 (dd, J₁ = 6.8 Hz, J₂ = 1.1 Hz, 1H, H-aromatic), 7.95-7.97 (m, 1H, H-aromatic), 10.82 (bs, 1H, NH).

¹³C-NMR (DMSO-D₆), δ: 14.3 (CH₃), 16.8 (CH₃), 62.1 (CH₂, C-8), 119.6, 124.3, 128.1, 129.2, 131.5, 134.8, 134.9 (CH, C-aromatic), 117.9, 136.5, 136.6, 138.8, 139.5 (C, C-aromatic), 167.7 (C, C-7).

UPLC-MS: Rt 2.57 (>95%) **MS (ESI)⁺:** 354.8 [M+H]⁺.

Ethyl 3-((3-chloro-2-methylphenyl)sulfonamido)benzoate (55)**(C₁₆H₁₆ClNO₄S; M.W.= 353.82)**Reagent: ethyl 3-aminobenzoate (**45**) (0.150 g, 0.66 mmol);Reagent: 3-chloro-2-methylbenzenesulfonyl chloride (**47**) (0.092 g, 0.55 mmol);

General Procedure 4;

Pink solid;

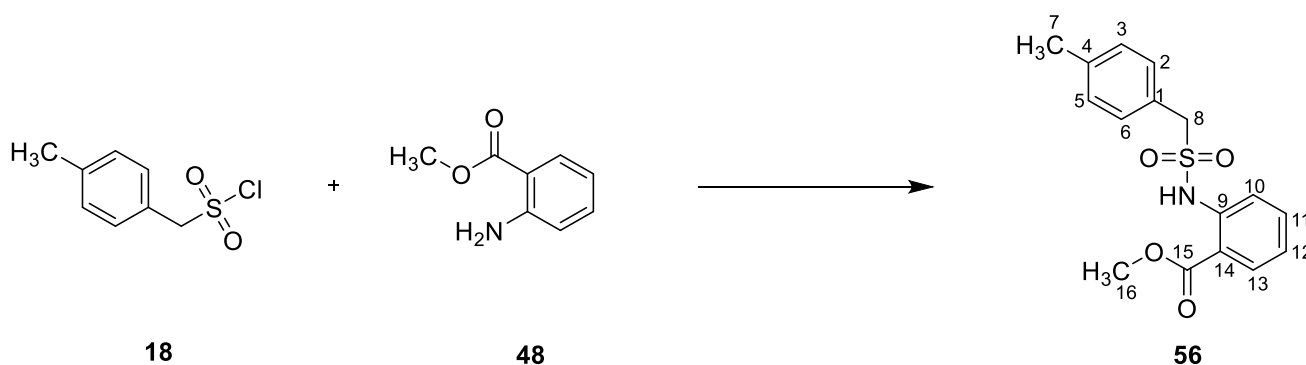
T.L.C. System: *n*-hexane-EtOAc 8:2 v/v, R_f: 0.38;Purification: Biotage Isolera One automated flash column chromatography (cartridge: SNAP KP SIL 25g, *n*-hexane-EtOAc 60:40 increasing to *n*-hexane-EtOAc 60:40 in 10CV);

Yield: 0.161 g (82%);

¹H-NMR (CDCl₃), δ: 1.30 (t, J = 7.1 Hz, 3H, H-9), 2.65 (s, 3H, H-16), 4.29 (q, J = 7.1 Hz, 2H, H-8), 6.99 (bs, 1H, NH), 7.14-7.17 (m, 1H, H-aromatic), 7.22-7.26 (m, 2H, H-aromatic), 7.49 (dd, J₁ = 7.0 Hz, J₂ = 1.1 Hz, 1H, H-aromatic), 7.60-7.61 (m, 1H, H-aromatic), 7.67-7.71 (m, 1H, H-aromatic), 7.88 (dd, J₁ = 6.8 Hz, J₂ = 1.1 Hz, 1H, H-aromatic).

¹³C-NMR (CDCl₃), δ: 14.2 (CH₃), 16.9 (CH₃), 61.5 (CH₂), 121.2, 124.2, 125.9, 126.6, 128.7, 131.7, 134.2 (CH, C-aromatic), 129.5, 135.2, 136.6, 137.2, 139.3 (C, C-aromatic), 165.9 (C, C-7).

UPLC-MS: Rt 2.27 (>99%) MS (ESI)⁺: 354.2 [M+H]⁺.

Methyl 2-((p-tolylmethyl)sulfonamido)benzoate (56)**(C₁₆H₁₇NO₄S; M.W.= 319.38)**

Reagent: p-tolylmethanesulfonyl chloride (**48**) (0.200 g, 0.97 mmol);

Reagent: methyl 2-aminobenzoate (**18**) (0.070 g, 0.44 mmol);

General Procedure 4;

White Solid;

T.L.C. System: *n*-hexane:EtOAc 8:2 v/v, R_f: 0.46;

Purification1: Biotage Isolera One automated flash column chromatography (cartridge: ZIP KP SIL 10g, *n*-hexane-EtOAc 100:0 increasing to *n*-hexane-EtOAc 60:40 in 15CV);

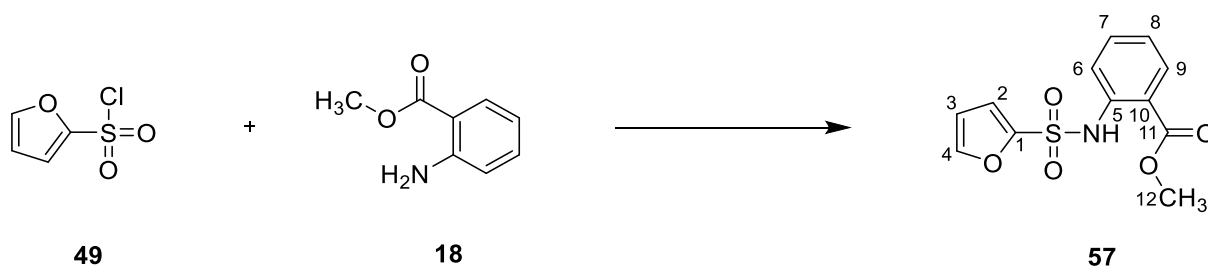
Purification 2: Biotage Isolera One automated flash column chromatography (cartridge: ZIP KP SIL 5g, *n*-hexane-DCM 100:0 increasing to *n*-hexane-DCM 0:100 in 15CV);

Yield: 0.019 g (15%);

¹H-NMR (CDCl₃), δ: 2.34 (s, 3H, H-7), 3.85 (s, 3H, H-16), 4.37 (s, 2H, H-8), 7.06-7.14 (m, 5H, H-aromatic), 7.50-7.53 (m, 1H, H-aromatic), 7.73-7.75 (m, 1H, H-aromatic), 8.02 (dd, J₁= 7.9 Hz, J₂= 1.6 Hz, 1H, H-aromatic), 10.28 (bs, 1H, NH).

¹³C-NMR (CDCl₃), δ: 21.1 (CH₃, C-7), 52.4 (CH₃, C-16), 58.0 (CH₂, C-8), 118.0, 122.6, 129.4, 130.5, 131.3, 134.7 (CH, C-aromatic), 115.4, 125.1, 138.7, 141.0 (C-aromatic), 167.9 (C, C-15).

UPLC-MS: Rt 2.30 (100%) MS (ESI)⁻: 318.0 [M-H]⁻.

Methyl 2-(furan-2-sulfonamido)benzoate (57)**(C₁₂H₁₁NO₅S; M.W.= 281.28)**Reagent: furan-2-sulfonyl chloride (**49**) (0.250 g, 1.80 mmol);Reagent: methyl 2-aminobenzoate (**18**) (0.226 g, 1.5 mmol);

General Procedure 4;

Pink solid;

T.L.C. System: *n*-hexane-EtOAc 8:2 v/v, R_f: 0.3;

Purification: Recrystallisation from EtOH;

Yield: 0.280 g (57%);

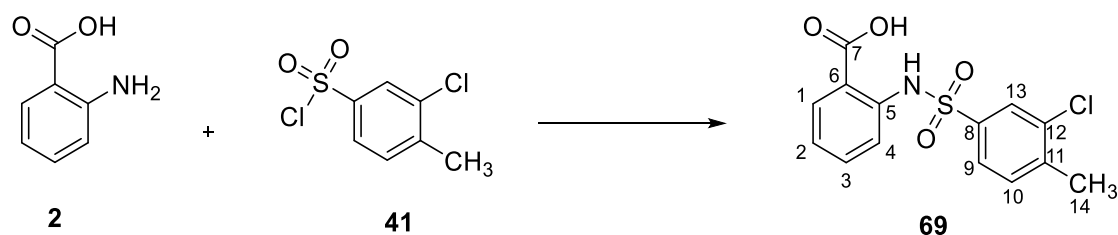
¹H-NMR (DMSO-D₆), δ: 3.84 (s, 3H, H-12), 6.65 (dd, J₁= 3.5 Hz, J₂= 1.7 Hz, 1H, H-aromatic), 7.24-7.27 (m, 2H, H-aromatic), 7.49 (dd, J₁= 8.2 Hz, J₂= 0.6 Hz, 1H, H-aromatic), 7.60-7.63 (m, 1H, H-aromatic), 7.89 (dd, J₁= 7.8, J₂= 1.3 Hz, 1H, H-aromatic), 7.96-7.98 (m, 1H, H-aromatic), 10.62 (bs, 1H, NH).

¹³C-NMR (DMSO-D₆), δ: 53.1 (CH₃, C-12), 112.2, 118.6, 121.3, 125.0, 131.4, 134.7, 148.6 (CH, C-aromatic), 119.6, 137.9, 147.1 (C-aromatic), 167.9 (C, C- 11).

UPLC-MS: Rt 2.10 (100%) MS (ESI)⁺: 282.0 [M+H]⁺.

9.2.5 Arylsulfonamido benzoic acids (69-70)

2-((3-Chloro-4-methylphenyl)sulfonamido)benzoic acid (69)

(C₁₄H₁₂ClNO₄S; M.W.= 325.76)Reagent: 2-aminobenzoic acid (**2**) (0.150 g, 1.11 mmol);Reagent: 3-chloro-4-methylbenzenesulfonyl chloride (**41**) (0.300 g, 1.33 mmol);

General Procedure 5;

Brown solid;

T.L.C. System: DCM-MeOH 9:1 v/v, R_f: 0.28;

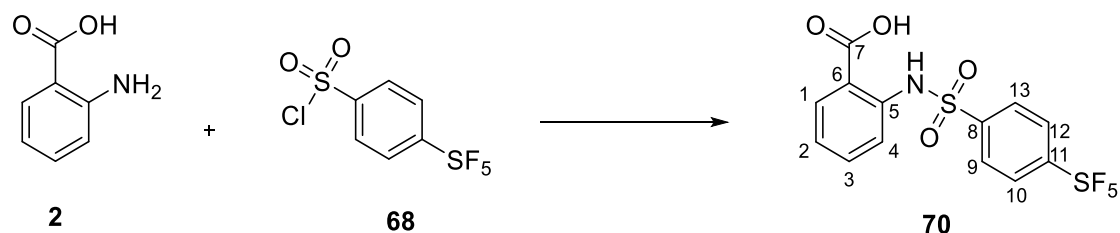
Purification: Biotage Isolera One automated flash column chromatography (cartridge: SNAP KP SIL 25g, DCM-MeOH 100:0 increasing to DCM-MeOH 80:20 in 15CV);

Yield: 0.220 g (61%);

¹H-NMR (DMSO-D₆), δ: 2.34 (s, 3H, H-14), 6.79-6.82 (m, 1H, H-aromatic), 7.19-7.23 (m, 1H, H-aromatic), 7.30 (d, J= 7.9 Hz, 1H, H-aromatic), 7.51 (d, J= 7.9 Hz, 1H, H-aromatic), 7.55-7.57 (m, 1H, H-aromatic), 7.73-7.74 (m, 1H, H-aromatic), 7.84-7.86 (m, 1H, H-aromatic), 11.07 (bs, 1H, NH), 13.11 (bs, 1H, OH).

¹³C-NMR (DMSO-D₆), δ: 14.5 (CH₃, C-14), 117.4, 120.2, 125.9, 129.3, 129.8, 131.3, 132.2 (CH, C-aromatic), 121.8, 136.8, 137.0, 141.7, 144.9 (C, C-aromatic), 170.0 (C, C-7) ppm.

UPLC-MS: Rt 2.18 (>96%) MS (ESI)⁺: 326.1 [M+H]⁺.

2-((4-(Pentafluorosulfonyl)phenyl)sulfonamido)benzoic acid (**70**)(C₁₃H₁₀F₅NO₄S₂; M.W.= 403.34)Reagent: 2-aminobenzoic acid (**2**) (0.057 g, 0.41 mmol);Reagent: 4-(pentafluorosulfonyl)benzenesulfonyl chloride (**68**) (0.150 g, 0.49 mmol);

General Procedure 5;

Brown solid;

T.L.C. System: *n*-hexane-EtOAc 2:8 v/v, R_f: 0.58;

Yield: 0.066 g (40%);

¹H-NMR (DMSO-D₆), δ: 7.17-7.21 (m, 1H, H-aromatic), 7.47-7.50 (m, 1H, H-aromatic), 7.56-7.60 (m, 1H, H-aromatic), 7.92 (dd, J₁= 7.9 Hz, J₂= 1.6 Hz, 1H, H-aromatic), 8.04 (d, J= 8.8 Hz, 2H, H-aromatic), 8.13 (d, 8.8 Hz, 2H, H-aromatic), 11.30 (bs, 1H, NH), 13.88 (bs, 1H, OH).

¹³C-NMR (DMSO-D₆), δ: 119.6, 124.5, 127.8, 128.7, 132.0, 134.9 (CH, C-aromatic), 118.3, 139.3, 142.9, 156.0 (C, C-aromatic), 169.9 (C, C-7).

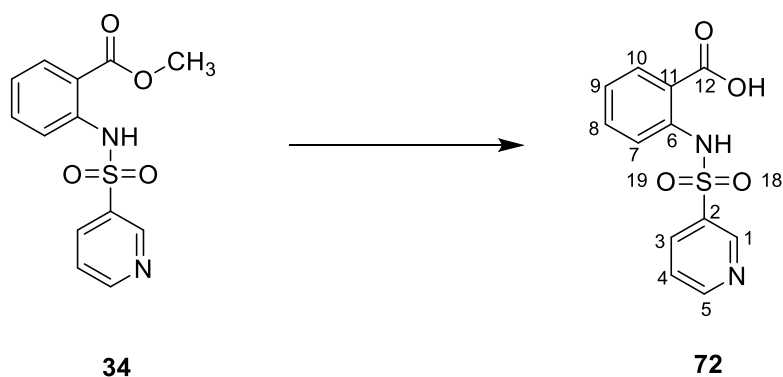
¹⁹F-NMR (DMSO-D₆), δ: 63.34 (d, J=151.6 Hz, 4F), 84.64 (m, 1F).

UPLC-MS: Rt 2.24 (>96%) MS (ESI)⁻: 402.1 [M-H]⁻.

9.2.6 Arylsulfonamido benzoic acid (72-76)

2-(Pyridine-3-sulfonamido)benzoic acid (72)

(C₁₂H₁₀N₂O₄S; M.W.= 278.28)



Reagent: methyl 2-(pyridine-3-sulfonamido)benzoate (**34**) (0.1 g, 0.34 mmol);

General Procedure 6;

Off-White Solid;

T.L.C. System: *n*-hexane-EtOAc 6:4 v/v, R_f: 0.20;

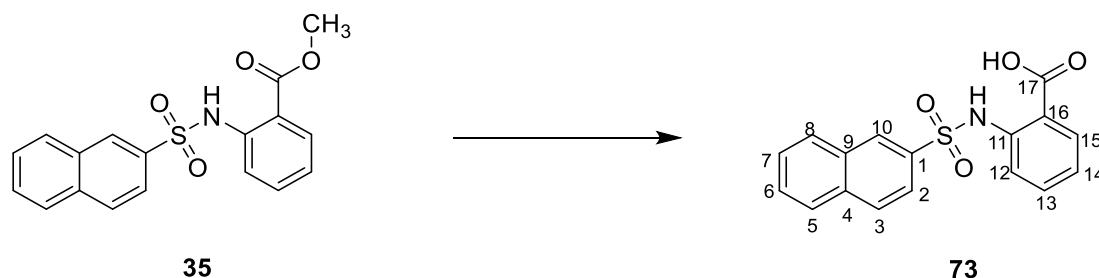
Purification: Recrystallisation from EtOH/Water;

Yield: 0.030 g (30%);

¹H-NMR (DMSO-D₆), δ: 7.17-7.20 (m, 1H, H-aromatic), 7.52-7.54 (m, 1H, H-aromatic), 7.57-7.59 (m, 1H, H-aromatic), 7.60-7.62 (m, 1H, H-aromatic), 7.90 (dd, J₁= 7.9 Hz, J₂= 1.5 Hz, 1H, H-aromatic), 8.19-8.22 (m, 1H, H-aromatic), 8.80-8.82 (m, 1H, H-aromatic), 8.95-8.97 (m, 1H, H-aromatic), 11.23 (bs, 1H, NH), 13.60 (bs, 1H, OH).

¹³C-NMR (DMSO-D₆), δ: 119.8, 124.4, 124.9, 132.0, 134.9, 135.4, 147.7, 154.4 (CH, C-aromatic), 118.3, 125.6, 135.6 (C, C-aromatic), 169.93(C, C- 12).

UPLC-MS: Rt 1.66 (99%) **MS (ESI)⁺:** 278.9 [M+H]⁺.

2-(Naphthalene-2-sulfonamido)benzoic acid (73)**(C₁₇H₁₃NO₄S; M.W.= 327.35)**

Reagent: methyl 2-(naphthalene-2-sulfonamido)benzoate (**35**) (0.080 g, 0.23 mmol);

General Procedure 6;

White Solid;

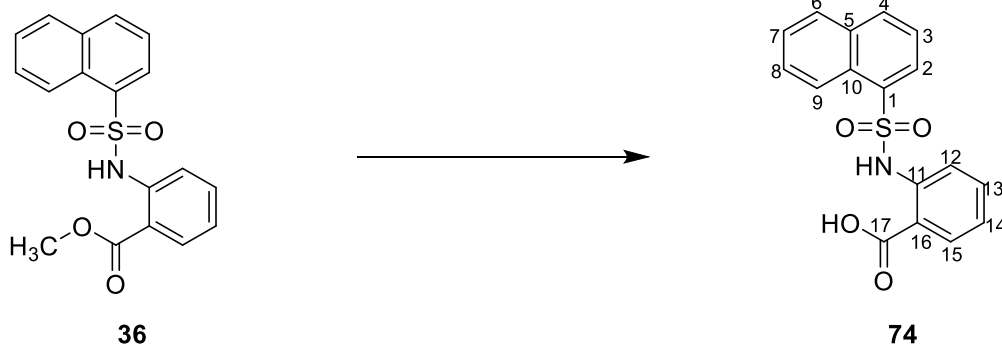
T.L.C. System: *n*-hexane-EtOAc 7:3 v/v, R_f: 0.20;

Yield: 0.051 g (68%);

¹H-NMR (DMSO-D₆), δ: 7.07-7.11 (m, 1H, H-aromatic), 7.51-7.55 (m, 1H, H-aromatic), 7.57-7.59 (m, 1H, H-aromatic), 7.66-7.69 (m, 1H, H-aromatic), 7.70-7.74 (m, 1H, H-aromatic), 7.76-7.79 (m, 1H, H-aromatic) 7.87 (d, J= 8.0 Hz, 1H, H-aromatic), 8.01 (d, J= 8.0 Hz, 1H, H-aromatic), 8.09 (d, J= 8.7 Hz, 1H, H-aromatic), 8.17 (d, J= 8.2 Hz, 1H, H-aromatic), 8.60 (s, 1H, H-10), 11.28 (bs, 1H, NH), 14.00 (bs, 1H, OH).

¹³C-NMR (DMSO-D₆), δ: 118.8, 122.2, 123.8, 128.30, 128.34, 129.0, 129.81, 129.85, 130.2, 131.9, 134.9 (CH, C-aromatic), 117.1, 132.0, 134.9, 136.0, 140.2 (C, C-aromatic), 170.2 (C, C-17).

UPLC-MS: Rt 2.12 (100%) MS (ESI)⁺: 328.1 [M+H]⁺.

2-(Naphthalene-1-sulfonamido)benzoic acid (74)**(C₁₇H₁₃NO₄S; M.W.= 327.35)**

Reagent: methyl 2-(naphthalene-1-sulfonamido)benzoate (**36**) (0.070 g, 0.2 mmol);

General Procedure 6;

Yellow Solid;

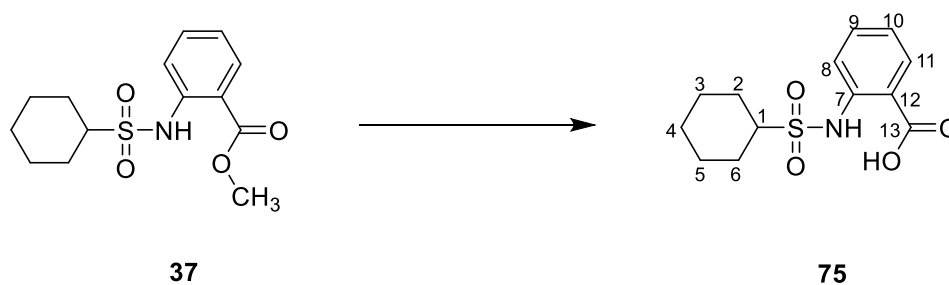
T.L.C. System: *n*-hexane-EtOA: 6:4 v/v, R_f: 0.10;

Yield: 0.059 g (90%);

¹H-NMR (DMSO-D₆), δ: 7.04-7.09 (m, 2H, H-aromatic), 7.48-7.53 (m, 2H, H-aromatic), 7.69-7.74 (m, 1H, H-aromatic), 7.76-7.80 (m, 1H, H-aromatic), 7.86 (d, J= 7.8 Hz, 1H, H-aromatic), 8.14 (d, J= 8.1 Hz, 1H, H-aromatic), 8.31 (d, J= 7.8 Hz, 1H, H-aromatic), 8.40 (d, J= 7.2 Hz, 1H, H-aromatic), 8.59 (d, J= 8.6 Hz, 1H, H-aromatic), 11.82 (bs, 1H, NH), 14.20 (bs, 1H, OH).

¹³C-NMR (DMSO-D₆), δ: 117.5, 123.2, 123.8, 124.9, 127.4, 127.6, 128.9, 131.0, 131.9, 134.9, 135.59 (CH, C-aromatic), 116.1, 129.8, 134.2, 140.5, 142.0 (C, C-aromatic), 170.3 (C, C-17).

UPLC-MS: Rt 2.09 (100%) **MS (ESI)⁺:** 328.1 [M+H]⁺.

2-(Cyclohexanesulfonamido)benzoic acid (75)**(C₁₃H₁₇NO₄S; M.W.= 283.34)**Reagent: methyl 2-(cyclohexanesulfonamido)benzoate (**37**) (0.050 g, 0.16 mmol);

General Procedure 6;

White Solid;

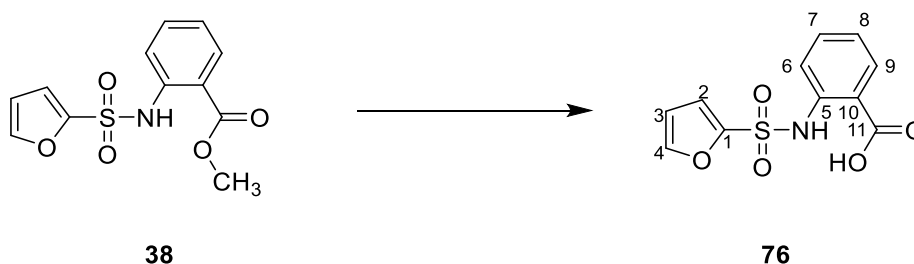
T.L.C. System: *n*-hexane-EtOAc 7:3 v/v, R_f: 0.20;Purification: Recrystallisation from DCM/*n*-hexane;

Yield: 0.011 g (26%)

¹H-NMR (DMSO-D₆), δ: 1.08-1.14 (m, 1H, H-cyclohexane), 1.17-1.26 (m, 2H, H-cyclohexane), 1.38-1.49 (m, 2H, H-cyclohexane), 1.53-1.60 (m, 1H, H-cyclohexane), 1.74-1.77 (m, 2H, H-cyclohexane), 1.97-2.00 (m, 2H, H-cyclohexane), 3.19-3.25 (m, 1H, H-1), 7.13-7.17 (m, 1H, H-aromatic), 7.58-7.62 (m, 1H, H-aromatic), 7.64 (dd, J₁= 8.3 Hz, J₂= 0.9 Hz, 1H, H-aromatic), 8.01 (dd, J₁= 7.9 Hz, J₂= 1.4 Hz, 1H, H-aromatic), 11.01 (bs, 1H, NH).

¹³C-NMR (DMSO-D₆), δ: 26.4, 25.0, 26.28(CH₂, C-cyclohexane), 60.0 (CH, C-1), 117.8, 122.8, 132.1, 135.0 (CH, C-aromatic), 132.2, 141.5 (C, C-aromatic), 170.5 (C, C-13).

UPLC-MS: Rt 2.04 (>99%) MS (ESI)⁻: 282.1 [M-H]⁻.

2-(Furan-2-sulfonamido)benzoic acid (76)**(C₁₁H₉NO₅S; M.W.= 267.02)**

Reagent: methyl 2-(furan-2-sulfonamido) benzoate (**38**) (0.150 g, 0.53 mmol);

General Procedure 6;

White Solid;

T.L.C. System: *n*-hexane-EtOAc 6:4 v/v, R_f: 0.10;

Purification: Recrystallisation from EtOH/Water;

Yield: 0.045 g (32%);

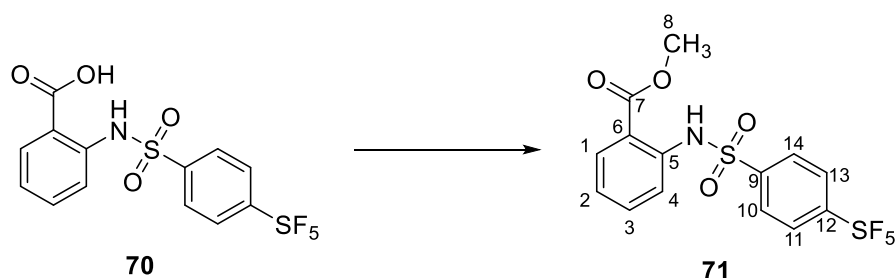
¹H-NMR (DMSO-D₆), δ: 6.66-6.68 (m, 1H, H-aromatic), 7.17-7.20 (m, 1H, H-aromatic), 7.35 (dd, J₁= 7.3 Hz, J₂= 0.6 Hz, 1H, H-aromatic), 7.52-7.54 (m, 1H, H-aromatic), 7.58-7.62 (m, 1H, H-aromatic) 7.94-7.97 (m, 2H, H-aromatic), 11.44 (bs, 1H, NH), 13.89 (bs, 1H, OH).

¹³C-NMR (DMSO-D₆), δ: 112.2, 118.6, 119.0, 124.8, 131.9, 135.0, 148.7 (CH, C-aromatic), 117.4, 139.5, 146.8 (C, C-aromatic), 170.2 (C, C-11).

UPLC-MS: Rt 1.81 (100%) MS (ESI): 266.0 [M-H]⁻.

9.2.7 Aryl(alkyl)esters (71, 77, 79)

Methyl 2-((4-(pentafluorosulfanyl)phenyl)sulfonamido)benzoate (71)

(C₁₄H₁₂F₅NO₄S₂; M.W.= 417.07)

Reagent: 2-((4-(pentafluorosulfanyl)phenyl)sulfonamido)benzoic acid (**70**) (0.050 g, 0.12 mmol);

General Procedure 7;

White solid;

T.L.C. System: *n*-hexane-EtOAc 7:3 v/v, R_f: 0.67;

Purification: Biotage Isolera One automated flash column chromatography (cartridge: SNAP KP SIL 10g, *n*-hexane-EtOAc 100:0 increasing to *n*-hexane-EtOAc 60:40 in 10CV);

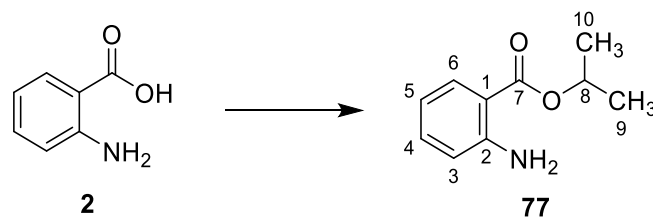
Yield: 0.022 g (43%);

¹H-NMR (DMSO-D₆), δ: 3.74 (s, 3H, H-8), 7.25-7.29 (m, 1H, H-aromatic), 7.41-7.44 (m, 1H, H-aromatic), 7.58-7.62 (m, 1H, H-aromatic), 7.81-7.83 (dd, J₁= 7.9 Hz, J₂= 1.3 Hz, 1H, H-aromatic), 7.96 (d, J=8.6 Hz, 2H, H-aromatic), 8.13 (d, J=8.6 Hz, 2H, H-aromatic), 10.48 (bs, 1H, NH).

¹³C-NMR (DMSO-D₆), δ: 52.9 (CH₃, C-8), 122.8, 125.6, 127.72, 127.75, 128.6, 131.4 (CH, C-aromatic), 121.2, 137.4, 143.1, 155.8 (C, C-aromatic), 167.4 (C, C-7).

¹⁹F-NMR (DMSO-D₆), δ: +63.35 (d, J=151.6 Hz, 4F), + 84.78 (m, 1F) ppm.

UPLC-MS: Rt 2.45 (>97%) MS (ESI)⁻: 416.1 [M-H]⁻.

Isopropyl 2-aminobenzoate (77) ⁽²⁵⁾**(C₁₃H₁₀NO₂; M.W.= 179.22)**Reagent: 2-aminobenzoic acid (**2**) (1.500 g, 10.93 mmol);

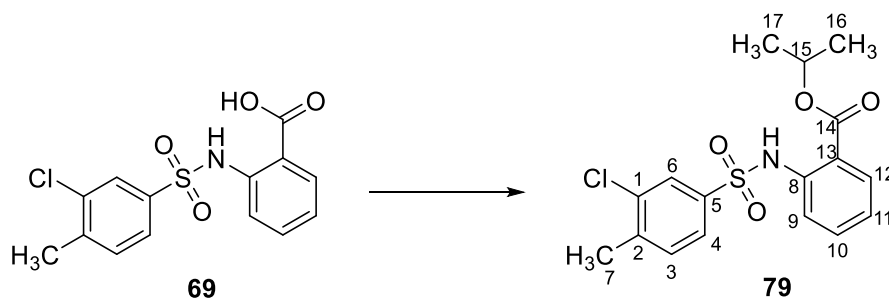
General Procedure 7;

Yellow oil;

T.L.C. System: *n*-hexane-EtOAc 8:2 v/v, R_f: 0.5;Purification: Flash column chromatography (*n*-hexane:EtOAc 100:0 v/v increasing to *n*-hexane:EtOAc 9:1 v/v);

Yield: 0.374 g (19%);

¹H-NMR (CDCl₃), δ: 1.28 (d, J= 6.2 Hz, 6H, H-9,10), 5.14 (m, 1H, H-8), 5.63 (bs, 2H, NH₂), 6.54-5.58 (m, 2H, H-aromatic), 7.15-7.19 (m, 1H, H-aromatic), 7.79 (dd, J₁= 7.8 Hz, J₂= 1.5 Hz, 1H, H-aromatic).**¹³C-NMR (CDCl₃), δ:** 22.0 (2xCH₃, C-9,10), 67.6 (CH, C-8), 116.2, 116.6, 131.2, 133.8 (CH, C-aromatic), 111.5, 150.4 (C, C-aromatic), 167.7 (C, C-7).

Isopropyl 2-((3-chloro-4-methylphenyl)sulfonamido)benzoate (**79**)(C₁₇H₁₈ClNO₄S; M.W.= 367.84)Reagent: 2-((3-chloro-4-methylphenyl)sulfonamido)benzoic acid (**69**) (0.1 g, 0.30 mmol);

General Procedure 7;

Colourless oil;

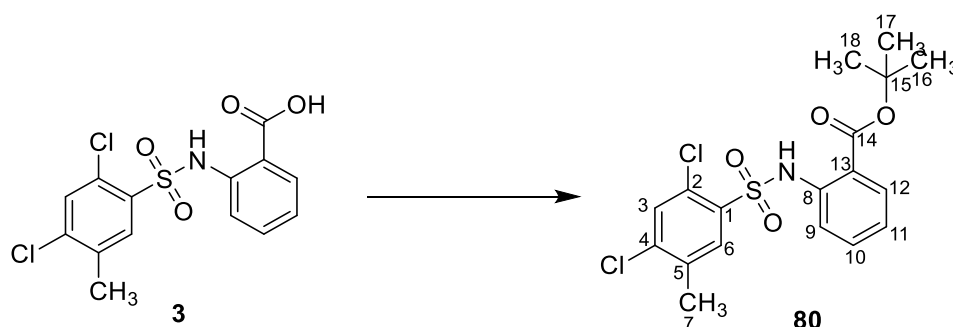
T.L.C. System: *n*-hexane-EtOAc 7:3 v/v, R_f: 0.67;Purification1: Biotage Isolera One automated flash column chromatography (cartridge: ZIP KP SIL 10g, *n*-hexane-EtOAc 100:0 increasing to *n*-hexane-EtOAc 70:30 in 10CV);Purification2: Biotage Isolera One automated flash column chromatography (cartridge: ZIP KP SIL 10g, *n*-hexane-EtOAc increasing to *n*-hexane-EtOAc 70:30 in 20CV);

Yield: 0.024 g (22%);

¹H-NMR (CDCl₃), δ: 1.26 (d, J= 6.2 Hz, 6H, H-16,17), 2.30 (s, 3H, H-7), 5.11-5.14 (m, 1H, H-15), 6.97-7.00 (m, 1H, H-aromatic), 7.17-7.19 (m, 1H, H-aromatic), 7.37-7.41 (m, 1H, H-aromatic), 7.52 (dd, J₁= 7.8 Hz, J₂= 1.9 Hz, 1H, H-aromatic), 7.59 (dd, J₁= 8.3 Hz, J₂= 1.0 Hz, 1H, H-aromatic), 7.74-7.76 (m, 1H, H-aromatic), 7.85 (m, 1H, H-aromatic), 10.68 (bs, 1H, NH) ppm.

¹³C-NMR (CDCl₃), δ: 20.2 (CH₃, C-7), 21.7 (2xCH₃, C-16,17), 69.5 (CH, C-15), 119.4, 123.2, 125.3, 127.7, 131.1, 131.3, 134.3 (CH, C-aromatic), 116.9, 135.1, 138.3, 140.1, 141.8 (C, C-aromatic), 167.3 (C, C-14).

UPLC-MS: Rt 2.77 (100%) MS (ESI)⁺: 368.8 [M+H]⁺.

9.2.8: *Tert*-Butyl(arylsulfonamido) benzoate (80-81)*Tert*-Butyl 2-((2,4-dichloro-5-methylphenyl)sulfonamido)benzoate (80)(C₁₈H₁₉Cl₂NO₄S; M.W.= 416.31)

Reagent: 2-((2,4-dichloro-5-methylphenyl)sulfonamido)benzoic acid (**3**) (0.150 g, 0.416 mmol);

General Procedure 8;

Yellow solid;

T.L.C. System: *n*-hexane-EtOAc 5:5 v/v, R_f: 0.72;

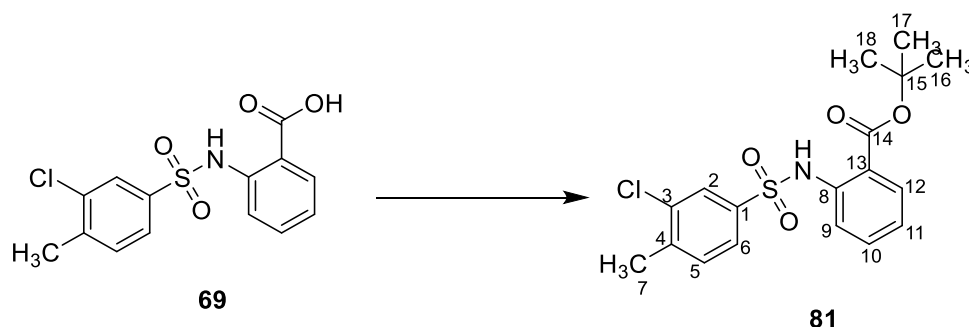
Purification: Biotage Isolera One automated flash column chromatography (cartridge: SNAP KP SIL 25g, *n*-hexane-EtOAc 100:0 increasing to *n*-hexane-EtOAc 60:40 in 15CV);

Yield: 0.035 g (20%);

¹H-NMR (CDCl₃), δ: 1.32 (s, 9H, H-16,17,18), 2.32 (s, 3H, H-7), 6.90-6.93 (m, 1H, H-aromatic), 7.26-7.30 (m, 1H, H-aromatic), 7.34 (s, 1H, H-6), 7.44 (dd, J₁= 7.3 Hz, J₂= 1.1 Hz, 1H, H-aromatic), 7.82 (dd, J₁= 6.3 Hz, J₂= 1.6 Hz, 1H, H-aromatic), 7.98 (s, 1H, H-3), 11.32 (bs, 1H, NH).

¹³C-NMR (CDCl₃), δ: 19.6 (CH₃, C-7), 28.1 (3xCH₃, C-16,17,18), 117.0, 122.4, 131.5, 131.8, 133.6, 133.9 (CH, C-aromatic), 83.0 (C, C-15), 129.8, 134.9, 134.5, 135.5, 139.5, 139.9 (C, C-aromatic), 167.0 (C, C-14).

UPLC-MS: Rt 2.38 (>97%) MS (ESI)⁻: 414.1 [M-H]⁻.

Tert-Butyl 2-((3-chloro-4-methylphenyl)sulfonamido)benzoate (81)**(C₁₈H₂₀ClNO₄S; M.W.= 381.87)**

Reagent: 2-((3-chloro-4-methylphenyl)sulfonamido)benzoic acid (**69**) (0.100 g, 0.30 mmol);

General Procedure 8;

White solid;

T.L.C. System: *n*-hexane-EtOAc 7:3 v/v, R_f: 0.57;

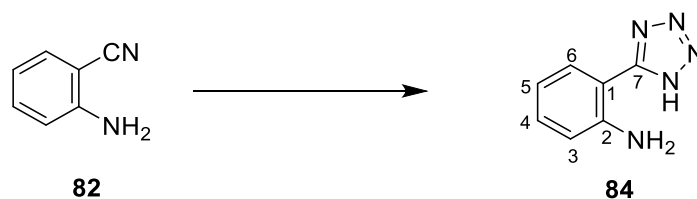
Purification: Biotage Isolera One automated flash column chromatography (cartridge: ZIP KP SIL 10g, *n*-hexane-EtOAc 100:0 increasing to *n*-hexane-EtOAc 70:30 in 10CV);

Yield: 0.026 g (22%);

¹H-NMR (CDCl₃), δ: 1.48 (s, 9H, H-16,17,18), 2.29 (s, 3H, H-7), 6.95-6.98 (m, 1H, H-aromatic), 7.18-7.20 (m, 1H, H-aromatic), 7.34-7.38 (m, 1H, H-aromatic), 7.51 (dd, J₁= 8.0 Hz, J₂= 1.8 Hz, 1H, H-aromatic), 7.56-7.58 (m, 1H, H-aromatic), 7.74 (d, J₁= 1.8 Hz, 1H, H-aromatic), 7.77-7.79 (m, 1H, H-aromatic), 10.76 (bs, 1H, NH).

¹³C-NMR (CDCl₃), δ: 20.2 (3xCH₃, C-16,17,18), 28.2 (CH₃, C-7), 119.6, 125.3, 127.7, 131.2, 131.3, 131.7, 135. (CH, C-aromatic), 83.1 (C, C-15), 117.9, 131.6, 134.0, 140.0, 141.7 (C, C-aromatic), 167.2 (C, C-14).

UPLC-MS: Rt 2.73 (>99%) MS (ESI): 380.2 [M-H]⁻.

9.2.9 (1*H*-Tetrazol-5-yl) anilines (84-85)2-(1*H*-Tetrazol-5-yl)aniline (84)(C₇H₇N₅; M.W.= 161.17)Reagent: 2-aminobenzonitrile (**82**) (1.0 g, 8.46 mmol);

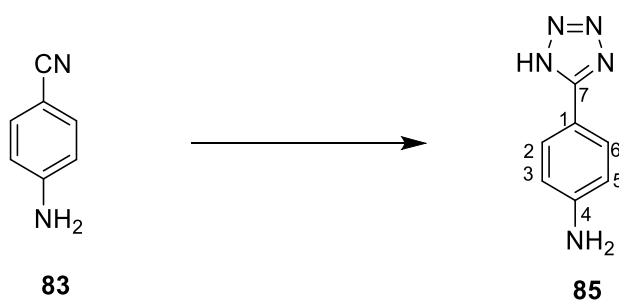
General Procedure 9;

Yellow Solid;

T.L.C. System: *n*-hexane-EtOAc 5:5 v/v, R_f: 0.58;Purification: Biotage Isolera One automated flash column chromatography (cartridge: SNAP KP 50g, *n*-hexane-EtOAc 100:0 increasing to *n*-hexane-EtOAc 0:100 in 10CV);

Yield: 0.723 g (53%);

¹H-NMR (DMSO-D₆), δ: 6.67-6.70 (m, 1H, H-aromatic), 6.88-6.92 (m, 1H, H-aromatic), 7.22-7.26 (m, 1H, H-aromatic), 7.72 (dd, J₁= 7.8 Hz, J₂= 1.3 Hz, 1H, H-aromatic), 9.66 (bs, 1H, NH).¹³C-NMR (DMSO-D₆), δ: 116.0, 116.8, 128.5, 132.3 (CH, C-aromatic), 105.0, 147.9 (C, C-aromatic), 155.3 (C, C-7).

4-(1H-Tetrazol-5-yl)aniline (85) ⁽²⁶⁾**(C₇H₇N₅; M.W= 161.17)**Reagent: 4-aminobenzonitrile (**83**) (1.0 g, 8.46 mmol);

General Procedure 9;

Yellow Solid;

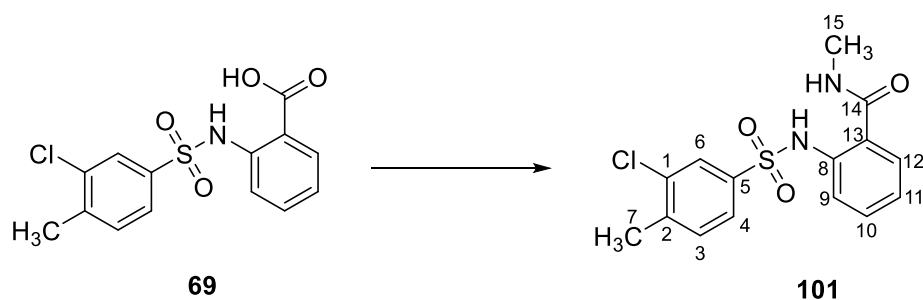
T.L.C. System: *n*-hexane-EtOAc 2:8 v/v, R_f: 0.30;

Purification: Trituration with EtOAc;

Yield: 0.451 g (33%);

¹H-NMR (DMSO-D₆), δ: 5.83 (bs, 2H, NH₂), 6.69 (d, J= 8.8 Hz, 2H, H-aromatic), 7.69 (d, J= 8.8 Hz, 2H, H-aromatic), 16.00 (bs, 1H, NH).¹³C-NMR (DMSO-D₆), δ: 116.0, 116.8, 128.5, 132.3 (CH, C-aromatic), 105.0, 147.9 (C, C-aromatic), 155.3 (C, C-7).

9.2.10 Alkyl(arylsulfonamido) carboxamide (101-105)

2-((3-Chloro-4-methylphenyl)sulfonamido)-*N*-methylbenzamide (101)(C₁₅H₁₅ClN₂O₃S; M.W.= 338.81)Reagent: 2-((3-chloro-4-methylphenyl)sulfonamido)benzoic acid (**69**) (0.100 g, 0.30 mmol);

General Procedure 10;

White solid;

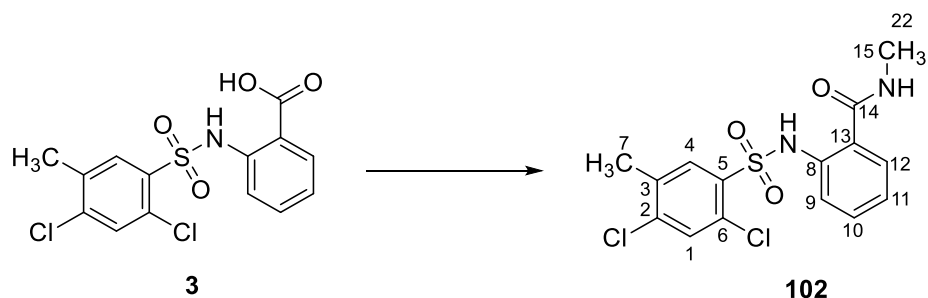
T.L.C. System: *n*-hexane-EtOAc 5:5 v/v, R_f: 0.40;Purification: Biotage Isolera One automated flash column chromatography (cartridge: ZIP KP SIL 10g, *n*-hexane-EtOAc 100:0 increasing to *n*-hexane-EtOAc 20:80 in 10CV);

Yield: 0.03 g (30%);

¹H-NMR (CDCl₃), δ: 2.39, (s, 3H, H-7), 2.94 (d, J= 4.8 Hz, 3H, H-15), 6.06 (bs, 1H, NH), 7.07-7.11 (m, 1H, H-aromatic), 7.26-7.29 (m, 1H, H-aromatic), 7.36 (d, J= 7.9 Hz, 1H, H-3), 7.42-7.46 (m, 1H, H-aromatic), 7.60 (dd, J₁= 8.1 Hz, J₂= 1.7 Hz, 1H, H-aromatic), 7.69 (d, J= 7.9 Hz, 1H, H-4), 7.79-7.81 (m, 1H, H-aromatic), 10.87 (bs, 1H, NH).

¹³C-NMR (CDCl₃), δ: 20.2 (CH₃), 26.7 (CH₃), 121.7, 123.8, 125.4, 126.5, 127.7, 131.1, 132.6 (CH, C-aromatic), 121.8, 135.0, 138.4, 138.5, 141.5 (C, C-aromatic), 168.8 (C, C-14).

UPLC-MS: Rt 2.11 (>99%) MS (ESI)⁺: 339.1 [M+H]⁺.

2-((2,4-Dichloro-5-methylphenyl)sulfonamido)-*N*-methylbenzamide (102)(C₁₅H₁₄Cl₂N₂O₃S; M.W.= 373.25)

Reagent: 2-((2,4-dichloro-5-methylphenyl)sulfonamido)benzoic acid (**3**) (0.100 g, 0.27 mmol);

General Procedure 10;

White solid;

T.L.C. System: *n*-hexane-EtOAc 5:5 v/v, R_f: 0.43;

Purification1: Recrystallisation from EtOH/Water;

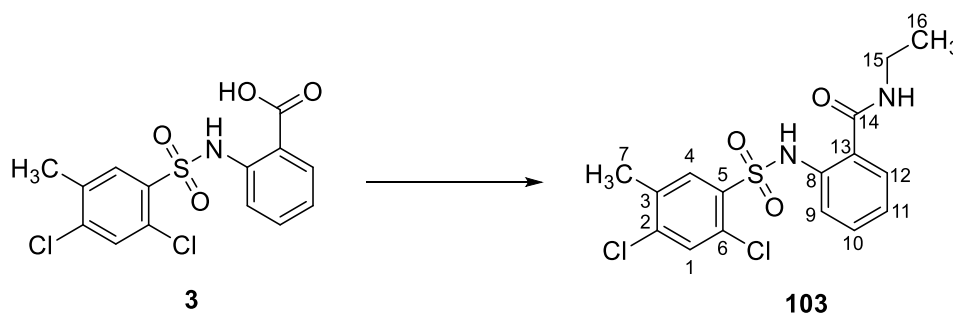
Purification2: Biotage Isolera One automated flash column chromatography (cartridge: ZIP KP SIL 10g, *n*-hexane-EtOAc 100:0 increasing to *n*-hexane-EtOAc 0:100 in 14CV);

Yield: 0.049 g (49%);

¹H-NMR (CDCl₃), δ: 2.41 (s, 3H, H-7), 3.02 (d, J=4.8 Hz, 3H, H-15), 6.17 (bs, 1H, NH), 7.02-7.05 (m, 1H, H-aromatic), 7.34-7.37 (m, 1H, H-aromatic), 7.40 (dd, J₁= 7.8 Hz, J₂= 1.0 Hz, 1H, H-aromatic), 7.45 (s, 1H, H-4), 7.54-7.57 (m, 1H, H-aromatic), 8.05 (s, 1H, H-1), 11.37 (bs, 1H, NH).

¹³C-NMR (CDCl₃), δ: 19.6 (CH₃), 26.8 (CH₃), 118.7, 122.9, 126.7, 131.7, 132.5, 133.3 (CH, C-aromatic), 120.6, 130.0, 135.2, 135.5, 138.0, 139.7 (C, C-aromatic), 168.9 (C, C-14).

UPLC-MS: Rt 2.23 (100%) MS (ESI)⁺: 375.1 [M+H]⁺.

2-((2,4-Dichloro-5-methylphenyl)sulfonamido)-*N*-ethylbenzamide (103)(C₁₆H₁₆Cl₂N₂O₃S; M.W.= 387.28)

Reagent: 2-((2,4-dichloro-5-methylphenyl)sulfonamido)benzoic acid (**3**) (0.100 g, 0.27 mmol);

General Procedure 10;

White solid;

T.L.C. System: *n*-hexane-EtOAc 6:4 v/v, R_f: 0.40;

Purification1: Recrystallisation from DCM/*n*-hexane;

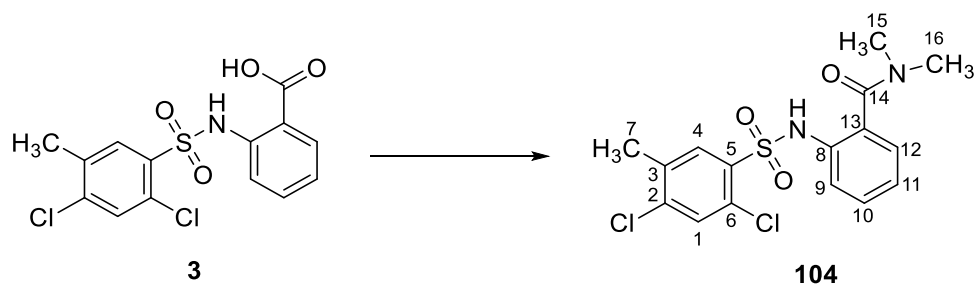
Purification2: Biotage Isolera One automated flash column chromatography (cartridge: ZIP KP SIL 5g, *n*-hexane-EtOAc 100:0 increasing to *n*-hexane-EtOAc 40:60 in 10CV);

Yield: 0.047 g (44%);

¹H-NMR (CDCl₃), δ: 1.28 (t, J= 7.2 Hz, 3H, H-16), 2.41 (s, 3H, H-7), 3.47-3.52 (m, 2H, H-15), 6.13 (bs, 1H, NH), 7.02-7.06 (m, 1H, H-aromatic), 7.34-7.37 (m, 1H, H-aromatic), 7.40-7.42 (m, 1H, H-aromatic), 7.45 (s, 1H, H-4), 7.55-7.57 (m, 1H, H-aromatic), 8.05 (s, 1H, H-1), 11.40 (bs, 1H, NH).

¹³C-NMR (CDCl₃), δ: 14.6 (CH₃), 19.6 (CH₃), 35.0 (CH₂, C-15), 118.7, 122.9, 126.7, 131.7, 132.5, 133.3 (CH, C-aromatic), 120.8, 130.0, 135.2, 135.5, 138.1, 139.7 (C, C-aromatic), 168.1 (C, C-14).

UPLC-MS: Rt 2.33 (>98%) MS (ESI)⁺: 389.1 [M+H]⁺.

2-((2,4-Dichloro-5-methylphenyl)sulfonamido)-*N,N*-dimethylbenzamide (104)(C₁₆H₁₆Cl₂N₂O₃S; M.W.= 387.28)Reagent: 2-((2,4-dichloro-5-methylphenyl)sulfonamido)benzoic acid (**3**) (0.100 g, 0.27 mmol);

General Procedure 10;

White solid;

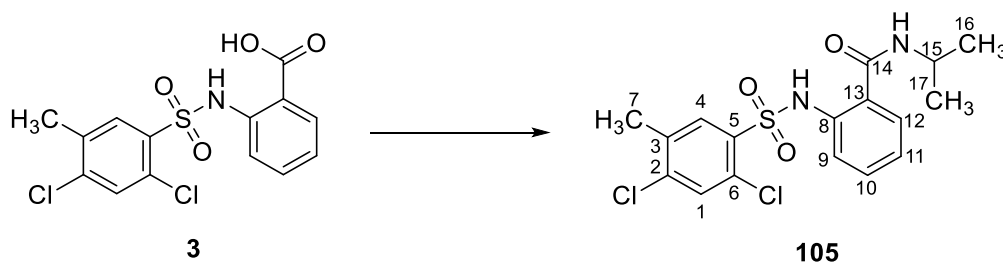
T.L.C. System: *n*-hexane-EtOAc 4:6 v/v, R_f: 0.50;Purification: Biotage Isolera One automated flash column chromatography (cartridge: ZIP KP SIL 10g, *n*-hexane-EtOAc 100:0 increasing to *n*-hexane-EtOAc 30:70 in 11CV);

Yield: 0.037 g (35%);

¹H-NMR (CDCl₃), δ: 2.37 (s, 3H, H-7), 2.79 (s, 3H), 3.10 (s, 3H), 7.09-7.12 (m, 1H, H-aromatic), 7.18-7.20 (m, 1H, H-aromatic), 7.32-7.36 (m, 1H, H-aromatic), 7.49 (s, 1H, H-4), 7.59-7.60 (m, 1H, H-aromatic), 7.93 (s, 1H, H-1), 8.88 (bs, 1H, NH) ppm.

¹³C-NMR (CDCl₃), δ: 19.6 (CH₃), 39.4 (CH₃), 39.6 (CH₃), 122.4, 124.0, 127.9, 130.8, 131.4, 133.2 (CH, C-aromatic), 126.1, 129.7, 135.1, 135.2, 135.7, 139.7 (C, C-aromatic), 169.3 (C, C-14) ppm.

UPLC-MS: Rt 2.18 (>97%) MS (ESI)⁺: 389.1 [M+H]⁺.

2-((2,4-Dichloro-5-methylphenyl)sulfonamido)-*N*-isopropylbenzamide (105)(C₁₇H₁₈Cl₂N₂O₃S; M.W.= 401.30)Reagent: 2-((2,4-dichloro-5-methylphenyl)sulfonamido)benzoic acid (**3**) (0.100 g, 0.27 mmol);

General Procedure 10;

White solid;

T.L.C. System: *n*-hexane-EtOAc 7:3 v/v, R_f: 0.38;Purification: Biotage Isolera One automated flash column chromatography (cartridge: ZIP KP SIL 10g, *n*-hexane-EtOAc 100:0 increasing to *n*-hexane-EtOAc 30:70 in 12CV);

Yield: 0.060 g (53%);

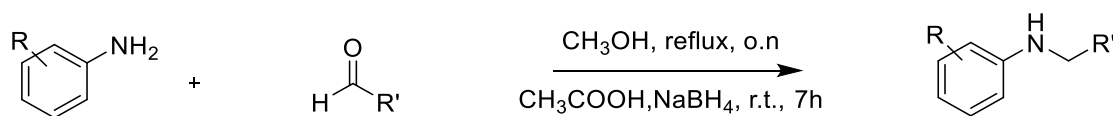
¹H-NMR (CDCl₃), δ: 1.19, d, J=6.5 Hz, 6H, H-16,17), 2.31 (s, 3H-H-7), 4.14-4.20 (m, 1H-H-15), 5.85 (bs, 1H, NH), 6.92-6.95 (m, 1H, H-aromatic), 7.24-7.27 (m, 1H, H-aromatic), 7.30 (dd, J₁= 7.8 Hz, J₂= 1.4 Hz, 1H, H-aromatic), 7.35 (s, 1H, H-aromatic), 7.45 (dd, J₁= 1.0 Hz, J₂= 8.4 Hz, 1H, H-aromatic), 7.96 (s, 1H, H-4), 11.32 (bs, 1H, NH).

¹³C-NMR (CDCl₃), δ: 19.6 (CH₃, C-7), 22.6 (2xCH₃, C-16,17), 42.1 (CH, C-15), 118.7, 122.9, 126.8, 131.7, 132.5, 133.4 (CH, C-aromatic), 120.8, 130.0, 135.2, 135.5, 138.1, 139.7 (C, C-aromatic), 167.5 (C, C-14).

UPLC-MS: Rt 2.43 (>97%) MS (ESI)⁺: 403.2 [M+H]⁺.

9.3 Synthesis of amine derivatives

General Procedure 11: arylamino derivatives (113-120, 129-134, 144-150) ⁽²⁷⁾



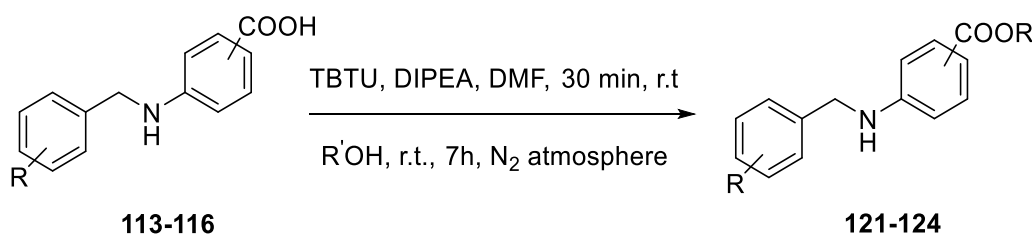
2, 18-19, 84-85, 96, 112

107-111, 125-128

113-120, 129-134, 144-150

A solution of the appropriate aryl benzaldehyde (1eq) and differently substituted anilines (1eq) in MeOH (2.5 mL/mmol) was refluxed overnight. The solvent was then removed under vacuum and the resulting residue was dissolved in acetic acid (3 mL/mmol). NaBH₄ (2 eq) was then added in portions at 20°C and the mixture was then stirred at room temperature for 7 hours. The reaction mixture was added of water (4 mL/mmol) and ethyl acetate (4 mL/mmol). The pH of the aqueous layer was adjusted to 5 by the addition of 1M NaOH. The water layer was extracted with ethyl acetate (3x10 mL/mmol). The combined organic layers were dried over MgSO₄ and concentrated under vacuum. The desired products were purified by flash column chromatography.

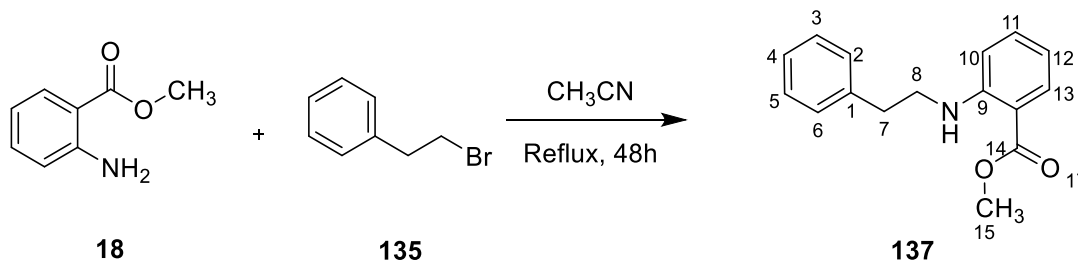
General Procedure 12: methyl((aryl)amino)benzoates (121-124) ⁽¹⁶⁾



113-116

121-124

The appropriate (aryl)amino benzoic acid (1 eq), TBTU (1 eq) and DIPEA (2 eq) was stirred in anhydrous DMF (1 mL/mmol eq), and the resulting mixture was stirred at room temperature for 30 min, under N₂ atmosphere. CH₃OH (1 eq) was then injected into the reaction mixture via syringe and stirring was continued at room temperature until completion of the reaction. The reaction mixture was diluted with DCM (10 mL/mmol eq) and the resulting mixture was extracted with sat. aq NH₄Cl (1x10 mL/mmol eq) and sat. aq NaHCO₃ (1x10 mL/mmol eq). The organic layer was dried over MgSO₄ and the solvent was evaporated under vacuum. The desired products were purified by flash column chromatography or recrystallisation.

Synthesis of methyl 2-(phenethylamino)benzoate (137) ⁽²⁸⁾**(C₁₆H₁₇NO₂; M.W.= 255.32)**

To a solution of (2-bromoethyl) benzene (0.150 g, 0.81 mmol) in MeCN (5 mL) was added methyl 2-aminobenzoate (0.122 g, 0.81 mmol) under nitrogen atmosphere. The resulting solution was stirred at reflux for 48 h. The formed salt was filtered off and the filtrate was concentrated under vacuum. The residue was dissolved in ethyl acetate (15 mL) and washed sequentially with water (10 mL) and brine (10 mL) and dried over sodium sulfate. The solvent was evaporated under reduced pressure and the residue was purified by flash column chromatography to obtain the pure compound.

Colourless Oil;

T.L.C. System: *n*-hexane-EtOAc 8:2 v/v, R_f: 0.55;

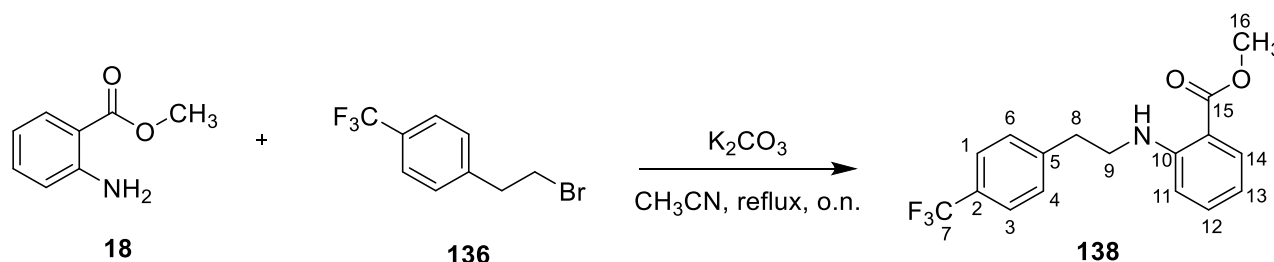
Purification: Biotage Isolera One automated flash column chromatography (cartridge: ZIP KP 10g, *n*-hexane-EtOAc 100:0 increasing to *n*-hexane-EtOAc 80:20 in 15CV);

Yield: 0.010 g (5%);

¹H-NMR (CDCl₃), δ: 2.90 (t, J= 7.5 Hz, 2H, H-7), 3.37 (t, J= 7.5 Hz, 2H, H-8), 3.76 (s, 3H, H-15), 6.49-6.52 (m, 1H, H-aromatic), 6.62-6.64 (m, 1H, H-aromatic), 7.12-7.15 (m, 1H, H-aromatic), 7.18-7.20 (m, 2H, H-aromatic), 7.23-7.29 (m, 3H, H-aromatic), 7.69 (bs, 1H, NH), 7.81-7.83 (m, 1H, H-aromatic).

¹³C-NMR (CDCl₃), δ: 51.4 (CH₃, C-15), 32.9, 44.5 (CH₂, C-7,8), 111.1, 114.5, 128.6, 127.7, 131.5, 131.7, 134.6 (CH, C-aromatic), 110.0, 139.2, 150.9 (C, C-aromatic), 168.9 (C, C-14).

UPLC-MS: Rt 2.58 (>97%) MS (ESI)⁺: 256.1 [M+H]⁺.

Synthesis of methyl 2-((4-trifluoromethyl)phenethylamino)benzoate (138) ⁽²⁹⁾**(C₁₇H₁₆F₃NO₂; M.W.= 323.32)**

A mixture of methyl 2-aminobenzoate (0.090 g, 0.59 mmol), 1-(2-bromoethyl)-4-(trifluoromethyl)benzene (0.150 g, 0.59 mmol), and K₂CO₃ (0.081 g, 0.59 mmol) in MeCN (2 mL) was stirred overnight under reflux. The mixture was extracted between ethylacetate (3 x 10 mL) and water (20 mL) and the organic layer was dried over sodium sulfate. The solvent was removed under vacuum and the residue was purified by flash column chromatography to obtain the pure compound.

Colourless oil;

T.L.C. System: *n*-hexane:EtOAc 9:1 v/v, R_f: 0.54;

Purification: Biotage Isolera One automated flash column chromatography (cartridge: ZIP KP SIL 30g, *n*-hexane-DCM 100:0 increasing to *n*-hexane-DCM 40:60 in 15CV);

Yield: 0.049 g (26%);

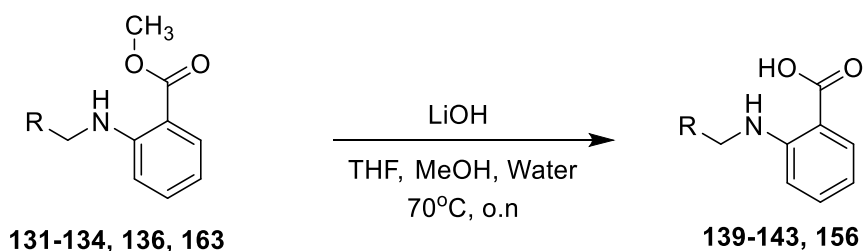
¹H-NMR (CDCl₃), δ: 3.06 (t, J = 7.2 Hz, 2H, H-8), 3.49-3.53 (m, 2H, H-9), 3.86 (s, 3H, H-16), 6.61-6.64 (m, 1H, H-aromatic), 6.70-5.72 (m, 1H, H-aromatic), 7.37-7.40 (m, 3H, H-aromatic), 7.59 (d, J = 8.0 Hz, 2H, H-aromatic), 7.80 (bs, 1H, NH), 7.93 (dd, J₁ = 8.0 Hz, J₂ = 1.6 Hz, 1H, H-aromatic).

¹³C-NMR (CDCl₃), δ: 35.4, 44.0 (CH₂, C-8,9) 51.4 (CH₃, C-16), 111.0, 114.8, 125.4, 125.5, 129.1, 131.78 (CH, C-aromatic), 125.4 (d, J = 37.3 Hz, C), 110.2, 134.6, 143.4, 150.7 (C-aromatic), 168.9 (C, C-15).

¹⁹F-NMR (CDCl₃), δ: -62.4 (s, 3F)

UPLC-MS: Rt 2.68 (100%) MS (ESI)⁺: 324.2 [M+H]⁺.

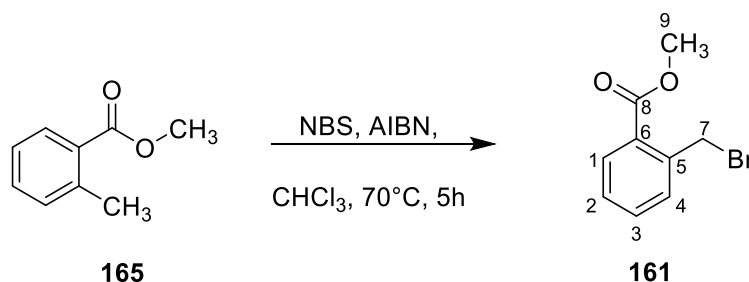
General Procedure 13: (aryl)amino)benzoic acids (139-143, 156) ⁽¹⁴⁾



To a solution of the appropriate methyl-(arylamino) benzoate (1 eq) in THF (7 mL/mmol), H₂O (3.5 mL/mmol), MeOH (3.5 mL/mmol) was added LiOH (3 eq). The reaction was stirred at 70°C overnight. After the reaction was allowed to cool to room temperature, the reaction mixture was acidified with 2M HCl. The product was extracted with ethyl acetate (3x10 mL/mmol). The organic layer was dried over MgSO₄ and evaporated under reduced pressure. The product was purified by flash column chromatography or recrystallisation.

Synthesis of: methyl 2-(bromomethyl) benzoate ^(30, 31)

(C₉H₉BrO₂; M.W.= 229.07)



To a solution of the starting methyl 2-methylbenzoate (1.0 g, 6.65 mmol) in 7 mL of CHCl₃, NBS (1.3 g, 7.31 mmol) and AIBN (0.013 g, 0.073 mmol) were added and the reaction was stirred at 70°C for 5 hours. The reaction was then cooled down to room temperature and the deposit of succinimide was filtered. The solvent was evaporated under reduced pressure. The crude product was then purified by flash column chromatography to obtain the pure product.

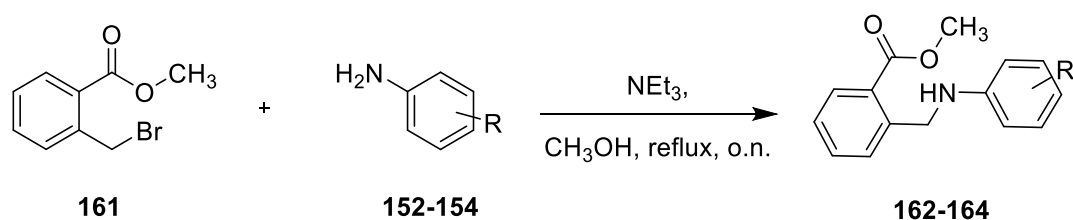
Yellow oil;

T.L.C. System: *n*-hexane-EtOAc 9:1 v/v, R_f: 0.57;

Purification: Biotage Isolera One automated flash column chromatography (cartridge: SNAP KP SIL 100g, *n*-hexane-EtOAc 100:0 increasing to *n*-hexane-EtOAc 80:20 in 15CV);

Yield: 1.25 g (82%);

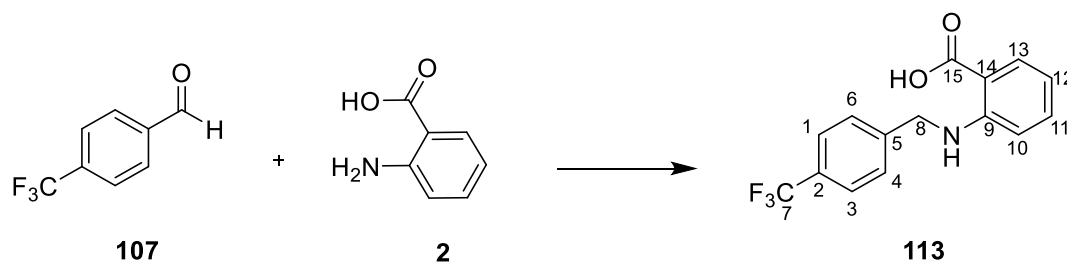
¹H-NMR (CDCl₃), δ: 3.95 (s, 3H, H-9), 4.98 (s, 2H, H-7), 7.38-7.40 (m, 1H, H-aromatic), 7.46-7.50 (m, 2H, H-aromatic), 7.98-8.00 (m, 1H, H-aromatic).

General Procedure 14: methyl 2-(aryl)amino)methyl)benzoates (162-164) ⁽³²⁾

A mixture of methyl 2-(bromomethyl)benzoate (1 eq), differently substituted anilines (1 eq) and TEA (1.5 eq) in methanol (1 mL/mmol) was heated at 85°C. overnight. The mixture was diluted with DCM, washed with saturated solution of NaHCO₃ (10 mL/mmol), dried over sodium sulfate and concentrated in vacuum. The crude products were purified by recrystallisation or flash column chromatography.

9.3.1 Arylamino derivatives (113-120, 129-134, 144-150)

2-((4-(Trifluoromethyl)benzyl)amino)benzoic acid (113)

(C₁₅H₁₂F₃NO₂, M.W.= 295.26)Reagent: 4-(trifluoromethyl)benzaldehyde (**107**) (0.300 g, 1.72 mmol);Reagent: 2-aminobenzoic acid (**2**) (0.236 g, 1.72 mmol);

General Procedure 10;

White solid;

T.L.C. System: *n*-hexane-EtOAc 7:3 v/v, R_f: 0.64;Purification1: Biotage Isolera One automated flash column chromatography (cartridge: SNAP ULTRA 25g, *n*-hexane-EtOAc 100:0 increasing to *n*-hexane-EtOAc 60:40 in 10CV);

Purification 2: Recrystallisation from EtOH/water;

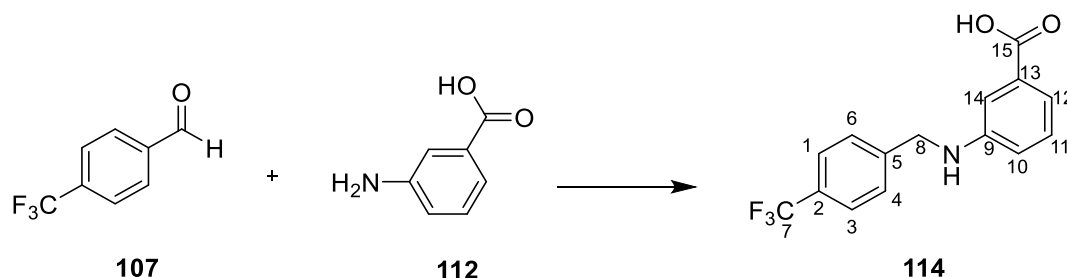
Yield: 0.087 g (17%);

¹H-NMR (CDCl₃), δ: 4.59 (s, 2H, H-8), 6.58 (m, 1H, H-aromatic), 6.67-6.70 (m, 1H, H-aromatic), 7.34-7.38 (m, 1H, H-aromatic), 7.50 (d, J= 7.9 Hz, 2H, H-aromatic), 7.63 (d, J= 7.9 Hz, 2H, H-aromatic), 8.05 (dd, J₁= 8.0 Hz, J₂= 1.5 Hz, 1H, H-aromatic), 8.20 (bs, 1H, NH), 11.22 (bs, 1H, OH).

¹³C-NMR (CDCl₃), δ: 46.4 (CH₂, C-8), 111.7, 115.6, 125.6, 125.7, 129.1, 129.4 (CH, C-aromatic), 109.1, 125.2, 127.0, 143.0, 151.3 (C, C-aromatic), 173.3 (C, C-15).

¹⁹F-NMR (CDCl₃), δ: -62.38 (3F).

UPLC-MS: Rt 2.29 (>99%) MS (ESI)⁺: 296.0 [M+H]⁺.

3-((4-(Trifluoromethyl)benzyl)amino)benzoic acid (114)**(C₁₅H₁₂F₃NO₂; M.W.= 295.26)**Reagent: 4-(trifluoromethyl)benzaldehyde (**107**) (0.300 g, 1.72 mmol);Reagent: 3-aminobenzoic acid (**112**) (0.236 g, 1.72 mmol);

General Procedure 11;

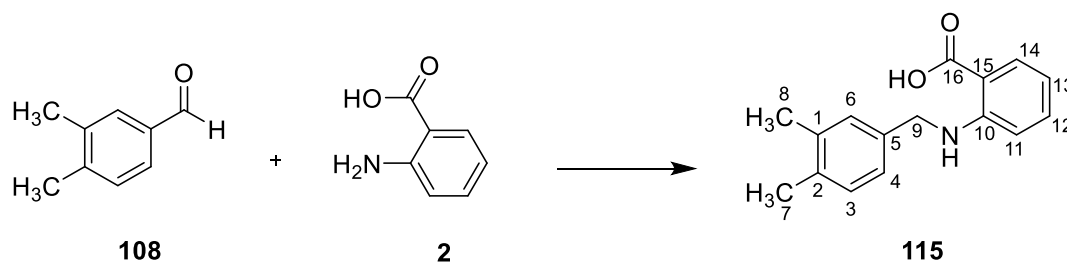
White solid;

T.L.C. System: *n*-hexane-EtOAc 7:3 v/v, R_f: 0.45;Purification1: Biotage Isolera One automated flash column chromatography (cartridge: SNAP KP SIL 25g, *n*-hexane-EtOAc 100:0 increasing to *n*-hexane-EtOAc 30:70 in 11CV);Purification2: Biotage Isolera One automated flash column chromatography (cartridge: SNAP KP SIL 10g, *n*-hexane-EtOAc 100:0 increasing to *n*-hexane-EtOAc 40:60 in 10CV);

Purification 3: Recrystallisation from EtOH;

Yield: 0.100 g (20%);

¹H-NMR (CDCl₃), δ: 4.49 (s, 2H, H-8), 6.83-6.85 (m, 1H, H-aromatic), 7.27-7.30 (m, 1H, H-aromatic), 7.35 (bs, 1H, NH), 7.39 (s, 1H, H-14), 7.50-7.54 (m, 3H, H-aromatic), 7.64 (d, J= 7.9 Hz, 2H, H-aromatic), 11.74 (bs, 1H, OH).¹³C-NMR (CDCl₃), δ: 47.6 (CH₂, C-8), 113.9, 125.2, 125.6, 125.72, 127.5, 129.4 (CH, C-aromatic), 125.76, 129.8, 130.2, 143.0, 147.70(C, C-aromatic), 171.8 (C, C-8).¹⁹F-NMR (CDCl₃), δ: -62.42 (3F).UPLC-MS: Rt 2.12 (99%) MS (ESI)⁺: 296.0 [M+H]⁺.

2-((3,4-Dimethylbenzyl)amino)benzoic acid (115)**(C₁₆H₁₇NO₂; M.W.= 255.32)**Reagent: 3,4-dimethylbenzaldehyde (**108**) (0.150 g, 1.12 mmol);Reagent: 2-aminobenzoic acid (**2**) (0.153 g, 1.72 mmol);

General Procedure 11;

White solid;

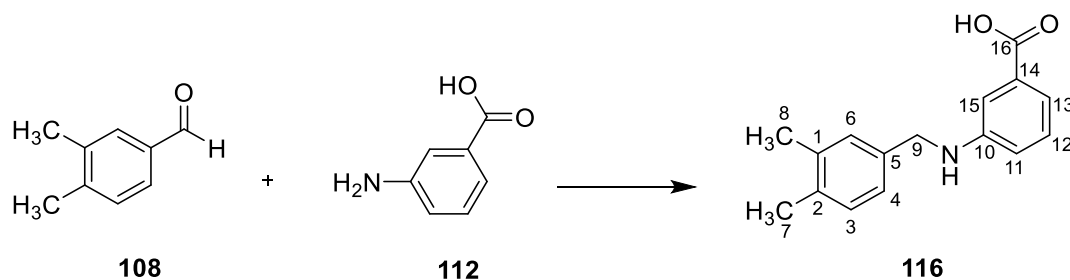
T.L.C. System: *n*-hexane-EtOAc 7:3 v/v, R_f: 0.50;Purification: Biotage Isolera One automated flash column chromatography (cartridge: SNAP KP SIL 25g, *n*-hexane-EtOAc 100:0 increasing to *n*-hexane-EtOAc 60:40 in 10CV);

Yield: 0.150 g (52%);

¹H-NMR (CDCl₃), δ: 2.18 (d, J= 3.7 Hz, 6H, H-7,8), 4.33 (s, 2H, H-9), 6.52-6.55 (m, 1H, H-aromatic), 6.58 (d, J= 8.4 Hz, 1H, H-aromatic), 7.00-7.05 (m, 3H, H-aromatic), 7.23-7.27 (m, 1H, H-aromatic), 7.91 (dd, J₁= 7.9 Hz, J₂= 1.6 Hz, 1H, H-aromatic), 8.22 (bs, 1H, NH) 11.36 (bs, 1H, OH).

¹³C-NMR (CDCl₃), δ: 19.4 (CH₃), 19.8 (CH₃), 46.7 (CH₂, C-9), 111.9, 114.9, 124.4, 128.3, 129.9, 132.62, 135.4 (CH, C-aromatic), 108.8, 135.6, 136.0, 136.9, 151.7 (C, C-aromatic), 173.6 (C, C-16).

UPLC-MS: Rt 2.34 (100%) MS (ESI)⁺: 256.1 [M+H]⁺.

3-((3,4-Dimethylbenzyl)amino)benzoic acid (116)**(C₁₆H₁₇NO₂; M.W.= 255.32)**Reagent: 3,4-dimethylbenzaldehyde (**108**) (0.200 g, 1.5 mmol);Reagent: 3-aminobenzoic acid (**112**) (0.205 g, 1.72 mmol);

General Procedure 11;

White solid;

T.L.C. System: *n*-hexane-EtOAc 7:3 v/v, R_f: 0.48;Purification: Biotage Isolera One automated flash column chromatography (cartridge: SNAP ULTRA 25g, *n*-hexane-EtOAc 100:0 increasing to *n*-hexane-EtOAc 50:50 in 10CV);

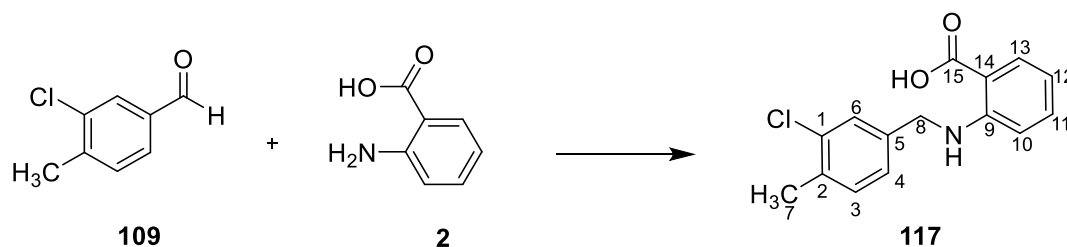
Purification2: Recrystallisation from EtOH/Water;

Yield: 0.097 g (26%);

¹H-NMR (CDCl₃), δ: 2.28 (d, J= 3.5 Hz, 6H, H-7,8), 4.32 (s, 2H, H-9), 6.42 (bs, 1H, NH), 6.85-6.88 (m, 1H, H-aromatic), 7.11-7.15 (m, 2H, H-aromatic), 7.26-7.28 (m, 2H, H-aromatic), 7.40-7.42 (m, 1H, H-aromatic), 7.47 (d, J= 7.6 Hz, 1H, H-aromatic), 11.71 (bs, 1H, OH).

¹³C-NMR (CDCl₃), δ: 19.4 (CH₃), 19.8 (CH₃), 48.0 (CH₂, C-9), 113.9, 118.0, 119.2, 125.0, 129.0, 129.31, 129.9 (CH, C-aromatic), 130.0, 135.7, 136.1, 136.9, 148.2 (C, C-aromatic), 171.5 (C, C-16).

UPLC-MS: Rt 2.13 (100%) MS (ESI)⁺: 256.1 [M+H]⁺.

2-((3-Chloro-4-methylbenzyl)amino)benzoic acid (117)**(C₁₅H₁₄ClNO₂; M.W.= 275.53)**Reagent: 3-chloro-4-methylbenzaldehyde (**109**) (0.150 g, 0.97 mmol);Reagent: 2-aminobenzoic acid (**2**) (0.133 g, 0.97 mmol);

General Procedure 11;

White solid;

T.L.C. System: *n*-hexane-EtOAc 7:3 v/v, R_f: 0.45;Purification1: Biotage Isolera One automated flash column chromatography (cartridge: SNAP KP SIL 50g, *n*-hexane-EtOAc 100:0 increasing to *n*-hexane-EtOAc 50:50 in 12CV);

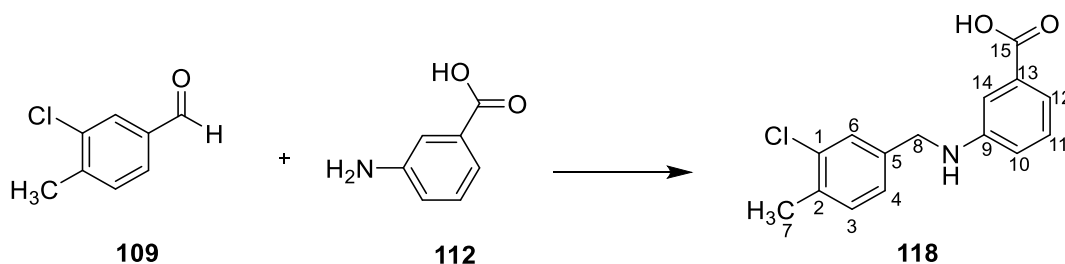
Purification2: Recrystallisation from EtOH/Water;

Yield: 0.058 g (21%);

¹H-NMR (CDCl₃), δ: 2.38 (s, 3H, H-7), 4.46 (s, 2H, H-8), 6.60-6.63 (m, 1H, H-aromatic), 6.65-6.68 (m, 1H, H-aromatic), 7.15-7.18 (m, 1H, H-aromatic), 7.21 (d, J= 7.8 Hz, 1H, H-aromatic), 7.34-7.37 (m, 2H, H-aromatic), 8.02 (dd, J₁= 7.8 Hz, J₂= 1.4 Hz, 1H, H-aromatic), 8.11 (m, 1H, H-aromatic), 10.77 (bs, 1H, NH), 12.73 (bs, 1H, OH).

¹³C-NMR (CDCl₃), δ: 19.7 (CH₃), 46.1 (CH₂, C-8), 111.8, 115.3, 125.0, 127.4, 131.2, 132.6, 135.6 (CH, C-aromatic), 108.9, 134.6, 134.8, 138.1, 151.4 (C, C-aromatic), 172.8 (C-15).

UPLC-MS: Rt 2.37 (100%) MS (ESI)⁺: 276.5 [M+H]⁺.

3-((3-Chloro-4-methylbenzyl)amino)benzoic acid (118)**(C₁₅H₁₄ClNO₂; M.W.= 275.73)**Reagent: 3-chloro-4-methylbenzaldehyde (**109**) (0.114 g, 0.73 mmol);Reagent: 3-aminobenzoic acid (**112**) (0.101 g, 0.73 mmol);

General Procedure 11;

Yellow solid;

T.L.C. System: *n*-hexane-EtOAc 7:3 v/v, R_f: 0.35;Purification1: Biotage Isolera One automated flash column chromatography (cartridge: SNAP KP SIL 25g, *n*-hexane-EtOAc 100:0 increasing to *n*-hexane-EtOAc 20:80 in 12CV);Purification2: Biotage Isolera One automated flash column chromatography (cartridge: ZIP KP SIL 5g, *n*-hexane-EtOAc 100:0 increasing to *n*-hexane-EtOAc 0:100 in 11CV);

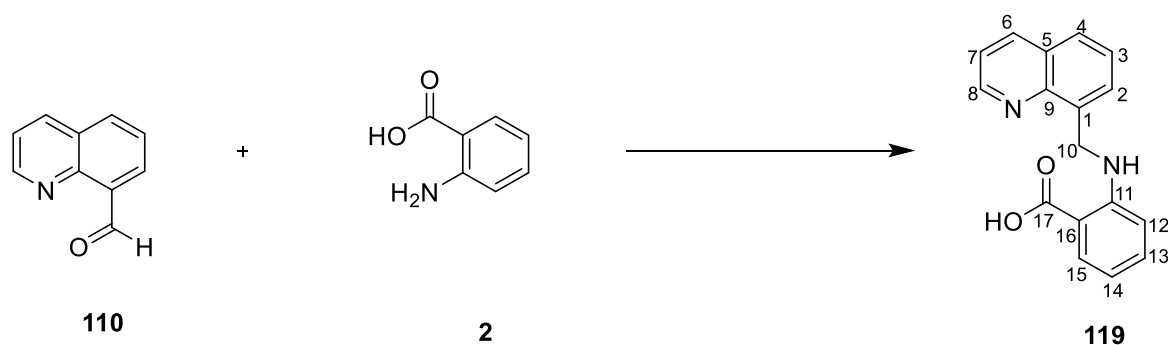
Purification3: Recrystallisation from EtOH/Water:

Yield: 0.057 g (28%);

¹H-NMR (CDCl₃), δ: 2.29 (s, 3H, H-7), 4.25 (s, 2H, H-8), 6.73-6.76 (m, 1H, H-aromatic), 7.08 (dd, J₁= 7.7 Hz, J₂= 1.5 Hz, 1H, H-aromatic), 7.13 (d, J= 7.7 Hz, 1H, H-aromatic), 7.16-7.19 (m, 1H, H-aromatic), 7.27-7.28 (m, 2H, H-aromatic), 7.35 (bs, 1H, NH) 7.38-7.40 (m, 1H, H-aromatic), 11.34 (bs, 1H, OH).

¹³C-NMR (CDCl₃), δ: 19.7 (CH₃, C-7), 47.3 (CH₂, C-8), 113.9, 118.0, 119.5, 125.6, 127.9, 129.3, 131.2 (CH, C-aromatic), 130.0, 134.6, 135.1, 138.1, 147.8 (C, C-aromatic), 171.3 (C, C-15).

UPLC-MS: Rt 2.16 (>96%) MS (ESI): 274.1 [M-H]⁻.

2-((Quinolin-8-ylmethyl)amino)benzoic acid (119)**(C₁₇H₁₄N₂O₂; M.W.= 278.31)**Reagent: quinoline-8-carbaldehyde (**110**) (0.100 g, 0.63 mmol);Reagent: 2-aminobenzoic acid (**2**) (0.086 g, 0.63 mmol);

General Procedure 11;

Yellow Solid;

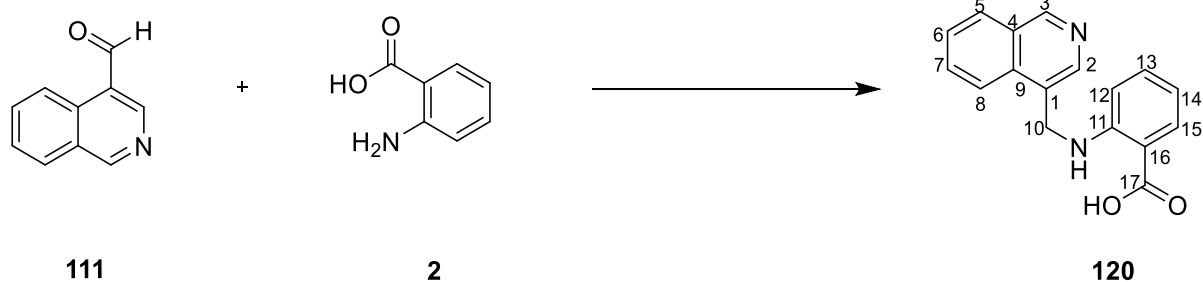
T.L.C. System: *n*-hexane-EtOAc 8:2 v/v, R_f: 0.60;Purification: Biotage Isolera One automated flash column chromatography (cartridge: ZIP KP SIL 30g, *n*-hexane-EtOAc 100:0 increasing to *n*-hexane-EtOAc 0:100 in 10CV);

Yield: 0.076 g (43%);

¹H-NMR (DMSO-D₆), δ: 5.08 (s, 2H, H-10), 6.52-6.55 (m, 1H, H-aromatic), 6.71 (dd, J₁= 8.5 Hz, J₂= 0.6 Hz, 1H, H-aromatic), 7.24-7.29 (m, 1H, H-aromatic), 7.54-7.57 (m, 1H, H-aromatic), 7.60 (dd, J₁= 8.2 Hz, J₂= 4.1 Hz, 1H, H-aromatic), 7.68-7.70 (m, 1H, H-aromatic), 7.80 (dd, J₁= 7.9 Hz, J₂= 1.5 Hz, 1H, H-aromatic), 7.90 (dd, J₁= 7.9 Hz, J₂= 1.1 Hz, 1H, H-aromatic), 8.41 (dd, J₁= 8.3 Hz, J₂= 1.7 Hz, 1H, H-aromatic), 8.49 (bs, 1H, NH), 8.98 (dd, J₁= 4.1 Hz, J₂= 1.7 Hz, 1H, H-aromatic), 12.51 (bs, 1H, OH).

¹³C-NMR (DMSO-D₆), δ: 42.6 (CH₂, C-10), 112.0, 114.7, 122.0, 126.8, 127.6, 127.8, 132.2, 134.8, 136.9, 150.2 (CH, C-aromatic), 110.7, 128.4, 137.0, 146.2, 151.2 (C, C-aromatic), 170.4 (C, C-17).

UPLC-MS: Rt 1.95 (100%) MS (ESI)⁺: 279.1 [M+H]⁺.

2-((Quinoline-3-ylmethyl)amino)benzoic acid (120)**(C₁₇H₁₄N₂O₂; M.W.= 278.31)**Reagent: quinoline-3-carbaldehyde (**111**) (0.100 g, 0.63 mmol);Reagent: 2-aminobenzoic acid (**2**) (0.066 g, 0.63 mmol);

General Procedure 11;

Yellow Solid;

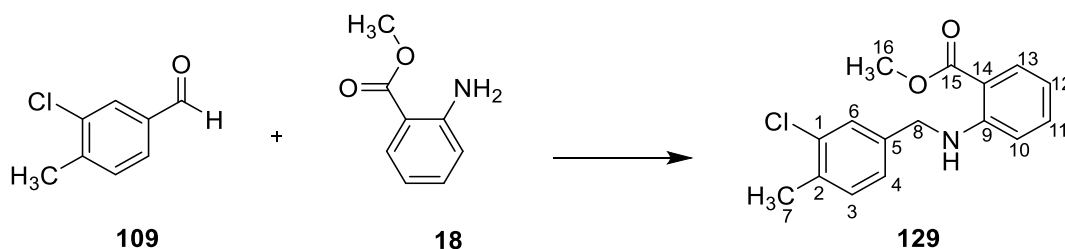
T.L.C. System: *n*-hexane-EtOAc 7:3 v/v, R_f: 0.25;Purification1: Biotage Isolera One automated flash column chromatography (cartridge: SNAP KP SIL 10g, *n*-hexane-EtOAc 100:0 increasing to *n*-hexane-EtOAc 0:100 in 15CV and EtOAc-MeOH 80:20 in 10 CV);Purification2: Recrystallisation from DCM/*n*-hexane;

Yield: 0.025 g (14%);

¹H-NMR (DMSO-D₆), δ: 4.72 (s, 2H, H-10), 6.56-6.60 (m, 1H, H-aromatic), 6.72 (d, J= 8.06 Hz, 1H, H-aromatic), 7.27-7.31 (m, 1H, H-aromatic), 7.57-7.61 (m, 1H, H-aromatic), 7.71-7.75 (m, 1H, H-aromatic), 7.83 (d, J= 8.1 Hz, 1H, H-aromatic), 7.96 (d, J= 8.1 Hz, 1H, H-aromatic), 8.01 (d, J= 8.1 Hz, 1H, H-aromatic), 8.24 (s, 1H, H-aromatic), 8.45 (bs, 1H, NH), 8.93 (s, 1H, H-aromatic), 12.76 (bs, 1H, OH).

¹³C-NMR (DMSO-D₆), δ: 112.1, 115.2, 127.2, 128.3, 129.1, 129.6, 132.2, 133.1, 134.9, 151.1 (CH, C-aromatic), 111.1, 127.9, 133.0, 147.3, 150.8 (C, C-aromatic), 170.4 (C, C-17).

UPLC-MS: Rt 1.62 (98%) MS (ESI)⁺: 279.1 [M+H]⁺.

Methyl 2-((3-chloro-4-methylbenzyl)amino)benzoate (129)**(C₁₆H₁₆ClNO₂; M.W.= 289.76)**Reagent: 3-chloro-4-methylbenzaldehyde (**198**) (0.100 g, 0.64 mmol);Reagent: 2-aminobenzoate (**18**) (0.098 g, 0.64 mmol);

General Procedure 11;

Grey solid;

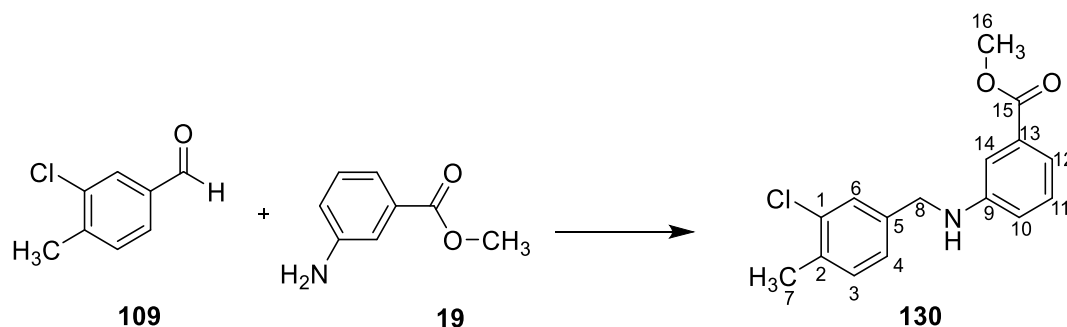
T.L.C. System: *n*-hexane-EtOAc 7:3 v/v, R_f: 0.72;Purification1: Biotage Isolera One automated flash column chromatography (cartridge: SNAP KP SIL 50g, *n*-hexane-EtOAc 100:0 increasing to *n*-hexane-EtOAc 60:40 in 13CV);Purification2: Biotage Isolera One automated flash column chromatography (cartridge: SNAP KP SIL 50g, *n*-hexane-DCM 100:0 increasing to *n*-hexane-DCM 30:70 in 10CV);Purification3: Biotage Isolera One automated flash column chromatography (cartridge: SNAP KP SIL 25g, *n*-hexane-DCM 100:0 increasing to *n*-hexane-DCM 30:70 in 10CV);

Yield: 0.049 g (26%);

¹H-NMR (CDCl₃), δ: 2.26 (s, 3H, H-7), 3.79 (s, 3H, H-16), 4.31 (d, J= 5.7 Hz, 2H, H-8), 6.50-6.54 (m, 2H, H-aromatic), 6.81 (bs, 1H, NH), 7.06 (dd, J₁= 7.8 Hz, J₂= 1.1 Hz, 1H, H-aromatic), 7.09 (d, J= 7.8 Hz, 1H, H-aromatic), 7.24 (s, 1H, H-6), 7.84 (dd, J₁= 7.9 Hz, J₂= 1.6 Hz, 1H, H-aromatic), 8.08 (m, 1H, H-aromatic).

¹³C-NMR (CDCl₃), δ: 19.7 (CH₃, C-7), 51.5 (CH₃, C-16), 46.2 (CH₂, C-8), 111.6, 115.1, 125.2, 127.6, 131.1, 131.6, 134.68 (CH, C-aromatic), 110.3, 134.64, 134.7, 138.3, 150.7 (C, C-aromatic), 169.1 (C, C-15).

UPLC-MS: Rt 2.69 (100%) MS (ESI)⁺: 290.0 [M+H]⁺.

Methyl 3-((3-chloro-4-methylbenzyl)amino)benzoate (130)**(C₁₆H₁₆ClNO₂; M.W.= 289.76)**Reagent: 3-chloro-4-methylbenzaldehyde (**109**) (0.100 g, 0.64 mmol);Reagent: 3-aminobenzoate (**19**) (0.098 g, 0.64 mmol);

General Procedure 11;

Yellow solid;

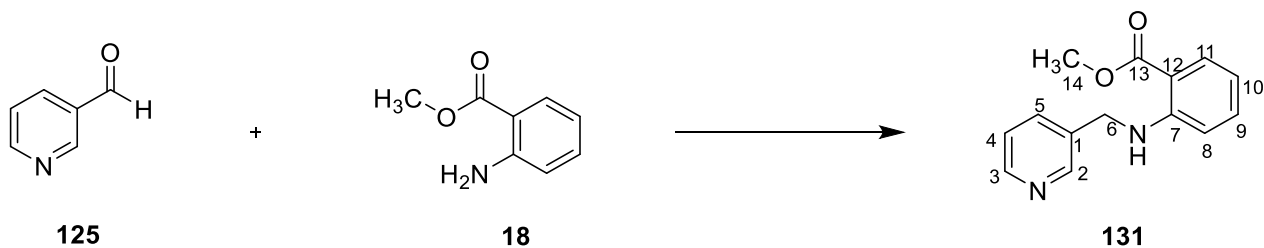
T.L.C. System: *n*-hexane-EtOAc 7:3 v/v, R_f: 0.60;Purification: Biotage Isolera One automated flash column chromatography (cartridge: SNAP KP SIL 25g, *n*-hexane-EtOAc 100:0 increasing to *n*-hexane-EtOAc 40:60 in 13CV);

Yield: 0.154 g (83%);

¹H-NMR (CDCl₃), δ: 2.38 (s, 3H, H-7), 3.91 (s, 3H, H-16), 4.19 (bs, 1H, NH), 4.34 (s, 2H, H-8), 6.78-6.80 (m, 1H, H-aromatic), 7.17 (dd, J₁= 7.8 Hz, J₂= 1.5 Hz, 1H, H-aromatic), 7.22 (d, J= 7.9 Hz, 1H, H-aromatic), 7.25 (d, J= 7.9 Hz, 1H, H-aromatic), 7.32-7.33 (m, 1H, H-aromatic), 7.37-7.38 (m, 1H, H-aromatic), 7.40-7.42 (m, 1H, H-aromatic).

¹³C-NMR (CDCl₃), δ: 19.7 (CH₃, C-7), 51.5 (CH₃, C-16) 47.5 (CH₂, C-8), 113.7, 117.4, 119.1, 125.6, 128.0, 129.2, 13.1 (CH, C-aromatic), 131.8, 134.6, 135.1, 138.0, 147.5 (C, C-aromatic), 167.4 (C, C-15).

UPLC-MS: Rt 2.44 (>99%) MS (ESI)⁺: 290.0 [M+H]⁺.

Methyl 2-((pyridin-3-ylmethyl)amino)benzoate (131)**(C₁₄H₁₄N₂O₂; M.W.= 242.28)**Reagent: nicotinaldehyde (**125**) (0.200 g, 1.86 mmol);Reagent: methyl 2-aminobenzoate (**18**) (0.281 g, 1.86 mmol);

General Procedure 11;

Yellow Oil;

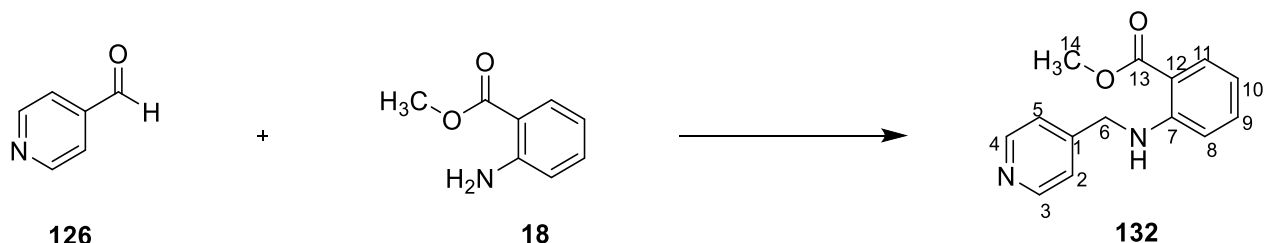
T.L.C. System: *n*-hexane-EtOAc 6:4 v/v, R_f: 0.30;Purification: Biotage Isolera One automated flash column chromatography (cartridge: ZIP KP 30g, *n*-hexane-EtOAc 100:0 increasing to *n*-hexane-EtOAc 20:80 in 15CV) ;

Yield: 0.427 g (90%);

¹H-NMR (CDCl₃), δ: 3.89 (s, 3H, H-14), 4.51 (d, J=5.7 Hz, 2H, H-6), 6.61 (d, J= 8.3 Hz, 1H, H-aromatic), 6.64-6.67 (m, 1H, H-aromatic), 7.28-7.30 (m, 1H, H-aromatic), 7.31-7.35 (m, 1H, H-aromatic), 7.69-7.72 (m, 1H, H-aromatic), 7.96 (dd, J₁= 8.0 Hz, J₂= 1.6 Hz, 1H, H-aromatic), 8.23 (bs, 1H, NH), 8.54-8.56 (m, 1H, H-aromatic), 8.65 (s, 1H, H-2).

¹³C-NMR (CDCl₃), δ: 51.6 (CH₃, C-14), 44.5 (CH₂, C-6), 111.5, 115.4, 123.6, 134.4, 134.7, 134.8, 148.6, 149.8 (CH, C-aromatic), 110.6, 131.7, 150.5 (C, C-aromatic), 169.1 (C, C-13).

UPLC-MS: Rt 1.40 (96%) MS (ESI)⁺: 243.1 [M+H]⁺.

Methyl 2-((pyridin-4-ylmethyl)amino)benzoate (132)**(C₁₄H₁₄N₂O₂; M.W.= 242.28)**Reagent: isonicotinaldehyde (**126**) (0.200 g, 1.86 mmol);Reagent: methyl 2-aminobenzoate (**18**) (0.282 g, 1.86 mmol);

General Procedure 11;

White Solid;

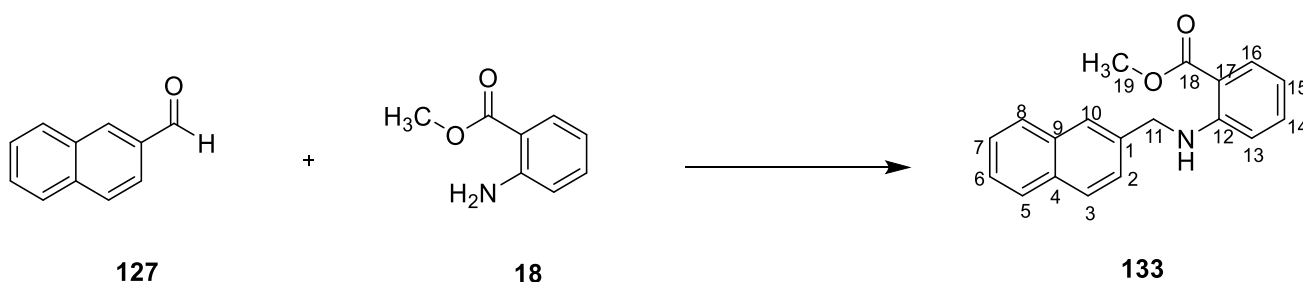
T.L.C. System: *n*-hexane-EtOAc 6:4 v/v, R_f: 0.25;Purification: Biotage Isolera One automated flash column chromatography (cartridge: ZIP KP 80g, *n*-hexane-EtOAc 100:0 increasing to *n*-hexane-EtOAc 40:60 in 15CV);

Yield: 0.403 g (89%);

¹H-NMR (CDCl₃), δ: 3.92 (s, 3H, H-14), 4.51 (d, J=5.6 Hz, 2H, H-6), 6.50 (d, J= 8.5 Hz, 1H, H-aromatic), 6.64-6.67 (m, 1H, H-aromatic), 7.29-7.33 (m, 3H, H-aromatic), 7.97 (d, J= 8.1 Hz, 1H, H-aromatic), 8.31 (bs, 1H, NH), 8.56-8.58 (m, 2H, H-aromatic).

¹³C-NMR (CDCl₃), δ: 51.6 (CH₃, C-14), 45.9 (CH₂, C-6), 111.5, 115.5, 121.8, 131.7, 134.6, 150.0 (CH, C-aromatic), 110.6, 148.4, 150.4 (C, C-aromatic), 169.1 (C, C-13).

UPLC-MS: Rt 1.44 (95%) MS (ESI)⁺: 243.1 [M+H]⁺.

Methyl 2-((naphthalen-2-ylmethyl)amino)benzoate (133)**(C₁₉H₁₇NO₂; M.W.= 291.35)**Reagent: 2-naphthaldehyde (**127**) (0.200 g, 1.28 mmol);Reagent: methyl 2-aminobenzoate (**18**) (0.193 g, 1.28 mmol);

General Procedure 11;

Yellow Solid;

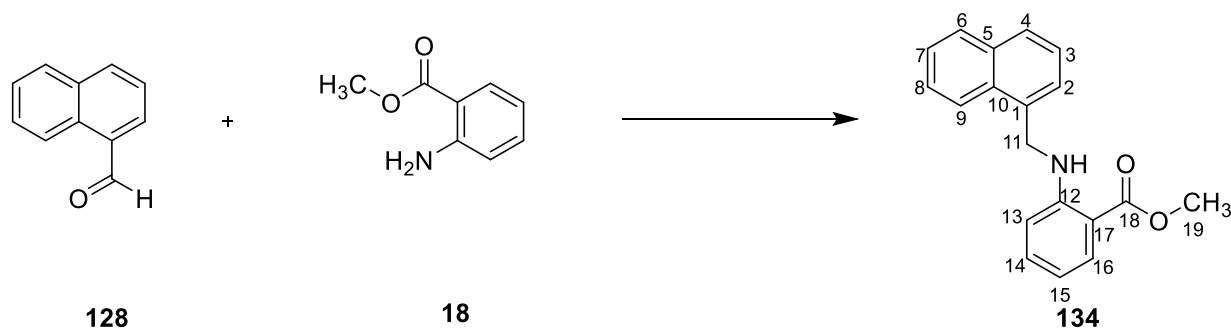
T.L.C. System: *n*-hexane-DCM 6:4 v/v, R_f: 0.64;Purification: Biotage Isolera One automated flash column chromatography (cartridge: ZIP KP 45g, *n*-hexane-DCM 100:0 increasing to *n*-hexane-DCM 20:80 in 15CV);

Yield: 0.285 g (76%);

¹H-NMR (CDCl₃), δ: 3.80 (s, 3H, H-19), 4.54 (d, J= 5.9 Hz, 2H, H-11), 6.50-6.54 (m, 1H, H-aromatic), 6.59 (d, J= 8.5 Hz, 1H, H-aromatic), 7.19-7.21 (m, 1H, H-aromatic), 7.35-7.37 (m, 1H, H-aromatic), 7.38-7.41 (m, 2H, H-aromatic), 7.70-7.72 (m, 2H, H-aromatic), 7.73-7.76 (m, 2H, H-aromatic), 7.86 (dd, J₁= 8.2 Hz, J₂= 1.6 Hz, 1H, H-aromatic), 8.20 (bs, 1H, NH).

¹³C-NMR (CDCl₃), δ: 51.5 (CH₃, C-19), 47.2 (CH₂, C-11), 111.8, 114.9, 125.3, 125.5, 125.6, 126.1, 127.70, 127.79, 128.4, 131.6, 134.6 (CH, C-aromatic), 110.3, 132.7, 133.5, 136.4, 151.0 (C, C-aromatic), 169.1 (C, C-18).

UPLC-MS: Rt 2.66 (100%) MS (ESI)⁺: 292.0 [M+H]⁺.

Methyl 2-((naphthalen-1-ylmethyl)amino)benzoate (134)**(C₁₉H₁₇NO₂; M.W.= 291.35)**Reagent: 1-naphthaldehyde (**128**) (0.200 g, 1.28 mmol);Reagent: methyl 2-aminobenzoate (**18**) (0.193 g, 1.28 mmol);

General Procedure 11;

White Solid;

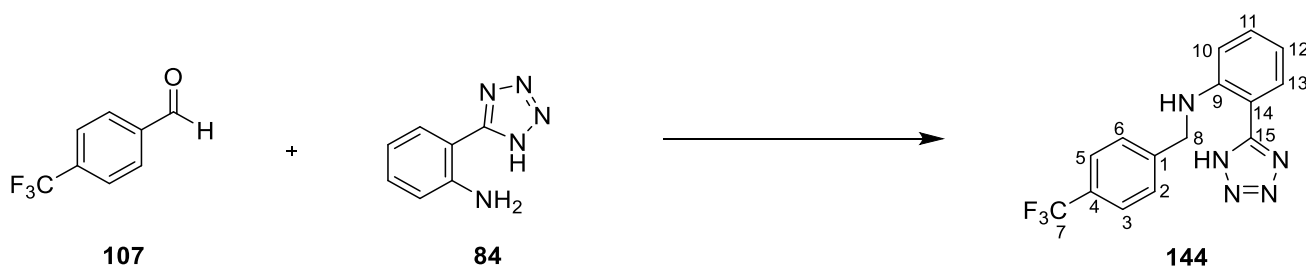
T.L.C. System: *n*-hexane-DCM 6:4 v/v, R_f: 0.51;Purification: Biotage Isolera One automated flash column chromatography (cartridge: ZIP KP 45g, *n*-hexane-DCM 100:0 increasing to *n*-hexane-DCM 20:80 in 10CV);

Yield: 0.295 g (79%);

¹H-NMR (CDCl₃), δ: 3.76 (s, 3H, H-19), 4.81 (d, J = 5.2 Hz, 2H, H-11), 6.53-6.57 (m, 1H, H-aromatic), 6.63 (d, J = 8.5 Hz, 1H, H-aromatic), 7.22-7.26 (m, 1H, H-aromatic), 7.32-7.35 (m, 1H, H-aromatic), 7.42-7.49 (m, 3H, H-aromatic), 7.71 (d, J = 8.3 Hz, 1H, H-aromatic), 7.81-7.83 (m, 1H, H-aromatic), 7.87 (dd, J₁ = 8.0 Hz, J₂ = 1.7 Hz, 1H, H-aromatic), 7.97 (d, J = 8.3 Hz, 1H, H-aromatic), 8.09 (bs, 1H, NH).

¹³C-NMR (CDCl₃), δ: 51.5 (CH₃, C-19), 44.9 (CH₂, C-11), 111.6, 114.9, 123.0, 125.1, 125.5, 125.7, 126.2, 127.9, 128.8, 131.6, 134.6 (CH, C-aromatic), 110.2, 131.3, 133.5, 133.8, 151.0 (C, C-aromatic), 169.0 (C, C-18).

UPLC-MS: Rt 2.66 (100%) MS (ESI)⁺: 292.0 [M+H]⁺.

2-(1H-Tetrazol-5-yl)-N-(4-(trifluoromethyl)benzyl)aniline (144)**(C₁₅H₁₂F₃N₅; M.W.= 319.29)**Reagent: 4-(trifluoromethyl)benzaldehyde (**107**) (0.100 g, 0.57 mmol);Reagent: 2-(1H-tetrazol-5-yl)aniline (**84**) (0.092 g, 0.57 mmol);

General Procedure 11;

White Solid;

T.L.C. System: *n*-hexane-EtOAc 6:4 v/v, R_f: 0.66;

Purification: Recrystallisation from EtOH/Water;

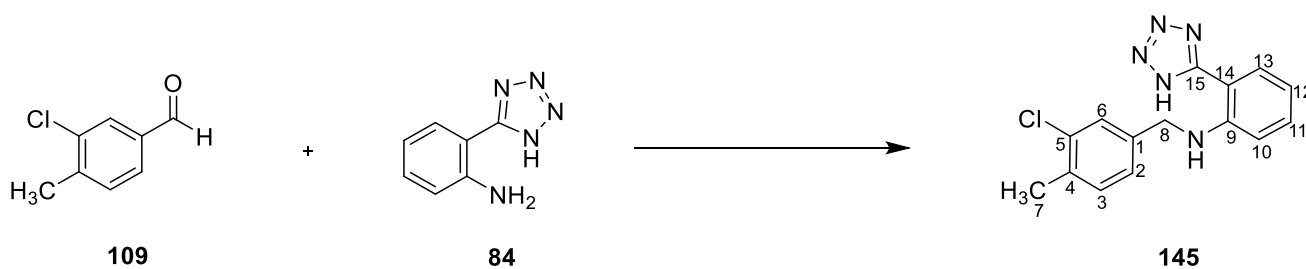
Yield: 0.059 g (32%);

¹H-NMR (DMSO-D₆), δ: 4.70 (s, 2H, H-8), 6.73-6.78 (m, 2H, H-aromatic), 7.28-7.31 (m, 1H, H-aromatic), 7.59 (d, J= 8.1 Hz, 2H, H-aromatic), 7.71 (d, J= 8.1 Hz, 2H, H-aromatic), 7.82-7.84 (m, 1H, H-aromatic)

¹³C-NMR (DMSO-D₆), δ: 46.1 (CH₂, C-8), 112.4, 116.3, 125.8, 128.1, 129.0, 132.7 (CH, C-aromatic), 106.3, 123.7, 127.9, 145.1, 146.7 (C-aromatic).

¹⁹F-NMR (DMSO-D₆), δ: -60.71 (s, 3F).

UPLC-MS: Rt 1.95 (>99%) MS (ESI)⁺: 320.1 [M+H]⁺.

N*-(3-Chloro-4-methylbenzyl)-2-(1*H*-tetrazol-5-yl)aniline (145)*(C₁₅H₁₄ClN₅; M.W.= 299.76)**Reagent: 3-chloro-4-methylbenzaldehyde (**109**) (0.096 g, 0.62 mmol);Reagent: 2-(1*H*-tetrazol-5-yl)aniline (**84**) (0.100 g, 0.62 mmol);

General Procedure 11;

White Solid;

T.L.C. System: *n*-hexane-EtOAc 6:4 v/v, R_f: 0.37;Purification1: Biotage Isolera One automated flash column chromatography (cartridge: SNAP KP 25g, *n*-hexane-EtOAc 100:0 increasing to *n*-hexane-EtOAc 20:80 in 15CV);

Purification2: Recrystallisation from DCM;

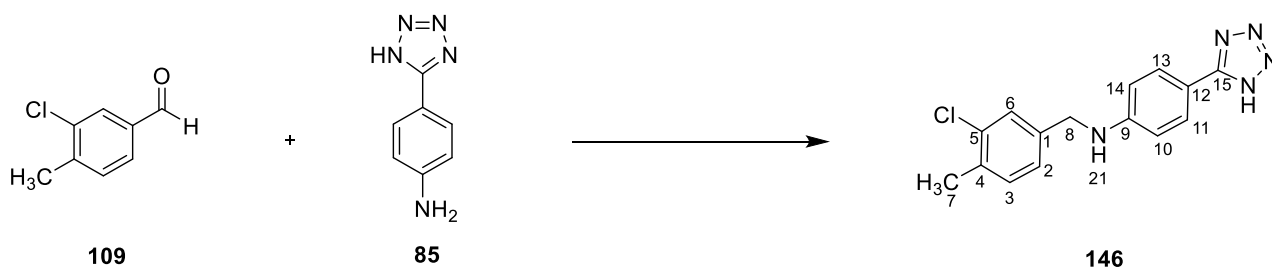
Purification3: Recrystallisation from EtOH/Water;

Yield: 0.036 g (25%);

¹H-NMR (DMSO-*D*₆), δ: 2.30 (s, 3H, H-7), 4.54 (s, 2H, H-8), 6.74-6.78 (m, 2H, H-aromatic), 7.25 (d, J= 7.5 Hz, 1H, H-aromatic), 7.30-7.32 (m, 2H, H-aromatic), 7.41 (s, 1H, H-6), 7.81 (d, J= 7.5 Hz, 1H, H-aromatic).

¹³C-NMR (DMSO-*D*₆), δ: 19.6 (CH₃, C-7), 45.8 (CH₂, C-8), 112.4, 116.2, 126.2, 127.7, 128.9, 131.8, 132.7 (CH, C-aromatic), 133.0, 133.7, 134.3, 138.7, 139.8 (C, C-aromatic), 149.7 (C, C-15).

UPLC-MS: Rt 2.33 (100%) MS (ESI)⁺: 300.0 [M+H]⁺.

N*-(3-Chloro-4-methylbenzyl)-4-(1*H*-tetrazol-5-yl)aniline (**146**)*(C₁₅H₁₄ClN₅; M.W.= 299.76)**Reagent: 3-chloro-4-methylbenzaldehyde (**109**) (0.096 g, 0.62 mmol);Reagent: 4-(1*H*-tetrazol-5-yl)aniline (**85**) (0.100 g, 0.62 mmol);

General Procedure 11;

White Solid;

T.L.C. System: DCM-MeOH 95:5 v/v, R_f: 0.75;

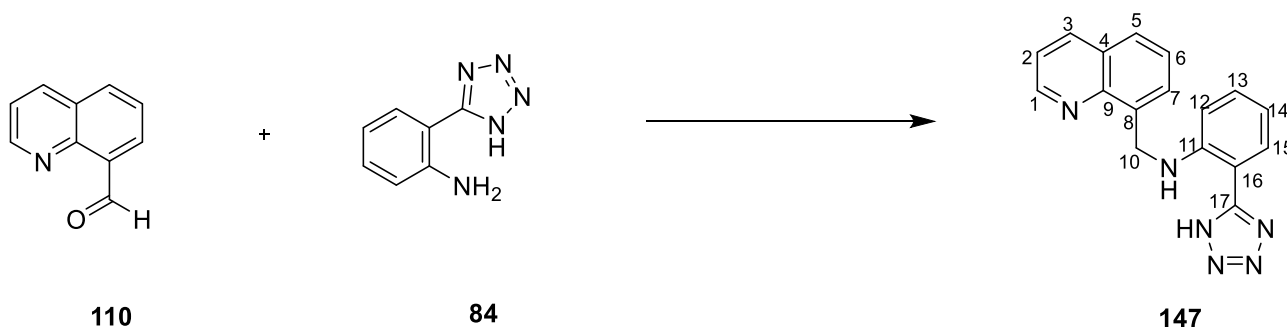
Purification: Biotage Isolera One automated flash column chromatography (cartridge: SNAP KP 25g, DCM-MeOH 100:0 increasing to DCM-MeOH 90:10 in 10CV);

Yield: 0.027 g (15%);

¹H-NMR (DMSO-*D*₆), δ : 2.29 (s, 3H, H-7), 4.33 (d, *J* = 5.9 Hz, 2H, H-8), 6.72 (d, 2H, *J* = 8.7 Hz, H-aromatic), 6.94 (t, *J* = 5.9 Hz, 1H, NH), 7.23 (d, *J* = 7.9 Hz, 1H, H-3), 7.31 (d, *J* = 7.9 Hz, 1H, H-2), 7.40 (s, 1H, H-6), 7.72 (d, *J* = 8.7 Hz, 2H, H-aromatic).

¹³C-NMR (DMSO-*D*₆), δ : 19.6 (CH₃, C-7), 45.4 (CH₂, C-8), 112.8, 126.4, 127.8, 128.6, 131.6 (CH, C-aromatic), 118.4, 133.8, 134.1, 140.0 (C, C-aromatic), 151.1 (C, C-14).

UPLC-MS: R_t 2.05 (>98%) MS (ESI)⁺: 300.1 [M+H]⁺.

N*-(Quinolin-8-ylmethyl)-2-(1*H*-tetrazol-5-yl)aniline (147)*(C₁₇H₁₄N₆; M.W.= 302.34)**Reagent: quinoline-8-carbaldehyde (**110**) (0.098 g, 0.62 mmol);Reagent: 2-(1*H*-tetrazol-5-yl)aniline (**84**) (0.100 g, 0.62 mmol);

General Procedure 11;

Yellow Solid;

T.L.C. System: *n*-hexane-EtOAc 5:5 v/v, R_f: 0.41;Purification1: Biotage Isolera One automated flash column chromatography (cartridge: SNAP KP 25g, *n*-hexane-EtOAc 100:0 increasing to *n*-hexane-EtOAc 0:100 in 15CV);

Purification2: Biotage Isolera One automated flash column chromatography (cartridge: SNAP KP 10g, DCM-MeOH 100:0 increasing to DCM-MeOH 98:2 in 15CV);

Purification3: Recrystallisation from EtOH/Water;

Yield: 0.023 g (12%);

¹H-NMR (DMSO-*D*₆), δ: 5.18 (s, 2H, H-10), 6.71-6.74 (m, 1H, H-aromatic), 6.75-6.78 (m, 1H, H-aromatic), 7.27-7.30 (m, 1H, H-aromatic), 7.55-7.58 (m, 1H, H-aromatic), 7.59-7.62 (m, 1H, H-aromatic), 7.73-7.75 (m, 1H, H-aromatic), 7.80-8.82 (m, 1H, H-aromatic), 7.90-7.92 (m, 1H, H-aromatic), 8.40-8.42 (m, 1H, H-aromatic), 8.98-9.00 (m, 1H, H-aromatic).

¹³C-NMR (DMSO-*D*₆), δ: 43.0 (CH₂, C-10), 112.3, 115.9, 122.0, 126.8, 127.7, 127.9, 128.9, 132.8, 136.9, 150.3 (CH, C-aromatic), 128.4, 146.2, 147.1 (C-aromatic).

UPLC-MS: Rt 1.68 (>96%) MS (ESI)⁺: 303.3 [M+H]⁺.

N*-(Quinolin-3-ylmethyl)-2-(1*H*-tetrazol-5-yl)aniline (**148**)*(C₁₇H₁₄N₆; M.W.= 302.34)**Reagent: quinoline-3-carbaldehyde (**111**) (0.097 g, 0.62 mmol);Reagent: 2-(1*H*-tetrazol-5-yl)aniline (**84**) (0.100 g, 0.62 mmol);

General Procedure 11;

Yellow Solid;

T.L.C. System: DCM-MeOH 98:2 v/v, R_f: 0.32;

Purification1: Trituration from MeOH;

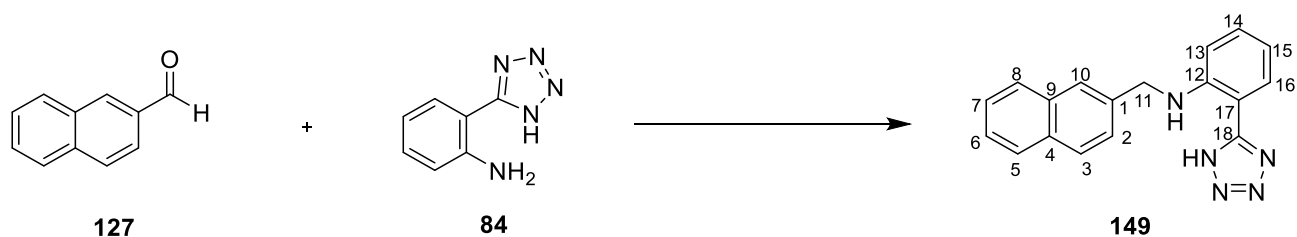
Purification2: Biotage Isolera One automated flash column chromatography (cartridge: SNAP KP 10g, DCM-MeOH 100:0 increasing to DCM-MeOH 90:10 in 20CV);

Yield: 0.0084 g (11%);

¹H-NMR (DMSO-*D*₆), δ: 4.82 (s, 2H, H-10), 6.5-6.78 (m, 1H, H-aromatic), 6.86-6.88 (m, 1H, H-aromatic), 7.29-31 (m, 1H, H-aromatic), 7.58-7.61 (m, 1H, H-aromatic), 7.72-7.75 (m, 1H, H-aromatic), 7.83-7.85 (m, 1H, H-aromatic), 7.92-7.95 (m, 1H, H-aromatic), 8.01-8.03 (m, 1H, H-aromatic), 8.29 (s, 1H, H-1), 8.97 (s, 1H, H-3).

¹³C-NMR (DMSO-*D*₆), δ: 49.0 (CH₂, C-10), 112.4, 116.3, 127.2, 128.3, 129.0, 129.1, 129.6, 132.6, 133.8, 151.2 (CH, C-aromatic), 106.7, 127.9, 132.9, 146.6, 147.3 (C-aromatic).

UPLC-MS: R_t 1.59 (>96%) MS (ESI)⁺: 303.1 [M+H]⁺.

N*-(Naphthalen-2-ylmethyl)-2-(1*H*-tetrazol-5-yl)aniline (149)*(C₁₈H₁₅N₅; M.W.= 301.35)**Reagent: 2-naphthaldehyde (**127**) (0.100 g, 0.64 mmol);Reagent: 2-(1*H*-tetrazol-5-yl)aniline (**84**) (0.103 g, 0.64 mmol);

General Procedure 11;

White Solid;

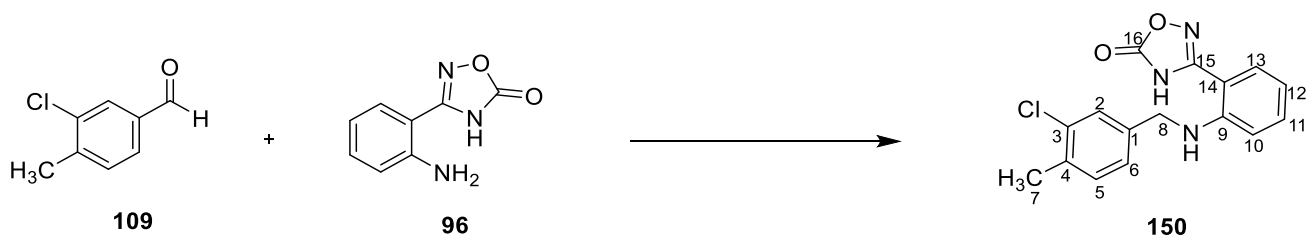
T.L.C. System: *n*-hexane-EtOAc 6:4 v/v, R_f: 0.57;Purification: Biotage Isolera One automated flash column chromatography (cartridge: SNAP KP 25g, *n*-hexane-EtOAc 100:0 increasing to *n*-hexane-EtOAc 30:70 in 15CV);

Yield: 0.144 g (75%);

¹H-NMR (DMSO-*D*₆), δ : 4.74 (s, 2H, H-11), 6.74-6.77 (m, 1H, H-aromatic), 6.85 (d, *J*=8.3 Hz, 1H, H-aromatic), 7.28-7.31 (m, 1H, H-aromatic), 7.47-7.52 (m, 2H, H-aromatic), 7.54 (d, *J*= 8.3 Hz, 1H, H-aromatic), 7.81-7.87 (m, 2H, H-aromatic), 7.90-7.92 (m, 3H, H-aromatic).

¹³C-NMR (DMSO-*D*₆), δ : 46.9 (CH₂, C-11), 112.5, 116.1, 125.8, 126.1, 126.1, 126.7, 128.0, 128.0, 128.6, 128.9, 132.70 (CH, C-aromatic), 132.72, 133.4, 137.8, 147.0 (C, C-aromatic).

UPLC-MS: Rt 1.97 (>98%) MS (ESI)⁻: 300.2 [M-H]⁻.

3-(2-((3-Chloro-4-methylbenzyl)amino)phenyl)-1,2,4-oxadiazol-5(4H)-one (150)**(C₁₆H₁₄ClN₃O₂; M.W.= 315.76)**Reagent: 3-chloro-4-methylbenzaldehyde (**109**) (0.070 g, 0.45 mmol);Reagent: 3-(2-aminophenyl)-1,2,4-oxadiazol-5(4H)-one (**96**) (0.080 g, 0.45 mmol);

General Procedure 11;

Off-White Solid;

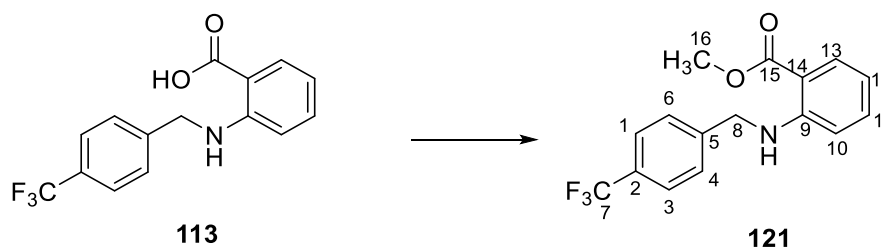
T.L.C. System: *n*-hexane-EtOAc 6:4 v/v, R_f: 0.57;Purification: Biotage Isolera One automated flash column chromatography (cartridge: SNAP KP 25g, *n*-hexane-EtOAc 100:0 increasing to *n*-hexane-EtOAc 20:80 in 12CV);

Yield: 0.057 g (40%);

¹H-NMR (DMSO-D₆), δ: 2.37 (s, 3H, H-7), 4.50 (s, 2H, H-8), 6.70-6.73 (m, 2H, H-aromatic), 7.08 (bs, 1H, NH), 7.21 (d, J= 7.2 Hz, 1H, H-aromatic), 7.30-7.33 (m, 2H, H-aromatic), 7.39 (s, 1H, H-2), 7.55 (d, J= 7.2 Hz, 1H, H-aromatic), 12.79 (bs, 1H, NH).¹³C-NMR (DMSO-D₆), δ: 19.6 (CH₃, C-7), 45.7 (CH₂, C-8), 112.3, 116.1, 126.2, 127.7, 129.0, 131.8, 133.3 (CH, C-aromatic), 105.5, 133.7, 134.3, 139.5, 146.9, 158.7 (C, C-aromatic), 159.5 (C, C-15).UPLC-MS: R_t 2.35 (>99%) MS (ESI)⁻: 314.1 [M-H]⁻.

9.3.2 Methyl((aryl)amino)benzoates (121-124)

Methyl 2-((4-(trifluoromethyl)benzyl)amino)benzoate (121)

(C₁₆H₁₄F₃NO₂; M.W.= 309.29)

Reagent: 2-((4-(trifluoromethyl)benzyl)amino)benzoic acid (**113**) (0.050 g, 0.17 mmol);

General Procedure 12;

Yellow solid;

T.L.C. System: *n*-hexane-EtOAc 7:3 v/v, R_f: 0.40;

Purification: Biotage Isolera One automated flash column chromatography (cartridge: SNAP KP SIL 10g, *n*-hexane-EtOAc 100:0 increasing to *n*-hexane-EtOAc 70:30 in 15CV);

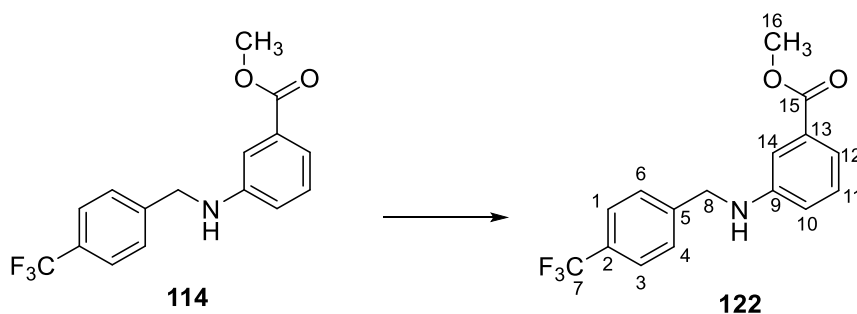
Yield: 0.023 g (44%);

¹H-NMR (CDCl₃), δ: 3.81 (s, 3H, H-16), 4.45 (d, J= 5.8 Hz, 2H, H-8), 6.45-6.48 (m, 1H, H-aromatic), 6.54-6.57 (m, 1H, H-aromatic), 7.20-7.24 (m, 1H, H-aromatic), 7.39 (d, J= 8.0 Hz, 2H, H-aromatic), 7.52 (d, J= 8.0 Hz, 2H, H-aromatic), 7.85-7.88 (m, 1H, H-aromatic), 8.18 (bs, 1H, NH).

¹³C-NMR (CDCl₃), δ: 51.6 (CH₃, C-16), 46.5 (CH₂, C-8), 111.5, 115.3, 125.6, 125.7, 131.7, 134.6 (CH, C-aromatic), 110.5, 125.6, 129.3, 143.1, 150.6 (C, C-aromatic), 169.1 (C, C-15).

¹⁹F-NMR (CDCl₃), δ: -62.43 (s, 3F).

UPLC-MS: Rt 2.60 (>98%) MS (ESI)⁺: 310.1 [M+H]⁺.

Methyl 3-((4-(trifluoromethyl)benzyl)amino)benzoate (122)**(C₁₆H₁₄F₃NO₂; M.W.= 309.29)**

Reagent: 3-((4-(trifluoromethyl)benzyl)amino)benzoic acid (**114**) (0.050 g, 0.17 mmol);

General Procedure 12;

White solid;

T.L.C. System: *n*-hexane-EtOAc 5:5 v/v, R_f: 0.61;

Purification: Biotage Isolera One automated flash column chromatography (cartridge: ZIP KP SIL 10g, *n*-hexane-EtOAc 100:0 increasing to *n*-hexane-EtOAc 50:50 in 10CV);

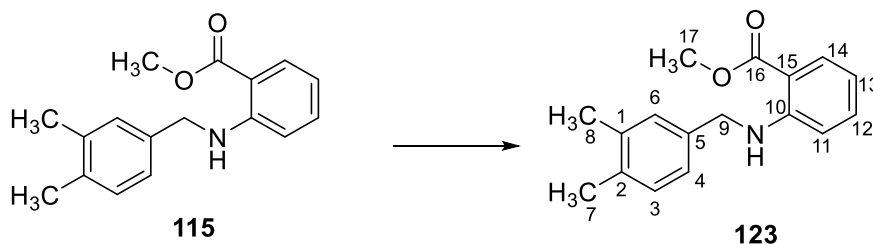
Yield: 0.020 g (38%);

¹H-NMR (CDCl₃), δ: 3.81 (s, 3H, H-16), 4.19 (bs, 1H, NH), 4.38 (s, 2H, H-8), 6.68-6.71 (m, 1H, H-aromatic), 7.13-7.17 (m, 1H, H-aromatic), 7.23-7.25 (m, 1H, H-aromatic), 7.31-7.34 (m, 1H, H-aromatic), 7.41 (d, J= 8.0 Hz, 2H, H-aromatic), 7.53 (d, J= 8.0 Hz, 2H, H-aromatic).

¹³C-NMR (CDCl₃), δ: 52.0 (CH₃, C-16), 47.7 (CH₂, C-8), 113.6, 117.3, 119.2, 125.6, 127.5, 129.3 (CH, C-aromatic), 123.0, 129.2, 131.2, 143.0, 147.5 (C, C-aromatic), 167.3 (C, C-15).

¹⁹F-NMR (CDCl₃), δ: -62.51 (s, 3F).

UPLC-MS: Rt 2.38 (>99%) MS (ESI)⁺: 310.1 [M+H]⁺.

Methyl 2-((3,4-dimethylbenzyl)amino)benzoate (123)**(C₁₇H₁₉NO₂; M.W.= 269.34)**Reagent: methyl 2-((3,4-dimethylbenzyl)amino)benzoate (**115**) (0.070 g, 0.27 mmol);

General Procedure 12;

Yellow solid;

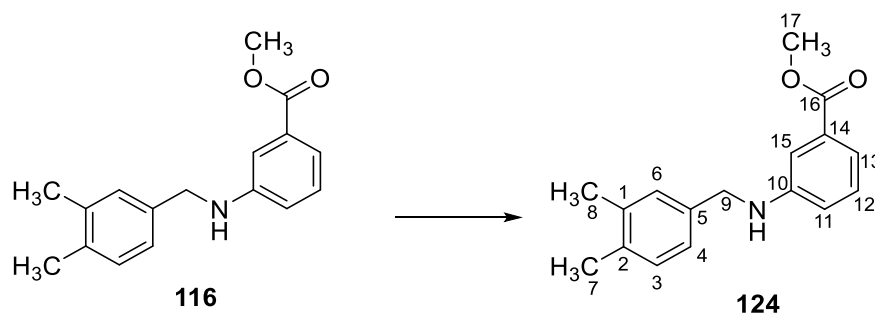
T.L.C. System: *n*-hexane-EtOAc 7:3 v/v, R_f: 0.65;Purification1: Biotage Isolera One automated flash column chromatography (cartridge: ZIP KP SIL 10g, *n*-hexane-EtOAc 100:0 increasing to *n*-hexane-EtOAc 70:30 in 10CV);Purification2: Biotage Isolera One automated flash column chromatography (cartridge: ZIP KP SIL 10g, *n*-hexane-EtOAc 100:0 increasing to *n*-hexane-EtOAc 80:20 in 10CV);Purification3: Biotage Isolera One automated flash column chromatography (cartridge: ZIP KP SIL 10g, *n*-hexane-EtOAc 100:0 increasing to *n*-hexane-EtOAc 90:10 in 10CV);

Yield: 0.010 g (13%);

¹H-NMR (CDCl₃), δ: 2.17 (d, J= 3.7 Hz, 6H, H-7,8), 3.77 (s, 3H, H-17), 4.30 (d, J=5.4 Hz, 2H, H-9), 6.49-6.52 (m, 1H, H-aromatic), 6.56-6.59 (m, 1H, H-aromatic), 7.00-7.02 (m, 2H, H-aromatic), 7.04 (s, 1H, H-aromatic), 7.20-7.23 (m, 1H, H-aromatic), 7.83 (dd, J₁= 8.0 Hz, J₂= 1.6 Hz, 1H, H-aromatic), 8.01 (bs, 1H, NH).

¹³C-NMR (CDCl₃), δ: 19.4 (CH₃), 19.8 (CH₃), 51.4 (CH₃, C-17), 46.83(CH₂, C-9), 111.6, 114.7, 124.5, 128.5, 129.9, 131.5, 134.6 (CH, C-aromatic), 110.1, 135.4, 136.2, 136.8, 151.0 (C, C-aromatic), 169.1 (C-16).

UPLC-MS: Rt 2.68 (>99%) MS (ESI)⁺: 270.1 [M+H]⁺.

Methyl 3-((3,4-dimethylbenzyl)amino)benzoate (124)**(C₁₇H₁₉NO₂; M.W.= 269.34)**

Reagent: methyl 3-((3,4-dimethylbenzyl)amino)benzoate (**116**) (0.070 g, 0.27 mmol);

General Procedure 12;

Yellow solid;

T.L.C. System: *n*-hexane-EtOAc 7:3 v/v, R_f: 0.60;

Purification1: Biotage Isolera One automated flash column chromatography (cartridge: ZIP KP SIL 10g, *n*-hexane-EtOAc 100:0 increasing to *n*-hexane-EtOAc 60:40 in 10CV);

Purification2: Biotage Isolera One automated flash column chromatography (cartridge: ZIP KP SIL 10g, *n*-hexane-EtOAc 100:0 increasing to *n*-hexane-EtOAc 70:30 in 10CV);

Yield: 0.019 g (26%);

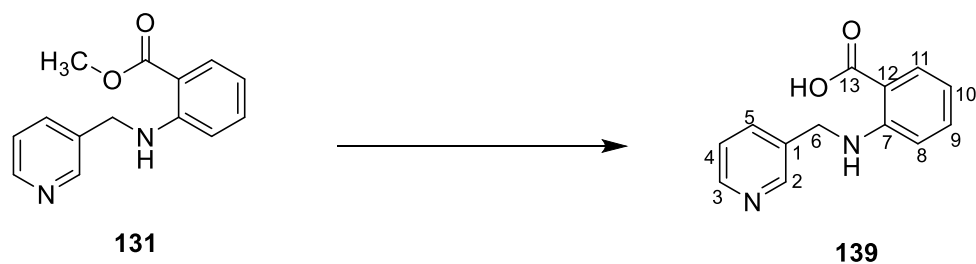
¹H-NMR (CDCl₃), δ: 2.18 (d, J= 2.5 Hz, 6H, H-7,8), 3.80 (s, 3H, H-17), 4.01 (bs, 1H, NH), 4.20 (s, 2H, H-9), 6.71 (dd, J₁= 8.0 Hz, J₂= 2.2 Hz, 1H, H-aromatic), 7.00-7.04 (m, 2H, H-aromatic), 7.06 (s, 1H, H-6), 7.11-7.15 (m, 1H, H-aromatic), 7.17 (s, 1H, H-15), 7.29 (d, J= 7.7 Hz, 1H, H-aromatic).

¹³C-NMR (CDCl₃), δ: 19.4 (CH₃), 19.8 (CH₃), 52.0 (CH₃, C-17), 48.0 (CH₂, C-9), 113.5, 117.2, 117.5, 118.6, 125.9, 129.0, 129.9 (CH, C-aromatic), 131.0, 135.7, 136.2, 136.9, 148.2 (C, C-aromatic), 167.5 (C, C-16).

UPLC-MS: Rt 2.42 (>99%) MS (ESI)⁺: 270.1 [M+H]⁺.

9.3.3 (Aryl)amino)benzoic acids (139-143, 156)

2-((Pyridin-3-ylmethyl)amino)benzoic acid (139)

(C₁₃H₁₂N₂O₂; M.W. = 228.25)

Reagent: methyl 2-((pyridin-3-ylmethyl)amino)benzoate (**131**) (0.100 g, 0.41 mmol);

General Procedure 13;

White Solid;

T.L.C. System: *n*-hexane-EtOA: 5:5 v/v, R_f: 0.30;

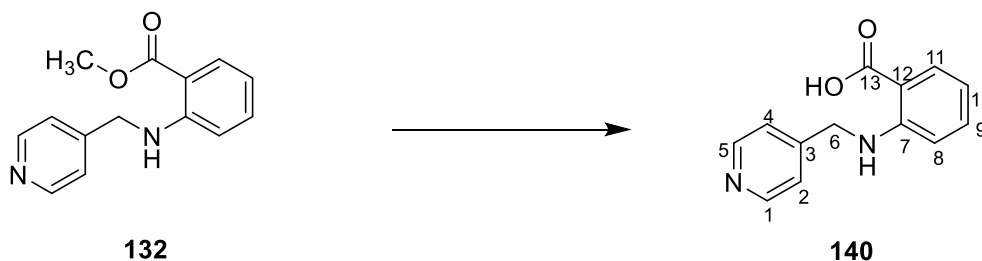
Purification: Recrystallisation from EtOH;

Yield: 0.026 g (28%);

¹H-NMR (DMSO-D₆), δ: 4.52 (s, 2H, H-6), 6.56-6.60 (m, 1H, H-aromatic), 6.69 (d, J = 8.4 Hz, 1H, H-aromatic), 7.29-7.30 (m, 1H, H-aromatic), 7.34 (dd, J₁ = 7.7 Hz, J₂ = 4.7 Hz, 1H, H-4), 7.73 (d, J = 7.7 Hz, 1H, H-5), 7.81 (dd, J₁ = 8.0 Hz, J₂ = 1.4 Hz, 1H, H-aromatic), 8.30 (bs, 1H, NH), 7.47 (d, J = 4.7 Hz, 1H, H-3), 8.59 (s, 1H, H-2), 12.76 (bs, 1H, OH).

¹³C-NMR (DMSO-D₆), δ: 43.7 (CH₂, C-6), 112.1, 115.2, 124.1, 132.2, 134.8, 135.3, 148.6, 149.1 (CH, C-aromatic), 111.1, 135.4, 150.8 (C, C-aromatic), 170.4 (C, C-13).

UPLC-MS: R_t 1.20 (>98%) MS (ESI)⁺: 229.1 [M+H]⁺.

2-((Pyridin-4-ylmethyl)amino)benzoic acid (140)**(C₁₃H₁₂N₂O₂; M.W.= 228.25)**Reagent: methyl 2-((pyridin-4-ylmethyl)amino)benzoate (**132**) (0.100 g, 0.41 mmol);

General Procedure 13;

White Solid;

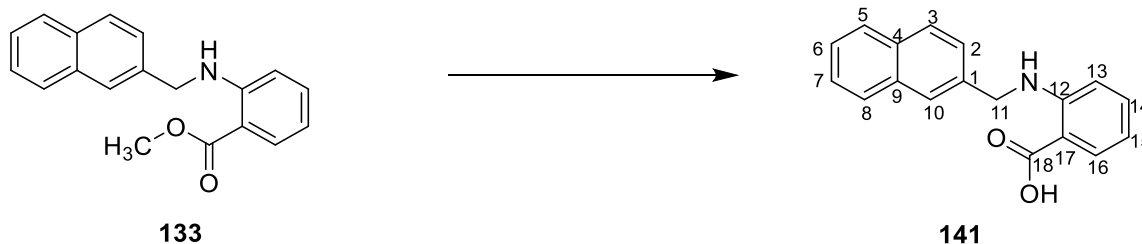
T.L.C. System: *n*-hexane-EtOAc 5:5 v/v, R_f: 0.20;

Purification1: Recrystallization from EtOH;

Purification2: Biotage Isolera One automated flash column chromatography (cartridge: SNAP KP 10g, *n*-hexane-EtOAc 100:0 increasing to *n*-hexane-EtOAc 0:100 in 6CV and EtOAc-MeOH 80:20 in 10CV);

Yield: 0.025 g (26%);

¹H-NMR (DMSO-D₆), δ: 4.54 (s, 2H, H-6), 6.53-6.56 (m, 1H, H-aromatic), 6.57-6.59 (m, 1H, H-aromatic), 7.24-7.28 (m, 1H, H-aromatic), 7.32 (d, J= 7.8 Hz, 2H, H-aromatic), 7.82 (d, J= 7.8 Hz, 2H, H-aromatic), 8.48-8.53 (m, 2H, H-aromatic + NH), 12.74 (bs, 1H, OH).**¹³C-NMR (DMSO-D₆), δ:** 45.1 (CH₂, C-6), 112.0, 115.6, 129.4, 132.2, 135.0, 150.6 (CH, C-aromatic), 118.6, 136.5, 149.8 (C, C-aromatic), 151.1 (C, C-13).**UPLC-MS: Rt 1.23 (100%) MS (ESI)⁺: 229.1 [M+H]⁺.**

2-((Naphthalen-2-ylmethyl)amino)benzoic acid (141)**(C₁₈H₁₅NO₂; M.W.= 277.32)**Reagent: methyl 2-((naphthalen-2-ylmethyl)amino)benzoate (**133**) (0.100 g, 0.34 mmol);

General Procedure 13;

White Solid;

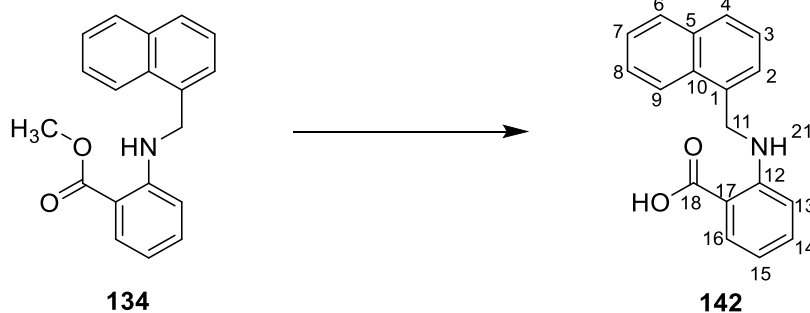
T.L.C. System: *n*-hexane-EtOA: 6:4 v/v, R_f: 0.84;

Yield: 0.084 g (89%);

¹H-NMR (DMSO-D₆), δ: 4.64 (s, 2H, H-11), 6.54-6.58 (m, 1H, H-aromatic), 6.72 (d, J= 8.2 Hz, 1H, H-aromatic), 7.27-7.30 (m, 1H, H-aromatic), 7.47-7.53 (m, 3H, H-aromatic), 7.82 (dd, J₁= 7.9 Hz, J₂= 1.5 Hz, 1H, H-aromatic), 7.85-7.88 (m, 2H, H-aromatic), 7.89-7.92 (m, 2H, H-aromatic), 8.41 (bs, 1H, NH), 12.68 (bs, 1H, OH).

¹³C-NMR (DMSO-D₆), δ: 45.5 (CH₂, C-11), 112.2, 115.0, 125.6, 126.0, 126.1, 126.7, 128.01, 128.04, 128.6, 132.1, 134.8 (CH, C-aromatic), 110.8, 132.7, 133.4, 137.5, 151.1 (C, C-aromatic), 170.5 (C, C-18).

UPLC-MS: Rt 2.32 (99%) MS (ESI)⁺: 278.0 [M+H]⁺.

2-((1-Naphthalen-1-ylmethyl)amino)benzoic acid (142)**(C₁₈H₁₅NO₂; M.W.= 277.32)**Reagent: methyl 2-((naphthalen-1-ylmethyl)amino)benzoate (**134**) (0.1 g, 0.34 mmol);

General Procedure 13;

White Solid;

T.L.C. System: *n*-hexane-EtOAc 7:3 v/v, R_f: 0.50;

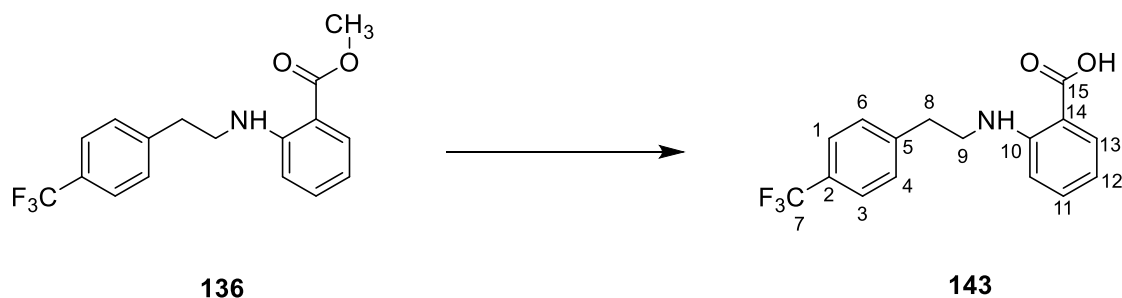
Purification: Recrystallisation from EtOH;

Yield: 0.039 g (41%);

¹H-NMR (DMSO-D₆), δ: 4.91 (s, 2H, H-11), 6.51-6.61 (m, 1H, H-aromatic), 6.78 (dd, J₁= 8.7 Hz, J₂= 0.4 Hz, 1H, H-aromatic), 7.32-7.35 (m, 1H, H-aromatic), 7.46-7.50 (m, 2H, H-aromatic), 7.55-7.61 (m, 2H, H-aromatic), 7.83 (dd, J₁= 7.9 Hz, J₂= 1.6 Hz, 1H, H-aromatic), 7.87 (dd, J₁= 7.4 Hz, J₂= 1.3 Hz, 1H, H-aromatic), 7.97-8.00 (m, 1H, H-aromatic), 8.11-8.12 (m, 1H, H-aromatic), 8.26 (bs, 1H, NH), 12.63 (bs, 1H, OH).

¹³C-NMR (DMSO-D₆), δ: 44.4 (CH₂, C-11), 112.1, 115.0, 123.8, 125.3, 126.0, 126.3, 126.7, 128.1, 129.0, 132.1, 134.9 (CH, C-aromatic), 110.7, 131.3, 133.9, 134.6 (C, C-aromatic), 170.4 (C, C-18).

UPLC-MS: R_t 2.33 (99%) MS (ESI)⁺: 278.1 [M+H]⁺.

2-((4-(Trifluoromethyl)phenethyl)amino)benzoic acid (143)**(C₁₆H₁₄F₃NO₂; M.W.= 309.29)**Reagent: methyl 2-((4-(trifluoromethyl)phenethyl)amino)benzoate (**136**) (0.035 g, 0.1 mmol);

General Procedure 13;

Pale Yellow Solid;

T.L.C. System: *n*-hexane-EtOAc 6:4 v/v, R_f: 0.10;

Purification: Recrystallisation from EtOH/Water;

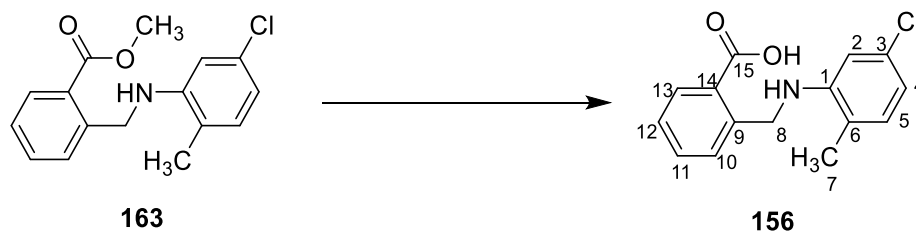
Yield: 0.005 g (16%);

¹H-NMR (CDCl₃), δ: 3.07 (t, J= 7.06 Hz, 2H, H-alkyl), 3.54 (t, J= 7.06 Hz, 2H, H-alkyl), 6.66-6.69 (m, 1H, H-aromatic), 6.74-6.76 (m, 1H, H-aromatic), 7.41 (d, J= 7.7 Hz, 2H, H-aromatic), 7.44-7.46 (m, 1H, H-aromatic), 7.62 (d, J= 7.7 Hz, 2H, H-aromatic), 7.72 (bs, 1H, NH), 8.01 (dd, J₁= 7.9 Hz, J₂= 1.3 Hz, 1H, H-aromatic), 11.24 (bs, 1H, OH).

¹³C-NMR (CDCl₃), δ: 35.3, 43.9 (2xCH₂, C-8,9), 111.2, 115.0, 125.5, 129.1, 132.7, 135.7 (CH, C-aromatic), 128.8 (d, J= 32.42 Hz, C) 102.5, 108.7, 143.1, 151.3 (C, C-aromatic), 173.2 (C, C-15).

¹⁹F-NMR (CDCl₃), δ: -62.3 (s, 3F).

UPLC-MS: Rt 2.37 (100%) **MS (ESI)⁺:** 310.1 [M+H]⁺.

2-(((5-Chloro-2-methylphenyl)amino)methyl)benzoic acid (**156**)**(C₁₅H₁₄ClNO₂; M.W.= 275.73)**Reagent: methyl 2-(((5-chloro-2-methylphenyl)amino)methyl)benzoate (**163**) (0.040 g, 0.13 mmol);

General Procedure13;

White Solid;

T.L.C. System: DCM-MeOH 98:2 v/v, Rf: 0.47;

Purification: Biotage Isolera One automated flash column chromatography (cartridge: SNAP KP SIL 10g, DCM-MeOH 100:0 increasing to DCM-MeOH 95:5 in 10CV) ;

Yield: 0.018 g (53%);

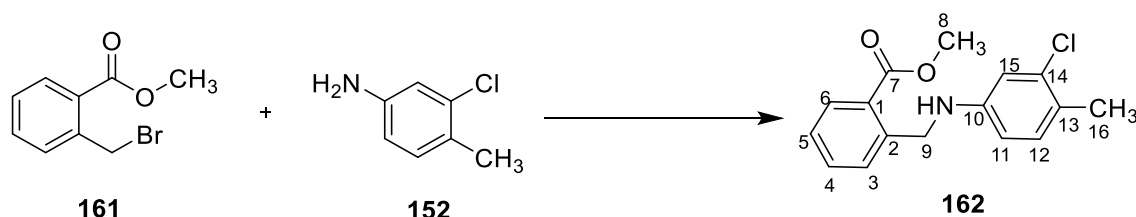
¹H-NMR (DMSO-D₆), δ: 2.14 (s, 3H, H-7), 4.68 (s, 2H, H-8), 5.94 (bs, 1H, NH), 6.23 (d, J= 2.0 Hz, 1H, H-2), 6.47 (dd, J₁= 7.8 Hz, J₂= 2.0 Hz, 1H, H-4), 6.97 (d, J= 7.8 Hz, 1H, H-5), 7.33-7.37 (m, 1H, H-aromatic), 7.42 (d, J= 7.3 Hz, 1H, H-aromatic), 7.49-7.52 (m, 1H, H-aromatic), 7.89 (dd, J₁= 7.7 Hz, J₂= 1.2 Hz, 1H, H-aromatic), 13.09 (bs, 1H, OH).

¹³C-NMR (DMSO-D₆), δ: 17.6 (CH₃, C-7), 45.2 (CH₂, C-8), 109.0, 115.3, 127.2, 128.0, 131.0, 131.4, 132.4 (CH, C-aromatic), 121.1, 130.1, 131.6, 141.3, 147.9 (C, C-aromatic), 169.1 (C, C-15).

UPLC-MS: Rt 2.19 (100%) MS (ESI)⁺: 276.0 [M+H]⁺.

9.3.4 Methyl 2-(aryl)amino)methyl)benzoates (162-164)

Methyl 2-(((3-chloro-4-methylphenyl)amino)methyl)benzoate (162)

(C₁₆H₁₆ClNO₂; M.W.= 289.76)Reagent: 3-chloro-4-methylaniline (**152**) (0.062 g, 0.43 mmol);Reagent: methyl 2-(bromomethyl)benzoate (**61**) (0.200 g, 0.87 mmol);

General Procedure14;

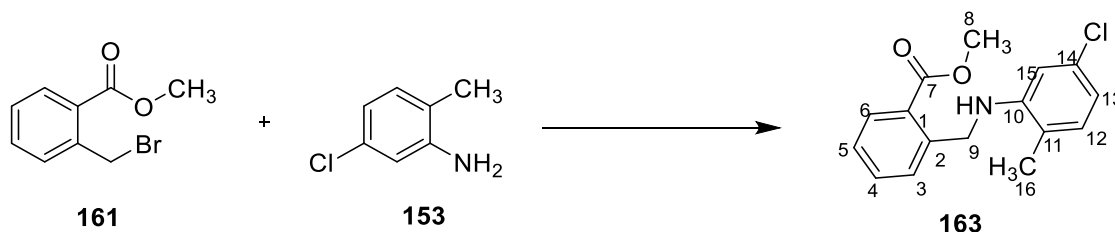
White Solid;

T.L.C. System: *n*-hexane-EtOAc 90:10 v/v, R_f: 0.40;Purification: Biotage Isolera One automated flash column chromatography (cartridge: ZIP KP SIL 30g, *n*-hexane-EtOAc 100:0 increasing to *n*-hexane-EtOAc 80:20 in 15CV) ;

Yield: 0.087 g (74%);

¹H-NMR (CDCl₃), δ: 2.24 (s, 3H, H-16), 3.93 (s, 3H, H-8), 4.46 (bs, 1H, NH), 4.65 (s, 2H, H-9), 6.24 (dd, J₁= 8.1 Hz, J₂=2.2 Hz, 1H, H-11), 6.65 (d, J= 2.2 Hz, 1H, H-15), 6.99 (d, J= 8.1 Hz, 1H, H-12), 7.34-7.37 (m, 1H, H-aromatic), 7.48-7.52 (m, 2H, H-aromatic), 7.99-8.01 (m, 1H, H-aromatic).

UPLC-MS: Rt 2.49 (90%) MS (ESI)⁺: 291.1 [M+H]⁺.

Methyl 2-(((5-chloro-2-methylphenyl)amino)methyl)benzoate (163)**(C₁₆H₁₆ClNO₂; M.W.= 289.76)**Reagent: 5-chloro-2-methylaniline (**153**) (0.062 g, 0.43 mmol);Reagent: methyl 2-(bromomethyl)benzoate (**61**) (0.200 g, 0.87 mmol);

General Procedure14;

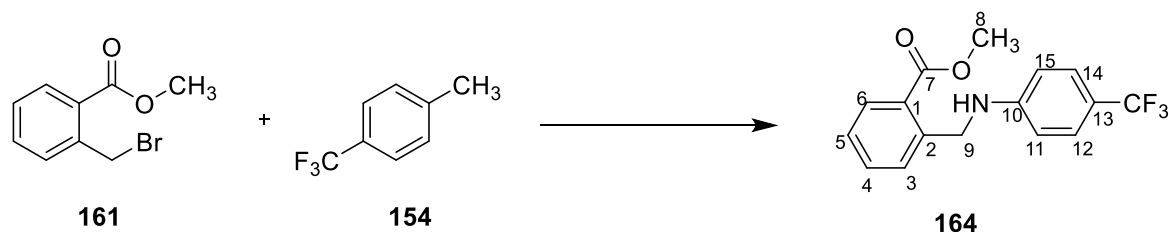
White Solid;

T.L.C. System: *n*-hexane-EtOAc 90:10 v/v, R_f: 0.40;Purification: Biotage Isolera One automated flash column chromatography (cartridge: SNAP KP SIL 25g, *n*-hexane-EtOAc 100:0 increasing to *n*-hexane-EtOAc 80:20 in 15CV) ;

Yield: 0.047 g (38%);

¹H-NMR (CDCl₃), δ: 2.03 (s, 3H, H-16), 3.83 (s, 3H, H-8), 4.39 (bs, 1H, NH), 4.61 (d, J= 6.1 Hz, 2H, H-9), 6.48 (d, J= 2.0 Hz, 1H, H-15), 6.51 (dd, J₁= 7.8 Hz, J₂=2.0 Hz, 1H, H-13), 6.86 (dd, J₁= 7.8 Hz, J₂= 0.7 Hz, 1H, H-aromatic), 7.26-7.29 (m, 1H, H-aromatic), 7.40-7.42 (m, 2H, H-aromatic), 7.90-7.92 (m, 1H, H-aromatic).

UPLC-MS: Rt 2.49 (97%) MS (ESI)⁺: 291.8 [M+H]⁺.

Methyl 2-(((4-(trifluoromethyl)phenyl)amino)methyl)benzoate (164)**(C₁₆H₁₄F₃NO₂; M.W.= 309.10)**Reagent: 1-methyl-4-(trifluoromethyl)benzene (**154**) (0.046 g, 0.28 mmol);Reagent: methyl 2-(bromomethyl)benzoate (**61**) (0.066 g, 0.28 mmol);

General Procedure14;

White Solid;

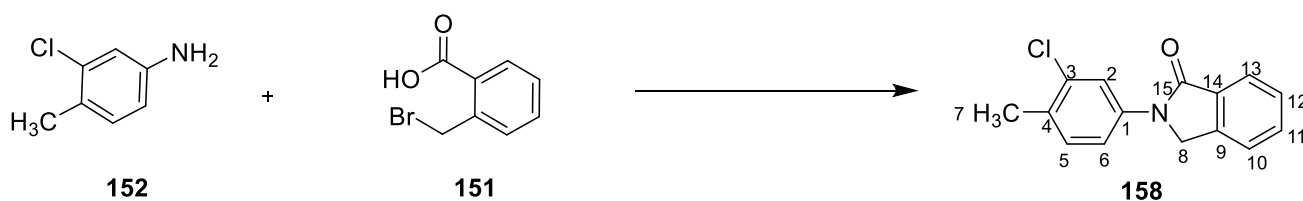
T.L.C. System: *n*-hexane-EtOAc 90:10 v/v, R_f: 0.40;Purification: Biotage Isolera One automated flash column chromatography (cartridge: SNAP KP SIL 25g, *n*-hexane-EtOAc 100:0 increasing to *n*-hexane-EtOAc 60:40 in 15CV);

Yield: 0.037 g (43%);

¹H-NMR (CDCl₃), δ: 3.84 (s, 3H, H-8), 4.63 (d, J= 6.2 Hz, 2H, H-9), 4.79 (bs, 1H, NH), 6.53 (d, J= 8.5 Hz, 2H, H-aromatic), 7.16-7.30 (m, 3H, H-aromatic), 7.40-7.41 (m, 2H, H-aromatic), 7.92-7.94 (m, 1H, H-aromatic).

¹⁹F-NMR (CDCl₃), δ: -62.06 (s, 3F)

UPLC-MS: Rt 2.44 (>96%) **MS (ESI)⁺:** 310.1 [M+H]⁺.

Lactam Derivatives (158-160)**2-(3-Chloro-4-methylphenyl)isoindolin-1-one (158)****(C₁₅H₁₂ClNO; M.W.= 257.72)**Reagent: 3-chloro-4-methylaniline (**152**) (0.108 g, 0.76 mmol);Reagent: 2-(bromomethyl)benzoic acid (**151**) (0.150 g, 0.69 mmol);

Off-White Solid;

T.L.C. System: *n*-hexane-EtOAc 6:4 v/v, R_f: 0.40;

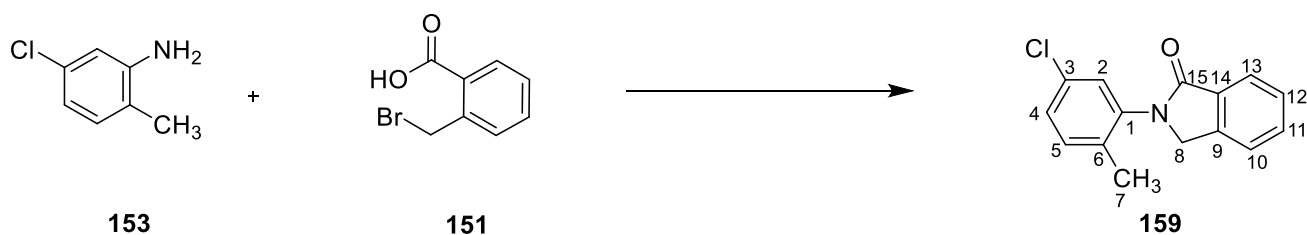
Purification: Recrystallisation from EtOH;

Yield: 0.063 g (37%);

¹H-NMR (DMSO-D₆), δ: 2.34 (s, 3H, H-7), 5.03 (s, 2H, H-8), 7.41-7.43 (m, 1H, H-aromatic), 7.54-7.57 (m, 1H, H-aromatic), 7.66-7.71 (m, 2H, H-aromatic), 7.72 (dd, J₁= 8.5 Hz, J₂= 2.3 Hz, 1H, H-6), 7.79-7.80 (m, 1H, H-aromatic), 8.09 (d, J= 2.3 Hz, 1H, H-2).

¹³C-NMR (DMSO-D₆), δ: 19.4 (CH₃, C-7), 50.8 (CH₂, C-8), 118.1, 119.7, 123.7, 123.8, 128.7, 131.8, 132.9 (CH, C-aromatic), 131.2, 132.6, 135.8, 139.0, 141.4 (C, C-aromatic), 167.2 (C, C-15).

UPLC-MS: Rt 2.32 (100%) **MS (ESI)⁺:** 258.0 [M+H]⁺.

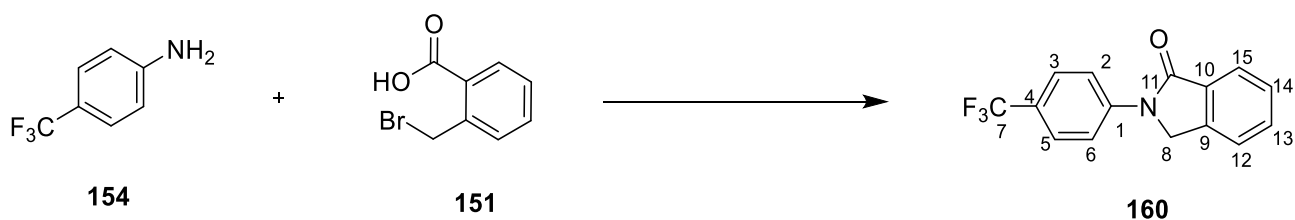
2-(5-Chloro-2-methylphenyl)isoindolin-1-one (159)**(C₁₅H₁₂ClNO; M.W.= 257.72)**Reagent: 5-chloro-2-methylaniline (**153**) (0.108 g, 0.76 mmol);Reagent: 2-(bromomethyl)benzoic acid (**151**) (0.150 g, 0.69 mmol);

Colourless oil;

T.L.C. System: *n*-hexane-EtOAc 7:3 v/v, R_f: 0.6;Purification1: Biotage Isolera One automated flash column chromatography (cartridge: SNAP KP 25g, *n*-hexane-EtOAc 100:0 increasing to *n*-hexane-EtOAc 60:40 in 10CV);Purification2: Biotage Isolera One automated flash column chromatography (cartridge: SNAP KP 10g, *n*-hexane-DCM 100:0 increasing to *n*-hexane-DCM 0:100 in 15CV);

Yield: 0.073 g (38%);

¹H-NMR (DMSO-D₆), δ: 2.16 (s, 3H, H-7), 4.89 (s, 2H, H-8), 7.36-7.40 (m, 2H, H-aromatic), 7.55-7.59 (m, 2H, H-aromatic), 7.66-7.71 (m, 2H, H-aromatic), 7.79 (d, J= 7.4 Hz, 1H, H-aromatic).¹³C-NMR (DMSO-D₆), δ: 17.9 (CH₃, C-7), 52.8 (CH₂, C-8), 123.7, 123.9, 127.8, 128.0, 128.6, 132.4, 132.6 (CH, C-aromatic), 130.8, 131.9, 135.6, 139.2, 142.9 (C, C-aromatic), 166.8 (C, C-15).UPLC-MS: R_t 2.10 (100%) MS (ESI)⁺: 258.0 [M+H]⁺.

2-(4-(Trifluoromethyl)phenyl)isoindolin-1-one (160)**(C₁₅H₁₀F₃NO; M.W.= 277.25)**Reagent: 4-(trifluoromethyl)aniline (**154**) (0.165 g, 1.02 mmol);Reagent: 2-(bromomethyl)benzoic acid (**151**) (0.2 g, 0.93mmol);

White Solid;

T.L.C. System: *n*-hexane-EtOAc 9:1 v/v, R_f: 0.20;

Purification: Recrystallisation from EtOH;

Yield: 0.087 g (32%);

¹H-NMR (CDCl₃), δ: 4.92 (s, 2H, H-8), 7.54-7.57 (m, 2H, H-aromatic), 7.64-7.68 (m, 1H, H-aromatic), 7.71 (d, J= 8.5 Hz, 2H, H-aromatic), 7.96-7.98 (m, 1H, H-aromatic), 8.05 (d, J= 8,5 Hz, 2H, H-aromatic).

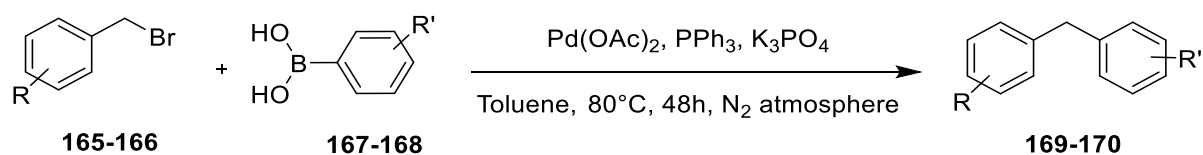
¹³C-NMR (CDCl₃), δ: 50.5 (CH₂, C-8), 118.5, 122.7, 124.4, 126.4, 128.6, 132.6 (CH, C-aromatic), 126.3 (d, J= 27.5 Hz, C, C-aromatic), 126.3, 126.4, 139.8, 142.0 (C, C-aromatic), 198.0 (C, C- 11).

¹⁹F-NMR (CDCl₃), δ: -62.06 (s, 3F)

UPLC-MS: Rt 2.28 (100%) MS (ESI)⁺: 278.0 [M+H]⁺.

9.4 Synthesis of methylene derivatives

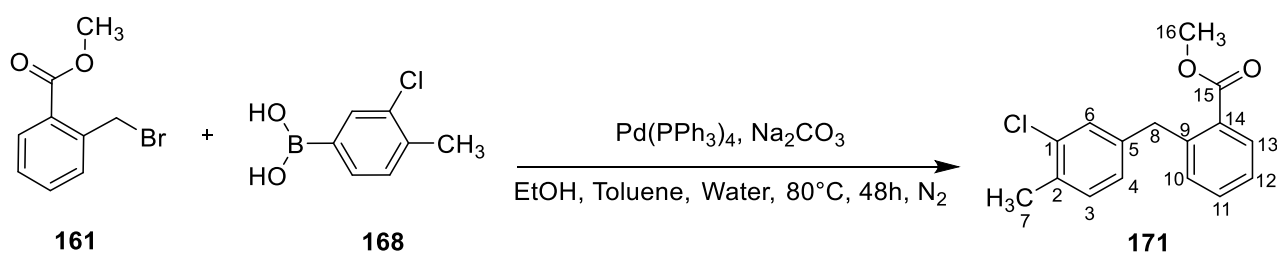
General Procedure 15: methyl(benzyl)benzoates (169-170) ⁽³³⁾



A round bottom flask was charged with Pd(OAc)₂ (0.001 eq), PPh₃ (0.002 eq), the appropriate arylboronic acid (1.5 eq), and K₃PO₄ (2 eq), under N₂ atmosphere. Then the appropriate benzyl bromide (1 eq) and toluene (4.5 mL/mmol) were added. The reaction was stirred at 80°C for 48 hours. The solution was diluted with diethyl ether (15 mL/mmol) and washed with NaOH 1M solution (10 mL/mmol), brine (10 mL/mmol) and then dried over MgSO₄. The residue obtained were purified by flash column chromatography.

Synthesis of methyl 2-(3-chloro-4-methylbenzyl)benzoate (171) ⁽³⁴⁾

((C₁₆H₁₅ClO₂; M.W.=274.74)



To a solution of (3-chloro-4-methylphenyl)boronic acid (0.111 g, 0.94 mmol) and (2-bromomethyl)benzoate (0.150 g, 0.65 mmol) in EtOH (1.5 mL), water (0.4 mL) and toluene (1.2 mL) was added Na₂CO₃ 1M (0.075 g, 0.72 mmol) and catalytic amount of Pd(PPh₃)₄. The reaction was stirred at 80°C for 2 days. The solution was then filtered through celite and the solvent was evaporated. The residue diluted with water and extracted with diethyl ether (3x10 mL). The organic layer was dried over MgSO₄ and evaporated under reduced pressure. The crude product was used for the next step without further purification.

Colourless oil;

T.L.C. System: *n*-hexane-DCM 6:4 v/v, R_f: 0.51;

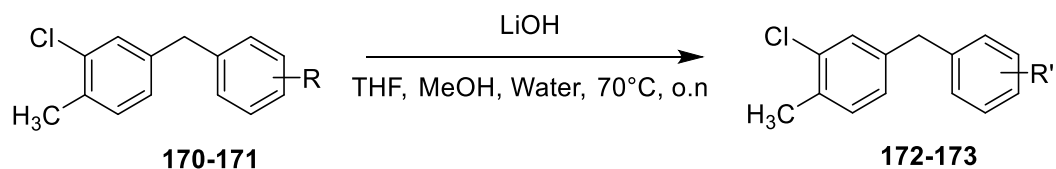
Yield: 0.100 g (56%)

¹H-NMR (CDCl₃), δ: 2.24 (s, 3H, H-7), 3.76 (s, 3H, H-16), 4.24 (s, 2H), 6.85-6.87 (m, 1H, H-aromatic), 7.03 (d, J= 7.9 Hz, 1H, H-aromatic), 7.04-7.06 (m, 1H, H-aromatic), 7.13 (d, J= 7.9 Hz, 1H, H-aromatic),

7.20-7.24 (m, 1H, H-aromatic), 7.35-7.38 (m, 1H, H-aromatic), 7.83 (dd, $J_1=7.8$ Hz, $J_2=1.3$ Hz, 1H, H-aromatic).

$^{13}\text{C-NMR}$ (CDCl_3), δ : 19.6 (CH_3), 51.8 (CH_3), 38.9 (CH_2), 126.7, 127.1, 129.4, 130.8, 131.0, 131.6, 132.30 (CH, C-aromatic), 129.80, 133.49, 134.19, 140.24, 141.71 (C, C-aromatic), 167.9 (C, C-15).

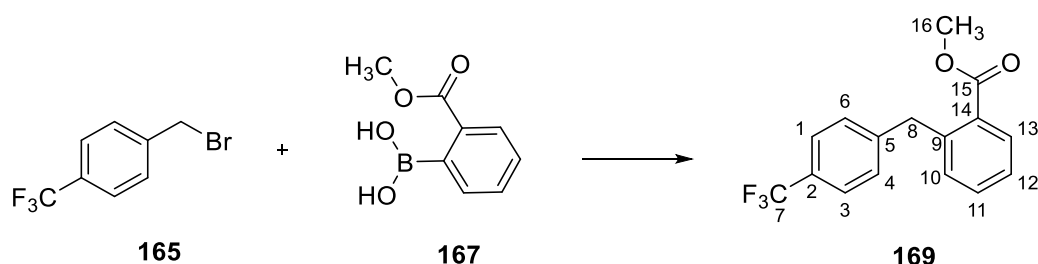
General Procedure 16: benzyl benzoic acids (172-173) ⁽¹⁴⁾



To a solution of the appropriate methyl-(arylamino) benzoate (1 eq) in THF (7 mL/mmol), H_2O (3.5 mL/mmol), MeOH (3.5 mL/mmol) was added LiOH (3 eq). The reaction was stirred at 70°C overnight. After the reaction was allowed to cool to room temperature, the reaction mixture was acidified with 2M HCl. The product was extracted with ethyl acetate (3x10 mL/mmol). The organic layer was dried over MgSO_4 and evaporated under reduced pressure. The product was purified by flash column chromatography or recrystallisation.

9.4.1 Methyl(benzyl)benzoates (169-170)

Methyl 2-(4-(trifluoromethyl)benzyl)benzoate (169)

(C₁₆H₁₃F₃O₂; M.W.= 294.09)Reagent: 1-(bromomethyl)-4-(trifluoromethyl)benzene (**165**) (0.150 g, 0.67 mmol);Reagent: (2-(methoxycarbonyl)phenyl)boronic acid (**167**) (0.170 g, 0.94 mmol);

General Procedure 15;

Colourless oil;

T.L.C. System: *n*-hexane-EtOAc 9:1 v/v, R_f: 0.61;Purification: Biotage Isolera One automated flash column chromatography (cartridge: SNAP KP SIL 25g, *n*-hexane-DCM 100:0 increasing to *n*-hexane-DCM 60:40 in 15CV);

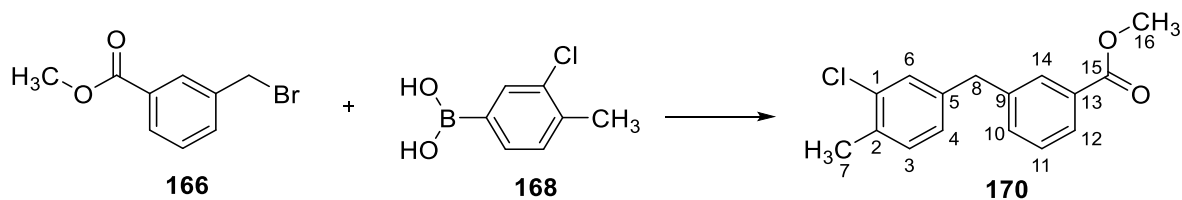
Yield: 0.074 g (37%);

¹H-NMR (CDCl₃), δ: 3.84 (s, 3H, H-16), 4.47 (s, 2H, H-8), 7.24-7.26 (m, 1H, H-aromatic), 7.27 (d, J= 8.2 Hz, 2H, H-aromatic), 7.33-7.37 (m, 1H, H-aromatic), 7.47-7.51 (m, 1H, H-aromatic), 7.53 (d, J= 8.2 Hz, 2H, H-aromatic), 7.97 (dd, J₁= 7.8 Hz, J₂= 1.4 Hz, 1H, H-aromatic).

¹³C-NMR (CDCl₃), δ: 52.0 (CH₃, C-16), 39.5 (CH₂, C-8), 125.4, 126.7, 128.1, 128.8, 129.0, 129.7 (CH, C-aromatic), 125.5, 128.3, 128.7, 141.1, 145.1 (C, C-aromatic), 167.7 (C, C-15).

¹⁹F-NMR (CDCl₃), δ: -62.40 (s, 3F).

UPLC-MS: Rt 2.54 (100%) MS (ESI)⁺: 295.9 [M+H]⁺.

Methyl 3-(3-chloro-4-methylbenzyl)benzoate (170)**(C₁₆H₁₅ClO₂; M.W.=274.74)**Reagent: methyl 3-(bromomethyl)benzoate (**166**) (0.100 g, 0.44 mmol);Reagent: (3-chloro-4-methylphenyl)boronic acid (**168**) (0.170 g, 0.94 mmol);

General Procedure 15;

Colourless oil;

T.L.C. System: *n*-hexane-EtOAc 9:1 v/v, R_f: 0.48;Purification: Biotage Isolera One automated flash column chromatography (cartridge: SNAP KP SIL 25g, *n*-hexane-EtOAc 100:0 increasing to *n*-hexane-EtOAc 80:20 in 15CV);

Yield: 0.070 g (58%);

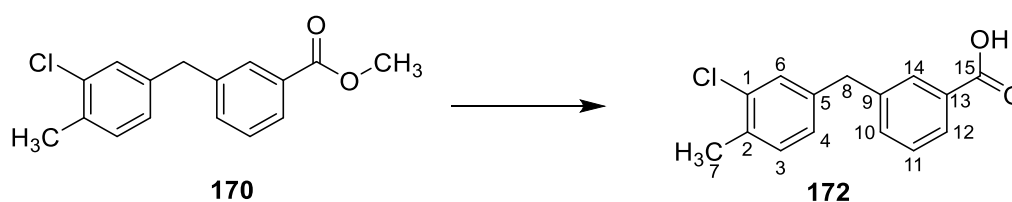
¹H-NMR (CDCl₃), δ: 2.25 (s, 3H, H-7), 3.83 (s, 3H, H-16), 3.88 (s, 2H, H-8), 6.89 (dd, J₁= 7.7 Hz, J₂= 1.3 Hz, 1H, H-aromatic), 7.06 (d, J= 7.7 Hz, 1H, H-aromatic), 7.08-7.10 (m, 1H, H-aromatic), 7.14-7.16 (m, 1H, H-aromatic), 7.27-7.30 (m, 1H, H-aromatic), 7.40-7.44 (m, 1H, H-aromatic), 8.01 (dd, J₁= 7.8 Hz, J₂= 1.3 Hz, 2H, H-aromatic), 7.79-7.83 (m, 2H, H-aromatic).

¹³C-NMR (CDCl₃), δ: 19.6 (CH₃), 52.1 (CH₃), 40.9 (CH₂), 127.1, 127.6, 128.6, 129.31, 131.0, 133.9, 140.9 (CH, C-aromatic), 129.33, 130.4, 133.4, 134.4, 139.7 (C, C-aromatic), 161.1 (C, C-15).

UPLC-MS: Rt 2.62 (>95%) MS (ESI)⁺: 275.0 [M+H]⁺.

9.4.2 Benzyl benzoic acids (172-173)

3-(3-Chloro-4-methylbenzyl)benzoic acid (172)

(C₁₅H₁₃ClO₂; M.W.= 260.72)Reagent: methyl 3-(3-chloro-4-methylbenzyl)benzoate (**170**) (0.050 g, 0.18 mmol);

General Procedure 16;

White solid;

T.L.C. System: *n*-hexane-EtOAc 6:4 v/v, R_f: 0.20;

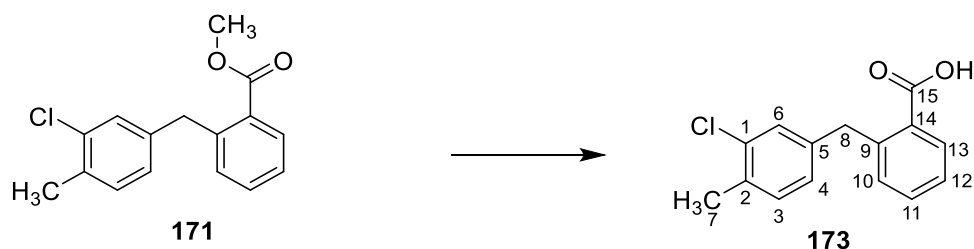
Purification: Precipitation in acid aqueous solution;

Yield: 0.032 g (74%);

¹H-NMR (CDCl₃), δ: 2.36 (s, 3H, H-7), 4.00 (s, 2H, H-8), 6.99-7.01 (m, 1H, H-aromatic), 7.12 (d, J= 7.6 Hz, 1H, H-aromatic), 7.18-7.20 (m, 1H, H-aromatic), 7.42 (d, J= 7.6 Hz, 1H, H-aromatic), 7.43-7.45 (m, 1H, H-aromatic), 7.96 (s, 1H, H-aromatic), 7.98-7.80 (m, 1H, H-aromatic), 11.31 (bs, 1H, OH).

¹³C-NMR (CDCl₃), δ: 19.6 (CH₃, C-7), 40.8 (CH₂, C-8), 127.1, 128.2, 128.8, 129.3, 130.5, 131.1, 134.0 (CH, C-aromatic), 129.4, 134.3, 134.4, 139.5, 141.1 (C, C-aromatic), 171.3 (C, C-15).

UPLC-MS: Rt 2.30 (>98%) MS (ESI)⁻: 259.56 [M-H]⁻.

2-(3-Chloro-4-methylbenzyl)benzoic acid (173)**(C₁₅H₁₃ClO₂; M.W.= 260.72)**Reagent: methyl 2-(3-chloro-4-methylbenzyl)benzoate (**171**) (0.096 g, 0.35 mmol);

General Procedure 16;

White solid;

T.L.C. System: *n*-hexane-EtOAc 6:4 v/v, R_f: 0.40;Purification: Biotage Isolera One automated flash column chromatography (cartridge: ZIP KP SIL 10g, *n*-hexane-EtOAc 100:0 increasing to *n*-hexane-EtOAc 40:60 in 14CV);

Yield: 0.061 g (67%);

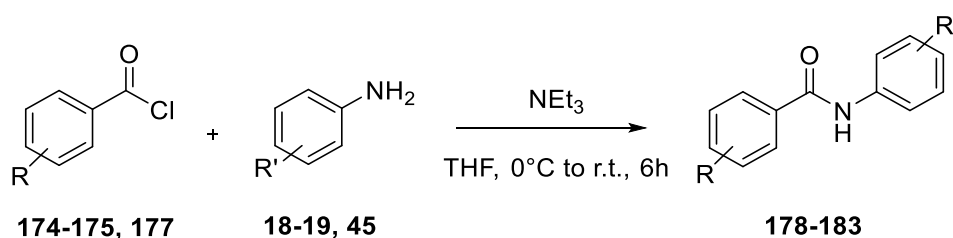
¹H-NMR (CDCl₃), δ: 2.24 (s, 3H, H-7), 4.31 (s, 2H, H-8), 6.88 (dd, J₁= 7.7 Hz, J₂= 1.5 Hz, 1H, H-4), 7.03 (d, J= 7.7 Hz, 1H, H-3), 7.06 (d, J= 1,5 Hz, 1H, H-6), 7.14-7.16 (m, 1H, H-aromatic), 7.25-7.28 (m, 1H, H-aromatic), 7.40-7.44 (m, 1H, H-aromatic), 8.01 (dd, J₁= 7.8 Hz, J₂= 1.3 Hz, 1H, H-aromatic), 11.36 (bs, 1H, OH).

¹³C-NMR (CDCl₃), δ: 19.6 (CH₃, C-7), 38.9 (CH₂, C-8), 126.6, 127.3, 129.4, 130.8, 131.7, 131.8, 133.1 (CH, C-aromatic), 128.2, 133.5, 134.2, 140.0, 142.8 (C, C-aromatic), 172.1 (C, C-15).

UPLC-MS: Rt 2.31 (>98%) MS (ESI)⁻: 259.1 [M-H]⁻.

9.5 Synthesis of amide derivatives

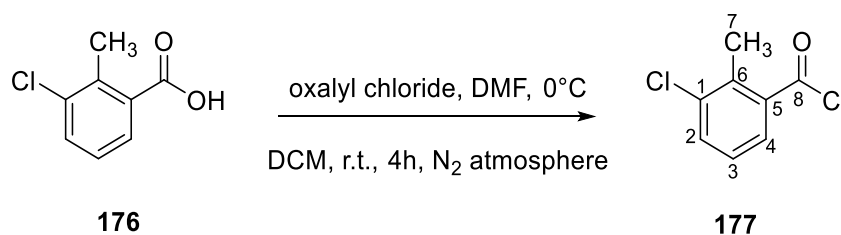
General Procedure 17: alkyl 2-arylamido benzoates (178-183) ⁽³⁵⁾



A solution of differently substituted benzoyl chloride (1 eq) in THF (1.5 mL/mmol) was slowly added at 0°C to a solution of the appropriate alkyl aminobenzoate (1.1 eq) and NEt₃ (1.1 eq) in THF (6.5 mL/mmol). The reaction was stirred at room temperature for 6 hours. The formed salt was removed by filtration and washed with THF. The solvent was removed under reduced pressure. The crude product was purified by flash column chromatography or recrystallization.

Synthesis of 3-chloro-2-methyl benzoyl chloride (177) ⁽³⁶⁾

(C₈H₆Cl₂O; M.W. = 189.04)



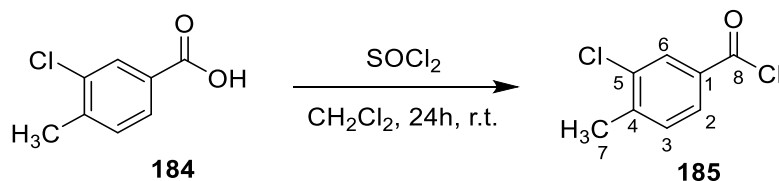
To a solution of 3-chloro-2-methyl carboxylic acid (0.3 g, 1.75 mmol) in dry DCM (5 mL) was added dropwise at 0°C oxalyl chloride (0.18 mL, 2.11 mmol), followed by addition of a catalytic amount (3 drops) of DMF. The reaction was stirred at room temperature, under nitrogen atmosphere for 4 hours. The solvent was then removed under vacuum to afford the desired product.

Yellow oil;

T.L.C. System: *n*-hexane-EtOAc 8:2 v/v, R_f: 0.60;

Yield: 0.303 g (92%);

¹H-NMR (CDCl₃), δ: 2.51 (s, 3H, H-7), 7.18-7.22 (m, 1H, H-aromatic), 7.53 (dd, J₁ = 1.2 Hz, J₂ = 7.0 Hz, 1H, H-aromatic), 7.93 (m, 1H, H-aromatic).

Synthesis of 3-chloro-4-methyl benzoyl chloride (185) ⁽³⁷⁾**(C₈H₆Cl₂O; M.W.= 189.04)**

SOCl₂ (0.696 g, 5.85 mmol) was added to a solution of 3-chloro-4-methyl benzoic acid (0.200 g, 1.17 mmol) in CH₂Cl₂ (2 mL). The mixture was stirred and refluxed for 24 hours, then evaporated until dryness to afford the desired product.

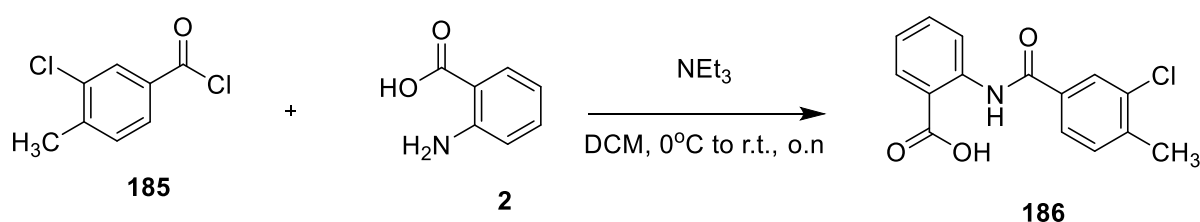
Yellow oil;

T.L.C. System: *n*-hexane-EtOAc 8:2 v/v, R_f: 0.60;

Yield: 0.110 g (50%);

¹H-NMR (CDCl₃), δ: 2.09 (s, 3H, H-7), 7.30 (d, J= 8.3 Hz, 1H, H3), 7.83 (dd, J₁= 8.3 Hz, J₂= 1.9 Hz, 1H, H-2), 8.01 (d, J= 1.9 Hz, 1H, H-aromatic).

¹³C-NMR (CDCl₃), δ: 20.6 (CH₃, C-7), 129.4, 131.3, 131.7 (CH, C-aromatic), 99.0, 124.2, 134.2 (C, C-aromatic), 144.6 (C, C-8).

Synthesis of 2-(3-chloro-4-methylbenzamido)benzoic acid (186) ⁽³⁸⁾**(C₁₅H₁₂ClNO₃; M.W.= 289.72)**

A mixture of anthranilic acid (0.020 g, 0.14 mmol), NEt₃ (0.018 g, 0.18 mmol) and CH₂Cl₂ (4 mL) was stirred at room temperature. 3-chloro-4-methyl benzoyl chloride (0.030 g, 0.15 mmol) was then added slowly at 0°C. The reaction was stirred overnight. The reaction mixture was washed with water and extracted with CH₂Cl₂ (20 mL x 2). The organic layers were combined, dried over sodium sulfate, and concentrated under reduced pressure. The product was purified by recrystallisation from EtOH/Water.

White solid;

T.L.C. System: *n*-hexane-EtOAc 7:3 v/v, R_f: 0.50;

Purification: Recrystallisation from EtOH;

Yield: 0.021 g (52%);

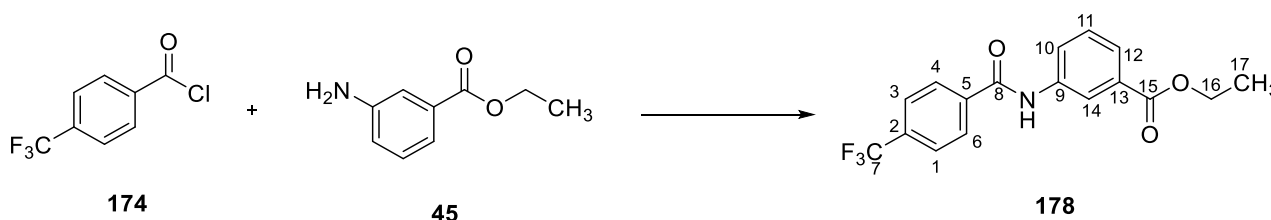
¹H-NMR (DMSO-D₆), δ: 2.48 (s, 3H, H-7), 7.19-7.22 (m, 1H, H-aromatic), 7.40 (d, J= 7.9 Hz, 1H, H-13), 7.68-7.72 (m, 1H, H-aromatic), 7.82 (dd, J₁= 7.9 Hz, J₂= 1.6 Hz, 1H, H-14), 7.83 (d, J= 1.6 Hz, 1H, H-10), 8.20 (dd, J₁= 8.0 Hz, J₂= 1.4 Hz, 1H, H-aromatic), 8.94-8.96 (m, 1H, H-aromatic), 11.85 (bs, 1H, NH).

¹³C-NMR (DMSO-D₆), δ: 20.2 (CH₃, C-15), 120.5, 122.9, 125.3, 128.4, 131.2, 131.9, 135.9 (CH, C-aromatic), 113.8, 134.0, 135.1, 140.5, 142.3 (C, C-aromatic), 164.5, 171.2 (C, C-carbonyl).

UPLC-MS: Rt 2.25 (99%) **MS (ESI)⁺:** 290.1 [M+H]⁺.

9.5.1 Alkyl 2-arylamido benzoates (178-183)

Ethyl 3-(4-(trifluoromethyl)benzamido)benzoate (178)

(C₁₇H₁₄F₃NO₃; M.W.= 337.30)

Reagent: 4-(trifluoromethyl)benzoyl chloride (**174**) (0.150 g, 0.72 mmol);

Reagent: ethyl 3-aminobenzoate (**45**) (0.130 g, 0.72 mmol);

General Procedure 17;

White solid;

T.L.C. System: *n*-hexane-EtOAc 8:2 v/v, R_f: 0.44;

Purification1: Recrystallisation from EtOH;

Purification 2: Biotage Isolera One automated flash column chromatography (cartridge: SNAP KP SIL 25g, *n*-hexane-EtOAc 100:0 increasing to *n*-hexane-EtOAc 60:40 in 10CV);

Purification 3: Biotage Isolera One automated flash column chromatography (cartridge: SNAP KP SIL 10g, *n*-hexane-EtOAc 100:0 increasing to *n*-hexane-EtOAc 65:30 in 10CV);

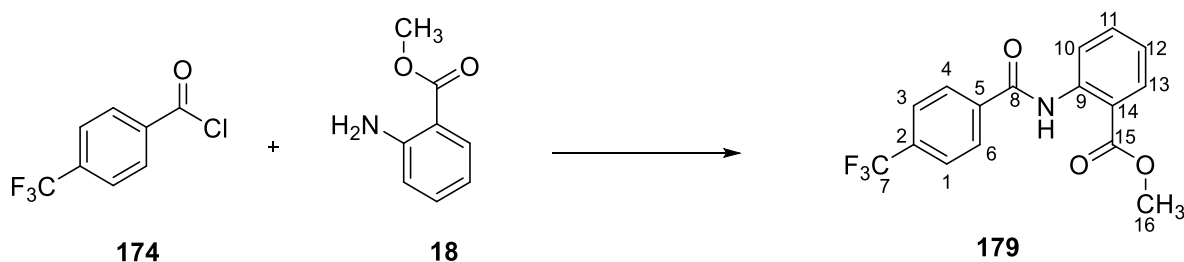
Yield: 0.117 g (44%);

¹H-NMR (DMSO-D₆), δ: 1.34 (t, J = 7.1 Hz, 3H, H-17), 4.35 (q, J = 7.1 Hz, 2H, H-16), 7.52-7.55 (m, 1H, H-aromatic), 7.72-7.74 (m, 1H, H-aromatic), 7.94 (d, J = 8.1 Hz, 2H, H-aromatic), 8.08-8.11 (m, 1H, H-aromatic), 8.19 (d, J = 8.1 Hz, 2H, H-aromatic), 8.43-8.45 (m, 1H, H-aromatic), 10.68 (bs, 1H, NH).

¹³C-NMR (DMSO-D₆), δ: 14.6 (CH₃, C-17), 61.3 (CH₂, C-16), 121.3, 124.3, 125.0, 125.2, 125.90, 125.93 (CH, C-aromatic), 129.1, 129.6, 130.8, 138.8, 139.6 (C, C-aromatic), 165.0, 166.0 (C, C-8,15).

¹⁹F-NMR (DMSO-D₆), δ: -61.33 (s, 3F).

UPLC-MS: Rt 2.31 (100%) MS (ESI)⁺: 338.2 [M+H]⁺.

Methyl 2-(4-(trifluoromethyl)benzamido)benzoate (179)**(C₁₆H₁₂F₃NO₃; M.W.= 323.27)**Reagent: 4-(trifluoromethyl)benzoyl chloride (**174**) (0.500 g, 2.39 mmol);Reagent: methyl 2-aminobenzoate (**18**) (0.362 g, 2.39 mmol);

General Procedure 17;

White solid;

T.L.C. System: *n*-hexane-EtOAc 7:3 v/v, R_f: 0.59;

Purification: Recrystallisation from EtOH;

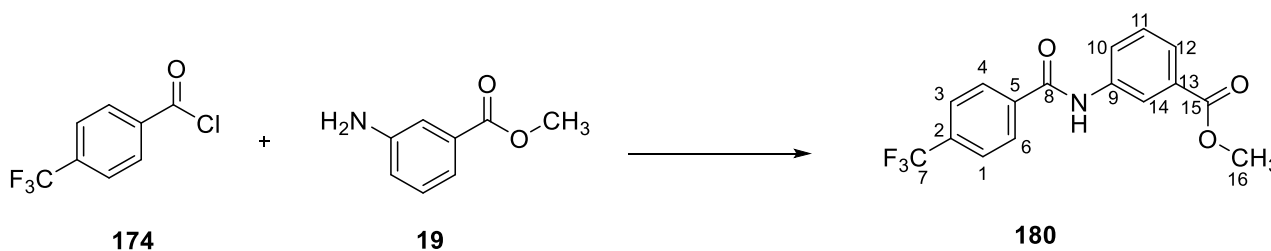
Yield: 0.275 g (37%);

¹H-NMR (DMSO-D₆), δ: 3.84 (s, 3H, H-16), 7.28-7.31 (m, 1H, H-aromatic), 7.69-7.33 (m, 1H, H-aromatic), 7.99 (d, J= 8.2 Hz, 2H, H-aromatic), 8.01-8.03 (m, 1H, H-aromatic), 8.16 (d, J= 8.2 Hz, 2H, H-aromatic), 8.46 (dd, J₁= 7.3 Hz, J₂= 1.0 Hz, 1H, H-aromatic), 11.59 (bs, 1H, NH).

¹³C-NMR (DMSO-D₆), δ: 53.1 (CH₃, C-16), 121., 125.3, 126.5, 128.5, 131.1, 134.7 (CH, C-aromatic), 118.6, 132.4, 138.6, 139.3, 140.8, (C, C-aromatic), 164.1, 168.3 (C, C-8,15).

¹⁹F-NMR (DMSO-D₆), δ: -61.41 (s, 3F).

UPLC-MS: Rt 2.52 (100%) MS (ESI)⁺: 324.2 [M+H]⁺.

Methyl 3-(4-(trifluoromethyl)benzamido)benzoate (180)**(C₁₆H₁₂F₃NO₃; M.W.= 323.27)**Reagent: 4-(trifluoromethyl)benzoyl chloride (**174**) (0.500 g, 2.39 mmol);Reagent: methyl 3-aminobenzoate (**19**) (0.362 g, 2.39 mmol);

General Procedure 17;

White solid;

T.L.C. System: *n*-hexane-EtOAc 7:3 v/v, R_f: 0.50;

Purification: Recrystallisation from EtOH;

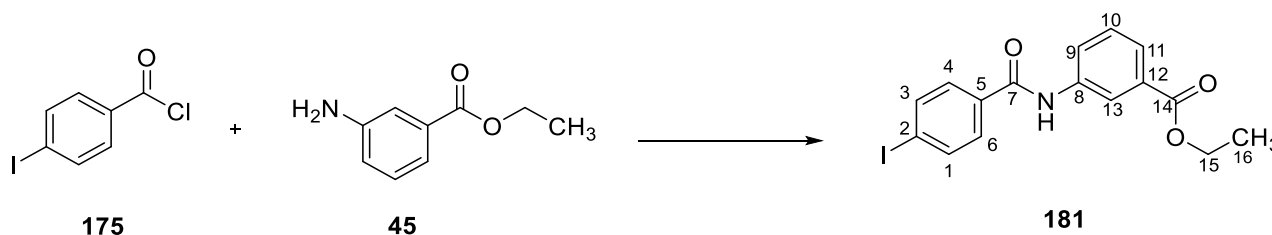
Yield: 0.700 g (90%);

¹H-NMR (CDCl₃), δ: 3.93 (s, 3H, H-16), 7.47-7.50 (m, 1H, H-aromatic), 7.70 (d, J= 8.3 Hz, 2H, H-aromatic), 7.85-7.87 (m, 1H, H-aromatic), 8.02 (d, J= 8.3 Hz, 2H, H-aromatic), 8.05-8.07 (m, 1H, H-aromatic), 8.15-8.17 (m, 1H, H-aromatic), 8.23 (bs, 1H, NH).

¹³C-NMR (CDCl₃), δ: 53.3 (CH₃, C-16), 121.9, 124.8, 125.9, 126.0, 127.6, 129.3 (CH, C-aromatic), 122.6, 124.6, 131.0, 133.7, 135.8, (C, C-aromatic), 164.6, 166.6 (C, C-8,15).

¹⁹F-NMR (CDCl₃), δ: -62.99 (s, 3F).

UPLC-MS: Rt 2.21 (100%) MS (ESI)⁺: 324.2 [M+H]⁺.

Ethyl 3-(4-iodobenzamido)benzoate (181)**(C₁₆H₁₄INO₃; M.W.= 395.20)**Reagent: 4-iodobenzoyl chloride (**175**) (0.500 g, 1.88 mmol);Reagent: ethyl 3-aminobenzoate (**45**) (0.309 g, 1.88 mmol);

General Procedure 17;

White solid;

T.L.C. System: *n*-hexane-EtOAc 8:2 v/v, R_f: 0.40;

Purification1: Recrystallisation from EtOH;

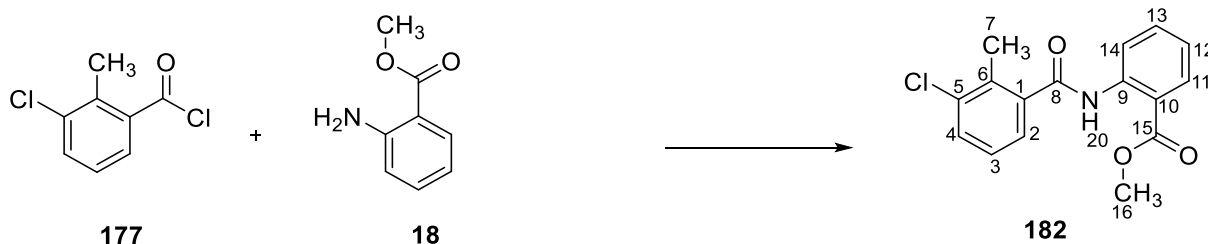
Purification 2: Biotage Isolera One automated flash column chromatography (cartridge: SNAP KP SIL 25g, *n*-hexane-EtOAc 100:0 increasing to *n*-hexane-EtOAc 60:40 in 10CV);

Yield: 0.270 g (37%);

¹H-NMR (CDCl₃), δ: 1.32 (t, J=7.1 Hz, 3H, H-16), 4.30 (q, J= 7.1 Hz, 2H, H-15), 7.37-7.40 (m, 1H, H-aromatic), 7.53 (d, J= 8.5 Hz, 2H, H-aromatic), 7.77 (d, J= 8.5 Hz, 2H, H-aromatic), 7.79-7.82 (m, 1H, H-aromatic), 7.85 (bs, 1H, NH), 7.97-7.99 (m, 1H, H-aromatic), 8.02-8.03 (m, 1H, H-aromatic),

¹³C-NMR (CDCl₃), δ: 14.3 (CH₃, C-16), 61.2 (CH₂, C-15), 121.0, 124.6, 125.8, 128.6, 129.3, 138.1 (CH, C-aromatic), 99.1, 131.4, 134.0, 137.8, (C, C-aromatic), 165.0, 166.1 (C, C-7,14).

UPLC-MS: Rt 2.21 (>99%) MS (ESI)⁻: 398.2 [M-H]⁻.

Methyl 2-(3-chloro-2-methylbenzamido)benzoate (182)**(C₁₆H₁₄ClNO₃; M.W.= 303.74)**Reagent: 3-chloro-2-methylbenzoyl chloride (**177**) (0.150 g, 0.79 mmol);Reagent: methyl 2-aminobenzoate (**18**) (0.120 g, 0.79 mmol);

General Procedure 17;

White solid;

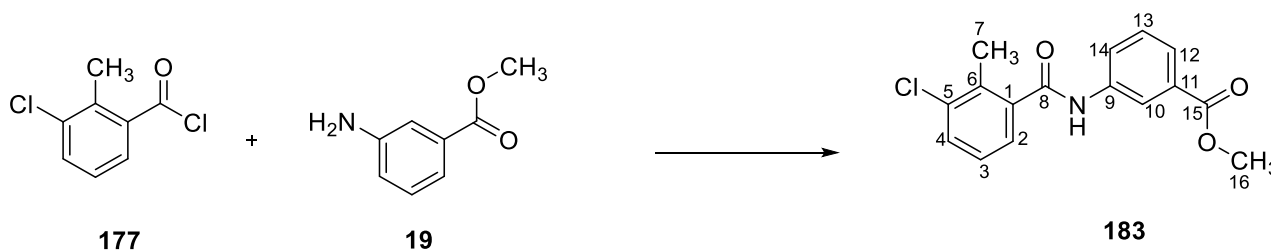
T.L.C. System: *n*-hexane-EtOAc 7:3 v/v, R_f: 0.50;Purification: Biotage Isolera One automated flash column chromatography (cartridge: SNAP KP SIL 25g, *n*-hexane-EtOAc 100:0 increasing to *n*-hexane-EtOAc 80:20 in 15CV);

Yield: 0.067 g (28%);

¹H-NMR (CDCl₃), δ: 2.57 (s, 3H, H-7), 3.93 (s, 3H, H-16), 7.16-7.20 (m, 1H, H-aromatic), 7.24-7.28 (m, 1H, H-aromatic), 7.48-7.51 (m, 2H, H-aromatic), 7.63-7.66 (m, 1H, H-aromatic), 8.11 (dd, *J*₁= 6.3 Hz, *J*₂= 1.5Hz, 1H, H-aromatic), 8.90-8.93 (m, 1H, H-aromatic), 11.45 (bs, 1H, NH).

¹³C-NMR (CDCl₃), δ: 17.1 (CH₃), 52.4 (CH₃), 123.0, 125.3, 126.0, 127.0, 131.0, 131.1, 134.3 (CH, C-aromatic), 115.3, 134.5, 136.1, 139.0, 141.4 (C, C-aromatic), 167.7, 168.7 (C, C-8, 15).

UPLC-MS: Rt 2.50 (>98%) MS (ESI)⁺: 304.1 [M+H]⁺.

Methyl 3-(3-chloro-2-methylbenzamido)benzoate (183)**(C₁₆H₁₄ClNO₃; M.W.= 303.74)**Reagent: 3-chloro-2-methylbenzoyl chloride (**177**) (0.150 g, 0.79 mmol);Reagent: methyl 3-aminobenzoate (**18**) (0.120 g, 0.79 mmol);

General Procedure 17;

White solid;

T.L.C. System: *n*-hexane-EtOAc 7:3 v/v, R_f: 0.50;Purification: Biotage Isolera One automated flash column chromatography (cartridge: SNAP KP SIL 25g, *n*-hexane-EtOAc 100:0 increasing to *n*-hexane-EtOAc 80:20 in 15CV);

Yield: 0.073 g (30%);

¹H-NMR (CDCl₃), δ: 2.40 (s, 3H, H-7), 3.77 (s, 3H, H-16), 7.08-7.12 (m, 1H, H-aromatic), 7.25-7.27 (m, 1H, H-aromatic), 7.36-7.39 (m, 2H, H-aromatic), 7.72-7.75 (m, 1H, H-aromatic), 7.80 (bs, 1H, NH), 7.95-7.97 (m, 1H, H-aromatic), 8.05 (s, 1H, H-10).

¹³C-NMR (CDCl₃), δ: 17.0 (CH₃), 52.2 (CH₃), 120.8, 124.4, 124.9, 125.8, 126.9, 129.3, 131.0 (CH, C-aromatic), 131.0, 134.2, 136.0, 138.0, 138.4 (C, C-aromatic), 166.6, 167.4 (C, C-8,15).

UPLC-MS: Rt 2.17 (100%) MS (ESI)⁺: 304.1 [M+H]⁺.

9.6 References

- 1: MCF-7 Cells. <http://www.mcf7.com> (accessed January 13, 2018).
- 2: TKCC-07. <http://www.pancreaticcancer.net.au> (accessed January 29, 2018).
- 3: HEK293. <http://www.hek293.com/> (accessed January 21, 2018).
- 4: Hayward, O. Design and Synthesis of Molecular Inhibitors of c-FLIP Activity as a Therapeutic Strategy to Target Breast Cancer Stem Cells. PhD Thesis. **2015**, Cardiff University.
- 5: Riss, L. T.; Moravec, R. A.; Niles, A. L.; Duellman, S.; Benink, H. A.; Worzella, T. J.; Minor, L. Cell viability assays. In *Assay guidance manual*, 1st ed.; Sittampalam, G. S.; Coussens, N. P.; Nelson, H.; Arkin, M.; Auld, D.; Austin, C.; Bejcek, B.; Glicksman, M.; Inglese, J.; Iversen, P. W.; Li, Z.; McGee, J., McManus, O.; Minor, L.; Napper, A., Peltier, J. M.; Riss, T.; Trask, O. J.; Weidner, J. Eds.; Bethesda (MD): Eli Lilly & Company and the National Center for Advancing Translational Sciences, 2013. Available from: <http://www.ncbi.nlm.nih.gov/books/NBK53196/>.
- 6: Chemical Computing Group, Montreal, Canada. <https://www.chemcomp.com> (accessed September 22, 2017).
- 7: Schrödinger, Cambridge, MA. <https://www.schrodinger.com> (accessed October 21, 2017).
- 8: Bowers, K. J.; Chow, E.; Xu, H.; Dror, R. O.; Eastwood, M. P.; Gregersen, B. A.; Klepeis, J. L.; Kolossváry, I.; Moraes, M. A.; Sacerdoti, F. D.; Salmon, J. K.; Shan, Y.; Shaw, D. E. Scalable algorithms for molecular dynamics simulations on commodity clusters. *Proceedings of the ACM/IEEE Conference on Supercomputing (SC06)*, Tampa, Florida, November 11–17, **2006**.
- 9: Peifer, C.; Kinkel, K.; Abadleh, M.; Schollmeyer, D.; Laufer, S. From five- to six-membered rings: 3,4-Diarylquinolinone as lead for novel p38MAP kinase inhibitors. *J. Med. Chem.* **2007**, *50*, 1213-1221.
- 10: Mishra, J. K.; Panda, G. Diversity-oriented synthetic approach to naturally abundant S-amino acid based benzannulated enantiomerically pure medium ring heterocyclic scaffolds employing inter- and intramolecular Mitsunobu reactions. *J. Comb. Chem.* **2007**, *9*, 321-338.
- 11: Soma, S.; Srikanth, K.; Banerjee, S.; Debnath, B.; Gayen, S.; Jha, T. 5-N-Substituted-2-(substituted benzsulphonyl) glutamines as antitumor agents. Part II: Synthesis, biological activity and QSAR study. *Bioorg. Med. Chem.* **2004**, *12*, 1413-1423.

- 12:** Naganawaa, A.; Saitoa, T.; Nagaoa, Y.; Egashiraa, H.; Iwahashia, M.; Kambea, T.; Koketsub, M.; Yamamotoc, H.; Kobayashib, M.; Maruyamaa, T.; Ohuchidad, S.; Nakaia, H.; Kondoa, K.; Todaa, M. Discovery of new chemical leads for selective EP1 receptor antagonists. *Bioorg. Med. Chem.* **2006**, *14*, 5562-5577.
- 13:** Surman, M. D.; Mulvihill, M. J.; Miller, M. J. Novel 1,4-benzodiazepines from acylnitroso-derived hetero-diels–alder cycloadducts. *Org. Lett.* **2002**, *4*, 139-141.
- 14:** Ohkata, K.; Tamura, Y.; Shetuni, B. B.; Takagi, R.; Miyanaga, W.; Kojima, S.; Paquette, L. A. Stereoselectivity control by oxaspiro Rings during diels–alder cycloadditions to cross-conjugated cyclohexadienones: the syn oxygen phenomenon. *J. Am. Chem. Soc.* **2004**, *126*, 16783-16792.
- 15:** Avila, C. M.; Lopes, A. B.; Gonçalves, A. S.; da Silva, L. L.; Romeiro, N. C.; Miranda, A. P. M.; Sant’Anna, C. M. R.; Barreiro, E. J.; Fraga, C. A. M. Structure-based design and biological profile of (*E*)-*N*-(4-Nitrobenzylidene)-2-naphthohydrazide, a novel small molecule inhibitor of I κ B kinase- β . *Eur. J. Med. Chem.* **2011**, *4*, 1245-1253.
- 16:** Suvarna, H. P.; Haushabhau, S. P.; Gwi, B. L.; Seo-Jung, H.; Hyun Jung, K.; Ji Young, K.; Ki, Y. K.; Sang Dal, R.; Jeong, I. R.; Jin, S. s.; Myung, A. B.; Mi-jin, P.; Dooseop, K.; Duck, H. L.; Jin, H. A. Discovery and optimization of adamantane carboxylic acid derivatives as potent diacylglycerol acyltransferase 1 inhibitors for the potential treatment of obesity and diabetes. *Eur. J. Med. Chem.* **2015**, *101*, 716-735.
- 17:** Wright, S. W.; Hageman, D. L.; Wright, A. S.; McClure, L. D. Convenient preparations of t-butyl esters and ethers from t-butanol. *Tetrahedron Lett.* **1997**, *42*, 7345-7348.
- 18:** Bjarne, D. H.; Palle, C. Substituted phenyl derivatives, their preparation and use. U.S. Patent 20020037905 A1, **2002**.
- 19:** Barker, E.; Crossley, R. Indazole derivatives which interact with the G protein-coupled receptor family, and their preparation, pharmaceutical compositions, and use against BRS-3 receptor-related disorders. U.S. Patent 2005056532, **2005**.
- 20:** Mizutani, T.; Nagase, T.; Sayaka, I.; Yasuhisa, M.; Takeshi, T.; Norihiro, T.; Shigeru, T.; Nagaaki, S. Development of novel 2-[4-(aminoalkoxy)phenyl]-4(3H)-quinazolinone derivatives as potent and selective histamine H3 receptor inverse agonists. *Bioorg. Med. Chem. Lett.* **2008**, *18*, 6041-6045.
- 21:** Soo Lee, K.; Kee, D. K. Efficient synthesis of primary amides from carboxylic acids using *N,N'*-carbonyldiimidazole and ammonium acetate in ionic liquid. *Synth. Commun.* **2011**, *41*, 3497-3500.

- 22:** Wydysh, E. A.; Medghalchi, S. M.; Vadlamudi, A.; Townsend, C A. Design and synthesis of small molecule glycerol 3-phosphate acyltransferase inhibitors. *J. Med. Chem.* **2009**, *52*, 3317-3327.
- 23:** Chen, X.; Zhou, S.; Qian, C. Preparation of thiophenols from substituted benzenesulfonyl chlorides. U.S. Patent 102531978 A, **2012**.
- 24:** Wyrwa, R.; Droescher, P.; Ring, S.; Elger, W.; Schneider, B.; Hillisch, A.; Reddersen, G.; Adamski, J. Preparation of aminosulfonyl- or aminosulfonylamino-substituted phenyl esters as estradiol prodrugs. W.O. Patent 2005113574 A1, **2005**.
- 25:** Dominic, J. E.; Lopez, M. On the reaction of anthranilic acid with thionyl chloride: iminoketene intermediate formation. *Indian. J. Chem. B.* **2007**, *64*, 519-523.
- 26:** Das, B.; Reddy, C. R.; Kumar, D. N.; Krishnaiah, M.; Narender, R. A simple, advantageous synthesis of 5-substituted 1H-tetrazoles. *Synlett.* **2010**, *3*, 391-394.
- 27:** Min, J.; Jian, L.; Feng, W.; Yichao, Z.; Feng, Z.; Xiaochun, D.; Weili, Z. A facile copper-catalyzed one-pot domino synthesis of 5,12-dihydroindolo[2,1-b]quinazolines. *Org. Lett.* **2012**, *14*, 1420-1423.
- 28:** Xiangdong, L.; Ming, C.; Xin X.; Ning, S.; Shi, L.; Yuanhong, L. Synthesis of multiple-substituted pyrroles via gold(I)-catalyzed hydroamination/cyclization cascade. *Org. Lett.* **2015**, *17*, 2984-2987.
- 29:** Barluenga, J.; Fañanás, F. J.; Sanz, R.; Marcos, C.; Ignacio, C. M. 2-Arylallyl as a new protecting group for amines, amides and alcohols. *ChemComm.* **2005**, *7*, 933-935.
- 30:** Laufer, S. A.; Ahrens, G. M.; Karcher, C. S.; Hering, S. J.; Niess, R. Design, synthesis, and biological evaluation of phenylamino-substituted 6,11-dihydro-dibenzo[b,e]oxepin-11-ones and dibenzo[a,d]cycloheptan-5-ones: novel p38 MAP kinase inhibitors. *J. Med. Chem.* **2006**, *49*, 7912-7915.
- 31:** Bernstein, R. P.; Aharony, D.; Albert, S. J.; Andisik, D.; Barthlow, G. H.; Bialecki, R.; Davenport, T.; Dedinas, F. R.; Dembofsky, T. B.; Koether, G.; Kosmider, J. B.; Kirkland, K.; Ohnmacht, J. C.; Potts, W.; Rumsey, L. W.; Shen, L.; Shenvi, A.; Sherwood, S.; Stollman, D.; Russell, K. Discovery of novel, orally active dual NK₁/NK₂ antagonists. *Bioorg. Med. Chem. Lett.* **2001**, *20*, 2769-2773.
- 32:** By Liu, Q.; Batt, D. G.; Delucca, G. V.; Shi, Q.; Tebben, A. J. Preparation of carbazole carboxamide compounds useful as kinase inhibitors. U. S. Patent 20100160303 A1, **2010**.
- 33:** Desforges, G.; Bombrun, A.; Quattropani, A. An efficient and expeditious synthesis of di- and trisubstituted amino-phenyl and -benzyl derivatives of tetrazole and [1,3,4]oxadiazol-2-one. *J. Comb. Chem.* **2008**, *10*, 671-680.

- 34:** Nobre, M. S.; Monteiro, L. A. Synthesis of diarylmethane derivatives from Pd-catalyzed cross-coupling reactions of benzylic halides with arylboronic acids. *Tetrahedron Lett.* **2004**, *45*, 8225-8228.
- 35:** Anselmia, E.; Abarbria, M.; Duchênea, A.; Langle-Lamandé, S.; Thibonnet, J. Efficient synthesis of substituted styrenes and biaryls (or heteroaryls) with regioselective reactions of ortho-, meta-, and para-bromobenzyl bromide. *Synthesis.* **2012**, *44*, 2023-2040.
- 36:** Van Dijk, T.; Burck, S.; Rong, M. K.; Rosenthal, J. A.; Nieger, M.; Slootweg, J. C.; Lammertsma, K. Facile synthesis of phosphamidines and phosphamidates using nitrilium ions as an imine synthon. *Angew. Chem. Int. Edit.* **2014**, *53*, 9068-9081.
- 37:** Sanjay, S.; Ting, L. L.; Yulin, L. Synthesis and in vitro evaluation of West Nile Virus protease inhibitors based on the 2-{6-[2-(5-Phenyl-4H{1,2,4}triazol-3-ylsulfanyl)acetylamino]benzothiazol-2ylsulfanyl}acetamide scaffold. *ChemMedChem.* **2013**, *8*, 994-1001.
- 38:** Xiaoke, G.; Xianglei, M.; Qian, Y.; Jing, X.; Lu, H.; Jianmin, J.; Jiaojiao, S.; Li, L.; Weilin, C.; Hongxi, C.; Jinlian, W.; Xiaojin, Z.; Haopeng, S.; Yiqun, T.; Qidong, Y. Discovery of 1-aryloxyethyl piperazine derivatives as Kv1.5 potassium channel inhibitors (part I). *Eur. J. Med. Chem.* **2014**, *81*, 89-94.